OXYGEN AND BORON ISOTOPE EFFECTS IN SYNTHETIC CALCITE

OXYGEN AND BORON ISOTOPE EFFECTS IN SYNTHETIC CALCITE

By JILLIAN WYMAN, B.Sc.

A Thesis Submitted to the School of Graduate Studies in Partial Fulfillment of the
Requirements for the Degree Master of Science

McMaster University

© Copyright by Jillian Wyman, August 2014

MASTER OF SCIENCE (2014) McMaster University
Earth and Environmental Science – Geochemistry Hamilton, Ontario

TITLE: Oxygen and Boron Isotope Effects in Synthetic Calcite

AUTHOR: Jillian Wyman, B.Sc. (Honours) (McMaster University)

SUPERVISOR: Dr. Sang-Tae Kim

NUMBER OF PAGES: xi, 194, xv

PRELIMINARIES

ABSTRACT

Natural calcium carbonates, such as foraminifera and speleothems, are ubiquitous on the Earth's surface and are essential subjects of study to the field of paleoclimatology. In particular, climate proxies using stable isotope and/or trace element concentrations of marine or continental carbonates largely rely on laboratory calibration studies in which carbonates are synthesized and their geochemical properties are carefully quantified. The boron isotope compositions of marine carbonates are a potentially powerful tool for the reconstruction of ancient seawater pH. If proven reliable, this tracer will allow systematic recording of paleooceanographic conditions, greatly assisting climatologists identifying historical fluctuations in atmospheric carbon dioxide concentrations.

The boron isotope-pH proxy relies on the hypothesis that only the charged borate ion, possessing a distinct boron isotope composition as a function of pH, is incorporated into the carbonate crystal lattice. In this study, abiotic calcite was synthesized in high ionic strength solutions (0.7 mol/kg) across a range of controlled pH conditions (low pH ~ 7.15, mid pH ~ 8.35 and high pH ~ 9.15). The magnitude of boron isotope fractionation (δ^{11}B) was determined to quantify the pH-dependence of $\delta^{11}B_{calcite}$ between the carbonate and the precipitating solution. The observed increase in boron isotope composition of calcite with pH is consistent with preferential incorporation of borate ion into the crystal lattice, however the sensitivity of the acid dissociation and isotope equilibrium constants render it difficult to ascertain its exclusive contribution to the boron isotope composition of calcite. Observed non-equilibrium effects further mask the interpretation of the underlying mechanisms, which must be understood precisely to validate the proxy. Ultimately, the relationship between the boron isotope composition of marine carbonates and ocean pH may provide objective evidence for ocean-CO_2 system alterations possibly stemming from human-induced climate change.

This research also evaluated the temperature- and pH-dependence of oxygen isotope fractionation (between calcite and water) in high ionic strength systems at 10, 25 and 40 °C over a pH range of 7.46-9.43. Our study is the first to assess oxygen isotope effects and fractionation behavior under these varied conditions while employing the constant addition method. Preliminary results support several working hypotheses in the field and have proven consistent with previously untested theoretical predictions.

ACKNOWLEDGEMENTS

I am very appreciative of the generous support that I have received from many individuals during my time at McMaster University. As an undergraduate student in the School of Geography and Earth Sciences, I was fortunate enough to receive instruction from enthusiastic and knowledgeable professors, which inspired me to pursue graduate studies in the same department. I am indebted to Dr. Sang-Tae Kim for his tireless and attentive supervision; it has been an honour to work alongside such an incredibly accomplished researcher. You have established an expectation of excellence that motivates others to realize their potential. Special thanks to Martin Knyf, who helmed the laboratory at all hours, and always with a healthy dose of humour. You administered the running of my 1000+ samples, assisting me from preparation to normalization with everything in between. Thank you for squeezing me into runs even when I wasn't "priority"!

I am forever grateful to our tight-knit MRSI Crew, who have steered the research ship confidently through rough and calm waters alike. To Chris Spencer, you define equilibrium… to Nick Randazzo and Kesia Ie: your unconditional friendship, calm demeanour while crunching data together and ever-readiness for a caffeine jolt is the stuff memories are made of… and to Captain Mohammed El-Shenawy, you are the essence of leadership and thinking outside of the box. Whether scrawling back-of-the-napkin calculations for me, walking me step-by-step through your whiteboard graphics, or bonding over potential research breakthroughs, our time together has been unforgettable. Your modesty and brilliance are inimitable. Thank you all.

I am thankful for research funding support provided by the Donors of the American Chemical Society – Petroleum Research Fund (ACS-PRF), Natural Science and Engineering Research Council (NSERC) Discovery Grant, Ontario Ministry of Research and Innovation – Ontario Research Fund (MRI-ORF), Canada Foundation for Innovation – Leaders Opportunity Fund (CFI-LOF), and also McMaster University, through Dr. Sang-Tae Kim. Thanks also to my committee members, Dr. Greg Slater and Dr. Lesley Warren, for their research guidance.

Thank you to my closest friends for their support over the past few years: Kayla, Sara G, Lauren, Caylea, Tori, Ben, Kathryn, Matthieu, Steffi, Andrew, Daryl, Sara O, Shawn and Mark. Chris R – you were there for me when I needed you most. Caitlin P – you continue to guide and inspire me to become the fullest, most fulfilled person I can be. To David Rossouw, I could not have done this without you; you epitomize what it means to be a scientist, with graphic talents second to none. Finally, I would like to thank my family: Dad, Mom, Jeff, Baba, Zayda and Ben. You have been with me every step of the way, providing motivation, encouragement, advice, and home cooked meals, and believing in me even when I didn't. I'm a long-course kinda girl – I've blended each of your academic/career paths for my own but I think I'm finally there. I love you all!

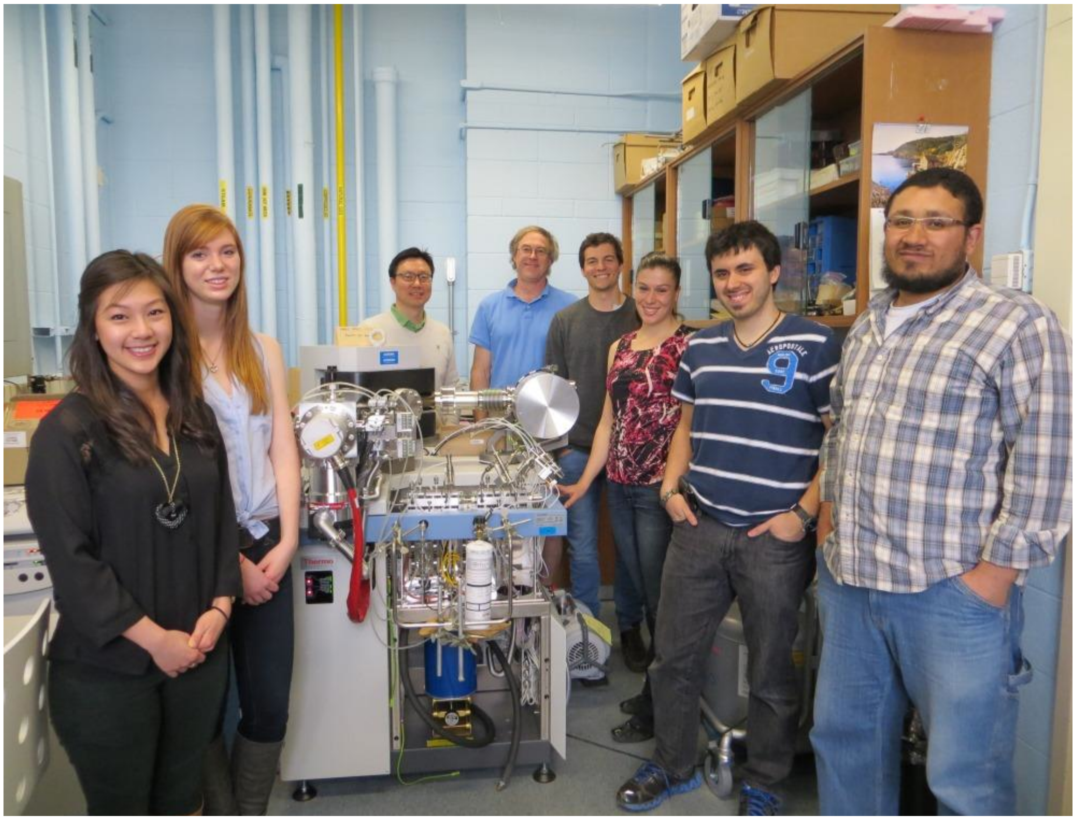

The McMaster Research Group for Stable Isotopologues (2013-2014). Pictured left to right: Kesia Ie, Victoria Tweedie, Sang-Tae Kim, Martin Knyf, Chris Spencer, Jillian Wyman, Nicolas Randazzo, Mohammed El-Shenawy.

DECLARATION OF ACADEMIC ACHIEVEMENT

Peer-reviewed publication:

Klein-Gebbinck, C., Kim, S.T., Knyf, M., and Wyman, J. (2014) A new online technique for the simultaneous measurement of the δ^{13}C value of dissolved inorganic carbon and the δ^{18}O value of water from a single solution sample using continuous-flow isotope ratio mass spectrometry. *Rapid Communications in Mass Spectrometry,* 28(5), 553-62. doi: 10.1002/rcm.6812.

Note: The above publication is not discussed in this thesis.

CONTENTS

Preliminaries

1 Introduction and Background

2 Aqueous Stable Isotope Geochemistry

3 Abiotic Carbonate Synthesis Techniques in Stable Isotope Geochemistry

6 Conclusions, Contributions and Future Prospects

LIST OF TABLES

LIST OF FIGURES

CHAPTER 1:

INTRODUCTION & BACKGROUND

1.1 Carbon dioxide and climate

Paleoclimatology relies on the identification of historical changes in climate by measuring variations in several important variables, including Earth's concentration of atmospheric carbon dioxide, average sea surface temperatures (SST), and oceanic circulation patterns. Any observed climate change can be traced back to each of these parameters, which themselves are intrinsically linked. Swedish scientist Arrhenius (1896) first quantified the greenhouse effect and postulated a resultant warming planet. Subsequent research conducted by Chamberlin (1898), who hypothesized a variety of geological processes potentially affecting atmospheric carbon dioxide concentrations [$CO_{2(atm)}$], built the foundation for future climatologists. Cenozoic (0-65 Ma) climate has varied in both direction and duration, with slow changes spanning tens of millions of years and others significantly more abrupt in nature. Although atmospheric carbon dioxide partial pressure (pCO_2) levels were higher in the Cenozoic than at present, controversy abounds regarding its accurate concentration on geological timescales. To obtain information on past climate conditions, geochemical and paleobiological indicators known as "proxies" can be used. Many climate models and proxies demonstrate consistent overlap and are in excellent agreement in their predicted CO_2 variations over the past 550 million years.

Ice core records are the most convincing evidence of globally averaged pCO_2 changes, demonstrating that climate change is tightly coupled with pCO_2. Unfortunately these robust archives only date back as far as ~ 420,000 years due to sheer length restrictions of coring (Petit et al., 1999). Hidden in the Earth are ancient environmental records however these dating clues only apply to the minutest representation of the planet's history. Instead, climatologists have turned to proxies in their quest to understand the carbon cycle spanning millions of years. Stable isotopes are intrinsic to many of these invaluable paleoproxies, as indicated by their abundant use in paleothermometry (e.g., McCrea, 1950), ocean circulation (e.g., Duplessy et al., 1984), and paleoproductivity (e.g., Meyer et al., 2011) reconstructions.

Climate change will affect the storage capacity of the oceanic carbon reservoir, the magnitude of which depends on several competing processes involving a $p\mathrm{CO}_2$ differential across the air-water interface (Fung, 2002). A warming of ocean water will be accompanied by freshening due to melting glaciers and ice caps – a combined effect that diminishes solubility, increases ocean stratification by restricting vertical mixing, and retards thermohaline circulation, overall leading to slower surface removal of surplus carbon (Fung, 2002). This accumulation of CO_2 leads to a downward shift in pH and subsequently higher dissolved CO_2 gas fractions of the carbonate system, potentially exceeding the natural buffering effect of seawater (Figure 1.1). Furthermore, rising $p\mathrm{CO}_2$ levels will inevitably alter seawater carbonate chemistry, as the surface ocean absorbs an increasing amount of this soluble gas (Klochko et al., 2009). The International Panel on Climate Change (2001) predicts that, if $p\mathrm{CO}_2$ continues to rise at the current rate, surface ocean CO_2 concentrations will triple preindustrial values by the end of this century. The ocean pH, in turn, would plummet 0.35 units, overwhelming the ocean's neutralizing capacity and undermining the function of marine ecosystems.

1.1.1 Defining pCO_2 and the role of oceans

Holding fifty times the amount of carbon present in the atmosphere, the oceans are a massive carbon sink and the primary control of $p\mathrm{CO}_2$ on short timescales (Foster, 2008). Understanding the ocean carbon cycle is crucial but complicated by the inability of CO_2 to simply dissolve in seawater. Instead, this gas reacts with water such that the total dissolved inorganic carbon (DIC) is comprised of four species: dissolved carbon dioxide ($CO_{2(aq)}$), carbonic acid (H_2CO_3), bicarbonate ion (HCO_3^-) and carbonate ion (CO_3^{2-}) (Zeebe et al., 1999). The relative distribution of these species is related to solution pH, controlled by a series of equilibrium reactions. These equilibrium constants are functions of solution temperature, pressure and salinity. The relative concentrations of these species are determined by the concentration of DIC with respect to the acid-titrating capacity of seawater, referred to as its alkalinity (Total ALK), which describes the total equivalence of ions that must be protonated in order to lower the pH of sea water to the acid dissociation constant (pK_a) of carbonic acid.

The world's oceans readily exchange CO_2 with the atmosphere; the extent to which CO_2 dissolves in water is determined by its partial pressure and the chemical reactions of the dissolved species with other solutes present. In seawater, the CO_2 system is described by several co-varying parameters, which can rarely be measured simultaneously:

1. Total dissolved inorganic carbon (DIC) and its constituent species
2. pH (NBS, total, free, or seawater scales)
3. CO_2 partial pressure ($p\mathrm{CO}_2$)

The ongoing exchange of CO_2 is mainly governed by the pCO_2 of surface waters: the gas will transfer into the ocean if atmospheric pCO_2 exceeds that of the surface waters, or transfer out of the ocean if the reverse is true. Temperature and ocean chemical composition control the pCO_2 of surface water, and these variables can be separated on the basis of their responses to glacial/interglacial climate changes. The determination of ancient ocean pH constrains pre-industrial pCO_2 and its control on atmospheric chemistry, providing a more comprehensive understanding of future implications resulting from these fluctuations. The development of an accurate proxy for paleo-pH is necessary with global warming, attributed to an industrial increase in the greenhouse gas $CO_{2(atm)}$, positioned at the forefront of environmental concerns.

Figure 1.2 details the dissolution of CO_2 in seawater by examining a series of chemical equations denoting its speciation steps. DIC is defined as the sum of $[CO_{2(aq)}]$, $[H_2CO_3]$, $[HCO_3^-]$ and $[CO_3^{2-}]$, with its species distribution pH-dependent. Modern surface waters possess a pH ~ 8.1, with HCO_3^- the most abundant carbonate species (~ 90% of DIC), followed by CO_3^{2-} (~ 10% of DIC) and $CO_{2(aq)}$ the least dominant, comprising < 1 % of DIC. At any given time, such little carbon exists within the carbonic acid species, H_2CO_3, that the concentrations of $CO_{2(aq)}$ and H_2CO_3 are usually combined as $[CO_{2(aq)}]$ (Wilson et al., 2012). The continuing addition of CO_2 to seawater is the fingerprint of anthropogenic ocean acidification; a lower pH will shift the balance between the three carbonate species, with $[CO_{2(aq)}]$ and $[HCO_3^-]$ increasing and $[CO_3^{2-}]$ decreasing (Klochko, 2009).

1.1.2 Current developed proxies for pCO_2

Recently developed climate proxies offer potential to deepen our understanding of the past carbon cycle. These proxies of past $p\mathrm{CO}_2$ enable reconstruction of $\mathrm{CO}_{2(\mathrm{atm})}$ variations over the last 15 Ma. As detailed by Henderson (2002), currently well-established isotope-derived proxies for reconstruction of the carbon cycle include those for ocean productivity ($^{231}\mathrm{Pa}/^{230}\mathrm{Th}$, U concentration), nutrient utilization (Cd/Ca, $\delta^{15}\mathrm{N}$, $\delta^{30}\mathrm{Si}$), alkalinity (Ba/Ca), pH ($\delta^{11}\mathrm{B}$), carbonate ion concentration (foraminiferal weight, Zn/Ca) and atmospheric CO_2 ($\delta^{11}\mathrm{B}$, $\delta^{13}\mathrm{C}$). Other developing climate proxies include bulk inorganic/organic carbon content in marine sediments, air bubbles trapped in ice cores, paleosols, boron isotopes in planktic foraminifera, alkenone and lipid biomarkers derived from haptophyte algae, and fossils from plants/leaves.

While $p\mathrm{CO}_2$ estimates are consistent across numerous approaches, many of these geochemical proxies are associated with relatively large uncertainties rendering it difficult to accurately constrain the changes occurring over time (Sigman and Boyle, 2000; Royer et al., 2001). Current gaps in knowledge of the paleo-pCO_2 record must be filled in order to provide a complete history of global climate and atmospheric carbon dioxide levels, and establish a predictable relationship between the two variables.

1.2 Calcium carbonate polymorphs

Calcium carbonate minerals occur widely in nature and comprise ~ 10 % of all sediments in the marine environment, thus are intrinsic to many biological functions and processes. Calcium carbonate primarily precipitates as calcite and aragonite, while vaterite is metastable under ambient conditions (Berner, 1975; Paquette and Reeder, 1990). Calcium carbonates are sensitive indicators of the global marine environment, serving as sedimentological records of both long-term and abrupt changes in the exogenic carbon cycle.

The three calcium carbonate polymorphs share the same chemistry and are thus characterized by their contrasting crystal structures (Figure 1.3). This thesis focuses on abiogenic calcite in particular: Figure 1.4 provides a view of the (001) calcite surface plane. These three polymorphs can be distinguished by their crystal Bravais lattices – orthorhombic (aragonite), rhombohedral (calcite) lattice, and hexagonal (vaterite). The structural details of vaterite are controversial but there is general agreement that the carbonate planes are parallel to the c axis, as opposed to perpendicular as observed in calcite and aragonite (Wang and Becker, 2009). At STP (room temperature and under normal atmospheric conditions), calcite is the most stable phase while the other two are metastable polymorphs which readily transform into the stable calcite phase (Figure 1.5) (Berner, 1975; Morse et al., 1997; Paquette and Reeder, 1990; Allen and Hönisch, 2012). Aragonite will crystallize preferentially under certain formation conditions; it exists as a stable mineral at higher pressures but not at higher temperatures. To avoid spontaneously converting to calcite, the pressure must increase to maintain stability with increasing temperature. Winland (1969) argues that mineral stability must be assessed relative to given pressure conditions and temperature conditions as well as associative substances; when chemical equilibrium with the environment is considered, aragonite has the lowest free energy of formation and is therefore the thermodynamically stable phase in shallow marine environments. A number of ions present in seawater can be substituted into the carbonate crystal structures, rendering it a questionable assumption that both calcite and aragonite will attain equilibrium with seawater given their differing lattice properties. The composition of each polymorph, with respect to its chemical equilibrium status with seawater, must therefore be known in order to identify the stable form of $CaCO_3$ in these conditions.

The transition between the calcite and aragonite precipitation phase-fields is determined by both the supersaturation state and the Mg:Ca of the solution. The degree of supersaturation (SI), with respect to calcium carbonate, is defined as: $S=[Ca^{2+}][CO_3^{2-}]/K_{sp}$ which represent the activities of calcium and carbonate ions in the solution, and the thermodynamic solubility product of calcite or aragonite, respectively. Heterogeneous nucleation can occur at lesser supersaturation than homogeneous nucleation, with the presence of different seed crystals having the potential to lower the activation energy barrier (Winland, 1969). The surface ocean is supersaturated with respect to $CaCO_3$, with the predominant mineralogy dictated by subtle variations in the aqueous magnesium-to-calcium (Mg:Ca) ion distribution as well as the biology of the secreting organism. Normal seawater has a Mg:Ca molar ratio of ~5.5 (Winland, 1969). According to the Doerner-Hoskins relation describing partitioning coefficients, calcite equilibrated with seawater at earth surface conditions should contain about 10 mole percent $MgCO_3$ (Winland, 1969).

Calcite growth requires a combination of high supersaturation of calcium carbonate and a Mg:Ca ratio much like modern seawater (compared to the lower ratio observed in fresh water); however, calcite will not precipitate above a certain ratio threshold (Morse et al., 1997). This ratio displays a distinct temperature dependence: aragonite will preferentially precipitate from seawater when Mg:Ca exceeds 4:1 at 10 °C and 1:1 at 25 °C (Morse et al., 1997). In natural systems, calcite typically incorporates magnesium into its lattice and can include over 20 mole percent $MgCO_3$ (Reddy and Wang, 1980; Paquette and Reeder, 1990; Morse et al., 1997). The synthesis of aragonite and calcite yields a very similar approach with the primary difference necessarily reflected by the Mg:Ca used to create the solution (Berner, 1975). Even subtle changes to the ratio will alter oceanic global carbonate deposition.

Earth has witnessed several cycles of aragonite and calcite seas (Figure 1.6), which themselves are indicative of seafloor spreading rates: more rapid spreading is associated with higher sea level and hydrothermal activity pumping calcium into the ocean while withdrawing magnesium through bedrock interactions, with "low-Mg calcite" primarily deposited (Wilkinson and Algeo, 1989). Oceanic calcium concentrations are lower, and magnesium concentrations higher, during periods of slower sea floor spreading coinciding with lower sea levels; these conditions favour aragonite and "high-Mg calcite" deposition (Wilkinson and Algeo, 1989). For context, early Paleozoic and the middle- to late-Mesozoic oceans were calcitic in nature, while aragonite characterized the early Mesozoic and Cenozoic seas (Lowenstein et al., 2001; Palmer amd Wilson, 2004). Based on shallow marine carbonates documenting secular oscillations in carbonate mineralogy, the Mg:Ca ratio has fluctuated between 1 and 5 over the past 560 million years (Wilkinson and Algeo, 1989). Aragonitic seas occur during periods of high Mg:Ca ~ 5 (from ~ 340 to ~ 170 Ma and the modern ocean) whereas calcitic seas are marked by low Mg:Ca ~ 1 (~ 550-340 Ma and ~ 170-40 Ma) (Stanley and Hardie, 1998).

The incorporation of magnesium into the calcite lattice has also been the subject of recent investigation. Its incorporation mechanism and subsequent influence on mineral properties have undergone intensive research to resolve questions surrounding its equilibrium status. Many studies indicate that magnesium in fact inhibits calcite nucleation and growth (e.g., Reddy and Wang, 1980; Mucci and Morse, 1984) due to the higher activation energy (~ 20%) required for Mg^{2+} dehydration (relative to Ca^{2+}) on the surface of a growing crystal, which functions as the rate limiting step during carbonate precipitation from solution (Nancollas and Purdie, 1945). In contrast, the larger cation sites present in the aragonite crystal structure can more easily accommodate magnesium ion substitution.

Both experimental studies (e.g., Tarutani et al., 1969; Kim et al., 2006) and natural sample data (e.g., Grossman and Ku, 1986; Muth-Bohm et al., 2000) indicate that aragonite has a slightly greater affinity for oxygen incorporation than calcite. The sign and magnitude of the aragonite-calcite enrichment of ~ 0.6 ‰ (Tarutani et al., 1969) to ~ 0.8 ‰ (Kim et al., 2006) at 25 °C is now well accepted in the literature.

Though rare in nature, assessing the chemical properties and behaviour of vaterite is essential to fully understand isotopic fractionation in carbonates. This has proven to be a difficult task due to the mineral's instability in aqueous solutions. Kim and O'Neil (1997) synthesized vaterite crystals and found them to be isotopically very light, in significant disequilibrium with the water, and controlled by varying diffusion rates of the different isotopic species of CO_2. In their experimental investigation, vaterite always formed with calcite in a saturated calcium bicarbonate solution, however calcite was the sole precipitate in solutions containing relatively high concentrations of calcium chloride and sodium bicarbonate; hybrid solutions produced a mixture of the two minerals. The amount of precipitated vaterite was inversely proportional to the precipitation rate.

To change the polymorph precipitating from seawater, the saturation state must be altered such that seawater is undersaturated with the more soluble polymorph (aragonite) but is supersaturated with a more stable polymorph (calcite). The $p\mathrm{CO}_2$ must lie between 2600 to 3500 μatm in order for seawater (S = 35, 25 °C, 1 atm) to be undersaturated with aragonite but supersaturated with calcite. Considering the current $p\mathrm{CO}_2$ is about 360 μatm, an order of magnitude change is necessary to produce a change from modern aragonitic seas to calcitic conditions. Other factors influencing saturation state, such as alkalinity, may reduce the degree of this requisite change.

1.3 Applications to Earth systems

Abiotic studies provide an important foundation upon which applied and/or biogenic research can build and accurately interpret their observations. Both types are integral to the formation of sound paleoclimate proxies. Laboratory studies, in which experiments are conducted under controlled, tightly monitored conditions, allow the variable of interest to be examined exclusively; this understanding can then be translated to living Earth systems, characterized by a dynamic and ever-evolving environment. While difficult to ascertain the role of each parameter due to multifactorial influences in the "real world", accruing relevant literature for both abiotic and biogenic studies is invaluable to the eventual integration of knowledge.

In this thesis, calcite was synthesized using homogeneous nucleation in an effort to isolate isotope fractionation behaviour. However, in nature, carbonate growth typically proceeds under heterogeneous conditions as crystals nucleate on an already-present substrate. Once the nature of isotope fractionation in select calcium carbonate minerals has been better established, heterogeneous nucleation offers a number of advantages to researchers (which will be further explored in Chapter 3) including a more accurate representation of crystal growth in Earth systems.

Similarly, the differing chemical and physical properties among calcite and aragonite carbonate polymorphs has several implications for evolving oceanic conditions with climate change. The modern ocean is predominantly aragonitic and the primary composition of corals, whereas foraminifera, chalk and coccoliths are calcitic in nature (Milliman, 1993). Ocean acidification is of prominent environmental concern; as per Henry's Law, heightened seawater dissolution of carbon dioxide will reduce the output of CO_3^{2-}, thereby reducing the ocean's carbonate state of saturation. As a result, the saturation horizon will rise, leaving less room for precipitation of calcium carbonate. Aragonite precipitation is favoured under these circumstances due to its increased solubility product and ubiquitous presence in warm, shallow waters. Subsequent reduction of photosynthetic coccolithic and foraminifera products possesses dire potential to disrupt the marine ecosystem.

Carefully calibrated laboratory studies, developed to assess the behaviour of these calcium carbonate polymorphs under a variety of experimental circumstances, is a pre-requisite to their examination in Earth systems. As a result of intricate distinctions in their crystal lattice, calcite and aragonite possess differing chemical and physical properties, which must first be understood under controlled conditions prior to disentangling their effects when manifested in nature. The delicate seawater calcium-to-magnesium ratio has fluctuated widely in the past and will continue to shift with Earth's changing climate. Thus, a fundamental understanding of key, influential factors is integral to forecasting alterations to the marine ecosystem balance related to climate change and the development of appropriate mitigation strategies.

1.4 Conclusions

Measured variations in Earth's concentration of atmospheric carbon dioxide form the foundation of paleoclimate research, which is integral to the field of climatology. It is only through the establishment of past climatic shifts that future climate change can be accurately predicted. The dynamic, ever-evolving Earth has undergone massive climate changes throughout its history; understanding the causes and linkages is essential to prioritize the factors driving these shifts and position them in an appropriate large-scale context. Figure 1.7 illustrates the purpose of this research from a progressively broader research perspective.

1.5 Thesis structure

Chapter 1 presented a big-picture link between this thesis research and the field of paleoclimatology, specifically pertaining to the study of aqueous stable isotope geochemistry. A synthesis of previous research completed on oxygen isotope fractionation between calcium carbonate, and the solution from which it grew ($\alpha_{\mathrm{CaCO3\text{-}H2O}}$), will be discussed in Chapter 2. Additionally, the boron isotope paleo-pH proxy is presented in great detail, linking the relevance of this research to its ongoing refinement. A brief introduction to mass spectrometry analysis procedure and primary calibration materials will be provided as necessary background information.

Chapters 3, 4 and 5 are written in "sandwich" format. Chapter 3 takes the form of a review article, discussing and assessing various abiogenic calcium carbonate synthesis methodologies. An outline of these approaches, and their corresponding rationale/objectives, will aid in the understanding of subsequent material presented in this thesis. Chapter 4 acts as an important stepping stone in the refinement of the boron isotope paleo-pH proxy, comparing the boron isotope composition of inorganic calcium carbonate samples with the calculated boron isotope composition of borate in order to evaluate the applicability of the proxy across calcite and aragonite polymorphs. Chapter 5 explores oxygen isotope effects in synthesized calcite crystals, assessing trends and discrepancies in oxygen isotope fractionation behavior across three different growth temperature values, three distinct stable pH conditions and a variety of precipitation rates.

The conclusions of this thesis are presented in Chapter 6. This will include a summary of the research conducted and the candidate’s specific contributions to research articles involving multiple authors. The applicability and relevance of this body of research to geochemistry will be discussed, in addition to suggestions for future work, aimed at the new graduate student who wishes to continue in the field.

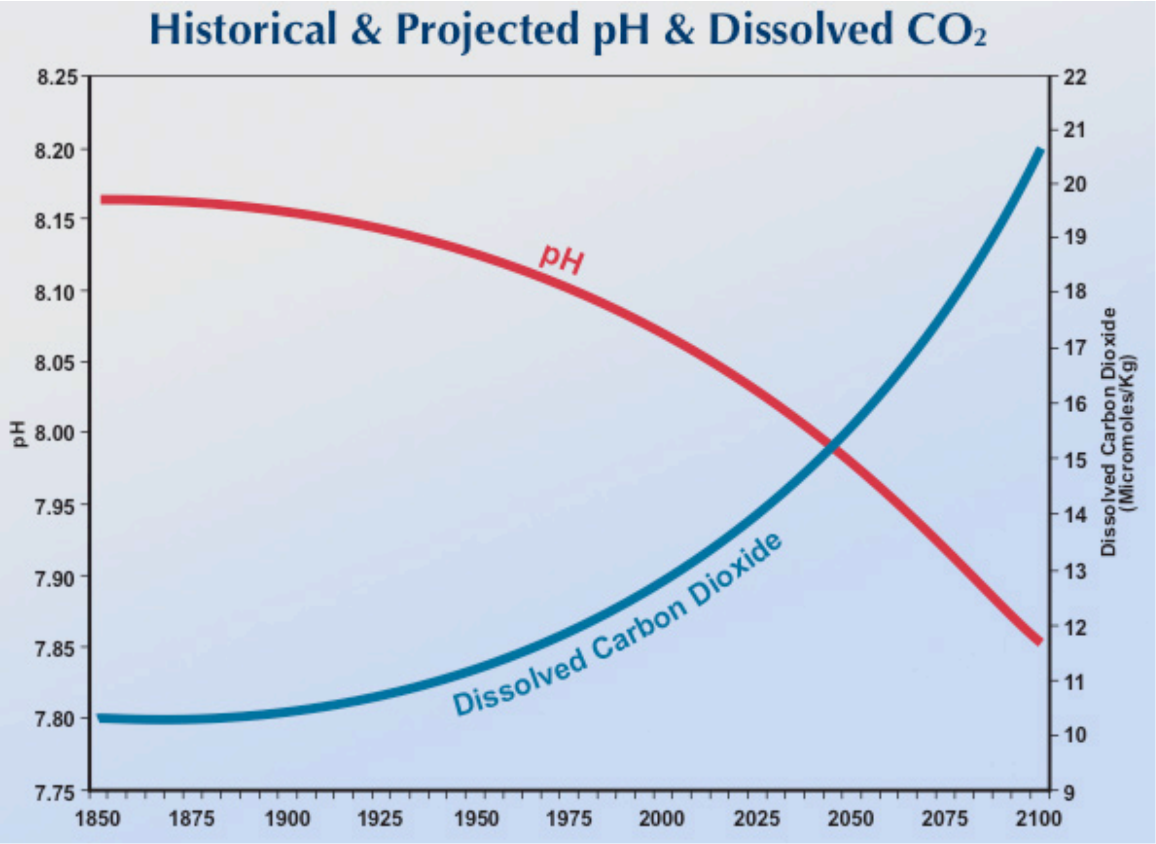

Figure 1.1: Predicted trend between dissolved carbon dioxide concentration and pH. (Feely et al., 2004)

An increase in the oceanic carbon dioxide concentration leads to more acidic conditions (marked by a lower pH), with potentially devastating effects on marine ecosystems.

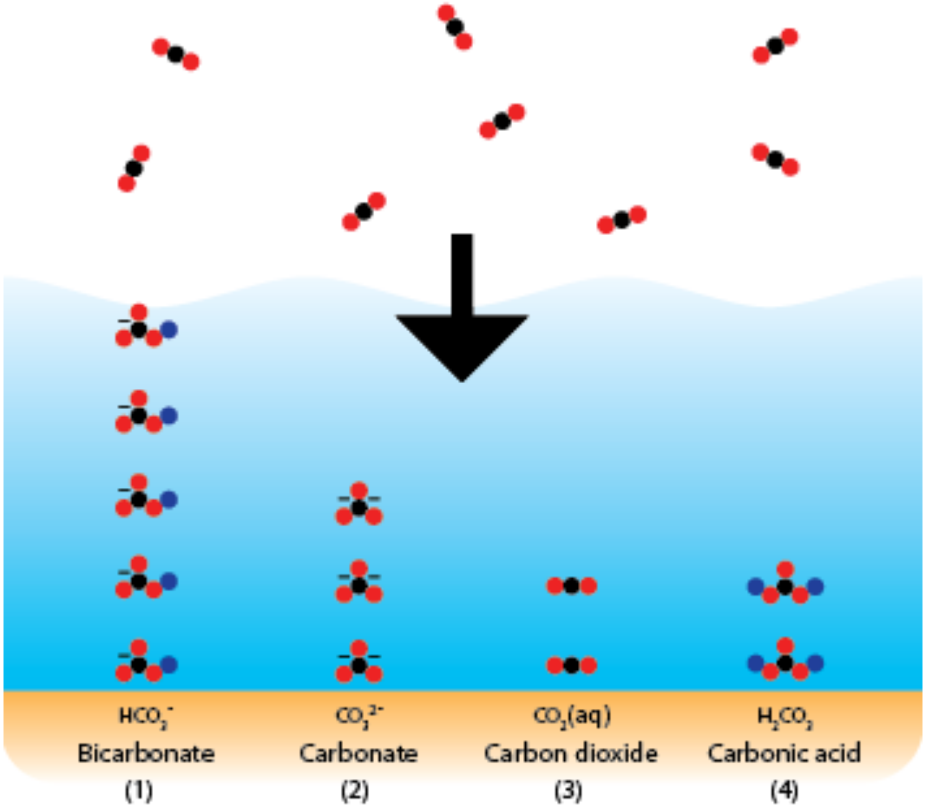

(1) $CO_{2(aq)} + H_2O \leftrightarrow H_2CO_3$ (2) $H_2CO_3 \leftrightarrow HCO_3^- + H^+$

(3) $HCO_3^- \leftrightarrow CO_3^{2-} + H^+$ (4) $CO_{2(aq)} + CO_3^{2-} + H_2O \rightarrow 2HCO_3^-$

Figure 1.2: Schematic illustration of oceanic carbonate system equilibria.

Upon reacting with water, carbon dioxide first converts to aqueous carbon dioxide ($CO_{2(aq)}$) and carbonic acid (H_2CO_3, Eq. 1). Carbonic acid rapidly dissociates and generates bicarbonate ions (HCO_3^-, Eq. 2), which then dissociate into carbonate ions (CO_3^{2-}, Eq. 3). The reactions driving Equations 1 and 2 also produce protons (H^+), which reduce the pH of the solution (pH is the negative logarithm of the proton concentration or activity, $-\log_{10}[H^+]$). It should be noted that the dissolution of CO_2 in seawater does not result in full dissociation into carbonate ions; the number of hydrogen ions produced, and the subsequent drop in pH, is reduced by the natural capacity of seawater to buffer against pH variations (Eq. 4). In this reaction, CO_2 is neutralized upon reacting with CO_3^{2-} to produce HCO_3^-. The HCO_3^- product of Eq. 4 circles back through the partial dissociation represented by Eq. 3, releasing protons and lowering the pH ("ocean acidification"), but this drop is far reduced compared to that experienced by an un-buffered system.

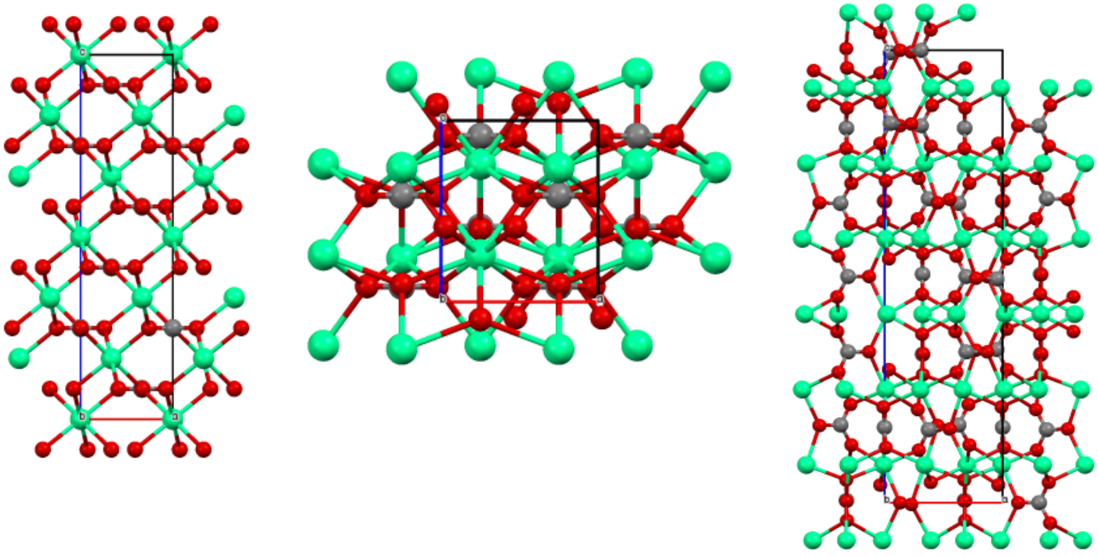

Calcite

Aragonite

Vaterite

Figure 1.3: A comparison of the polymorphs of calcium carbonate.

From left to right: Unit cells for calcite, aragonite and vaterite. Calcite displays trigonal crystal system, aragonite displays orthorhombic and vaterite belongs to the hexagonal crystal system. Calcite and vaterite exhibit sixfold coordination of oxygen (red) atoms around the central calcium (green) atoms, while aragonite exhibits ninefold coordination. Vaterite octahedra are highly distorted relative to those formed in calcite. Additionally, calcite and vaterite display an elongated c axis versus aragonite's shortened axis. Thus, calcite and vaterite carbonate groups are widely spaced (4.05 Å and 4.01 Å, respectively) whereas aragonite possesses closer carbonate spacing (2.9 Å). *Constructed in Mercury CSD 2.0*.

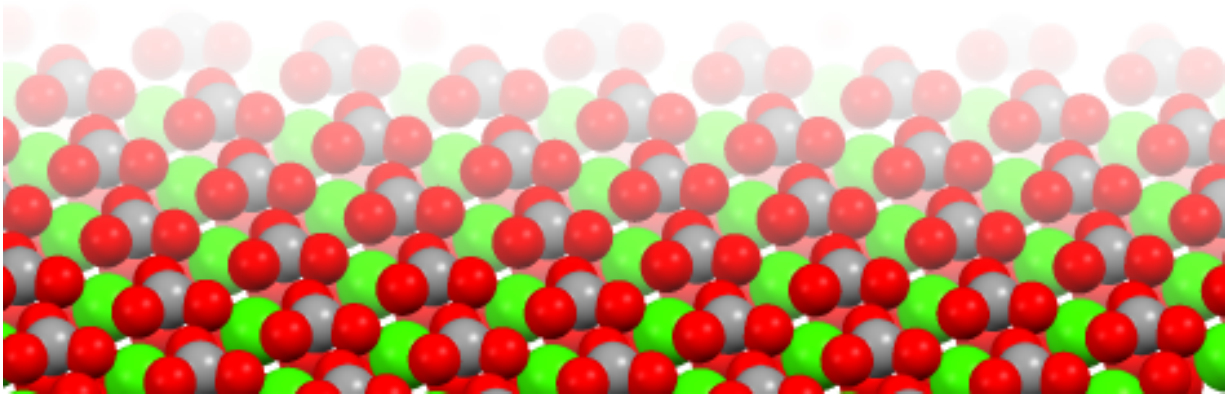

Figure 1.4: The (001) calcite surface.

An atomistic view of an atomically flat (001) surface of calcite, displaying in-plane three-fold coordination of the oxygen (red) about the carbon (grey) atom. *Constructed in Mercury CSD 2.0*.

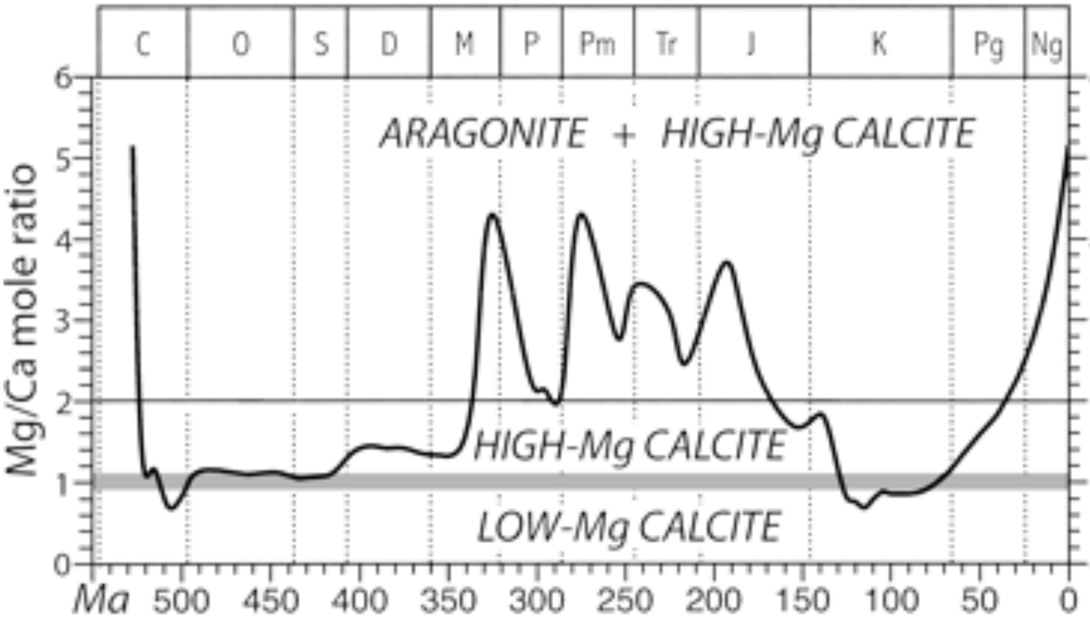

Figure 1.5: Secular oscillations in the Mg:Ca ratio of seawater over the past 500 Ma. (Stanley, 2002)

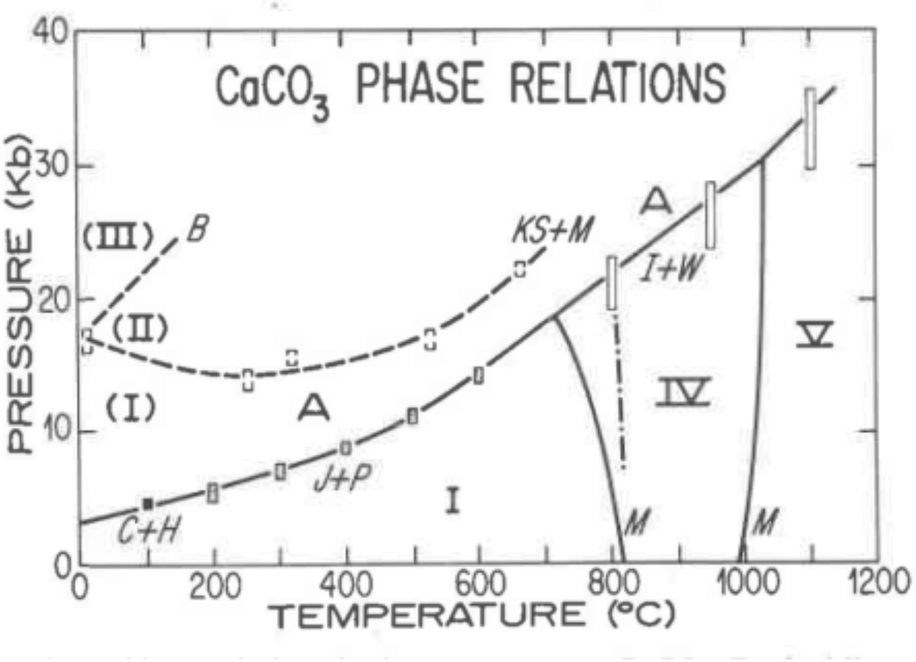

Figure 1.6: Temperature-pressure phase diagram of calcium carbonate (Carlson, 1980).

At room temperature and pressure, calcite is the stable mineral form of calcium carbonate. Aragonite becomes more stable than calcite only at high pressure [approximately 3500 bars (350 MPa) at 25°C and 7000 bars (700 MPa) at 300°C], consistent with its greater density.

Dashed lines represent metastable equilibria. "A" denotes aragonite while "I" through "V" represent calcite polymorphs. Data from Crawford and Hoersch, 1972 (C+H); Johannes and Puhan, l971 (J+P); Irving and Wyllie, 1973 (I+W); Mirwald, 1976 (M); Kondo et al., 1972 (KS+M); Bridgman, 1939 (B).

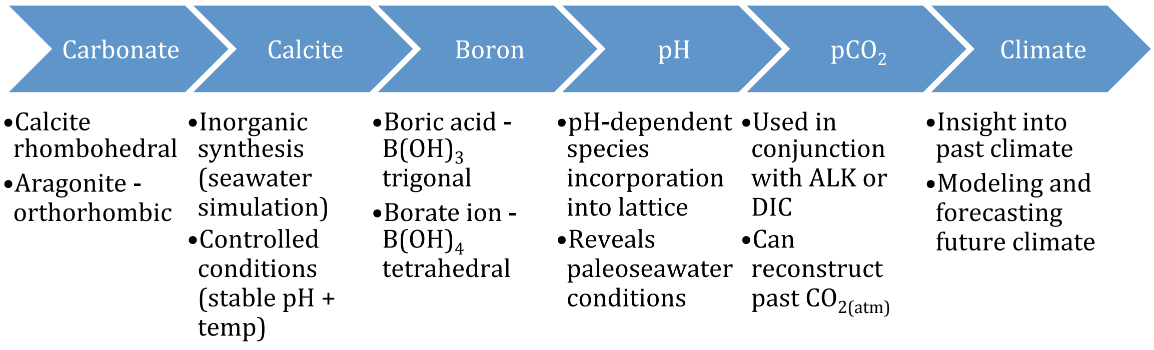

Figure 1.7: Fundamental research objectives.

A "big-picture" flowchart describing the aims of this boron study, from the narrow focus on marine carbonates expanding to their role in reconstructing past climate conditions.

References

Arrhenius, S. On the Influence of Carbonic Acid in the Air upon the Temperature of the Ground. *Philosophical Magazine and Journal of Science, 5(41),* 237-276.

Allen, K. A., & Hönisch, B. (2012). The planktic foraminiferal B/Ca proxy for seawater carbonate chemistry: A critical evaluation. *Earth and Planetary Science Letters*, *345-348*, 203–211. doi:10.1016/j.epsl.2012.06.012

Berner, R. A. (1975). The Role of Magnesium in the Crystal Growth of Calcite and Aragonite From Sea Water. *Geochimica et Cosmochimica Acta*, *39*, 489–504.

Carlson, W. D. (1980). The calcite-araqonite equilibrinm: effects of Sr substitution aid anion brientational disorder. *American Mineralogist,* 65, 1252-1262.

Chacko, T., & Deines, P. (2008). Theoretical calculation of oxygen isotope fractionation factors in carbonate systems. *Geochimica et Cosmochimica Acta*, *72*(15), 3642–3660. doi:10.1016/j.gca.2008.06.001

Chamberlin, T. C. (1898). An attempt to frame a working hypothesis of the cause of glacial periods on an atmospheric basis. *J. Geol.,* 7, 545-584.

Duplessy, J., Shackleton, N. J., Matthewsa, R. K., Prell, W., Ruddiman, W. F., Hendy, C. H., … Yvette, G. (1984). 13C Record of Benthic Foraminifera in the Last Interglacial Ocean : Implications for the Carbon Cycle and the Global Deep Water Circulation. *Quaternary Research*, *21*, 225–243.

Feely, R. A., Sabine, C. L., Lee, K., Berelson, W., Kleypas, J., Fabry, V. J., and Millero, F. J. (2004). Impact of anthropogenic CO_2 on the $CaCO_3$ system in the oceans. *Science,* 305, 362-366.

Foster, G. L. (2008). Seawater pH, pCO2 and [CO2−3] variations in the Caribbean Sea over the last 130 kyr: A boron isotope and B/Ca study of planktic foraminifera. *Earth and Planetary Science Letters*, *271*(1-4), 254–266. doi:10.1016/j.epsl.2008.04.015

Fung, B. M. (2002). 13C NMR studies of liquid crystals. *Progress in Nuclear Magnetic Resonance Spectroscopy*, *41*(3-4), 171–186. doi:10.1016/S0079-6565(02)00048-1

Grossman, E., & Ku, T. (1986). Oxygen and carbon isotope fractionation in biogenic aragonite: Temperature effects. *Chemical Geology*, *59*, 59–74.

Henderson, G. (2002). New oceanic proxies for paleoclimate. *Earth and Planetary Science Letters*, 203, 1-13.

Kim, S-T., Hillaire-Marcel, C., & Mucci, A. (2006). Mechanisms of equilibrium and kinetic oxygen isotope effects in synthetic aragonite at 25°C. *Geochimica et Cosmochimica Acta*, *70*(23), 5790–5801. doi:10.1016/j.gca.2006.08.003

Kim, S-T., & O'Neil, J. (1997). Equilibrium and nonequilibrium oxygen isotope effects in synthetic carbonates. *Geochimica et Cosmochimica Acta*, *61*(16), 3461–3475.

Klochko, K., Cody, G. D., Tossell, J. A., Dera, P., & Kaufman, A. J. (2009). Re-evaluating boron speciation in biogenic calcite and aragonite using 11B MAS NMR. *Geochimica et Cosmochimica Acta*, *73*(7), 1890–1900. doi:10.1016/j.gca.2009.01.002

Lowenstein, T. K., Timofeeff, M. N., Brennan, S. T., Hardie, L. A., & Demicco, R. V. (2001). Oscillations in Phanerozoic Seawater Chemistry: Evidence From Fluid Inclusions. *Science*, *294*, 1086–1089.

McCrea, J. M. (1950). On the isotopic chemistry of carbonates and a paleotemperature scale. *Journal of Chemical Physics*, *18*(6), 849–857.

Mercury CSD 2.0 - new features for the visualization and investigation of crystal structures, C. F. Macrae, I. J. Bruno, J. A. Chisholm, P. R. Edgington, P. McCabe, E. Pidcock, L. Rodriguez- Monge, R. Taylor, J. van de Streek and P. A. Wood. (2008). *J. Appl. Cryst.*, 41, 466-470.

Meyer, K., Yu, M., Jost, A., Kelley, B. & Payne, J. (2011) δ13C evidence that high primary productivity delayed recovery from end-Permian mass extinction. *Earth Planet. Sci. Lett.,* 302, 378-384.

Milliman, J. D. (1993) Production and accumulation of calcium carbonate in the ocean: Budget of a nonsteady state. *Global Biogeochemical Cycles*, *7*(4), 927-957.

Morse, J. W., Wang, Q., & Tsio, M. Y. (1997). Influences of temperature and Mg : Ca ratio on CaCO 3 precipitates from seawater. *Geology*, *25*(1), 85–87. doi:10.1130/0091-7613(1997)025<0085

Mucci, A., & Morse, J. W. (1984). The solubility of calcite in seawater solutions of various magnesium concentration , Zi = 0 .697 m at 25 °C and one atmosphere total pressure. *Geochimica et Cosmochimica Acta*, *48*(1982), 815–822.

Muth-Bohm, J., Becker, A., & Faisal, F. (2000). Suppressed molecular ionization for a class of diatomics in intense femtosecond laser fields. *Physical review letters*, *85*(11), 2280–3. Retrieved from http://www.ncbi.nlm.nih.gov/pubmed/10977991

Nancollas, B. G. H., & Purdie, N. (1945). The Kinetics of Crystal Growth. *Quarterly Reviews*, 1–20.

Palmer, T., & Wilson, M. (2004). Calcite precipitation and dissolution of biogenic aragonite in shallow Ordovician calcite seas. *Lethaia*, *37*(4), 417–427. doi:10.1080/00241160410002135

Paquette, J., & Reeder, R. J. (1990). New Type of Compositional Zoning in Calcite: Insights Into Crystal Growth Mechanisms. *Geology*, *18*, 1244–1247.

Petit, J. R., Raynaud, D., Basile, I., Chappellaz, J., Ritz, C., Delmotte, M., … Pe, L. (1999). Climate and atmospheric history of the past 420,000 years from the Vostok ice core, Antarctica. *Nature*, *399*, 429–436.

Reddy, M. M., & Wang, K. K. (1980). Crystallization of calcium carbonate in the presence of metal ions. *Journal of Crystal Growth*, *50*(2), 470–480. doi:10.1016/0022-0248(80)90095-0

Royer, D. L., Wing, S. L., Beerling, D. J., Jolley, D. W., Koch, P. L., Hickey, L. J., & Berner, R. a. (2001). Paleobotanical evidence for near present-day levels of atmospheric CO2 during part of the tertiary. *Science (New York, N.Y.)*, *292*(5525), 2310–3. doi:10.1126/science.292.5525.2310

Sigman, D. M., & Boyle, E. A. (2000). Glacial/Interglacial Variations in Atmospheric Carbon Dioxide. *Nature*, *407*(October), 859–869.

Stanley, S. M., & Hardie, L. A. (1998). Secular oscillations in the carbonate mineralogy of reef-building and sediment-producing organisms driven by tectonically forced shifts in seawater chemistry. *Palaeogeography, Palaeoclimatology, Palaeoecology*, *144*, 3–19.

Stanley, S. (2002). Low-magnesium calcite produced by coralline algae in seawater of Late Cretaceous composition. *PNAS*, 99(24), 15323-15326.

Tarutani, T., Clayton, R. N., & Mayeda, T. K. (1969). The effect of polymorphism and magnesium substitution on oxygen isotope fractionation between calcium carbonate and water. *Geochimica et Cosmochimica Acta*, *33*, 987–996.

Urey, H. C. (1947). The Thermodynamic Properties of Isotopic Substances. *Journal of the Chemical Society,* 562-581.

Wang, J. & Becker, U. (2009). Structure and carbonate orientation of vaterite (CaCO3). *American Mineralogist*, 94, 380-386.

Wilkinson, B. H., & Algeo, T. J. (1989). Sedimentary Carbonate Record of Calcium-Magnesium Cycling. *American Journal of Science*, *289*, 1158–1194.

Wilson, J. D., Barker, S., & Ridgwell, A. (2012). Assessment of the spatial variability in particulate organic matter and mineral sinking fluxes in the ocean interior: Implications for the ballast hypothesis. *Global Biogeochemical Cycles*, *26*(4), 15p. doi:10.1029/2012GB004398

Winland, H. D. (1969). Stability of Calcium Carbonate Polymorphs in Warm, Shallow Seawater. *SEPM Journal of Sedimentary Research*, *Vol. 39*(4). doi:10.1306/74D71E92-2B21-11D7-8648000102C1865D

Wolf-Gladrow, D. A., Zeebe, R. E., Klaas, C., Körtzinger, A., & Dickson, A. G. (2007). Total alkalinity: The explicit conservative expression and its application to biogeochemical processes. *Marine Chemistry*, *106*(1-2), 287–300. doi:10.1016/j.marchem.2007.01.006

Zeebe, R. E., Wolf-Gladrow, D. A., & Jansen, H. (1999). On the time required to establish chemical and isotopic equilibrium in the carbon dioxide system in seawater. *Marine Chemistry*, *65*(3-4), 135–153. doi:10.1016/S0304-4203(98)00092

Zhou, G-T., & Zheng, Y.-F. (2003). An experimental study of oxygen isotope fractionation between inorganically precipitated aragonite and water at low temperatures. *Geochimica et Cosmochimica Acta*, *67*(3), 387–399.

CHAPTER 2:

AQUEOUS STABLE ISOTOPE GEOCHEMISTRY

2.1 Introduction to aqueous geochemistry

The isotopic composition of a mineral is strongly dependent on the nature of its chemical bonds, principally determined by its electronic structure. However, certain physicochemical differences arise due to an overall change in mass number as a result of quantum mechanical effects. For example, one additional neutron can significantly slow a reaction and thereby alter the resultant infrared spectrum emission. Isotope fractionation occurs when two phases of the same substance possess differing isotope ratios, which are either equilibrium- or kinetics-driven processes.

At equilibrium, the stable isotope fractionation factor (α) is defined as the ratio of any two isotopes in a given chemical compound, divided by the ratio of any two isotopes in a different chemical compound. That is, $\alpha_{A\text{-}B}=R_A/R_{B.}$ Isotope geochemistry reports isotopic composition of compounds on a relative (rather than absolute) scale using delta notation, where $\delta = \left(\frac{R_{Sa}}{R_{st}} - 1\right) * 1000$ with both Sample (Sa) and Standard (St) measured in the laboratory by conventional mass spectrometry. Kinetic isotope effects, which occur under unidirectional and irreversible processes, are also responsible for fractionation. Quantifying these effects provides insight on reaction pathways and mass dependent relationships. Mass spectrometers are complex pieces of equipment used to measure isotopic abundances by separating charged atoms based on their charge and behaviour in magnetic and/or electric fields. An online continuous-flow isotope ratio mass spectrometer (CF-IRMS), used in the McMaster University Research Group for Stable Isotopologues (MRSI) laboratory, is depicted in Figure 2.1.

The use of isotopes as a paleoclimate tool was first proposed in 1947 by Harold Urey, who described the interphase partitioning of two stable isotopes of an element as a "special case" in which a negligible change in pressure offers a considerable advantage over other established geothermometers. In order to apply this thermometer, isotopic equilibrium must be achieved, which requires products to be in chemical equilibrium. Thus, minerals in a rock determined to be in isotope equilibrium presents strong evidence that the rock is in chemical equilibrium. Stable isotopes continue to gain popularity in geochemistry studies, demonstrating great potential for reconstructing past climate and allowing a longitudinal examination of natural system dynamics. Initiated by Urey's (1947) groundbreaking paper, the application of stable isotopes to carbonate studies was subsequently explored by Emiliani (1955), Epstein et al. (1951, 1953) and McCrea (1950). In the nineteen-eighties, combining this newfound knowledge with ongoing polar ice-core research, marine carbonates firmly established themselves as an invaluable resource for paleoclimate reconstructions. Stable isotopes have been progressively incorporated into proxies, which are used to infer past climatic changes in instances where variables cannot be directly measured for the past. However, these variables affect the chemistry and biology of the marine sedimentary record in a measurable way and are thus representative of the past environment by "proxy". The following discussion aims to highlight the application of oxygen and boron stable isotopes to marine carbonate studies and evaluate their potential role in proxy development and contribution to further research.

2.2 Oxygen isotope studies

The most abundant element on Earth, oxygen occurs in compounds of all phases, many of which are thermally stable over a broad spectrum of temperatures. Due to the large mass difference and high abundance of the light isotope (^{16}O ~ 99.757%, ^{17}O ~ 0.038%, ^{18}O ~ 0.205%), the $^{18}O/^{16}O$ is typically determined to be 1:500 in natural samples. Calcium carbonates are intrinsic to paleoclimatic and paleoenvironmental reconstructions by means of oxygen isotope analysis. Since Urey (1947) laid out its theoretical basis, an abundance of data has accumulated for oxygen isotope fractionation in carbonate-water ($CaCO_3$-H_2O) systems. However, these theoretical calculations are not without controversy, and empirical measurements as well as natural observations of oxygen isotope fractionation factors have also undergone considerable scrutiny. An explicit differentiation of the three terms is as follows: "theoretical" refers to statistical mechanical calculations that have not been measured in the lab or observed *in situ*, while "empirical" describes natural setting circumstances or a real-world environment, in contrast to "experimental" data which indicates laboratory-generated information under controlled conditions.

The study of marine carbonates has recently been popularized due to their importance in understanding oxygen isotope fractionation in the CO_2-H_2O system. Therefore, determining the extent to which the $CaCO_3$-CO_2-H_2O system controls stable isotope fractionation is essential to supplement the ongoing archive of Earth's climate history. While the $\delta^{18}O$ value of carbonates are commonly used as paleothermometry tools (e.g., Epstein et al., 1953; Broecker, 1986; Lea et al., 2000), comparisons of experimental results versus natural carbonate samples indicate that chemical (isotopic) equilibrium is not always achieved in natural settings, complicating their role in temperature reconstructions (Gabitov et al., 2012). Thermodynamically, the state of equilibrium (thus marking the onset of precipitation) is unaffected by auxiliary parameters such as precipitation rate and pH variance (e.g., Kim et al., 2006). The oxygen isotopic fractionation between carbonate and water ($1000\ln\alpha_{\mathrm{CaCO3\text{-}H2O}}$) has also been used to estimate carbonate precipitation temperature (McCrea, 1950; Epstein et al., 1953; Tarutani et al., 1969; Kim and O'Neil, 1997). Such fractionation factors are typically first calculated theoretically using laboratory-determined vibrational frequencies, or naturally-derived measurements from systems in geochemical equilibrium. Doubt has been cast upon the validity of laboratory calibrations due to the difficulty of precipitating calcite in oxygen isotope equilibrium, which itself is promoted by slow growth rates according to Tarutani et al. (1969) and Kim and O'Neil (1997).

Experimentally determined oxygen isotope fractionation factors for the aqueous CO_2-H_2O system, specific to individual carbonate species differing at room temperature, have been reported by Usdowski and Hoefs (1990), Beck et al. (2005) and Zeebe (2007). Derivation of oxygen isotope temperatures requires quantification of the pH-dependence of the oxygen isotope compositions in the carbonate-water system (Hoefs, 2009). Oxygen isotopes are typically measured using an isotope ratio mass spectrometer, with $\delta^{18}O$ values normalized to the recommended values for the international reference materials NBS-19, SMOW, and SLAP. Carbonate $\delta^{18}O$ values are typically calculated using a CO_2–H_2O oxygen isotopic fractionation factor of 1.04120 (O'Neil et al., 1975) and an acid-liberated CO_2–calcite oxygen isotopic acid fractionation factor of 1.01025 at 25 °C (Sharma and Clayton, 1965).

For isotopic analysis, oxygen must be extracted from its surrounding compound, which can be accomplished using a variety of techniques. Sharma and Clayton (1965) outline the fluorination process necessary to measure the carbonate $\delta^{18}O$ value ($\delta^{18}O_{carbonate}$). Certain carbonates (i.e., magnesite, siderite) require higher reaction temperatures (90-150 °C) to isolate $CO_{2(g)}$ (Rosenbaum and Sheppard, 1986). Most stable isotope laboratories turn to the method developed by McCrea (1950) to analyze the oxygen isotope composition of carbonates. Phosphoric acid and carbonate react to liberate gaseous carbon dioxide; however, it comprises only two-thirds of the oxygen in carbonate, necessitating the application of an "acid fractionation factor" (AFF) to obtain its true isotopic composition. The so-called isotope effect is influenced by the metal cation attached to carbonate in the reactant, as well as the reaction temperature and preparation procedure. Much research has been dedicated to obtaining an accurate AFF, which is essential in the interpretation of all carbonate data. There are currently a number of published AFF and the possibility exists that many are in error, severely hampering efforts to determine thermodynamic and physical constraints in natural systems.

Practical difficulties also arise with the use of natural samples, casting doubt upon the validity of oxygen isotopes as a paleothermometry tool. Isotopic heterogeneity has been documented in biogenic and abiogenic calcites synthesized under controlled, constant conditions (Dietzel et al., 2009; Barras et al., 2010). Furthermore, the initial isotopic composition of the natural fluid growth medium is often unknown; Rollion-Bard et al. (2008) reported a depletion in δ^{18}O of 3 ‰ in early-precipitated calcite versus later-precipitated calcite, despite the absence of alteration and both biominerals belonging to the foraminifera. They attributed this depletion to the elevated pH at the onset of precipitation, thereby increasing the isotopically light CO_3^{2-} component in the calcifying fluid. Coplen (2007) suggests that true thermodynamic equilibrium in the calcite-water oxygen-isotope system is achieved in a stable geochemical environment experiencing very low growth rates. At their Devils Hole, Nevada study site, Coplen et al. (1994) reported the precipitation of calcite in carbon isotopic equilibrium and were able to rule out oxygen isotopic disequilibrium after examining several lines of evidence. Additionally, water temperature and chemistry conditions of the cave have been nearly constant since the early 1930s (Winograd and Pearson, 1976). Thus, these factors comprise the modern research requirements for a natural environment to be well suited as a “natural laboratory to calibrate the calcite-water oxygen isotope geothermometer” (Coplen, 2007). Of course, this claim is not without controversy, and will be further explored in subsequent chapters.

The δ^{18}O value of precipitated carbonates is determined by the relative proportion of DIC species present in the parent solution (McCrea, 1950; Zeebe et al., 1999; Zeebe, 2007). Since this distribution is pH-dependent, the $\delta^{18}O_{carbonate}$ is a function of solution pH. In their investigations involving biogenic carbonates, Spero et al. (1997) reported these parameters to be inversely related, however Kim et al. (2006) determined that no relationship in fact exists by measuring the same δ^{18}O value for synthetic aragonites precipitated at two different pH values of 8.22 and 10.77. Thus, any δ^{18}O variations cannot be attributed to changing pH at the site of calcification. Rather, extraneous oxygen introduced during the processing of a calcium carbonate shell influences its $^{18}O/^{16}O$ signature and thus colours the true temperature determination derived from their proposed carbonate-water paleotemperature scale (Epstein et al., 1951). Additionally, inherent variations in $^{18}O/^{16}O$ over Earth's history complicate the precise comparison of this oxygen ratio in marine shells versus the surrounding water.

Numerous experimental studies have been conducted to determine the oxygen isotopic fractionation between inorganically precipitated calcite and water (Tarutani et al., 1969; Kim and O'Neil, 1997; Jiménez-López et al., 2001, 2004; Zhou and Zheng, 2003). As is the nature of scientific evolution, each of these reports build upon past knowledge in an effort to constrain variables and optimize their study's precision. For example, Kim and O'Neil (1997) recommended an increase of 0.28 for the temperature coefficient (i.e., slope, or 1000lnα value) proposed by Tarutani et al. (1969) to comply with Friedman and O'Neil (1977), while Coplen (2007) suggested an increase of 0.25 for the 1000lnα value reported by Kim and O'Neil (1997) in accordance with the use of a CO_2-calcite oxygen isotopic acid fractionation factor of 1.01025. These various calcite-water fractionation expressions have been refined, under carefully selected precipitation methods and temperature-specific conditions, to produce calcite that is in apparent equilibrium with its surrounding water. Conflicting mineralogical affinity data reported by Zhou and Zheng (2003) has since been widely discounted due to unsatisfactory documentation of their methodology (e.g., Kim and O'Neil, 2006; Coplen, 2007).

Chacko and Deines (2008) also obtained fractionation data through theoretical calculations using the methods of statistical mechanics. Their calculations are in agreement with Chacko et al. (1991) and Schauble et al. (2006). Such mutual corroboration between theoretical and empirical evidence indicates that true equilibrium fractionation factors have indeed been derived independently for each of these systems. This conclusion, however, contrasts with the fractionation data provided by Coplen (2007). Their Devils Hole karst yielded substantially larger calcite-water fractionations; if this natural sample datum accurately reflects equilibrium fractionations in the calcite-water system, as the authors believe it does, then previous calibrations (theoretical and empirical alike) are all in error. However, the Devils Hole data may prove to be incorrect since modern-day water temperature and isotopic composition "cannot unequivocally be demonstrated to be the same as that responsible for calcite precipitation" (Chacko and Deines, 2008).

Clearly, the carbonate-water oxygen isotopic fractionation factor requires re-evaluation and careful calibration given the current discrepancy between theoretical, laboratory, and natural samples. A more precise definition of isotopic equilibrium and disequilibrium conditions is imperative to more accurately constrain $\alpha_{\mathrm{CaCO3\text{-}H2O}}$ values representative of true equilibrium and subsequently determine carbonate precipitation temperature, a parameter intrinsic to paleoenvironmental reconstructions.

2.3 Boron isotope studies

2.3.1 Introduction

Boron has two stable isotopes, ^{10}B and ^{11}B, which are present in 20% and 80% abundances, respectively. This element holds great promise as a geochemical tracer, with a relatively long residence time of ~ 20 million years (Pearson and Palmer, 2000), little variation within oceanic isotope compositions over the past ~21 million years (Rollion-Bard et al., 2011), hovering around 39.61 ‰ (Foster et al., 2010) and pH-dependent incorporation behaviour into carbonates (Milliman, 1974; Furst et al., 1976; Vengosh et al., 1991). Boron displays a large isotopic mass difference therefore identical samples and normalizing standards are necessary to correct for any resulting mass fractionation (Foster et al., 2006). In modern marine carbonates, boron is found in concentrations ranging from 1-100 ppm (Milliman, 1974; Furst et al., 1976; Vengosh et al., 1991). Boron isotope compositions are expressed as $\delta^{11}B$, defined as parts per thousand deviation from NBS 951 international boron reference material, where $\delta^{11}B = (\frac{11B/10Bsample}{11B/10Bstandard} - 1)*1000$. In aqueous solution, boron occurs as two species, trigonally-coordinated boric acid $B(OH)_3$ and tetrahedrally-coordinated borate $B(OH)_4^-$. These species each possess unique bond strengths and vibrational frequencies, resulting in isotopic fractionation (~ 20 ‰) between the two forms, with ^{11}B preferentially found in the $B(OH)_3$ form. Their differentiating isotopic fractionation behaviour and equilibrium values are strongly influenced by pH, a characteristic that has attracted widespread interest among paleoclimate researchers (Hemming and Hanson, 1992; Sanyal et al., 2000). This defines its power as a climate proxy since any variations in the boron isotope composition of foraminifera signify past changes in oceanic pH. The boron isotopic compositions of modern marine carbonates lie within a relatively narrow range (22.1 ‰ relative to NBS SRM95) for all samples regardless of their origin (i.e., biogenic, abiogenic, warm water, cold water, aragonitic, or calcitic) (Hemming and Hanson, 1992). Since the isotopically lighter tetrahedral borate is preferentially incorporated into the carbonate lattice, the dissolved seawater boron becomes isotopically heavy, which accounts for the high $\delta^{11}B$ values observed in seawater.

Several key studies have examined the applicability of carbonate boron isotopic composition to climate reconstruction techniques (Hemming and Hanson, 1992; Sanyal et al., 1995; Pearson and Palmer, 2000; Hönisch and Hemming, 2005). Simultaneous application of these proxies will provide insight into the state of the paleo-carbonate system and link the saturation state of the oceans with changing carbon dioxide concentrations. The boron-isotope approach to paleoclimatology is founded on the assumption that rising $p\mathrm{CO}_2$ values will mean more carbon dioxide is dissolved in the surface ocean, thus lowering its pH. These pH values can then be determined by measurement of the boron-isotope composition of calcium carbonate ($\delta^{11}B_{carb}$) precipitated from the seawater. This proxy aims to demonstrate the coupling between surface ocean chemistry and the atmosphere, as recorded in marine archives, allowing for quantitative estimation of ancient atmospheric $p\mathrm{CO}_2$ values not achievable by ice cores (Hemming and Honisch, 2007).

2.3.2 Dissociation constant of boric acid

As illustrated in Figure 2.2, the two most abundant aqueous boron species are trigonal boric acid, $B(OH)_3$, and tetrahedral borate ion, $B(OH)_4^-$ in seawater; polynuclear boron species (i.e., $B_3O_3(OH)_4^-$, $B_4O_5(OH)_4^{2-}$, $B_5O_6(OH)_4^-$) are chemically negligible at their typical seawater concentrations of ~ 0.4 mmol/kg (Klochko et al., 2006). These predominant species are strongly pH-dependent (Hershey et al., 1986) and equilibrate rapidly (Zeebe et al., 2001) according to the following equation:

$$B(OH)_3 + H_2O \rightleftharpoons H^+ + B(OH)_4^-$$

$$\text{where } K_B = [B(OH)_4^-][H^+]/[B(OH)_3]$$

The concentration of each species can be calculated as a function of pH once the acid dissociation constant, expressed as (pK_B), is applied (Dickson, 1990; Pagani et al., 2005). The experimental conditions in which the constant is quantified and applied must be similar. Varying such conditions, such as temperature and chemical constituents, will alter the reaction pathways and result in a suboptimal selection of pK_B. In addition, the pH scale used to determine the pK_B value must be identical to that used for the dissociation constants for CO_2 equilibria, to ensure an accurate estimation of pCO_2 from pH. Assuming the dissociation constant of boric acid $pK_B = 8.597$ (at 25 °C), borate ion accounts for ~ 28.5 % of boron species in modern seawater (pH ~ 8.2).

The pH can be identified using the total scale (pH_T), free scale (pH_F), seawater scale (pH_{SWS}), or NBS scale (pH_{NBS}). The latter is defined with low ionic-strength (I = ~ 0.1 mol/kg), standard buffer solutions, each having an assigned pH. Such pH quantification methodology is incompatible with high ionic-strength solutions such as seawater (I = ~ 0.7 mol/kg), which alters the liquid junction potential by several millivolts (Dickson, 1992, 1993; Hansson, 1973). Therefore, directly recording pH is not appropriate due to the electrical potential charge differential observed between solution and electrode. Instead, the pH_T scale was introduced, in which synthetic seawater-containing sulfate ions exist as the standard state and buffers of high ionic strength are assigned their own pH values (Hansson, 1973). The pH_{SWS} scale is only appropriate for fluoride-containing system, while the pH_F scale focuses primarily on the hydrogen ion concentrations, though it oversimplifies sulphur concentrations and activity coefficients, therefore its use is limited.

The application of the boron isotope-pH proxy in paleoseawater pH reconstructions is founded on the origin of marine foraminifera in natural seawater. The ionic strength is an inorganic experiment consideration to mimic the incorporation of boron into carbonates in the natural environment. As discussed above, experimental pH measurements are necessarily converted from the pH_{NBS} to the pH_T scales (Dickson, 1990). This is so accomplished with a pH buffer of similar ionic concentration to the experimental solutions, termed the Tris buffer as it is based on 2-amino-2-hydroxymethyl-1,3-propanediol, and is now widely used to define seawater pH scales. Thus, the pH_T values can be accurately compared to the dissociation of boric acid in seawater.

With a pK_B value of 8.597 at 25 °C, boron speciation is predominantly trigonal in nature at $pH < 8.6$ and tetrahedral at $pH > 8.6$ (Dickson, 1990; Hemming and Hanson, 1992; Klochko et al., 2006). The distribution of $B(OH)_3$ and $B(OH)_4^-$ in solution also depends on temperature, pressure, salinity (Dickson, 1990), and solution composition (Hansson, 1973). Hershey et al. (1986) demonstrated that borate ion activity, which describes the tendency to interact with other dissolved chemical species, varies with solution composition. Therefore, depending on the concentration of Mg, Ca, Na and/or K concentrations of ancient oceans, dissolved boron may have behaved differently. This is in contrast to the ongoing assumption that the activity of dissolved boron species has been constant through time.

2.3.3 Boron isotope equilibrium constant

The equilibrium isotope exchange reaction between boric acid and borate is:

$$^{10}B(OH)_3 + {}^{11}B(OH)_4 \rightleftharpoons {}^{11}B(OH)_3 + {}^{10}B(OH)_4$$

$$\text{where } {}^{11\text{-}10}K_B = \frac{[^{11}B(OH)_3][^{10}B(OH)_4-]}{[^{10}B(OH)_3][^{11}B(OH)_4-]}$$

The isotope equilibrium constant can be determined either theoretically or experimentally. The former accounts for the different vibrational energies of the two boron coordinations but these calculations are environmentally-sensitive and subject to the theoretical quantification of molecular forces (Kakihana et al., 1977; Klochko et al., 2006). Until recently, the boron isotope equilibrium constant ($^{11\text{-}10}K_B$) was cited as 1.0194, a theoretical calculation performed by Kakihana et al. (1977); this value has since been re-evaluated and a majority of follow-up studies have reported larger $^{11\text{-}10}K_B$ values (Table 2.1). The enrichment in ^{11}B of $B(OH)_3$ relative to $B(OH)_4^-$ can be attributed to the differing molecular coordinations and vibrational frequencies of aqueous boron species (Kakihana et al., 1977; Vengosh et al., 1991; Hemming and Hönisch, 2007; Hönisch et al., 2007) by ~ 27 ‰ (Klochko et al., 2006). The relationship between the boron isotope composition of carbonate ($\delta^{11}B_{carb}$) in seawater and pH is described as:

$$pH = pK_B + \log \frac{[B(OH)_4-]}{[B(OH)_3]}$$

where pH = -log [H+], pK_B= -log K_B, K_B is an equilibrium constant and the square brackets denote total concentrations of $B(OH)_3$ and $B(OH)_4^-$ in all forms (e.g., free $B(OH)_4^-$ plus ion pairs). The difference between pH measured in solutions of ^{11}B (^{11}pH) and the pH of solutions containing solely ^{10}B (^{10}pH) can be written as:

$$^{11}pH - {}^{10}pH = p^{11}K_B - p^{10}K_B + \log \frac{[11B(OH)_3][10B(OH)_4-]}{[10B(OH)_3][11B(OH)_4-]}$$

$$\text{where } p^{11}K_B - p^{10}K_B = \log({}^{11\text{-}10}K_B).$$

Figure 2.3 shows the $\delta^{11}B$ of the aqueous boron species vs. seawater pH, which was generated by combining the equation outlining the distribution of aqueous boron species and the equilibrium boron isotope exchange reaction (Hemming and Hanson, 1992). Based on the dissociation of $B(OH)_3$ in seawater, the relative proportions of $B(OH)_3$ and $B(OH)_4^-$ in seawater are present as a function of pH, with trigonal $B(OH)_3$ being enriched in ^{11}B relative to $B(OH)_4^-$ (Figure 2.4).

As observed by Klochko et al. (2006), carbonates precipitated at higher pH displayed higher $\delta^{11}B$ values versus those precipitated at lower pH. However, complicating this observation was the fact that boron isotope compositions of these laboratory-controlled precipitates trended near or below the theoretical isotope exchange constant for seawater borate proposed by Kakihana et al. (1977). Such downward offset contradicts the mass balance of boron isotope systematics in solution, which dictates that the isotopic composition of a carbonate precipitated in a given solution should be equal or greater than the isotopic composition of borate ions in that solution since aqueous borate comprises the lowest (i.e., lightest) end member (Zeebe et al., 2003). This inexplicable observation casts doubt upon the “borate curve” itself as well as the accompanying, likely underestimated, $^{11\text{-}10}K_B$ value (Zeebe et al., 2003, 2005; Pagani et al., 2005).

2.3.4 The boron isotope paleo-pH proxy

Introduction

The boron isotope paleo-pH proxy is founded on three working hypotheses: (1) the relative proportion of boric acid ($B(OH)_3$) and borate ($B(OH)_4^-$) in seawater is a function of seawater pH; (2) at equilibrium, the tetrahedrally-coordinated borate ion is depleted in ^{11}B relative to trigonally-coordinated boric acid; and (3) borate is exclusively incorporated into marine carbonates without a significant kinetic isotope effect. However, these assumptions have recently undergone considerable scrutiny. An independent assessment of each reveals calculation discrepancies in various reports of the isotope fractionation factor, a need to ascertain the role of biological vital effects, and the possibility that some boric acid may indeed be incorporated into the crystal structure. Thus, the reliability of the proxy has been challenged. Constraints must be placed on these controversial components in order for the boron proxy to be broadly accepted within the scientific community as a paleoclimate reconstruction tool. Further debate exists surrounding the fractionation factor, which varies among theoretical and empirical estimates: among the most widely cited values are the theoretically-calculated fractionation factor of 1.0194 at 25 °C proposed by Kakihana et al. (1977) versus the empirically-derived fractionation factor of 1.0272 determined by Klochko et al. (2006).

There has been a flurry of activity to recalculate and remeasure the isotope fractionation between aqueous boron species (e.g., Liu and Tossell, 2005; Pagani et al., 2005; Zeebe, 2005). Most studies attempt to refine the fractionation factor using *ab initio* calculations of the theoretical isotope effect based on the vibrational energies of the two coordinations. All but one of these results is significantly greater than determined by Kakihana, ranging from 1.0176 to 1.030, indicating the uncertainties in vibration frequency data and assumptions used in the calculations. Using a range of total boron concentrations in spectrophotometric measurements, Klochko et al. (2006) published a new boron isotope equilibrium constant of 1.0272, which is consistent with *ab initio* calculations. This remains the favoured value due to its strictly experimental basis, independent of theoretical deductions.

Deviation from the $\delta^{11}B_{B(OH)4}$–pH curve under equilibrium conditions can be attributed to several factors, as summarized by Pagani et al. (2005): (1) the isotopic fractionation occurring between solid phase and solution may differ from that between aqueous boron species, creating an offset in isotopic composition from the dissolved species; (2) equilibrium may not describe the bulk ambient solution and carbonate interaction, but instead a chemically distinct site-specific "pool"; (3) in the solid phase, boron speciation may comprise both trigonal and tetrahedral species, the proportion of which changes as a function of pH; (4) the theoretical $\delta^{11}B_{B(OH)4}$–pH relationship is erroneous. Alternatively, boron incorporation into carbonates may be associated with non-equilibrium isotope fractionation if one boron species is preferentially and irreversibly incorporated over the other. This may occur if growth rate is rapid relative to exchange rates, thereby introducing kinetic isotopic fractionation upon uptake. Under these circumstances, $\delta^{11}B_{carb}$ reflects the isotopic composition of both the dissolved boron species that is incorporated in addition to the associated kinetic fractionation. The magnitude of this fractionation is dynamic and will alter under varying conditions.

The proxy is additionally complicated by inherent uncertainties associated with secular variations in $\delta^{11}B_{carbonate}$ and environmental reconstructions exceeding the residence time of boron in the ocean, which are cumulatively significant factors (Pagani et al., 2005; Honisch and Hemming, 2005). In response to the published critique by Pagani et al. (2005), Honisch and Hemming (2005) constructed six empirical calibration curves to confirm the validity of the theoretical fractionation factor presented by Kakihana et al. (1977), designed as a rigorous test of the proxy. The empirical results were consistent with previous theoretical calculations, providing strong support for the applicability of the boron paleo-pH proxy to planktonic foraminifera. Oceanic pH, the borate to carbonate ratio in seawater, temperature, mineralogy, biological influences and kinetic factors are all important controls which account for the very narrow boron isotopic range observed in marine carbonates.

Boron incorporation into carbonate minerals

Compared to modern seawater total boron concentrations of 4.8 ppm, the boron concentrations in marine carbonates analyzed to date are relatively high (40-100 ppm), indicating that marine calcification acts as a substantial sink for boron. While oceanic surface waters are supersaturated with respect to calcite and aragonite, direct precipitation of inorganic calcium carbonate is rare due to the presence of various constituents (e.g., magnesium, phosphates and dissolved organic compounds) rendering conditions unfavourable for carbonate precipitation by inhibiting the formation of $CaCO_3$ nuclei (Berner, 1975; Mucci, 1986).

The boron isotope-pH proxy is founded on the exclusive incorporation of the borate ion into the crystal lattice. This was first postulated following the observation of different boron isotope signatures in clay and seawater, indicating the uptake of charged, isotopically light borate into clays (Schwarcz et al., 1969). Both Vengosh et al. (1991) and Hemming and Hanson (1992) affirmed this fractionation behaviour in marine carbonates. Ion substitution dynamics appear to be polymorph-specific, as the larger tetrahedral borate anion is substituted into the smaller lattice sites in aragonite, while the smaller trigonal boric acid is substituted into the larger lattice sites in calcite. Due to differences in crystal size and coordination, trace elements partition differently between calcite and aragonite. For example, divalent cations larger than Ca^{2+} are more easily incorporated into aragonite's carbonate site than calcite (Mucci and Morse, 1982), while SO_4^{2-} substitutes into the calcite crystal structure preferentially over aragonite (Kitano et al., 1979). When it comes to boron incorporation in carbonates, the bond length it shares with oxygen must be considered; since the B-O bond length is ~ 7% larger than that of C-O in trigonal coordination, and the anion site in aragonite is smaller in volume than calcite (37.77 Å and 40.87 Å respectively), then trigonally-coordinated boron will be more compatible with calcite (Hemming et al., 1995).

Since the size of both boric acid and borate ion are comparable to that of carbonate ion, either could substitute into the carbonate lattice. Charge balance considerations necessitate that substitution of borate could be charge-balanced by the coupled substitution of an alkali for calcium while substitution of boric acid would substitute for carbonate and calcium. Since the B-O bond length of 0.137 nm for trigonal boron is similar to the C-O bond length of 0.128 nm (Kakihana et al., 1977), boron is likely substituting in the CO_3^{2-} site of the crystal lattice. Cation sites within the aragonite crystal structure are sufficiently large to allow substitution of larger ions such as magnesium, strontium and barium. Subsequent research has focused on possible mechanisms for this preferential incorporation of $B(OH)_4^-$ into calcite and aragonite (e.g., Kitano et al., 1978; Hemming and Hanson, 1992; Hemming et al., 1995; Tossell, 2006).

In their study of boron uptake in synthetic carbonates, Kitano et al. (1978) originally observed that boron uptake is greater in aragonite than calcite by a factor of 3-5 and that the presence of magnesium in the parent solutions heightened boron uptake in calcite compared to magnesium-free solutions, observations later verified by Hemming et al. (1995). A higher content of boron in marine biogenic aragonite relative to calcite (15 to 9 ppm, respectively) is also well corroborated (e.g., Furst et al., 1976; Vengosh et al., 1991; Hemming et al., 1995). This can be explained by the abundance of organic matter in calcite, contrasted with the location of boron in the inorganic constituents of the shell, as opposed to the organic matrix (Furst et al., 1976). Such differences in boron concentrations among the various calcium carbonate polymorphs may be attributed to biogenic effects, which dictate the inclusion (corals) or exclusion (gastropods) of aqueous boron species (Vengosh et al., 1991).

Sen et al. (1994) suggested that carbonate boron incorporation mechanisms may also be influenced by the various species coordinations, which can be assessed with ^{11}B magic angle spinning nuclear magnetic resonance (MAS NMR) spectroscopy analysis. Their study differentiated the local coordinations of natural calcite and aragonite, synthetic calcite and aragonite, and a phase-changed calcite: natural and synthetic calcite contained 90% boric acid and 10% borate, the natural and synthetic aragonite contained only borate, and the altered calcite contained only boric acid. This remarkable observation indicates that boron incorporation into calcite may require a coordination change. Prior to this, Kitano et al. (1978) had hypothesized the presence of borate in both polymorphs, though its abundance in aragonite far exceeds calcite. This is consistent with Hemming et al. (1995) who provided isotopic data revealing that borate is preferentially incorporated in aragonite relative to calcite. Thus, if $B(OH)_4^-$ is indeed the predominant species interacting with the carbonate surface, then boron must change in coordination from tetrahedral to trigonal upon its incorporation into calcite, which will be reflected in the relative partitioning behaviour if this coordination alteration is energetically or kinetically hindered.

Hemming et al. (1995, 1998) suggested the presence of a structural barrier in calcite dictating this quantitative change from tetrahedral to trigonal coordination without significant isotopic fractionation, which would support the exclusive incorporation of borate into carbonate minerals from aqueous solutions. Tossell (2006) further hypothesized the existence of an intermediate phase during the coordination change (Figure 2.5). In this scenario, boron incorporation cannot be described simply by the adsorption of borate to the carbonate surface, but rather chemical reactions between HCO_3^- and $B(OH)_3$ or $B(OH)_4^-$ occur during the early growth phase. Termed "chemosorption", this stage sees $B(OH)_2CO_3$ isomers of either trigonal or tetrahedral coordination form on the surface.

However, δ^{11}B variability in calcite samples from follow-up empirical studies (Sanyal et al., 1995, 2000, 2001; Hönisch et al., 2004) and the systematic observation that aragonite is enriched in ^{11}B relative to calcite are in marked contrast to the NMR results reported by Sen et al. (1994). The coordination change from tetrahedral in solution to trigonal in calcite detected by Sen et al. (1994) and Hemming et al. (1998) was investigated further by Klochko et al. (2009), who determined an equal presence of trigonally and tetrahedrally coordinated boron in biogenic carbonates. Larger positive deviations of δ^{11}B in carbonates relative to aqueous borate were detected at lower pH values, indicating that the incorporation of trigonally-coordinated boron is important at lower pH. This is to be expected since the relative concentration of trigonally-coordinated boron increases with decreasing pH. Incorporation of both boric acid and borate into carbonates would yield an overall higher boron isotopic composition than expected if only borate was incorporated, as boric acid is enriched in ^{11}B relative to the tetrahedral species.

However, Klochko et al. (2009) noted a significant amount of boron in trigonal coordination, correlating to a far higher enrichment in ^{11}B than that reported in the literature for both biogenic and inorganic carbonates. By extension, a change in coordination from trigonal to tetrahedral must indeed occur, which Ruiz-Agudro et al. (2012) hypothesize may be the limiting factor for boron incorporation into calcite. This argument may also explain why boron is preferentially incorporated into aragonite relative to calcite, as observed by Hemming et al. (1995). Moreover, variations in calcite growth rates may affect the relative proportions of trigonally and tetrahedrally coordinated boron found in carbonate samples (Sen et al., 1994; Klochko et al., 2009; Rollion-Bard et al., 2011), associated with the time needed to undergo the coordination change rather than both species actually being incorporated. The results obtained by Ruiz-Agudo et al. (2012) suggest that tetrahedrally-coordinated boron is predominantly incorporated into calcite, and that the offset found between δ^{11}B in carbonates and the solution from which they precipitated can be attributed to isotopic fractionation associated with the change in coordination from tetrahedrally-coordinated to trigonally-coordinated boron.

Abiogenic versus biogenic sampling

Significant isotopic offsets have been observed between inorganic, biogenic calcification, and foraminifera species compared to the reported empirical δ^{11}B-pH relationship (Sanyal et al., 2001). These discrepancies can be attributed to species-specificity, differences in microenvironment pH and/or due to diurnal differences in the relative proportion of calcite precipitated (Zeebe et al., 2003; Sanyal et al., 2001). In their study of corals, Hemming et al. (1998) determined more positive boron isotope values occurred during periods of high primary productivity, enhanced symbiont photosynthetic activity and a resultant higher pH. Vital effects may account for the offset observed between δ^{11}B and the theoretical $\delta^{11}B_{B(OH)4}$ values in planktic foraminifera (Hönisch et al., 2007). Laboratory-based studies cannot possibly recreate true conditions, however coral and foraminifera culture experiments best mimic the natural environment while controlling its associated parameters. The overall shape of the borate curve initially generated theoretically by Kakihana et al. (1977) (and subsequently empirically by

Klochko et al., 2009) has been reproduced by an abundance of coral and foraminifera experiments over a spectrum of pH values, each demonstrating a variable offset (e.g., Honisch et al., 2004; Sanyal et al., 2001).

Natural samples are ideally obtained from shallow sediment cores to minimize dissolution effects (Honisch et al., 2007), contain high boron concentrations to satisfy current analytical limitations, and do not alter seawater composition when secreting the carbonate. The *Siderastrea sidereal* coral, composed of aragonite, contains a high concentration of boron (approximately 60 ppm) and grows at the epidermis which comes into direct contact with seawater (Hemming and Hanson, 1992). Compared to internal shell growth observed in molluscs and/or species containing lower boron concentrations, this coral constitutes an ideal specimen for the application of boron isotope-pH proxy (Hemming and Hanson, 1992).

Hemming and Hanson (1992) attributed the range in boron isotope composition to the fact that only the aqueous borate ion is involved in reactions incorporating boron into the carbonate crystal structure, since their compiled data closely matched the isotopic composition of the tetrahedral species in seawater. However, boron isotope values reported by Vengosh et al. (1991) did not plot as reliably, necessitating an investigation to correctly interpret the proxy. Unknown pH, salinity and temperature values at sample localities each contribute uncertainty to the study of modern carbonates; controls on boron uptake and fractionation cannot be analyzed quantitatively. Therefore, Hemming et al. (1995) initiated a laboratory-based study to grow synthetic calcite from an ionic strength akin to seawater over a range of boron concentrations, which confirmed the original findings. A key additional observation was the lack of mineralogical influence on isotope composition, which set the stage for the boron isotope proxy. A subsequent empirical study (Sanyal et al., 2000) also reported the tight coupling between boron isotope isotopes in synthetic inorganic carbonates and the pH of the growth solution over a range of pH values.

In the past, boron isotopes were analyzed by inserting samples containing ~ 5 μg boron into a positive ion thermal mass spectrometer (PTIMS), although foraminiferal carbonates did not satisfy these sizing constraints. Paleoceanographers have since benefitted from the introduction of the negative ion thermal mass spectrometer (NTIMS), in which analyses can be executed with smaller sample sizes (~1 ng) (Hemming and Hanson, 1994). However, this instrument has been associated with notable in-run fractionation and mass interferences (Sanyal et al., 1995; Foster et al., 2006). The multi-collector inductively coupled plasma mass spectrometer (MC-ICPMS) has proven the best instrument in this instance: its stability allows for machine-induced fractionation to be easily corrected, requiring only marginally larger sample sizes, yielding rapid isotopic analysis relative to the other approaches, and achieving < 1 ‰ precision (Foster, 2008).

2.3.5 Insight into past studies

At a given pH value, Hemming et al. (1995) determined the boron isotope compositions of synthesized carbonate to equal that of the borate ion, although pH gradients have been reported in studies implementing a similar methodology (e.g., Paquette and Reeder, 1995). Such experimental considerations must be taken into account when evaluating Hemming et al. (1995) reports of no crystal precipitation during the initial two days of their study, in which the pH of the experiments increased from 5.6 to 8.0. Had any crystals indeed precipitated during this period of dynamic pH fluctuation, the intended pH range achieved upon stabilizing would not be accurately reflected. When trying to determine the equivalence of $\delta^{11}B_{B(OH)4}$, a stable pH must be maintained over the course of carbonate synthesis, otherwise boron incorporation would occur over a range of pH values and yield a faulty comparison baseline.

To explain the relatively light $\delta^{11}B$ values of their marine carbonates, Hemming and Hanson (1992) reasoned that borate was exclusively incorporated into the crystal structure. This tetrahedral species would have interacted with the growing crystal surfaces, reflected by changing crystal geometry in high boron concentration growth conditions (Hemming et al., 1995). However, nuclear magnetic resonance (NMR) imaging reveals the equivalent coexistence of trigonal and tetrahedral boron coordinations in biogenic calcite (Klochko et al., 2009). It must be noted that this test is not necessarily indicative of which molecule is incorporated from solution; boron may alter coordination with 3 or 4 oxygen atoms during adsorption and transform into borocarbonate upon incorporation. The large offset present between boric acid and borate ion isotopes is a valuable indirect marker for boron species incorporation.

Sanyal et al. (2000) synthesized calcium carbonates under ambient laboratory conditions in the presence of seed material over a small range of pH (7.9-8.6) in artificial seawater. Their goal was to determine the relationship between the pH of the parent solution and the boron isotope composition of the synthetic carbonates, then quantify the extent to which biogenic effects influence boron isotope composition. Sanyal et al. (2000)

reported no potential kinetic effects due to the agreement between their $\delta^{11}B_{B(OH)4}$ versus pH curve and that of Kakihana et al. (1977). The findings of Sanyal et al. (2000) oppose those of Hemming et al. (1995) since $\delta^{11}B_{carbonate}$ is lighter than $\delta^{11}B_{B(OH)4}$, indicating potential biogenic limits of this proxy. However, calcite growth varied among the different pH values and Sanyal et al. (2000) did not confirm the isotopic equilibrium of their experimental system, therefore this conclusion may not accurately portray the overall role of kinetic effects in the synthesis of calcium carbonate. An additional consideration is that Sanyal et al. (2000) included starting solutions with total boron concentrations (B_T) of 74 ppm (6.8 mmol/kg H_2O), around 15 times that of natural seawater (~ 4.8 ppm, or 0.4 mmol/kg H_2O). Klochko et al. (2006) determined that an increase in boron concentration by a factor of 125 (600 ppm or 0.05 mol/kg H_2O) has no observable effect on the boron isotope equilibrium exchange between aqueous boric acid and borate, although it is not known how higher boron concentrations influence overall boron uptake and associated boron isotope fractionation between the calcium carbonate and the mother solution.

Sanyal et al. (2000) was instrumental to the reconstruction of past oceanic pH using the boron isotopic composition ($\delta^{11}B$) of foraminifera, clearly demonstrating the relationship between changing ocean pH with the global carbon cycle. Their research has also linked $\delta^{11}B$ of inorganic calcite with the pH of artificial seawater, providing further support for the hypothesis that $B(OH)_4^-$ is the dominant species incorporated into calcite's structure. However, instituting both a temperature control and confirmation of isotopic equilibrium would better portray the role of kinetic effects in calcium carbonate synthesis.

Inconsistencies between Hemming et al. (1992, 1995) and Sanyal et al. (2000) may be attributed to the different experimental methods implemented in each study. While Hemming et al. (1995) synthesized their calcite with a modified free-drift method, in which the solution was not stirred and therefore uniform distribution of the precipitating solution could not be guaranteed, Sanyal et al. (2000) used the pH-stat system with continuous monitoring of pH. Hemming et al. (1992) had employed a similar experimental setup in which vertical pH gradients were present, potentially explaining the difference in boron isotopic compositions between the inorganic calcites, although Sanyal et al. (2000) later discounted this possibility in their rapidly stirred, steady-state reactor experimental setup. Instead, they concluded that inorganic calcite co-precipitation experiments display a strong δ^{11}B value dependence on solution pH. Additionally, the unknown offset of carbonate-borate boron isotope compositions between Hemming et al. (1995) and Sanyal et al. (2000) may be attributed to varying ionic strengths of the two studies. The desired pH was obtained manually in both cases: the former by adjusting $p\text{CO}_2$ in the reaction chamber, and the latter through the addition of acids and bases (HCl and NaOH) with sodium carbonate injections to maintain constant pH spanning the synthesis duration. Both Hemming et al. (1995) and Sanyal et al. (2000) successfully correlated the boron isotope composition of calcium carbonate with solution pH however the differing results remain unresolved. For advancement of the boron isotope-pH proxy, further research is required to ascertain potential effects in a spectrum of species over a larger pH range, better constrain the experimental variables, and resolve the offset in $\delta^{11}\text{B}_{\text{carbonate}}$ compared to the predicted equilibrium $\delta^{11}\text{B}_{\text{B(OH)4}}$ between these two studies.

While the primary assumption of the boron isotope-pH proxy assumes that $\delta^{11}B_{carbonate} = \delta^{11}B_{B(OH)4}$, the relationship between $\delta^{11}B_{B(OH)4}$ and pH is based on a model generated from a *theoretical* value. In their cultured experiments, Sanyal et al. (2000) measured isotopic composition values deviating from the slope of a theoretical curve, indicating its imperfection. If the established relationship is indeed assumed to be correct then an *empirical* correction can be applied, extrapolated from the results of these inorganic carbonate precipitation experiments. If the empirical value is in fact correct then the $\delta^{11}B_{carbonate}$-pH relationship is faulty and, subsequently, estimates of ocean pH derived from the theoretical model are in error. Regardless of questions surrounding boron incorporation, diagenesis considerations and the exact mechanism of isotopic inheritance, the sensitivity of the $\delta^{11}B_{carbonate}$-pH curve must be better understood in order to appropriately evaluate the uncertainties and variables affecting it.

When using boron as a pH proxy, changes in growth rate, the pH of the calcifying fluid, and the crystallographic form in which boron is incorporated must also be carefully considered, as each these factors may influence amount of boron incorporated and its isotopic signature. In their inorganic calcite growth experiments, Sanyal et al. (2000) reported time requirements of 24, 12, and 3 h to precipitate 100 mg of calcite on 200 mg of seed at pH values of 7.9, 8.3, and 8.6, respectively – an eight-fold increase in growth rate from pH 7.9 to 8.6. As documented by Turner (1982), rapid reactions involving isotope exchange, including crystallization, are more susceptible to kinetic effects by preferentially fractionating the lighter isotope into the reaction product. It is expected that, with increasing growth rate, kinetic fractionation would result in $\delta^{11}B$ values deviating increasingly from the trend parallel to the $B(OH)_4^-$ curve. Using *in situ* Atomic Force Microscopy (AFM) to study coprecipitation of boron by calcite as a function of pH, supersaturation and boron concentration, Ruiz-Agudro et al. (2012) suggested that variations in the calcification rate, or the calcite crystallographic form in which boron is incorporated, must also be considered (in addition to changes in pH) when using boron in carbonates as a pH proxy. These factors also have the potential to influence the amount of boron incorporated during growth and possibly the boron isotopic signature.

2.3.6 Conclusions and future work

The boron isotope-pH proxy and surrounding controversy has been described in detail. Briefly, the oceanic system is comprised of two dominant species of dissolved boron, boric acid [$B(OH)_3$)] and borate [$B(OH)_4^-$], the relative concentrations of which change with pH. At low pH (< 8.6), boron is predominantly in the form of boric acid, while borate exists primarily at high pH (> 8.6). The stable isotope ^{11}B is enriched in $B(OH)_3$ compared to $B(OH)_4^-$, with an effective isotopic fractionation on the order of 27 ‰ between the two boron species (Klochko et al., 2006). Therefore, the isotopic composition of the dissolved species is dependent upon the relative concentration of the dissolved species, which changes with pH. A diverse range of biogenic and inorganic marine carbonates record boron isotopic compositions approximating the boron isotopic composition of $B(OH)_4^-$ at modern seawater pH, therefore borate species must be incorporated into marine carbonates (Hemming and Hanson, 1992). A number of follow-up studies have supported this interpretation over a wide range of pH values (7.7-9.0), including empirical calibration studies on planktonic foraminifera (Sanyal et al., 1996,

2001) as well as studies in which calcium carbonate has been inorganically precipitated (Hemming et al., 1995; Sanyal et al., 2000). It is now widely accepted that borate is predominantly incorporated into the aragonite crystal lattice with no observed fractionation while the incorporated species in calcite is 90% boric acid, a differential potentially resulting in heavier boron isotopic composition of calcite relative to aragonite.

However, a systematic depletion in $\delta^{11}B$ relative to the expected value for aqueous $B(OH)_4^-$ has been observed. Klochko et al. (2006) cited several potential mechanisms: $\delta^{11}B$ of biogenic carbonates may have been influenced by pH adjustment at the site of calcification, vital effects are species-specific and not constant with pH, and/or boron partitioning during carbonate mineralization may create non-equilibrium enrichment of $\delta^{11}B$ in the experimental carbonates. All of these circumstances introduce a large error in the pH estimate. Klochko et al. (2009) subsequently suggested that $\delta^{11}B$-enriched boric acid may also be incorporated into the carbonate lattice in addition to borate, thus increasing the overall boron isotopic composition of the carbonate than that expected from exclusive borate incorporation. The value of $\delta^{11}B_{carbonate}$ will differ from the theoretical $\delta^{11}B_{B(OH)4}$ if boric acid is also incorporated into the carbonate (which may result from changes in pH and/or growth rate), as suggested by numerous studies (e.g., Pagani et al., 2005; Klochko et al., 2009; Rollion-Bard et al., 2011). The reliability of boron isotopes as a paleo-pH proxy is called into question under these circumstances. The change in coordination from tetrahedral (in solution) to trigonal (in calcite) may explain the offset reported between $\delta^{11}B$ in carbonates and the solution from which they precipitated, however this clearly indicates that the relationship between boron composition and seawater pH is far more complicated than initially suggested. Finally, the role of kinetic effects related to changes in growth rate may also help to explain some of the variability of the data reported in the literature. The development of growth rate corrections for boron content in marine biocarbonates, using controlled culture experiments focused on species with different calcification rates, is a logical step to advance the use of boron as a pH proxy.

The boron isotope paleo-pH proxy can only be applied upon appropriate selection of the boric acid dissociation (pK_B) and boron isotope fractionation constant ($^{11\text{-}10}K_B$). In addition, boron partitioning and coordination in calcium carbonates must be characterized and constrained at any given pH value, and vital effects influencing $\delta^{11}B$ of biogenic carbonates must be absent or known. To estimate ancient ocean pH and pCO_2 conditions, the application of boron isotopes in marine carbonates is founded upon three pillars to the proxy: (1) aqueous boron speciation is pH-dependent, governed by the boric acid dissociation constant (pK_B); (2) isotope exchange occurring between aqueous boric acid and borate ions, the latter possessing a distinctly lighter isotopic compositions, is controlled by the boron isotope fractionation constant ($^{11\text{-}10}K_B$); (3) borate is preferentially incorporated into both inorganic and biogenic carbonates without further fractionation. Of these three listed items, the first two have been experimentally constrained (Dickson, 1990; Klochko et al., 2006, respectively). However, the partitioning of boron species in carbonates and the magnitude of isotope fractionation associated with the incorporation of boron as either boric acid or borate remains largely unresolved.

Application of empirically-derived relationships to the boron isotope paleo-pH proxy allows scientifically sound reconstruction of surface seawater pH (Sanyal et al., 1995) and variations in atmospheric $p\mathrm{CO}_2$. The previous assumption of only borate being incorporated into the carbonate crystal structure is intrinsic to the boron isotope-pH proxy application to paleoseawater conditions. If this is indeed true, the carbonate isotope composition should mirror that of the borate sharing the same pH value, therefore seawater pH can be determined at the time of carbonate formation provided proper calibration of the proxy. The proxy is not necessarily invalidated if dual incorporation of species occurs however it is significantly complicated. As will be explored in this thesis, while not placing further constraints upon the proxy, abiotic observations of mineral-specific non-equilibrium effects associated with boron uptake provide important insight into environmental conditions when applied to the biogenic realm.

Reconstruction of paleo-pH yields important clues to paleo-$p\mathrm{CO}_2$ concentrations and subsequently provides objective evidence for ocean-CO_2 system alterations possibly stemming from human-induced climate change. To minimize outside influences (e.g., dissolution effects), samples should be collected from areas of low productivity and large shell size fractions (Honisch et al., 2007). However, the ambiguity associated with inferring formation environments (e.g., temperature and salinity) of natural samples renders the proxy far from robust; external conditions can be better controlled with cultured samples, as performed by Sanyal et al. (1996), although biogenic effects during carbonate precipitation must then be quantified. These culture studies allow species-specific vital effects to be examined, which will prove to be an important knowledge link as the proxy continues to be refined. Laboratory simulations, in which all variables are controlled, provide the most useful experimental basis at this point in time. For the proxy to advance, all aspects of its foundation must first be fully understood and established.

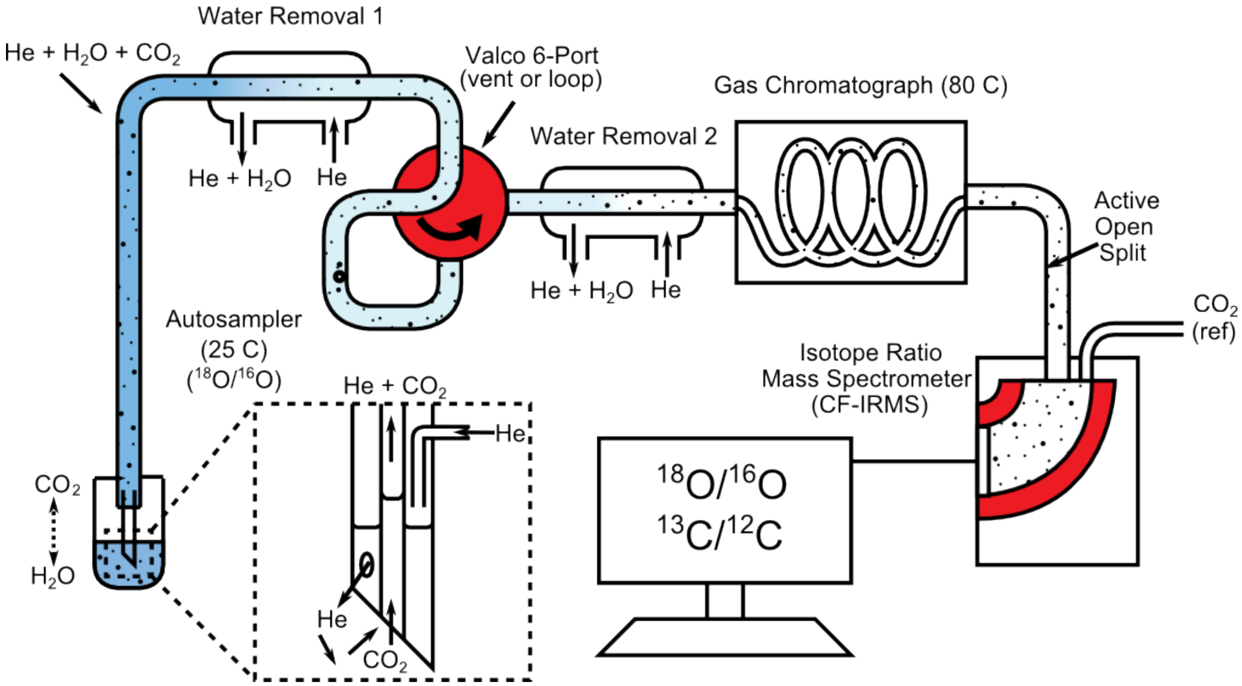

Figure 2.1: Analytical line for Finnigan Gas Bench II autosampler online with an isotope ratio mass spectrometer.

The McMaster University Research Group for Stable Isotopologues employs a Gas Bench II headspace autosampler with a Thermo Finnigan Delta plus XP isotope ratio mass spectrometer. For the purposes of this thesis, the GasBench II is used to measure the oxygen isotope composition of water and carbon isotope composition of DIC.

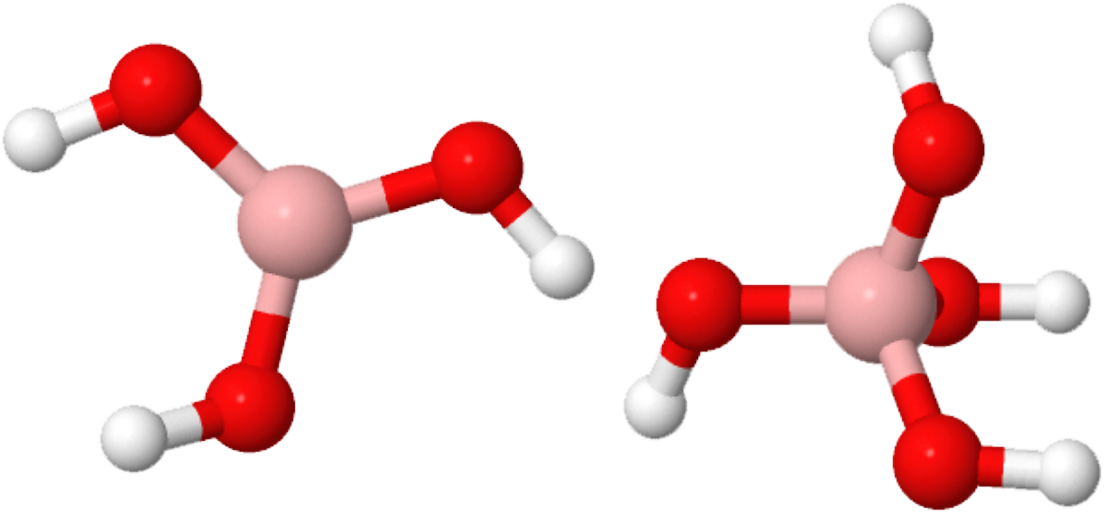

Figure 2.2: Molecular configurations of the dominant aqueous boron species in seawater.

Left: Boric acid, $B(OH)_3$, molecular structure. The unit cell is comprised of four such molecules. Right: Addition of one hydroxide molecule yields the borate ion, $B(OH)_4^-$, structure. *Constructed in Mercury CSD 2.0*.

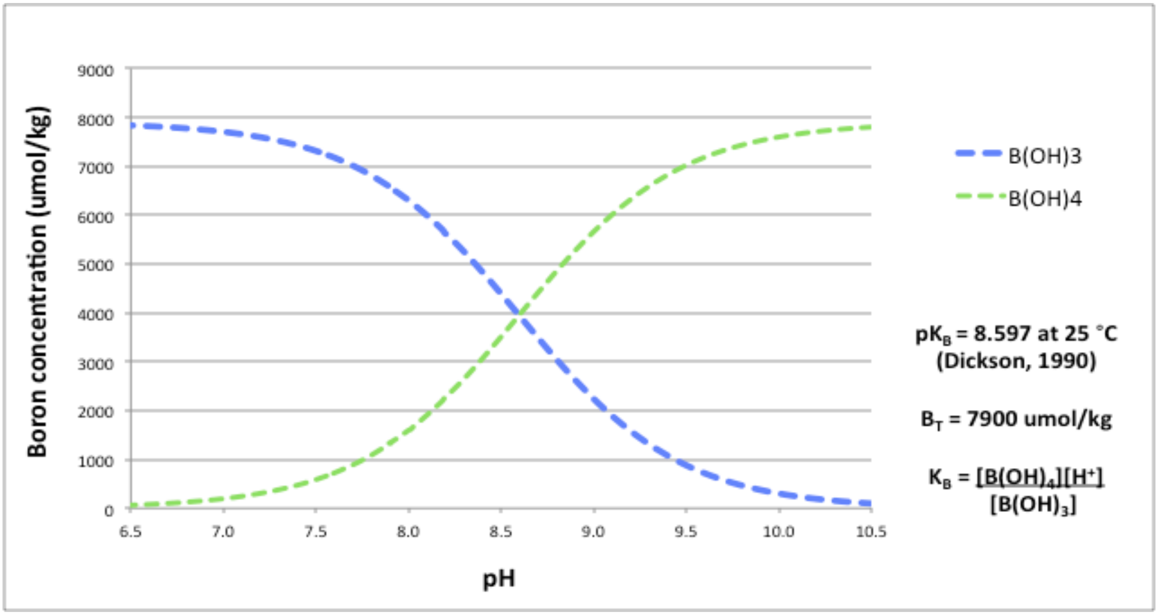

Figure 2.3: Distribution of aqueous boron species as a function of pH.

The pH-dependent speciation behavior calculated using pK_B = 8.597 (Dickson, 1990).

Table 2.1: Previously established boric acid dissociation constants (from Klein-Gebbinck, 2013)

Author(s)	Treatments/Methods	Isotope Equilibrium Constant ($^{11\text{-}10}K_B$)
Kakihana et al., 1977	Ion-exchange separation based on reduced partition function ratios and using spectroscopic data for molecular vibrations	1.0194
Palmer et al., 1987	Adsorption of B from seawater onto marine clay	1.033
Oi, 2000	*Ab initio* molecular orbital theory calculating vibrational frequency at the optimized structure	1.026
Pagani et al., 2005	Best fit with inorganic carbonate precipitation experiments conducted in artificial seawater	1.0267
Zeebe, 2005	*Ab initio* molecular orbital theory and spectroscopic data for molecular vibrations	≥1.030
Liu and Tossell, 2005	*Ab initio* molecular orbital theory using the "water droplet" method	1.027
Tossell, 2005	Quantum mechanical calculations considering vibrational, rotational, and translational contributions to the free energy	1.0322
Bryne et al., 2006	Experimental observations of chemical equilibrium in 0.6 mol kg^{-1} H_2O KCl	1.0285
Klochko et al., 2006	Experimental observations of chemical equilibrium in "pure water", 0.6 mol kg^{-1} H_2O KCl, and 0.7 mol kg^{-1} synthetic seawater, at 25 and 40°C, with 0.01-0.05 mol kg^{-1} total boron concentrations	1.0308, 1.0250, and 1.0272, respectively
Rustad and Bylaska, 2007	*Ab initio* molecular dynamics using Fourier transformation of the velocity autocorrelation function to obtain vibrational densities	1.028

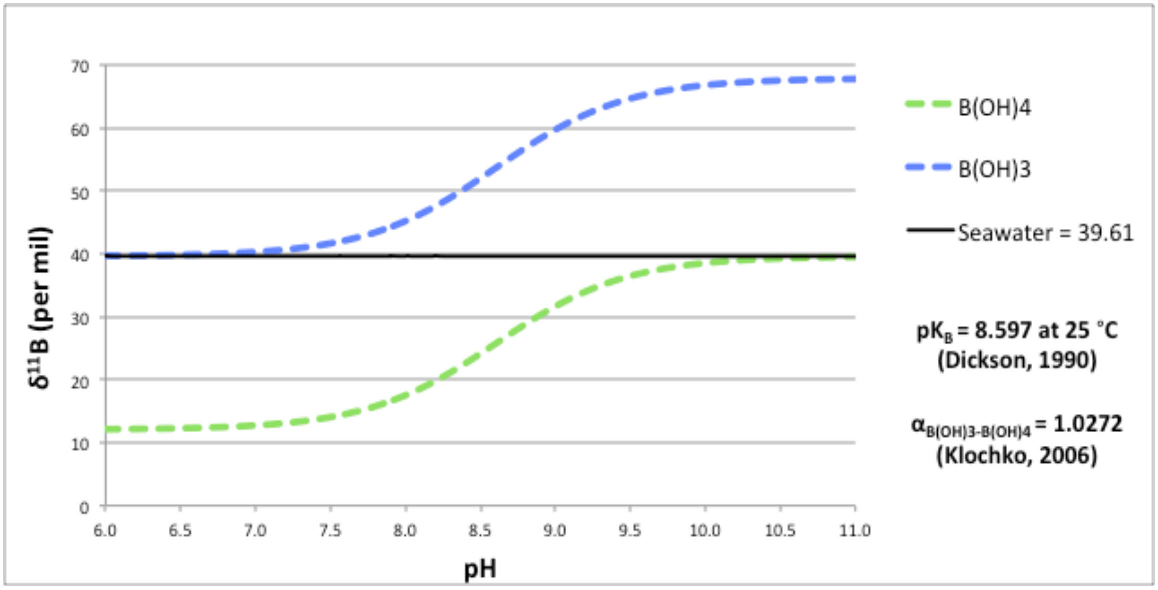

Figure 2.4: "The borate curve" δ^{11}B of $B(OH)_4^-$ in seawater as a function of pH.

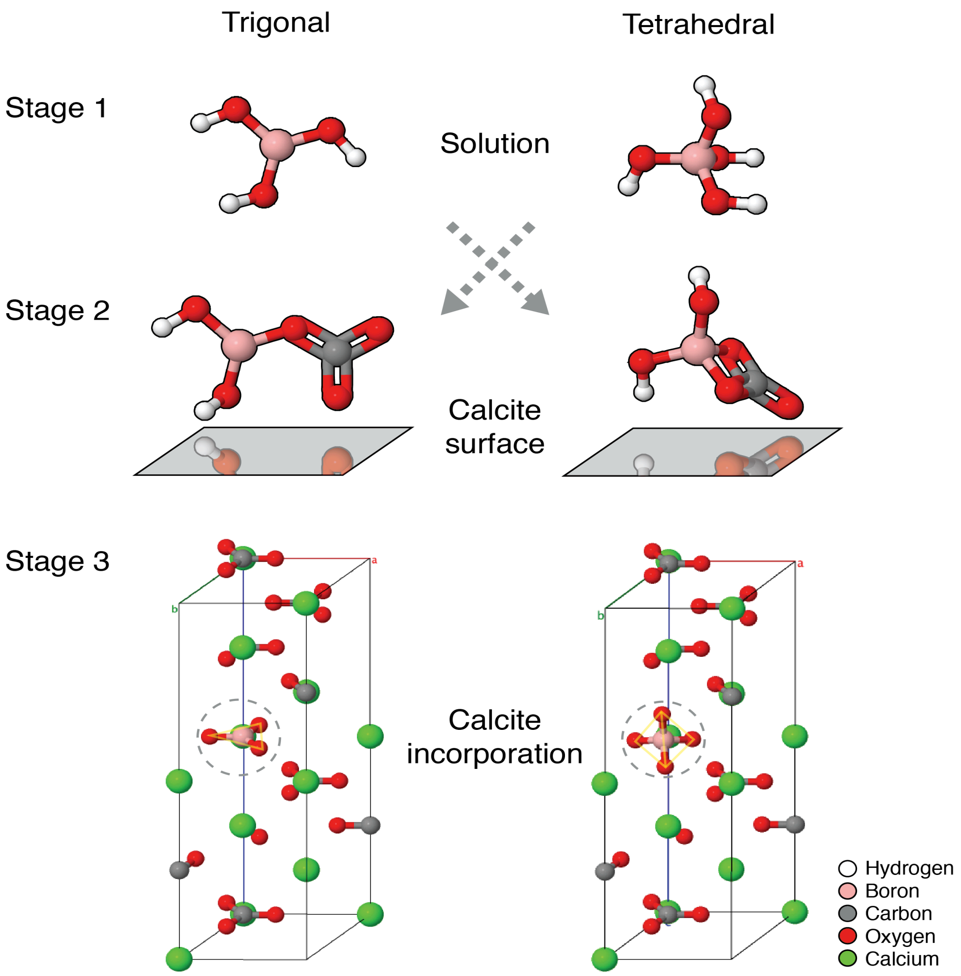

Figure 2.5: Potential "chemosorption" mechanism of boron incorporation into calcium carbonate. *Constructed in Mercury CSD 2.0.*

Schematic model of molecular structures are adopted from Tossell (2006) and Klochko (PhD Dissertation), associated with six chemical reactions as indicated below.

(1) $B(OH)_3 + H_2O \rightarrow B(OH)_4^- + H^+$

(2) $^{10}B(OH)_3 + {}^{11}B(OH)_4^- \rightarrow {}^{11}B(OH)_3 + {}^{10}B(OH)_4^-$

(3) $B(OH)_3 + HCO_3^- \rightarrow B(OH)_2CO_3^- + H_2O$

(4) $B(OH)_4^- + HCO_3^- \rightarrow B(OH)_2CO_3^- + H_2O + OH^-$

(5) $B(OH)_2CO_3^- + H_2O \rightarrow B(OH)_3 + HCO_3^-$

(6) $B(OH)_2CO_3^- + H_2O + OH^- \rightarrow (OH)_4^- + HCO_3^-$

References

Atekwana, E. A., & Krishnamurthy, R. V. (1998). Seasonal Variations of Dissolved Inorganic Carbon and δ^{13}C of Surface Waters: Application of a Modified Gas Evolution Technique. *Journal of Hydrology*, *205*, 265–278.

Barras, C., Duplessy, J-C., Geslin, E., Michel, E., & Jorissen, F. J. (2010). Calibration of δ^{18}O of cultured benthic foraminiferal calcite as a function of temperature. *Biogeosciences*, *7*(4), 1349–1356. doi:10.5194/bg-7-1349-2010

Beck, W. C., Grossman, E. L., & Morse, J. W. (2005). Experimental studies of oxygen isotope fractionation in the carbonic acid system at 15°, 25°, and 40°C. *Geochimica et Cosmochimica Acta*, *69*(14), 3493–3503. doi:10.1016/j.gca.2005.02.003

Berner, R. A. (1975). The Role of Magnesium in the Crystal Growth of Calcite and Aragonite From Sea Water. *Geochimica et Cosmochimica Acta*, *39*, 489–504.

Billups, K. (2002). Late Miocene through early Pliocene deep water circulation and climate change viewed from the sub-Antarctic South Atlantic. *Palaeogeography, Palaeoclimatology, Palaeoecology*, *185*, 287–307.

Broecker, W. S. (1982). Glacial to Interglacial Changes in Ocean Chemistry. *Prog. Oceanog.*, *11*, 151–197.

Broecker, W. S. (1986). Oxygen isotope constraints on surface ocean temperatures. *Quaternary Research*, *26*(1), 121–134. doi:10.1016/0033-5894(86)90087-6

Chacko, T., & Deines, P. (2008). Theoretical calculation of oxygen isotope fractionation factors in carbonate systems. *Geochimica et Cosmochimica Acta*, *72*(15), 3642–3660. doi:10.1016/j.gca.2008.06.001

Chacko, T., Mayeda, T. K., Clayton, R. N., & Goldsmith, J. R. (1991). Oxygen and carbon isotope fractionations between CO2 and calcite. *Geochimica et Cosmochimica Acta*, *55*(10), 2867–2882. doi:10.1016/0016-7037(91)90452-B

Coplen, T. B., Winograd, I. J., Landwehr, J. M., Riggs, A. C. (1994). 500,000-Year Stable Carbon Isotopic Record from Devils Hole, Nevada. *Science, 263(5145)*, 361-365.

Coplen, T. B. (2007). Calibration of the calcite–water oxygen-isotope geothermometer at Devils Hole, Nevada, a natural laboratory. *Geochimica et Cosmochimica Acta*, *71*(16), 3948–3957. doi:10.1016/j.gca.2007.05.028

Dickson, A. (1990). Thermodynamics of the dissociation of boric acid in synthetic seawater from 273.15 to 318.15 K. *Deep Sea Research Part A. Oceanographic Research Papers, 37(5),* 755-766.

Dickson, A. G. (1992). pH buffers for sea water media based on the total hydrogen ion concentration scale ANDREW G. *Deep-Sea Research*, *40*(1), 107–118.

Dickson, A. G. (1993). The measurement of sea water pH. *Marine Chemistry*, *44*(2-4), 131–142. doi:10.1016/0304-4203(93)90198-W

Dietzel, M., Tang, J., Leis, A., & Köhler, S. J. (2009). Oxygen isotopic fractionation during inorganic calcite precipitation — Effects of temperature, precipitation rate and pH. *Chemical Geology*, *268*(1-2), 107–115. doi:10.1016/j.chemgeo.2009.07.015

Dreybrodt, W., & Scholz, D. (2011). Climatic dependence of stable carbon and oxygen isotope signals recorded in speleothems: From soil water to speleothem calcite. *Geochimica et Cosmochimica Acta*, *75*(3), 734–752. doi:10.1016/j.gca.2010.11.002

Duplessy, J., Shackleton, N. J., Matthewsa, R. K., Prell, W., Ruddiman, W. F., Hendy, C. H., … Yvette, G. (1984). 13C Record of Benthic Foraminifera in the Last Interglacial Ocean : Implications for the Carbon Cycle and the Global Deep Water Circulation. *Quaternary Research*, *21*, 225–243.

Emiliani, C. (1953). Pleistocene temperatures. J. Geol. 63, 538-578.

Emrich, K., Ehhalt, D., & Vogel, J. (1970). Carbon Isotope Fractionation During the Precipitation of Calcium Carbonate. *Earth and Planetary Science Letters*, *8*(September 1969), 363–371.

Epstein, S., Buchsbaum, R., Lowenstam, H., & Urey, H. (1953). Revised Carbonate-Water Isotopic Temperature Scale. *Geological Society of America Bulletin*, *11*, 1315–1326. doi:10.1130/0016-7606(1953)64

Foster, G.L. (2008). Seawater pH, pCO2 and [CO2−3] variations in the Caribbean Sea over the last 130 kyr: A boron isotope and B/Ca study of planktic foraminifera. *Earth and Planetary Science Letters*, *271*(1-4), 254–266. doi:10.1016/j.epsl.2008.04.015

Foster, Gavin L., Ni, Y., Haley, B., & Elliott, T. (2006). Accurate and precise isotopic measurement of sub-nanogram sized samples of foraminiferal hosted boron by total evaporation NTIMS. *Chemical Geology*, *230*(1-2), 161–174. doi:10.1016/j.chemgeo.2005.12.006

Foster, G. L., von Strandmann, P. A. P., & Rae, J. W. (2010). Boron and magnesium isotopic composition of seawater. *Geochem. Geophys. Geosyst., 11,* Q08015, doi:10.1029/2010GC003201.

Friedman, I., & O'Neil, J. R. (1977). Data of Geochemistry. Chapter KK. Compilation of Stable Isotope Fractionation Factors of Geochemical Interest. US Government Printing Office.

Furst, M., Lowestam, H.A., & Burnett, D. S. (1976). Radiographic study of the distribution of boron in recent mollusc shells. *Geochim. Cosmochim. Acta, 40*, 1381–1386

Gabitov, R. I., Watson, E. B., & Sadekov, A. (2012). Oxygen isotope fractionation between calcite and fluid as a function of growth rate and temperature: An in situ study. *Chemical Geology*, *306-307*, 92–102. doi:10.1016/j.chemgeo.2012.02.021

Grossman, E., & Ku, T. (1986). Oxygen and carbon isotope fractionation in biogenic aragonite: Temperature effects. *Chemical Geology*, *59*, 59–74.

Hansson, I. (1973). A new set of pH-scales and standard buffers for sea water. *Deep-Sea Research*, *20*, 479–491.

Hemming, N G, & Hanson, G. N. (1992). Boron isotopic composition and concentration in modern marine carbonates. *Geochimica et Cosmochimica Acta*, *56*, 537–543.

Hemming, N Gary, Reeder, R. J., & Hanson, G. N. (1995). Mineral-fluid partitioning and isotopic fractionation of boron in synthetic calcium carbonate. *Geochimica et Cosmochimica Acta*, *59*(2), 371–379.

Hershey, J. P., Fernandez, M., Milne, P. J., Millero, J., & Hal, F. (1986). The ionization of boric acid in NaCI , Na-Ca-Cl and Na-Mg-Cl solutions at 25 ° C. *Geochimica et Cosmochimica Acta*, *50*(4), 143–148.

Hoefs, J. (2009). Stable Isotope Geochemistry. Sixth Edition. Springer. 285p.

Hönisch, B., Hemming, N. G., Grottoli, a. G., Amat, a., Hanson, G. N., & Bijma, J. (2004). Assessing scleractinian corals as recorders for paleo-pH: Empirical calibration and vital effects. *Geochimica et Cosmochimica Acta*, *68*(18), 3675–3685. doi:10.1016/j.gca.2004.03.002

Hönisch, Bärbel, Hemming, N. G., & Loose, B. (2007). Comment on "A critical evaluation of the boron isotope-pH proxy: The accuracy of ancient ocean pH estimates" by M. Pagani, D. Lemarchand, A. Spivack and J. Gaillardet. *Geochimica et Cosmochimica Acta*, *71*(6), 1636–1641. doi:10.1016/j.gca.2006.07.045

Jimenez-Lopez, C., Caballero, E., Huertas, F. J., & Romanek, C. S. (2001). Chemical, mineralogical and isotope behavior, and phase transformation during the precipitation of calcium carbonate minerals from intermediate ionic solution at 25 ° C. *Geochimica et Cosmochimica Acta*, *65*(19), 3219–3231.

Jiménez-López, C., Romanek, C. S., Huertas, F. J., Ohmoto, H., & Caballero, E. (2004). Oxygen isotope fractionation in synthetic magnesian calcite. *Geochimica et Cosmochimica Acta*, *68*(16), 3367–3377. doi:10.1016/j.gca.2003.11.033

Kakihana, H., Kotaka, M., Satoh, S., Nomura, M., & Okamoto, M. (1977). Fundamental Studies on the Ion-Exchange Separation of Boron Isotopes. *Bulletin of the Chemical Society of Japan*, *50*(1), 158–163.

Kim, S-T., Hillaire-Marcel, C., & Mucci, A. (2006). Mechanisms of equilibrium and kinetic oxygen isotope effects in synthetic aragonite at 25°C. *Geochimica et Cosmochimica Acta*, *70*(23), 5790–5801. doi:10.1016/j.gca.2006.08.003

Kim, S-T., & O'Neil, J. (1997). Equilibrium and nonequilibrium oxygen isotope effects in synthetic carbonates. *Geochimica et Cosmochimica Acta*, *61*(16), 3461–3475.

Kitano, Y., Okumura, M., & Idogaki, M. (1978). Coprecipitation of borate-boron with calcium carbonate. *Geochemical Journal*, *12*, 183–189.

Kitano, Y., Okumura, M., & Idogaki, M. (1979). Influence of borate-boron on crystal form of calcium carbonate. *Geochemical Journal*, *13*, 223–224.

Klochko, K., Cody, G. D., Tossell, J. A., Dera, P., & Kaufman, A. J. (2009). Re-evaluating boron speciation in biogenic calcite and aragonite using 11B MAS NMR. *Geochimica et Cosmochimica Acta*, *73*(7), 1890–1900. doi:10.1016/j.gca.2009.01.002

Klochko, K., Kaufman, A. J., Yao, W., Byrne, R. H., & Tossell, J. a. (2006). Experimental measurement of boron isotope fractionation in seawater. *Earth and Planetary Science Letters*, *248*(1-2), 276–285. doi:10.1016/j.epsl.2006.05.034

Lea, D., Pak, D., & Spero, H. (2000). Climate impact of late quaternary equatorial pacific sea surface temperature variations. *Science (New York, N.Y.)*, *289*(5485), 1719–24. Retrieved from http://www.ncbi.nlm.nih.gov/pubmed/10976060

Liu, Y., & Tossell, J. (2005). Ab initio molecular orbital calculations for boron isotope fractionations on boric acids and borates. *Geochimica et Cosmochimica Acta*, *69*(16), 3995–4006. doi:10.1016/j.gca.2005.04.009

Lynch-Stieglitz, J., Stocker, T. F., Broecker, W. S., & Fairbanks, R. G. (1995). The Influence of Air-Sea Exchange on the Isotopic Composition of Oceanic Carbon: Observations and Mo. *Global Biogeochemical Cycles*, *9*(4), 653–665.

McCrea, J. M. (1950). On the isotopic chemistry of carbonates and a paleotemperature scale. *Journal of Chemical Physics*, *18*(6), 849–857.

Mercury CSD 2.0 - new features for the visualization and investigation of crystal structures, C. F. Macrae, I. J. Bruno, J. A. Chisholm, P. R. Edgington, P. McCabe, E. Pidcock, L. Rodriguez- Monge, R. Taylor, J. van de Streek and P. A. Wood. (2008). *J. Appl. Cryst*., 41, 466-470.

Mickler, P. J., Banner, J. L., Stern, L., Asmerom, Y., Edwards, R. L., & Ito, E. (2004). Stable isotope variations in modern tropical speleothems: Evaluating equilibrium vs. kinetic isotope effects. *Geochimica et Cosmochimica Acta*, *68*(21), 4381–4393. doi:10.1016/j.gca.2004.02.012

Milliman, J. D. (1974). Marine Carbonates. Springer-Verlag (1974), 375p.

Mix, A. C., & Fairbanks, R. G. (1985). North Atlantic surface-ocean control of Pleistocene deep-ocean circulation. *Earth and Planetary Science Letters*, *73*, 231–243.

Mook, W., Bommerson, J., & Staverman, W. (1974). Carbon isotope fractionation between dissolved bicarbonate and gaseous carbon dioxide. *Earth and Planetary Science Letters*, *22*, 169–176.

Mook, W. & de Vriess, J. (2000). Environmental Isotopes in the Hydrological Cycle. Principles and Applications. Volume 1: Introduction - Theory, Methods, Review.

Mucci, A. (1986). Influence of temperature on the composition of magnesian calcite overgrowths precipitated from seawater. *Geochimica et Cosmochimica Acta*, *51*, 1977–1984.

Mucci, Alfonso, & Morse, J. W. (1982). The incorporation of Mg and Sr into calcite overgrowths : influences of growth rate and solution composition. *Geochimica et Cosmochimica Acta*, *47*, 217–233.

O’Neil, J. R., Adami, L. H. and Epstein, S. (1975). Revised value for the ^{18}O fractionation between CO_2 and H_2O at 25^0C. *Journal of Research of the U.S. Geological Survey*, *3(5)*, 623-624.

Oppo, D. W., & Fairbanks, R. G. (1987). Variability in the deep and intermediate water circulation of the Atlantic Ocean during the past 25,000 years : Northern Hemisphere modulation of the Southern Ocean. *Earth and Planetary Science Letters*, *86*, 1–15.

Pagani, M., Lemarchand, D., Spivack, A., & Gaillardet, J. (2005). A critical evaluation of the boron isotope-pH proxy: The accuracy of ancient ocean pH estimates. *Geochimica et Cosmochimica Acta*, *69*(4), 953–961. doi:10.1016/j.gca.2004.07.029

Paquette, J., & Reeder, R. J. (1995). Relationship between surface structure , growth mechanism , and trace element incorporation in calcite. *Science*, *59*(4), 735–749.

Pearson, P. N., & Palmer, M. R. (2000). Atmospheric carbon dioxide concentrations over the past 60 million years. *Nature*, *406*(6797), 695–9. doi:10.1038/35021000

Raymo, M. E., Ruddiman, W. F., Shackleton, N. J., & Oppo, D. W. (1990). Evolution of Atlantic-Pacific d13C gradients over the last 2.5 m.y. *Earth and Planetary Science Letters*, *97*, 353–368.

Rollion-Bard, C., Erez, J., & Zilberman, T. (2008). Intra-shell oxygen isotope ratios in the benthic foraminifera genus Amphistegina and the influence of seawater carbonate chemistry and temperature on this ratio. *Geochimica et Cosmochimica Acta*, *72*(24), 6006–6014. doi:10.1016/j.gca.2008.09.013

Rollion-Bard, Claire, Chaussidon, M., & France-Lanord, C. (2011). Biological control of internal pH in scleractinian corals: Implications on paleo-pH and paleo-temperature reconstructions. *Comptes Rendus Geoscience*, *343*(6), 397–405. doi:10.1016/j.crte.2011.05.003

Romanek, C., Grossman, E., & Morse, J. (1992). Carbon isotopic fractionation in synthetic aragonite and calcite : Effects of temperature and precipitation rate. *Geochimica et Cosmochimica Acta*, *56*, 419–430.

Romanov, D., Kaufmann, G., & Dreybrodt, W. (2008). δ13C profiles along growth layers of stalagmites: Comparing theoretical and experimental results. *Geochimica et Cosmochimica Acta*, *72*(2), 438–448. doi:10.1016/j.gca.2007.09.039

Rosenbaum, J., & Sheppard, S. (1986). An isotopic study of siderites, dolomites and ankerites at high temperatures*. *Geochimica et Cosmochimica Acta*, *50*(645), 4–7.

Rubinson, M., & Clayton, R. N. (1969). Carbon-13 fractionation between aragonite and calcite. *Geochimica et Cosmochimica Acta*, *33*, 997–1002.

Ruiz-Agudo, E., Putnis, C. V., Kowacz, M., Ortega-Huertas, M., & Putnis, a. (2012). Boron incorporation into calcite during growth: Implications for the use of boron in carbonates as a pH proxy. *Earth and Planetary Science Letters*, *345-348*, 9–17. doi:10.1016/j.epsl.2012.06.032

Sanyal, A, Hemming, N. G., Hanson, G. N., & Broecker, W. (1995). Evidence for a higher pH in the glacial ocean from boron isotopes in foraminifera. *Nature*, *373*, 234–236.

Sanyal, A, Nugent, M., Reeder, R. J., & Bijma, J. (2000). Seawater pH control on the boron isotopic composition of calcite : Evidence from inorganic calcite precipitation experiments. *Geochimica et Cosmochimica Acta*, *64*(9), 1551–1555.

Sanyal, Abhijit, Bijma, J., Spero, H. J., & Lea, D. W. (2001). Empirical relationship between pH and the boron isotopic composition of Globigerinoides sacculifer: Implications for the boron isotope paleo-pH proxy. *Paleoceanography*, *16*(5), 515–519.

Schauble, E. a., Ghosh, P., & Eiler, J. M. (2006). Preferential formation of 13C–18O bonds in carbonate minerals, estimated using first-principles lattice dynamics. *Geochimica et Cosmochimica Acta*, *70*(10), 2510–2529. doi:10.1016/j.gca.2006.02.011

Schwarcz, H. P., Agyei, E. K., & Mcmullen, C. C. (1969). Boron Isotopic Fractionation During Clay Adsorption From Seawater. *Earth and Planetary Science Letters*, *6*, 1–5.

Sen, S., Stebbins, J. F., Hemming, N. G., & Ghosh, B. (1994). Coordination environments of B impurities in calcite and aragonite polymorphs; A ^{11} B MAS NMR study. *American Mineralogist, 79*, p. 819-825

Sharma, T., & Clayton, R. N. (1985). Measurement of O18/O16 ratios of total oxygen of carbonates. *Geochimica et Cosmochimica Acta*, *29*, 1347–1353.

Spero, H. J., Bijma, J., Lea, D. W., & Bemis, B. E. (1997). Effect of seawater carbonate concentration on foraminiferal carbon and oxygen isotopes. *Nature*, *390*, 497–500.

Tarutani, T., Clayton, R. N., & Mayeda, T. K. (1969). The effect of polymorphism and magnesium substitution on oxygen isotope fractionation between calcium carbonate and water. *Geochimica et Cosmochimica Acta*, *33*, 987–996.

Tossell, J. a. (2006). Boric acid adsorption on humic acids: Ab initio calculation of structures, stabilities, 11B NMR and 11B,10B isotopic fractionations of surface complexes. *Geochimica et Cosmochimica Acta*, *70*(20), 5089–5103. doi:10.1016/j.gca.2006.08.014

Turner, J. V. (1982). Kinetic fractionation of carbon-13 during calcium carbonate precipitation. *Geochimica et Cosmochimica Acta*, *46*(7), 1183–1191. doi:10.1016/0016-7037(82)90004-7

Urey, H. C. (1947). The Thermodynamic Properties of Isotopic Substances. *Journal of the Chemical Society,* 562-581.

Usdowski, E., & Hoefs, J. (1990). Kinetic 13C/12C and 18O/16O effects upon dissolution and outgassing of CO2 in the system CO2-H2O. *Chemical Geology (Isotope Geosciences Edition)*, *80*, 109–118.

Vengosh, A., Kolodny, Y., Starinsky, A., Chivas, A. R., & McCulloch, M. T. (1991). Coprecipitation and isotopic fractionation of boron in modern biogenic carbonates. *Geochimica et Cosmochimica Acta*, *55*(10), 2901–2910. doi:10.1016/0016-7037(91)90455-E

Venz, K. A., & Hodell, D. A. (2002). New evidence for changes in Plio ^ Pleistocene deep water circulation from Southern Ocean ODP Leg 177 Site 1090. *Palaeogeography, Palaeoclimatology, Palaeoecology*, *182*, 197–220.

Vincent, E., & Berger, W. H. (1985). Carbon Dioxide and Polar Cooling in the Miocene: The Monterey Hypothesis. *Geophysical Monograph Series*, *32*, 455–468.

Winograd, I. J., & Pearson F. J. Jr. (1976). Major carbon 14 anomaly in a regional carbonate aquifer: Possible evidence for megascale channeling. *South Central Great Basin, Water Resour. Res., 12(6)*, 1125–1143, doi:10.1029/WR012i006p01125.

Zachos, J. C., Dickens, G. R., & Zeebe, R. E. (2008). An early Cenozoic perspective on greenhouse warming and carbon-cycle dynamics. *Nature*, *451*(7176), 279–83. doi:10.1038/nature06588

Zachos, J., Pagani, M., Sloan, L., Thomas, E., & Billups, K. (2014). Trends , Global Rhythms , Aberrations to Present in. *Science*, *292*(5517), 686–693.

Zeebe, R. (2007). An explanation of the effect of seawater carbonate concentration on foraminiferal oxygen isotopes. *Geochimica et Cosmochimica Acta*, *63*(13), 2001–2007.

Zeebe, R. E., Sanyal, A., Ortiz, J. D., & Wolf-Gladrow, D. A. (2001). A theoretical study of the kinetics of the boric acid–borate equilibrium in seawater. *Marine Chemistry*, *73*(2), 113–124. doi:10.1016/S0304-4203(00)00100-6

Zeebe, R. E., Wolf-Gladrow, D. A., & Jansen, H. (1999). On the time required to establish chemical and isotopic equilibrium in the carbon dioxide system in seawater. *Marine Chemistry*, *65*(3-4), 135–153.

Zhou, G.-T., & Zheng, Y.-F. (2003). An experimental study of oxygen isotope fractionation between inorganically precipitated aragonite and water at low temperatures. *Geochimica et Cosmochimica Acta*, *67*(3), 387–399.

Zuddas, P., & Mucci, A. (1994). Kinetics of calcite precipitation from seawater : I . A classical chemical kinetics description for strong electrolyte solutions. *Science*, *58*(20), 4353–4362.

CHAPTER 3:

ABIOTIC CARBONATE SYNTHESIS TECHNIQUES IN STABLE ISOTOPE GEOCHEMISTRY

INVITED REVIEW

Abiotic Carbonate Synthesis Techniques in Stable Isotope Geochemistry

Jillian Wyman[a*] and Sang-Tae Kim[a]

[a]School of Geography and Earth Sciences, McMaster University, 1280 Main Street West, Hamilton, ON L8S 4K1, Canada

*Corresponding author: Jillian Wyman (wymanjv@mcmaster.ca)

In preparation for: Chemie der Erde

3.1 Introduction

Calcium carbonates, such as foraminifera and speleothems, are ubiquitous on Earth's surface and are essential subjects of study to the field of paleoclimatology. Their global presence and importance in the geologic record has yielded extensive investigation into calcium carbonate precipitation behaviour in aqueous solutions. In particular, paleoclimate proxies using stable isotope and/or trace element concentrations of marine or continental carbonates largely rely on laboratory calibration studies in which carbonates are synthesized and their geochemical properties are carefully quantified. The precipitation of calcium carbonates has been examined comprehensively in the field of stable isotope geochemistry subsequent to McCrea's (1950) pioneering study. The proposed paleotemperature scale is founded upon the temperature-dependent oxygen isotope fractionation between carbonate and water under equilibrium precipitation conditions. While the past five decades have witnessed innumerate follow-up studies employing a wide variety of experimental techniques to synthesize calcium carbonate minerals, several key innovative studies have markedly improved the approach in its entirety (e.g., Gruzensky, 1967; Tarutani et al., 1969; Romanek et al., 1992; Jiménez-López et al., 2004; Kim et al., 2006, 2007; Dietzel et al., 2009; Gabitov et al., 2012). These methods have been continually modified to satisfy current research needs, reflect improved technological advancements, and comply with intra-laboratory equipment intricacies. This review summarizes and differentiates the most common abiotic carbonate synthesis techniques, which can be distinguished by four broad approaches: (1) free drift; (2) degassing; (3) constant addition and (4) CO_2 diffusion.

Since McCrea (1950) published the first temperature-based oxygen isotope fractionation relationship between calcite and water, various novel precipitation techniques have been developed to improve upon the current understanding of equilibrium oxygen, carbon and calcium isotope fractionation between carbonate minerals and water. Differences between the oxygen isotope fractionation factors proposed by Kim and O'Neil (1997) and Gabitov et al. (2012) can be attributed to experimental intricacies associated with different precipitation methods. Researchers must carefully consider the method by which to grow abiogenic carbonates, as complexities specific to each technique can play a significant role in their success in research. The specific need for thermal, chemical and/or isotopic equilibrium conditions must be assessed independently to determine which technique is most appropriate for the desired experimental purpose. This review paper will chronicle the development of carbonate synthesis techniques over the last fifty years in the field of stable isotope geochemistry, thus providing a foundation upon which future studies can base their research objectives and optimize their research methodology.

3.2 Seeded versus non-seeded growth experiments

Calcium carbonate minerals can be synthesized by one of two precipitation mechanisms: spontaneous nucleation (homogeneous growth) or seeded nucleation (heterogeneous growth). The former is characterized by the absence of a solid interface (e.g., Garside, 1982) while the latter occurs in the presence of a solid interface (e.g., Romanek et al., 1992). These are differentiated by precipitation processes and rate constants, although this variation has proven difficult to quantify (Garside, 1982; Romanek et al., 1992). A rate constant is calculated from an individual run to distinguish crystal growth mechanisms for mineralogically pure seed; it should be constant among different runs unless different mechanisms are acting within or between runs.

The overgrowth or seeded nucleation method occurs upon crystal material ("seed") previously added to the solution prior to initiation of the precipitation experiment. The presence of seed offers several benefits over its unseeded precipitation counterpart. A state of supersaturation, and subsequent spontaneous nucleation, is not necessary for mineral growth to proceed. Unlike spontaneous precipitation experiments, the overgrowth approach allows reliable measurement of the crystal growth rate (Nancollas and Gardner, 1974; Reddy, 1977; Reddy and Wang, 1980). In their exploration of crystal growth kinetics of calcium oxalate monohydrate from supersaturated solutions, Nancollas and Gardner (1974) determined that well-characterized hydroxyapatite seed material proved accurate in measuring relative changes of ionic concentrations from the parent solution as small as 0.02 %. The use of seed crystals eliminates the nucleation process present in carbonate precipitation experiments under supersaturated conditions; mineral growth upon nuclei is the sole remaining process, isolating the measurement of growth kinetics. Seeded precipitation is therefore preferentially selected for kinetic studies examining the mechanism of calcium carbonate precipitation. The preparation of seed material also allows mineralogical control (beneficial for any carbonate experiment) with measurable and quantifiable grain sizes easily adjusted for the desired experimental purpose (Nancollas and Gardner, 1974; Romanek et al., 1992).

Seeded crystal growth thus provides an accurate simulation for studies aiming to recreate natural conditions, because precipitation invariably occurs on an already existing surface (the mineral itself or a metal with available sites for adsorption of lattice ions). As such, field conditions can be much better mimicked with seeded growth studies than via spontaneous precipitation, in which surface characteristics are not well known and vary significantly over the course of an experiment. Factors such as secondary nucleation and the effect of foreign ions can also be studied under highly reproducible conditions. The primary limiting factor to seeded precipitation experiments is the resulting isotopic heterogeneity between the seed and overgrowth (e.g., Romanek et al., 1992).

To permit accurate determination of fractionation factors, the amounts of seed and overgrowth must be carefully monitored. For example, calculation of overgrowth carbon isotope composition (δ^{13}C) requires knowledge of δ^{13}C value of initial seed, δ^{13}C value of final solid, and the associated fraction of overgrowth, which comprises the difference between final and initial solid weights divided by the final solid weight (Romanek et al., 1992). Typically, the fraction of overgrowth precipitated is quantified using the mass and concentration of the titrants added. Uncertainty in the fraction of overgrowth can lead to significant error in the quantification of isotope fractionation factor, the magnitude of which is larger for slower rate runs due to limited production of overgrowth.

Recent seeded precipitation experiments have provided important practical implications relating crystal growth with stable isotope equilibrium and fractionation processes. Dietzel et al. (2009) modeled their kinetic data against the currently accepted apparent equilibrium fractionation value proposed by Kim and O’Neil (1997) and observed a distinct trend in the oxygen isotope fractionation of calcite with varying precipitation rates. Using a secondary ion mass spectrometer (SIMS), Gabitov et al. (2012) measured oxygen isotope fractionation between calcite and water across multiple calcitic growth layers. The crystal centre was characterized by reduced oxygen isotope fractionation, implying kinetics-related alteration for spontaneous nucleation and early stages of seeded nucleation (at high growth rates). The outer edge of the crystal was marked by an increasing trend towards the previously proposed equilibrium fractionation (Kim and O’Neil, 1997), suggesting that seeded nucleation occurs nearer equilibrium at reduced growth rates. Thus, crystal growth and precipitation rates have proven to be determining factors in the method of isotopic fractionation, both theoretically and empirically (Kim and O'Neil, 1997; Dietzel et al., 2009; Gabitov et al., 2012; Watkins et al., 2013). Seeded precipitation experiments allow further investigation of the kinetic fractionation contribution to the overall isotopic fractionation within the carbonate mineral growth system.

3.3 Selected abiotic carbonate synthesis techniques

3.3.1 Free drift

Gruzensky (1967) was the founding father of free drift experiments, in which individual carbonate crystals precipitate from a sealed solution. His procedure set the stage for a plethora of follow-up studies (e.g., Paquette and Reeder, 1990, 1995; Lemarchand et al., 2004; Hemming et al., 2005; Gabitov et al., 2012). A prepared parent solution is left to interact with escaping gaseous carbon dioxide, altering initial equilibrium conditions and therefore solution pH. Free drift carbonate mineral synthesis studies can be employed in both open and closed systems. Often, multi-minerals are produced as a result of solution heterogeneity and differing growth mechanisms, yielding data difficult to interpret (Rubinson and Clayton, 1969; Emrich et al., 1970; Turner, 1982). Certain open system methods offer greater mineralogical, chemical, and isotope control over the course of precipitation; these variables have been maintained simultaneously by Morse (1974) and Romanek et al. (1992), using the pH-stat and chemo-stat techniques, respectively.

Carbonate precipitation occurs once the experimental solution reaches supersaturated conditions with respect to a specific polymorph of $CaCO_3$ (i.e., calcite or aragonite). While the concentration of calcium ions in the parent solution is assumed constant during the course of each experiment, it is important to quantify the amount of calcium ions removed from the solution through precipitation and concentration of the dissolved CO_3^{2-} species in the experimental solution to determine the saturation index of the solution (Lemarchand et al., 2004).

In the classic approach, illustrated in Figure 3.1, solid ammonium carbonate sublimates to produce NH_3 and CO_2. Under ambient conditions, ammonium carbonate crystals decompose according to the following reaction:

$$(NH_4)_2CO_3 \rightarrow 2NH_3(g) + CO_2(g) + H_2O(g)$$

Gaseous species NH_3 and CO_2 then dissolve and diffuse into an aqueous solution of calcium and ammonium chloride ($CaCl_2{\cdot}NH_4Cl$), with further dissociation occurring as a function of solution temperature and salinity according to the equilibrium reaction schemes described in Lemarchand et al. (2004). These reactions yield an increase in both total alkalinity and pH of the solution, and thus enhance supersaturation conditions with respect to calcite: $\Omega = [Ca^{2+}][CO_3^{2-}]/K_{sp}$, where K_{sp} represents the solubility product of calcite in the experimental solution. The degree of supersaturation is controlled by the rate of CO_2 gas supply to the system via sublimation. Upon reaching the targeted value, carbonate (i.e., calcite or aragonite) crystals nucleate along the aqueous surface, beaker walls, and substrate of the immersed glass tubing. The beakers are titrated with an aqueous solution of ammonium carbonate to achieve desired carbonate alkalinity values, limiting the development of significant pH gradients.

Jiménez-López et al. (2001, 2004) innovated the free-drift system to enable control over the carbonic acid system, and thus pH, stabilizing isotopic equilibrium over the course of carbonate precipitation. A closed-system approach was adapted to examine the effect of progressive dissolution and investigate the influence of recrystallization reactions on calcium carbonate precipitation kinetics and isotopic partitioning. In this experiment, pH was maintained while the chemical composition (i.e., Ca^{2+}) of the solution drifted towards chemical equilibrium. Crystal growth upon the induced nuclei was driven primarily by the dissolution of NH_3 into the reacting solution from an underlying reservoir of ammonium acetate (NH_4Ac), while calcium was removed from solution via calcium carbonate precipitation of solid carbonate; pH was thus maintained by the hydrolysis of ammonia gas. The carbonic acid system chemistry remained stable while solution saturation state approached equilibrium as precipitation ensued. Parent solution consisting of $CaCl_2$, $MgCl_2$ and $NaHCO_3$ was placed within watch glasses supported by pedestals atop an argon-rich enclosure. An NH_4Ac reservoir underlying the pedestals evaporated NH_3 into the system, which then dissolved within the parent solution, driving spontaneous nucleation and resultant magnesian calcite crystal growth. The carbonic acid system ensured a relatively constant state of isotopic equilibrium throughout carbonate precipitation. The bulk and isotope chemistry of the carbonic acid system thus remained relatively stable while the solution saturation state approached equilibrium, induced by carbonate precipitation. A pseudo-constant pH was achieved by the hydrolysis of ammonia gas simultaneous with precipitation-driven consumption of calcium ions.

Extensive investigation into the chemical and isotope compositions of free drift precipitation experiments has revealed several influencing factors responsible for variations in solution pH, including: (1) degassing of $CO_{2(aq)}$; (2) dissolution of $NH_{3(g)}$; (3) generation of H^+ during carbonate formation, and (4) dissolution of $CO_{2(g)}$ into the NH_4Ac reservoir. As noted in Jiménez-López et al. (2001), the first factor, degassing of $CO_{2(aq)}$ from the parent solution, is an important consideration in the initial experimental stage. This period is marked by significant gaseous exchange between the master and NH_4Ac solutions and resultant increase in $\delta^{13}C$ value of dissolved inorganic carbon (DIC). CO_2 outgassing may yield the preferential escape of lighter isotopes due to the relative diffusion coefficients for molecules of different mass (Usdowski and Hoefs, 1990). No correlation between oxygen isotope fractionation and the mineralogy of the precipitate was observed over the experimental duration. Likewise, when the initial gas phase comes into physical contact with the master solution, $CO_{2(g)}$ is exsolved from solution and solution pH consequentially increase according to the following chemical reactions: $CO_3^{2-}{}_{(aq)} + 2H^+{}_{(aq)} \rightleftharpoons HCO_3^-{}_{(aq)} + H^+{}_{(aq)} \rightleftharpoons H_2CO_3^-{}_{(aq)} \rightleftharpoons H_2O_{(l)} + CO_{2(g)}$. Over time, the degree of disequilibrium is diminished as a constant pCO_2 is reached. An increase in pH can also be attributed to the dissolution of $NH_{3(g)}$ in the master solution based on the equilibria $H_2O_{(l)} + NH_{3(g)} \rightleftharpoons NH_4^+{}_{(aq)} + OH^-{}_{(aq)}$. Assuming the system approached chemical equilibrium, this dissolution would require the pH of the parent solution to increase ~1 pH unit over the course of an experiment. The exsolution of $CO_{2(aq)}$ from the master solution into the headspace and underlying NH_4Ac reservoir act as a sink for CO_2, raising the pH in the master solution.

3.3.2 Degassing

A well-differentiated subset of the free drift method, the degassing technique involves the removal of dissolved gas from its aqueous housing solution. That is, solutions are continuously bubbled with a CO_2/N_2 gas mixture; the onset of precipitation is associated with drifting solution chemistry and pH as calcium and carbonate ions are consumed. "Passive" degassing can be differentiated from "forced" degassing primarily by the hastened reaction speed. Forced, or active, degassing typically involves bubbling of pre-purified nitrogen gas (saturated with water of identical oxygen isotope composition as the parent solutions) through the solution to remove carbon dioxide present in the parent solution. Passive degassing does not bubble nitrogen gas but rather allows the carbon dioxide to degas freely into the overlying headspace. The two experimental setups, depicted in Figure 3.2a and 3.2b, closely resemble one another. Both methods achieve chemical equilibrium and subsequently induce supersaturation, spontaneous nucleation, and resultant calcium carbonate mineral precipitation according to the following reaction scheme (Kim et al., 2007):

$$H_2O + CO_{2(aq)} \rightleftharpoons H_2CO_{3(aq)}$$
$$Ca^{2+}_{(aq)} + 2HCO^-_{3\,(aq)} \rightleftharpoons CaCO_{3(s)} + H_2CO_{3(aq)}$$

In accordance with Le Chatelier's principle, the inter-media pCO_2 differential necessitates degassing of CO_2 to the surrounding atmosphere. Solution chemistry and pH values slowly drift as a result of the degassing and consumption of calcium and carbonate ions during precipitation. Reduced experimental duration may minimize these shifts in pH. While this technique was first employed to synthesize calcite at thermal equilibrium, solutions were stored at temperatures differing from their precipitation conditions, potentially resulting in isotopic and chemical disequilibrium as these processes do not occur at the same rate (Beck et al., 2005). Assuming a mid-pH range of 8.0-8.7, the low temperature solutions (13.6, 18.0, 19.9 °C) would have required approximately 8 hours to establish isotopic equilibrium (as extrapolated from Beck et al., 2005); even colder temperatures necessitate equilibration times on the scale of days to weeks. Without establishing baseline equilibrium conditions, the measured oxygen isotope composition of calcium carbonate ($\delta^{18}O_{carbonate}$) does not accurately reflect the system temperature. Kim et al. (2007) updated these findings by providing sufficient time for both chemical and isotopic equilibrium to be achieved based upon solution pH and temperature.

Kim et al. (2007) employed the passive degassing technique to synthesize aragonite at 0 and 25 °C. Upon thermal and isotopic equilibration of DIC, rapid bubbling of CO_2 ensued to increase solubility prior to the addition of $MgCl_2•6H_2O$ and $CaCl_2•2H_2O$. Once mixed, the solution was sealed and CO_2 was allowed to degas into the headspace of the container causing precipitation of $CaCO_3$ as aragonite dictated by the Mg:Ca molar ratio of 4:1. The reported aragonite-water fractionation factor is consistent with that obtained by both forced degassing and constant addition techniques (Kim et al., 2007).

A slightly different approach was taken by Tarutani et al. (1969), in which carbon dioxide was bubbled through a solution containing sodium bicarbonate and sodium chloride to precipitate calcite or calcite-vaterite mixtures. This approach renders it difficult to constrain the mineralogy of precipitates. Moreover, upon addition of all chemical components, the solution was immediately prepared for precipitation. The reduced reproducibility observed at lower temperatures can be attributed to inadequate time allotment for thermal and isotopic equilibrium to be achieved (Beck et al., 2005). In addition, to minimize the isotopic change in parent solution over the course of carbonate precipitation due to evaporation, the nitrogen gas was run through with water of equal oxygen isotope composition to the parent solution. Carbonate precipitation occurred once water-saturated N_2 removed sufficient CO_2 to initiate spontaneous nucleation (e.g., Tarutani et al., 1969).

Since precise quantification of precipitation rate was not possible due to spontaneous nucleation of carbonate at the onset of precipitation using this technique, Tarutani et al. (1969) altered the nitrogen flow rate during inorganic carbonate synthesis. Precipitation rate and $1000\ln\alpha_{\text{carbonate-water}}$ were determined to be independent of one another under these experimental conditions, ruling out the influence of growth rate on biogenic carbonate oxygen isotopic fractionation.

In an effort to reinvestigate and ascertain this reported relationship, Kim and O'Neil (1997) modified the traditional degassing experimental setup and installed an apparatus designed for two different types of bubbling. Pure CO_2 gas was bubbled through their sodium bicarbonate solution then, once thermal equilibrium was established, water-saturated nitrogen gas was introduced slowly through the solutions to remove CO_2 (Kim and O'Neil, 1997). The apparatus is connected in series, ensuring equal flow of nitrogen gas throughout. To explore factors influencing precipitation rate, Kim and O'Neil (1997) altered the bubble size and frequency, with Type I producing large bubbles sequentially by passing nitrogen gas through a tube with no constriction, and Type II generating many small bubbles at once by passing nitrogen gas through a glass frit filter. The latter yielded a higher pH (~ 0.5 units), indicating it to be the more effective approach for removal of carbon dioxide. Kim and O'Neil (1997) observed precipitation rate to vary as a function of flow rate, bubble size, and CO_2 removal. As a result, they refined three fractionation relationships ($\alpha_{\text{calcite-H2O}}$, $\alpha_{\text{otavite-H2O}}$ and $\alpha_{\text{witherite-H2O}}$), provided insight into non-equilibrium fractionation behaviour in carbonates and presented evidence linking calcium carbonate isotope fractionation behavior with precipitation rate.

An apparent drawback of the degassing technique is the inability to maintain initial chemical and isotope equilibrium conditions. Onset of precipitation is marked by the removal of Ca^{2+}, CO_2, and CO_3^{2-} from solution, thereby altering chemical and isotopic equilibrium. Jiménez-López and Romanek (2004) employed the degassing technique to quantify the carbon isotope composition of siderite ($\delta^{13}C_{carbonate}$) and attributed drift in their $\delta^{13}C_{carbonate}$ values to the continuous exsolution of $CO_{2(g)}$ from solution, rendering it difficult to accurately quantify carbon isotope fractionation. McCrea's (1950) groundbreaking study has since been widely improved upon, as experimental procedures have been tweaked to establish initial chemical and isotopic equilibrium, as well as to minimize chemical and isotopic drift of oxygen throughout precipitation (e.g., Kim and O'Neil, 1997; Kim et al., 2007). Control over carbon isotope composition is also being actively tested.

3.3.3 Constant addition

The constant addition method exists as a culmination of past techniques, encompassing the "fluidized bed" (e.g., Chou and Wollast, 1984; Chou et al., 1989), "chemo-stat" (e.g., Mucci and Morse, 1983; Romanek et al., 1992) and "pH-stat" (e.g., Lorens, 1981; Kazmierczak et al., 1982) approaches with suitable modifications implemented as required. This technique was devised to control isotopic and chemical equilibrium of the parent solution by continuously adding CO_3^{2-} ions to replace those consumed during precipitation (Mucci and Morse, 1984; Kim et al., 2006, 2007). The constant addition system requires a steady state environment for carbonate precipitation spanning the course of the experiment, providing reliable measurements of the crystal growth rate in both the presence and absence of additive substances (i.e., seed) (Reddy and Wang, 1980).

The "fluidized bed" reactor emerged as the earliest version of the constant addition system in the nineteen eighties. The premise of this reactor is centred on fluid mechanics, adjusting flow to ensure fluid velocity is equal to the steady state of the solid particles in constant suspension; a particle that has escaped to the less dense overhead medium will immediately fall back to the fluidized bed below (Chou and Wollast, 1984). Therefore, it is possible to obtain a homogeneous suspension for a given height and flow rate of the fluid. By altering the pumping rate, and thereby the renewal of fresh solution, it is possible to vary the residence time and concentration of the fluid in the reactor. This approach possesses a distinct advantage over other methods as it allows evaluation of various chemical conditions without manipulating the solid phase, but instead by abruptly altering the composition of the input solution and ensuring a constant input supply of reactants (Chou et al., 1989). Difficulty arises in the maintenance of steady state conditions. These fluctuations alter solution pH and ion concentrations, which in turn affect the saturation state and overall precipitation kinetics under study.

Inspired by the fluidized bed reactor, Zhong and Mucci (1993) introduced an appropriate alternative to this method, the "constant addition" system. The original version was modified with two sequential changes: addition of a gas phase, and the cease of circulation within the reacting solution. The introduction of a gas phase to the system promotes mixing of the solid and liquid phases in the solution and holds constant the

$p\mathrm{CO}_2$ at a predetermined value (Zhong and Mucci, 1993). Meanwhile, solution would no longer be removed from the reacting chamber, greatly simplifying the technique.

In the constant addition system, designed by Mucci and Morse (1982) in its infancy, reactant solution is simply added to the reactor at a constant rate, thereby attaining and maintaining steady state conditions throughout the experimental duration. This method is characterized by the addition of two titrant solutions containing DIC and calcium ion species, respectively. A fully saturated (with respect to a given calcium carbonate polymorph, i.e., calcite or aragonite) bulk solution is prepared and, ideally, stored to achieve thermal, chemical and isotopic equilibrium. Upon establishing these baseline conditions, precipitation is initiated by slowly injecting the two titrant solutions into the parent solution, creating a state of supersaturation and resultant calcium carbonate precipitation. Carefully crafted chemical conditions, ensuring replenishment of ions via titrant addition, allows chemical and isotopic equilibrium to be maintained independent of experimental duration (Romanek et al., 1992; Kim et al., 2006). As hypothesized by Zuddas and Mucci (1994), equilibrium conditions within the constant addition system rely on finely tuned precipitation rate, which is dictated by titrant injection rate.

One subset of the constant addition system is the “chemo-stat” technique, in which mineral precipitation reactions are conducted in an open system over a wide range of precipitation rates. Constant composition conditions are achieved through the use of a dual syringe pump that dispenses two titrants in equal amounts. The temperature of solutions is held constant by circulating water from a temperature-controlled water bath and a water-jacketed glass reaction vessel. Romanek et al. (1992) adapted the "open-system chemo-stat" technique used by Mucci and Morse (1983) to study supersaturation and carbon isotope composition conditions. In this modified approach, Romanek et al. (1992) maintained supersaturation of the parent solution and precipitated carbonate under various precipitation rates and temperatures, subsequently measuring carbon isotope fractionation factors $\alpha_{\text{CO2-calcite}}$ and $\alpha_{\text{CO2-aragonite}}$ under known chemical, isotopic and thermal equilibrium using seeded carbonate overgrowth. Another division of the constant addition system, the "pH-stat" method was developed to advance the seeded growth technique by allowing the kinetics of crystallization to be studied over a broad spectrum of supersaturation states under constant pH conditions. Both "chemo-stat" and "pH-stat" methods can be conducted with or without seed as resources allow; seeded crystal synthesis allows researchers to control mineralogy however the procedure is further complicated by correction factors to differentiate crystal overgrowth from the internal seeding.

Within the constant addition umbrella system, difficulty can be encountered using the highly sensitive "chemo-stat" approach, which often requires several rounds of experimentation before achieving a successful run, necessarily defined by a stable solution composition. Typically, the onset of each experimental run is marked by dynamic fluctuations dependent on the reaction rate and the difference between initial and steady-state boundary conditions. The "pH-stat" system is also not without its challenges, requiring a truly closed system to prevent gas exchange between the air and solution and subsequent alteration of $p\text{CO}_2$ values. In addition, analytical uncertainty is introduced due to electrode drift over the course of a precipitation; to minimize error, the controller should be bypassed entirely and syringe pump injection should proceed directly into the solution.

Control over chemical and isotopic equilibrium was greatly enhanced by the addition of carbonate-forming ions (e.g., Ca^{2+} and CO_3^{2-}) to replace those consumed by precipitation, as employed by Mucci and Morse (1983), Romanek et al. (1992) and Kim et al. (2006, 2007). In the "open-system chemo-stat" technique (Mucci and Morse, 1983) adaptation by Romanek et al. (1992), stock solution containing $NaHCO_3$, NaCl, and $CaCl_2 \cdot H_2O$ was bubbled with a CO_2/N_2 mixture to ensure the solution was undersaturated with respect to $CaCO_3$. Two titrants containing $CaCl_2$ and $NaHCO_3$ were also prepared. A CO_2/N_2 gas mixture was actively bubbled through the carbon-bearing solutions to maintain carbon isotopic equilibrium. Selected seed material (i.e., calcite or aragonite depending on the desired precipitated polymorph) was then added to the stock solution to initiate precipitation, providing a nucleus upon which overgrowth proceeded. Both titrants were continuously injected into the stock solution using a peristaltic pump to maintain supersaturation and precipitation by replenishing calcium and carbonate ions. Injection rate and solution chemistry controlled the precipitation rate. The experiment was conducted under temperature-controlled conditions using a circulating water bath to maintain thermal equilibrium. The addition of titrant solution and ongoing stirring of the solution ensured initial chemical equilibrium conditions were held constant over the experimental duration, while continuous bubbling of CO_2/N_2 gas mixture through the $NaHCO_3$ titrant and stock solutions maintained isotopic equilibrium. With this intricate technique, the stock solution maintained a constant state of supersaturation, calcium carbonate precipitated at an adjustable temperature and precipitation rate, and the carbon isotope composition of seed overgrowth was quantified under chemical, isotopic, and thermal equilibrium conditions.

The "closed-system constant addition" method enables carbonate precipitation to occur under stable thermal, chemical and isotopic equilibrium conditions. Illustrated in Figure 3.3, Kim et al. (2006) modified the constant addition method with an experimental setup resembling the "chemo-stat" technique but without the ongoing pumping of the CO_2/N_2 gas mixture through the titrant and stock solutions. This permits relative maintenance of oxygen isotope composition of the parent solution, and thus oxygen isotope equilibrium among DIC, through replenishment of ions by titrant addition.

The constant addition method has proven effective in providing precise measurements of oxygen isotope fractionation between aragonite and water (Kim et al., 2006) in addition to carbon isotopic fractionation between calcite and DIC (Romanek et al., 1992). The experiments proceed under conditions of constant oxygen isotope composition, accomplished with the addition of titrant possessing similar isotopic composition to the parent solution. Chemical equilibrium (with respect to DIC) is achieved prior to mixing under stable titrant temperature and ongoing precipitation progress. As illustrated by Romanek et al. (1992) in their innovative "chemo-stat" design, a continuous stream of CO_2/N_2 mixture through both the titrant and bulk solution is required to maintain a constant carbon isotope composition ($\delta^{13}C_{DIC}$). This approach, however, is associated with drifting oxygen isotope composition ($\delta^{18}O_{H2O}$). Such a limitation may be remedied by ensuring prior equilibration of CO_2 with the parent solution, although this has yet to be tested. Minimizing the off-gassing of CO_2 may also reduce carbon isotope composition drift of the solution DIC, which may be achieved by creating a closed system for the parent solution in which headspace is non-existent. Furthermore, high-density plastic or glass containers for bulk and titrant solutions may reduce CO_2 diffusion through the container walls.

3.3.4 CO_2 diffusion

The CO_2 diffusion method was first developed by Dietzel and Usdowski (1996) in their assessment of trace element (strontium) partitioning in galena, covellite, and calcite. The technique was further refined to determine the oxygen isotope fractionation between calcite and water (Dietzel et al., 2009). Founded on the principle of diffusion, an inner solution housing high pCO_2 is contained in an outer solution comprised of calcium ions, an NH_4Cl buffer, and overall low pCO_2 conditions (Figure 3.4) (Tang et al., 2008; Dietzel et al., 2009). The CO_2 leaks across a diffusive polyethylene membrane separating the two solutions, inducing a CO_2 flux to crystallize calcium carbonate from an aqueous solution. The concentration of dissolved inorganic carbon (DIC) in the outer solution increases until a critical saturation index for spontaneous calcite precipitation is achieved. The applied CO_2-diffusion technique is used as a simple mixed-flow reactor where the CO_2 flux may be varied simply by altering the thickness or type of the membrane, or by adjusting the chemical composition of the solution (e.g., pH, HCO_3^- or Ca^{2+} concentration).

In the CO_2 diffusion technique, the buffer and pH-stat titration technique ensures a stable solution pH throughout the course of the precipitation experiment, although ionic concentrations are not similarly controlled due to the consumption of calcium ions without replenishment in the outer solution (as is accounted for in the constant addition system). However, the rate of diffusion (i.e., precipitation rate) dictates the depletion of inner solution $p\text{CO}_2$ and, by extension, the final isotopic compositions. Carbonate precipitation rate is thus controlled by the CO_2 flux through the membrane. This flux can be precisely determined by adjusting the membrane thickness and the respective pH of the inner and outer solutions; in principle, a thinner membrane and a lower pH of the inner solution induces a higher CO_2 flux due to shorter diffusion lengths, and an elevated CO_2 gradient between the solutions. In order to accurately portray equilibrium oxygen isotopic fractionation, precipitation rate and/or initial equilibrium conditions must be controlled. Moreover, the CO_2 diffusion technique cannot measure carbon isotope fractionation due to the continuous transfer of CO_2 between solutions out of chemical equilibrium. Alteration of oxygen isotope compositions of DIC may also be associated with the transfer of DIC (mainly in the form of CO_2) although the overall drift is likely negligible.

Diffusion of CO_2 is controlled by the partial pressure gradient, inducing a flux of DIC from the inner to outer solution, which houses solution of constant pH. Since the diffusion of negatively charged CO_3^{2-} species requires a simultaneous diffusion of corresponding cations, the CO_2 molecules diffuse through the membrane with no net charge transfer. Consequently, no significant DIC transfer occurs if the inner solution contains sodium bicarbonate without the addition of gaseous CO_2. Notably, Dietzel et al. (2009) allowed insufficient time after preparing parent solutions to ensure initial isotopic equilibrium was achieved, casting doubt upon the reliability of their results. Dietzel et al. (2009) attributed this variability to altered solution pH and precipitation rate, although another influencing factor may be at play, as indicated by the large variability between experiments of similar pH and precipitation rate.

The CO_2 diffusion method is characterized by three distinct stages: (1) CO_2 diffusion through the membrane into the outer solution; (2) CO_2 diffusion and fast precipitation at elevated saturation with respect to calcite; (3) CO_2 diffusion and slow precipitation at lower saturation with respect to calcite. The overall reaction yields equal consumption of CO_2 and OH^-. NaOH was added to maintain pH; the rate of addition (i.e. amount of added over time) represents the flux of CO_2 from the inner to outer solution. The linear slope reflects a nearly constant pCO_2 in the inner solution as CO_2 diffuses to the outer solution at a constant rate, inducing calcite precipitation. The slope for the second stage is more than double that of the first, indicating $n > 1$ in the above equations and fast precipitation at relatively high degrees of saturation. The third stage is marked by lesser slope, indicating $n < 1$ and therefore slow precipitation at rather low saturation. Both latter stages consume NaOH linearly with time, suggesting negligible changes of pCO_2 in the inner solution and a constant rate of CO_2 diffusion to the outer solution.

3.4 Discussion and conclusions

The $CaCO_3$ system is especially interesting for isotope fractionation studies, as it can provide both equilibrium and kinetic data simultaneously on both carbon and oxygen isotope effects (Chacko and Deines, 2008). Control over thermal, chemical and isotopic equilibrium is controlled by temperature, pressure, pH, precipitation rate, growth rate and growth method (Romanek et al., 1992; Kim and O'Neil, 1997; Beck et al., 2005; Dietzel et al., 2009). However, these parameters have only been studied empirically. In their assessment of abundant natural cave speleothem data, Coplen (2007) and Tremaine et al. (2011) both indicate that true equilibrium conditions have not yet been achieved in the laboratory. Experimental precipitation experiments are executed over a short timeframe relative to the environment, as reflected by the rapid carbonate growth rate compared to that observed in speleothem deposits (Watkins and Nielsen, 2013). Therefore, robust experimentation is required to accumulate a comprehensive understanding of growth rate, as well as other equilibrium parameters, to justify the continued usage of empirically-derived equilibrium fractionation factors applied to the majority of modern paleothermometry studies.

To examine equilibrium effects, either the free drift or pH-stat synthesis methods can be employed depending on the desired experimental conditions. Free drift experiments should be conducted when current data is insufficient in describing precipitation kinetics and element partitioning behaviour of mixed cation carbonates. Experiments carried out by this method may serve as a starting point for future chemo-stat experiments to clarify the solid-solution state relationships of mixed-cation carbonates and provide a base level understanding to determine the origin of natural low temperature carbonates of similar chemistry (Romanek et al., 2009).

One drawback of the degassing and constant addition methods in their currently engineered states is the inability to quantify precipitation rate. This statistic can be used to determine the extent to which equilibrium conditions have been achieved. For example, trace element literature (e.g., Dromgoole and Walter, 1990; DeVillers et al., 1995) suggests that chemical equilibrium will be better achieved when employing a slower precipitation rate. Neither of the two homogeneous nucleation methods can precisely determine precipitation rate due to (1) the unpredictable number and size of the nuclei on which carbonate growth occurs and (2) the dynamic nature of carbonate growth surface area over precipitation duration; however, it can be calculated with alternative synthesis methods employing heterogeneous nucleation (i.e., seeded growth) which have been successfully applied to carbonate kinetics studies (Zhong and Mucci, 1993). While many studies have measured and discussed the empirical relevance of precipitation rate, new research has indicated that precipitation amount provides equal insight into equilibrium conditions. Controversy surrounds the importance of precipitation rate versus precipitation amount on stable isotope fractionation between natural carbonates and their environmental solutions. A comparison of experimental results and natural carbonate samples indicates that chemical (isotopic) equilibrium is not always attained in nature; therefore potential influencing factors must be evaluated independently to discern the circumstances under which true equilibrium conditions are achieved.

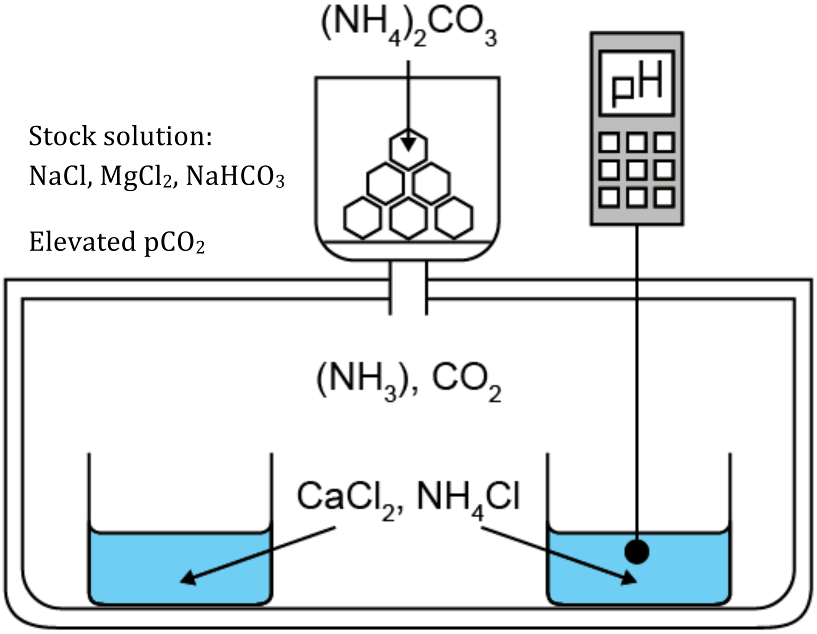

Figure 3.1: Free drift

Solid ammonium carbonate overlying the reaction vessel sublimates to produce NH_3 and CO_2 gases, which then diffuse and dissociate into an aqueous solution of calcium and ammonium chloride ($CaCl_2$-NH_4Cl). This results in an increase of the total alkalinity (Total ALK) and pH of the solution and a subsequent increase in the supersaturation conditions with respect to calcite ($\Omega = [Ca][CO_3]/K_{sp}$). The NH_3/NH_4 system acts as a pH buffer to moderate pH and minimize variance in isotopic composition over the course of experimentation.

Modified schematic of Jiménez-López et al. (2001) and Lemarchand et al. (2004).

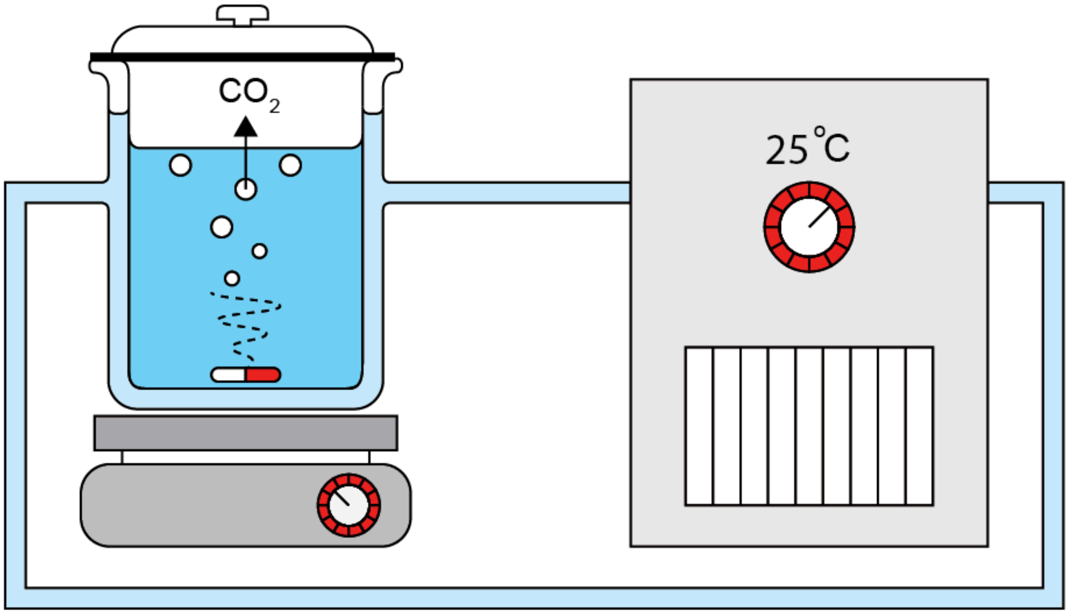

Figure 3.2a: Passive degassing

A starting parent solution is contained in a closed system reaction chamber connected to a constant-temperature water bath. This degassing approach allows CO_2 to degas freely into the overlying headspace. Over time, equilibration of atmospheric and solution pCO_2 is achieved and supersaturation conditions (with respect to calcium carbonate) are established. Carbonate precipitation commences shortly thereafter.

Modified schematic of Kim et al. (2007)

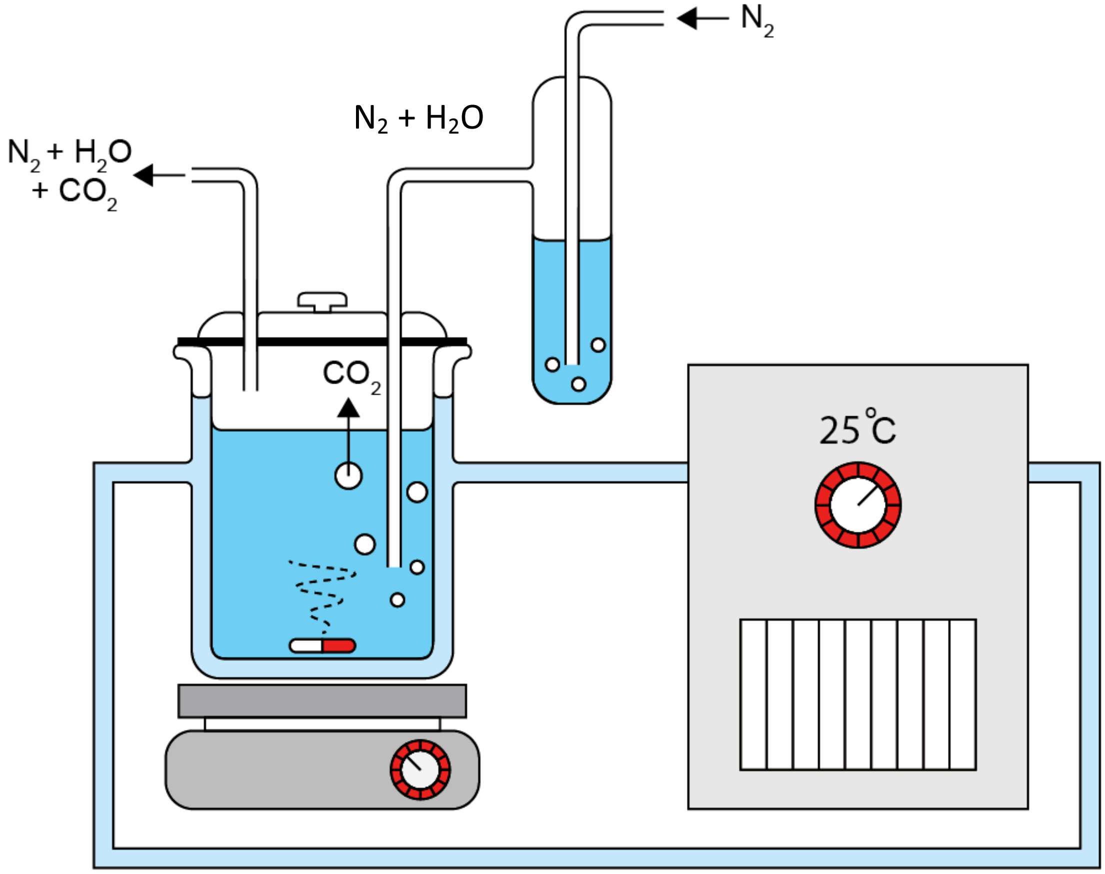

Figure 3.2b: Active degassing

A starting parent solution is contained in a semi-open-system reaction chamber connected to a constant-temperature water bath. Pre-purified nitrogen gas, saturated with water of identical oxygen isotope composition to the experimental solutions, is bubbled slowly through the solutions to remove CO_2. Slow is defined as approximately 20 bubbles per minute and fast is defined as 48 bubbles per minute (Kim and O'Neil, 1997). This bubbling induces supersaturation, spontaneous nucleation, and precipitation of calcium carbonate. The bubbling of nitrogen gas through the solution aims to catalyze the precipitation process, stabilizing the rate of carbon dioxide gas removal. The solution-atmospheric $p\mathrm{CO}_2$ gradient is largest at the beginning and smallest at the end of the experiment.

Modified schematic of Kim and O'Neil (1997).

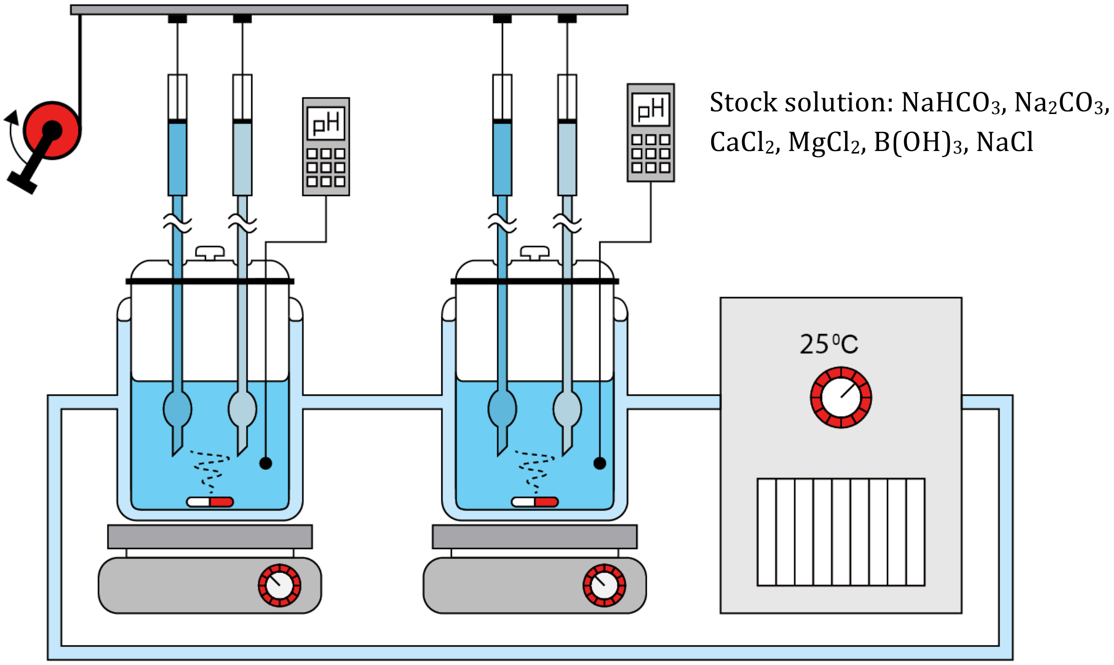

Figure 3.3: Modified constant addition

Closed reaction chambers are connected in series to a circulating constant-temperature water bath. Two titrant solutions (one $NaHCO_3$ and/or Na_2CO_3 solution and one $CaCl_2$ solution, with or without Mg^{2+} depending on the pH of the experiment) are simultaneously injected at a constant and selected rate by a dual syringe pump into an air-tight Teflon reaction vessel housing a thermally and isotopically equilibrated Na-Mg-Cl-CO_3 or Na-Ca-Mg-Cl-CO_3 starting solution at a predetermined [Mg]:[Ca] ratio depending on the desired carbonate polymorph growth. To prevent isotopic stratification and ensure solution homogeneity, a floating magnetic stirrer is used throughout precipitation. The constant addition technique allows maintenance of isotopic, thermal and chemical equilibrium conditions.

Modified schematic of Kim et al. (2006).

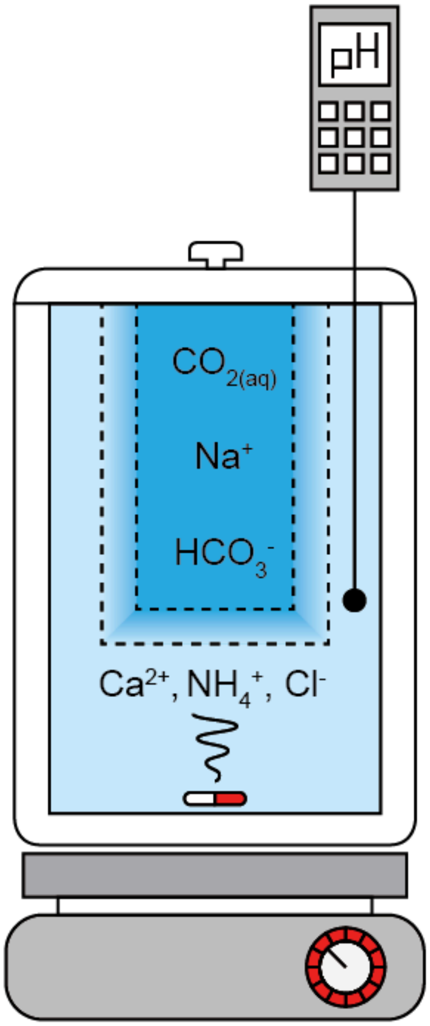

Figure 3.4: CO_2 diffusion

In a temperature-controlled chamber, an inner solution housing high pCO_2 is contained in an outer solution comprised of calcium ions, an NH_4Cl buffer, and lower pCO_2 conditions. The CO_2 diffuses across a polyethylene membrane (2mm) separating the two solutions. The concentration of dissolved inorganic carbon (DIC) in the outer solution increases until a critical saturation index for spontaneous calcium carbonate precipitation is achieved. To ensure homogeneity and avoid grinding of crystals, a floating magnetic stir bar is included in the outer solution throughout experimentation.

Modified schematic of Dietzel et al. (2009).

References

Beck, W. C., Grossman, E. L., & Morse, J. W. (2005). Experimental studies of oxygen isotope fractionation in the carbonic acid system at 15°, 25°, and 40°C. *Geochimica et Cosmochimica Acta*, *69*(14), 3493–3503. doi:10.1016/j.gca.2005.02.003

Busenberg, E., & Plummer, L. N. (1986). The solubility of BaCO3 (witherite) in CO3-H2O solutions between 0 and 90 C , evaluation of the association constants of BaHCO3(aq) and BaCO3(aq) between 5 and 80 C , and a preliminary evaluation of the thermodynamic properties of B. *Geochimica et Cosmochimica Acta*, *50*, 2225–2233.

Chacko, T., & Deines, P. (2008). Theoretical calculation of oxygen isotope fractionation factors in carbonate systems. *Geochimica et Cosmochimica Acta*, *72*(15), 3642–3660. doi:10.1016/j.gca.2008.06.001

Chou, L., & Wollast, R. (1984). Study of the Weathering of Albite at Room Temperature and Pressure With a Fluidized Bed Reactor. *Geochimica et Cosmochimica Acta*, *48*(11), 2205-2217.

Chou, L. Garrels, R., & Wollast, R. (1989). Comparative Study of the Kinetics and Mechanisms of Dissolution of Carbonate Minerals. *Chemical Geology*, 78, 269-282.

Coplen, T. B. (2007). Calibration of the calcite–water oxygen-isotope geothermometer at Devils Hole, Nevada, a natural laboratory. *Geochimica et Cosmochimica Acta*, *71*(16), 3948–3957. doi:10.1016/j.gca.2007.05.028

de Villiers, S., Nelson, B.K., &Chivas, A.R. (1995). Biological controls on coral Sr/Ca and δ18O reconstructions of sea surface temperatures. *Science*, 269, 1247–1249

Dietzel, M., Tang, J., Leis, A., & Köhler, S. (2009). Oxygen isotopic fractionation during inorganic calcite precipitation — Effects of temperature, precipitation rate and pH. *Chemical Geology*, *268*(1-2), 107–115. doi:10.1016/j.chemgeo.2009.07.015

Dietzel, M., Tang, J., Leis, A., & Köhler, S. J. (2009). Oxygen isotopic fractionation during inorganic calcite precipitation — Effects of temperature, precipitation rate and pH. *Chemical Geology*, *268*(1-2), 107–115. doi:10.1016/j.chemgeo.2009.07.015

Dietzel, M., & Usdowski, E. (1996). Coprecipitation of Ni2+, Co2+, and Mn2+ with galena and covellite, and of Sr2+ with calcite during crystallization via diffusion of H2S and CO2 through polyethylene at 20C: Power law and Nernst law control of trace element partitioning. *Chemical Geology*, *131*, 55–65.

Dromgoole, E. L., & Walter, L. M. (1990). Inhibition of calcite growth rates by Mn2+ in CaC12 solutions at 10, 25, and 50°C. *Geochimica et Cosmochimica Acta*, *54*(1984), 2991–3000.

Emrich, K., Ehhalt, D., & Vogel, J. (1970). Carbon Isotope Fractionation During the Precipitation of Calcium Carbonate. *Earth and Planetary Science Letters*, *8*(September 1969), 363–371.

Gabitov, R. I., Watson, E. B., & Sadekov, A. (2012). Oxygen isotope fractionation between calcite and fluid as a function of growth rate and temperature: An in situ study. *Chemical Geology*, *306-307*, 92–102. doi:10.1016/j.chemgeo.2012.02.021

Gabitov, R., Watson, B., & Sadekov, A. (2012). Oxygen isotope fractionation between calcite and fluid as a function of growth rate and temperature: An in situ study. *Chemical Geology*, *306-307*, 92–102. doi:10.1016/j.chemgeo.2012.02.021

Garside, J. (1982). Nucleation. In G H Nancollas (Ed.), *Biological Mineralization and Demineralization SE - 3* (Vol. 23, pp. 23–35). Springer Berlin Heidelberg. doi:10.1007/978-3-642-68574-3_3

Gruzensky, P. M. (1967). Growth of Calcite Crystals. In H. S. Peiser (Ed.), *Crystal Growth* (pp. 365–367). Oxford University Press.

Jiménez-López, C., Romanek, C. S., Huertas, F. J., Ohmoto, H., & Caballero, E. (2004). Oxygen isotope fractionation in synthetic magnesian calcite. *Geochimica et Cosmochimica Acta*, *68*(16), 3367–3377. doi:10.1016/j.gca.2003.11.033

Kazmierczak, T. F., Tomson, M. B., & Nancollas, G. H. (1982). Crystal growth of calcium carbonate: A controlled composition kinetic study. *J. Phys. Chem.*, 86, 103-107.

Kim, S-T., & O'Neil, J. (1997). Equilibrium and nonequilibrium oxygen isotope effects in synthetic carbonates. *Geochimica et Cosmochimica Acta*, *61*(16), 3461–3475.

Kim, S-T., Hillaire-Marcel, C., & Mucci, A. (2006). Mechanisms of equilibrium and kinetic oxygen isotope effects in synthetic aragonite at 25°C. *Geochimica et Cosmochimica Acta*, *70*(23), 5790–5801. doi:10.1016/j.gca.2006.08.003

Kim, S-T., O'Neil, J., Hillaire-Marcel, C., & Mucci, A. (2007). Oxygen isotope fractionation between synthetic aragonite and water: Influence of temperature and Mg2+ concentration. *Geochimica et Cosmochimica Acta*, *71*(19), 4704–4715. doi:10.1016/j.gca.2007.04.019

Lemarchand, D., Wasserburg, G., & Papanastassiou, D. (2004). Rate-controlled calcium isotope fractionation in synthetic calcite. *Geochimica et Cosmochimica Acta*, *68*(22), 4665–4678. doi:10.1016/j.gca.2004.05.029

Lorens, B. (1980). Sr, Cd, Mn and Co distribution coefficients in calcite as a function of calcite precipitation rate. *Geochimica et Cosmochimica Acta*, *45*(2), 553-561.

McCrea, J. M. (1950). On the isotopic chemistry of carbonates and a paleotemperature scale. *Journal of Chemical Physics*, *18*(6), 849–857.

Mucci, A., & Morse, J. W. (1982). The incorporation of Mg and Sr into calcite overgrowths : influences of growth rate and solution composition. *Geochimica et Cosmochimica Acta*, *47*, 217–233.

Mucci, A., & Morse, J. W. (1984). The solubility of calcite in seawater solutions of various magnesium concentration , Zi = 0.697 m at 25 °C and one atmosphere total pressure. *Geochimica et Cosmochimica Acta*, *48*(1982), 815–822.

Nancollas, G.H., & Gardner, G. L. (1974). Kinetics of crystal growth of calcium oxalate monohydrate. *Journal of Crystal Growth*, *21*(2), 267–276. doi:10.1016/0022-0248(74)90014-1

Reddy, M. M. (1977). Crystallization of calcium carbonate in the presence of trace concentrations of phosphorus-containing anions. *Journal of Crystal Growth*, *41*, 287–295.

Reddy, M. M., & Wang, K. K. (1980). Crystallization of calcium carbonate in the presence of metal ions. *Journal of Crystal Growth*, *50*(2), 470–480. doi:10.1016/0022-0248(80)90095-0

Romanek, C., Grossman, E., & Morse, J. (1992). Carbon isotopic fractionation in synthetic aragonite and calcite: Effects of temperature and precipitation rate. *Geochimica et Cosmochimica Acta*, *56*(1), 419–430. doi:10.1016/0016-7037(92)90142-6

Romanek, C. S., Jiménez-López, C., Navarro, A. R., Sánchez-Román, M., Sahai, N., & Coleman, M. (2009). Inorganic synthesis of Fe–Ca–Mg carbonates at low temperature. *Geochimica et Cosmochimica Acta*, *73*(18), 5361–5376. doi:10.1016/j.gca.2009.05.065

Rubinson, M., & Clayton, R. N. (1969). Carbon-13 fractionation between aragonite and calcite. *Geochimica et Cosmochimica Acta*, *33*, 997–1002.

Tang, J., Köhler, S. J., & Dietzel, M. (2008). Sr2+/Ca2+ and 44Ca/40Ca fractionation during inorganic calcite formation: I. Sr incorporation. *Geochimica et Cosmochimica Acta*, *72*(15), 3718–3732. doi:10.1016/j.gca.2008.05.031

Tarutani, T., Clayton, R. N., & Mayeda, T. K. (1969). The effect of polymorphism and magnesium substitution on oxygen isotope fractionation between calcium carbonate and water. *Geochimica et Cosmochimica Acta*, *33*, 987–996.

Tremaine, D. M., Froelich, P. N., & Wang, Y. (2011). Speleothem calcite farmed in situ: Modern calibration of δ18O and δ13C paleoclimate proxies in a continuously-monitored natural cave system. *Geochimica et Cosmochimica Acta*, *75*(17), 4929–4950. doi:10.1016/j.gca.2011.06.005

Turner, J. V. (1982). Kinetic fractionation of carbon-13 during calcium carbonate precipitation. *Geochimica et Cosmochimica Acta*, *46*(7), 1183–1191. doi:10.1016/0016-7037(82)90004-7

Usdowski, E., & Hoefs, J. (1990). Kinetic 13C/12C and 18O/16O effects upon dissolution and outgassing of CO2 in the system CO2-H2O. *Chemical Geology (Isotope Geosciences Edition)*, *80*, 109–118.

Watkins, J. M., Nielsen, L. C., Ryerson, F. J., & DePaolo, D. J. (2013). The influence of kinetics on the oxygen isotope composition of calcium carbonate. *Earth and Planetary Science Letters*, *375*, 349–360. doi:10.1016/j.epsl.2013.05.054

Watkins, J., & Nielsen, L. (2013). The influence of kinetics on the oxygen isotope composition of calcium carbonate. *Earth and Planetary Science Letters*, *375*, 349–360. doi:10.1016/j.epsl.2013.05.054

Watson, E. B. (2004). A conceptual model for near-surface kinetic controls on the trace-element and stable isotope composition of abiogenic calcite crystals. *Geochimica et Cosmochimica Acta*, *68*(7), 1473–1488. doi:10.1016/j.gca.2003.10.003

Zhong, S., & Mucci, A. (1993). Calcite precipitation in seawater using a constant addition technique: A new overall reaction kinetic expression. *Geochimica et Cosmochimica Acta*, *57*(7), 1409–1417. doi:10.1016/0016-7037(93)90002-E

Zuddas, P., & Mucci, A. (1994). Kinetics of calcite precipitation from seawater : I . A classical chemical kinetics description for strong electrolyte solutions. *Science*, *58*(20), 4353–4362.

CHAPTER 4:

INVESTIGATION OF BORON ISOTOPE SYSTEMATICS IN THE $CaCO_3$-CO_2-H_2O-NaCl SYSTEM

Investigation of Boron Isotope Systematics in the $CaCO_3$-CO_2-H_2O-NaCl System

Jillian Wyman[a], Christa D. Klein Gebbinck[a], Michael J. Henehan[b], Gavin Foster[b], Sang-Tae Kim[a]

[a]School of Geography and Earth Sciences, McMaster University, 1280 Main Street West, Hamilton, ON L8S 4K1, Canada

[b]Ocean and Earth Science, National Oceanography Centre Southampton, University of Southampton Waterfront Campus, European Way, Southampton SO14 3ZH, UK

*Corresponding author: Sang-Tae Kim (sangtae@mcmaster.ca)

In preparation for: Geochimica et Cosmochimica Acta

Abstract

The boron isotope compositions of marine carbonates are a potentially powerful tool for the reconstruction of ancient seawater pH. If proven reliable, this proxy will allow systematic recording of paleooceanographic conditions, greatly assisting climatologists identifying historical fluctuations in atmospheric carbon dioxide concentrations. In this study, boron speciation in inorganic calcite and aragonite – as well as the magnitude of boron isotope fractionation between the carbonate and its parent solution – was quantified in high ionic strength solutions (0.7 mol/kg) across a range of controlled pH conditions: low pH ~ 7.15, mid pH ~ 8.35 and high pH ~ 9.15. These abiotic experiments were designed to spontaneously nucleate the two calcium carbonate polymorphs to identify the dependence of carbonate boron isotope composition ($\delta^{11}B_{carbonate}$) on the pH of the parent solution. Both aragonite and calcite displayed a distinct correlation between boron isotope composition and solution pH, supporting one of the pillars to the hypothesis, namely the preferential incorporation of the lighter borate ($B(OH)_4^-$) ion into the crystal lattice. However, the chemical composition of this study's solutions disallow the application of an exact boric acid dissociation constant and isotope equilibrium constant, rendering exclusive incorporation of $B(OH)_4^-$ difficult to confirm. Boron isotope compositions of marine carbonate therefore require further quantification from artificial seawater solutions comprising select constituents such that appropriate constants can be applied to more clearly verify the proxy.

4.1 Introduction

The Vostok ice core records ongoing cyclic fluctuations in Earth's atmospheric carbon dioxide partial pressure ($p\mathrm{CO}_2$) levels over the Pleistocene glacial cycles (Barnola et al., 1987; Jouzel et al., 1987). However, such robust environmental archives are limited to the past ~ 420, 000 years (Petit et al., 1999). Climatologists instead rely on proxies, preserved physical characteristics of the past, in their quest to understand Earth's history over several million years – a timespan not recordable by direct measurements. The evolution of Earth's atmospheric carbon dioxide concentrations must be fully pieced together to differentiate natural changes from those out of the ordinary and position future climate change within a geological context. Proxies developed to quantify ice volume and temperature changes (i.e., δD and δ^{18}O) are exceptionally well aligned with the ice core record, denoting $p\mathrm{CO}_2$ as a driving factor behind Earth's oscillating climate (Petit et al., 1999).

The study of marine carbonates has recently been popularized due to the influence of CO_2-water interactions on oxygen isotopic compositions (Usdowski and Hoefs, 1990; Beck et al., 2005; Zeebe, 2007). Ice core records indicate that $p\mathrm{CO}_2$ oscillated between 80 and 300 parts per million by volume (ppmv) over the last four glacial cycles (Petit et al., 1999). Using boron isotopes in planktic foraminifer shells, Hönisch et al. (2009) constructed a record of sea surface $p\mathrm{CO}_2$, concluding that modern levels are the highest they have been in the last 2.1 million years. Seawater carbonate chemistry is subsequently altered as the surface ocean absorbs an increasing amount of this soluble gas (Klochko et al., 2009). The oxygen isotope fractionation factor ($1000\ln\alpha_{CaCO3\text{-}H2O}$) is integral to the derivation of ocean surface temperatures; thus, understanding the CO_2-water system is essential to supplement the ongoing archive of Earth's climate history (Hoefs, 2009). To minimize uncertainty intrinsic to any natural, dynamic system, settings in which all variables are controlled must first be examined to lay the foundation of understanding. In this experimental study, inorganic carbonates were synthesized over a three-year timeline, consisting of three- to four-week series of individual experimental durations, under constant temperature and pH conditions.

Boron holds great promise as a geochemical tracer, with a relatively long residence time of ~ 20 million years (Lemarchand et al., 2002), little variation within oceanic isotope compositions over the past ~ 21 million years (Spivack et al., 1987; Rollion-Bard et al., 2011) and pH-dependent boron isotope incorporation behaviour into carbonates (Milliman, 1974; Furst et al., 1976; Vengosh et al., 1991). The dominant isotopic fractionation process occurs as an equilibrium exchange reaction between trigonally-coordinated boric acid ($B(OH)_3$) and tetrahedrally-coordinated borate ($B(OH)_4^-$). These species equilibrate rapidly (Zeebe et al., 2001) and their relative abundance is strongly pH-dependent (Hershey et al., 1986).

The boron isotope paleo-pH proxy is based on three assumptions: (1) the relative proportion of boric acid [$B(OH)_3$] and borate [$B(OH)_4^-$] in seawater is a function of seawater pH; (2) at equilibrium, the tetrahedrally-coordinated borate ion is depleted in ^{11}B relative to trigonally-coordinated boric acid; (3) borate is exclusively incorporated into marine carbonates without a significant kinetic isotope effect. This approach to paleoclimatology is founded on the observation that rising $p\mathrm{CO}_2$ values increase the dissolved carbon dioxide content in the surface ocean, thus lowering its pH. These pH values can then be determined by measuring the boron isotope composition of calcium carbonate ($\delta^{11}\mathrm{B}_{\mathrm{carbonate}}$) precipitated from the seawater. Fundamental to the boron incorporation process is the equilibrium state necessarily achieved by the precipitating carbonate and parent solution (Vengosh et al., 1991). Among the tenets of the proxy is the hypothesis that only borate is incorporated into the crystal lattice without fractionation, therefore the boron isotope composition of the carbonate should equal that of the borate. Hemming et al. (1995) and Hemming and Hanson (1992) both observed similar boron isotope compositions of calcite, aragonite and borate, indeed suggesting that the ion is adsorbed on to the crystal surface and structurally incorporated into both polymorphs despite their different crystal coordinations.

This proxy aims to demonstrate the coupling between surface ocean chemistry and the atmosphere as recorded in marine archives, allowing for quantitative estimation of ancient atmospheric $p\mathrm{CO}_2$ values. However, controversy exists over the possibility that some boric acid may indeed be incorporated into the crystal structure. In this study, aragonite and calcite were synthesized at a range of stable pH values from 7.10 to 9.18 using total scale, with a thermostated modified constant addition technique.

Since oxygen isotope fractionation behavior in marine carbonates is well established in the field, comparing and contrasting this study's oxygen isotope fractionation with published values – and using the observed trends to discern information about the lesser-known boron isotope fractionation behavior – highlights the importance of using known relationships as a baseline for examining the stable isotope systematics of those that are not as well established (i.e., boron). This study is the first to link oxygen and boron isotope effects in abiotic aragonite and calcite samples; additional control of carbon isotope systematics is integral to the development of a multi-element approach, which has remarkable potential to improve the robustness of the boron isotope paleo-pH proxy and provide a foundational model for refining other paleoclimate proxies.

4.2 Experimental methods

4.2.1 Experimental setup

This study employed the unseeded pH-stat method, a modified version of the constant addition technique. In this approach, parent solution is simply added to the reactor at a constant rate, thereby attaining and maintaining steady state conditions throughout the experimental duration. The pH-stat technique was developed to study the kinetics of crystallization over a broad spectrum of supersaturation states under constant pH conditions. This is achieved through the use of a dual syringe pump that dispenses two titrants in equal amounts. These titrants are injected simultaneously at a predetermined continuous rate of 0.50 mL/hr into an airtight Teflon® reaction vessel that has been both thermally and isotopically equilibrated. The starting solution reaches a state of supersaturation (with respect to calcium carbonate) prior to addition of the two titrant solutions, with subsequent spontaneous nucleation marked by a phase change from the dissolved inorganic carbon species to carbonate precipitation. Calcium carbonate is thus precipitated without the use of seed material. The chemical compositions of all involved solutions are carefully controlled to achieve stable pH over the experimental duration and precipitation of the desired polymorph.

The temperature of solutions is held constant (25 ± 0.04 °C) by circulating water from a temperature-controlled water bath (25 ± 0.01 °C) and a water-jacketed glass reaction vessel. Solution homogeneity is maintained with a floating magnetic stirrer throughout precipitation. Aliquots of experimental solution are collected for oxygen, carbon and boron isotope analysis both at the onset and conclusion of each experiment. Solution temperature and pH are monitored daily using a Thermo Scientific Traceable® digital thermometer and ROSS® Sure-Flow combination pH electrode, respectively; the electrode is calibrated with NIST-traceable pH buffers (4.00, 7.00, and 10.00) as well as a Tris buffer (8.38 and 8.25). The buffers are stored in a temperature-controlled water bath at 25 ± 0.01 °C to ensure consistency between all experimental solutions. Upon termination of each experiment, solutions are filtered, dried overnight in a 70 °C oven then subsequently collected for isotopic analysis.

4.2.2 Solution preparation

Experimental starting solutions were gravimetrically prepared using deionized water (~18 MΩ cm) and ACS grade $NaHCO_3$ and Na_2CO_3, the ratio of which was dependent on the targeted initial pH as well as the concentrations of boric acid and sodium chloride. The solution remained in a temperature-monitored water bath (25 ± 0.01 °C) for a minimum of seven days to ensure that the DIC species and water reached oxygen isotopic equilibrium. ACS grade $MgCl_2 \bullet 6H_2O$ and $CaCl_2 \bullet 2H_2O$ were added to the equilibrated starting solutions immediately preceding experimental synthesis. To precipitate aragonite, the ratio of $MgCl_2•6H_2O$ to $CaCl_2•2H_2O$ was adjusted to 4:1; this ratio was reduced to 0.13 for calcite precipitation (Morse et al., 2007). The completed starting solution was then enclosed in a reaction chamber maintained at 25.00 ± 0.04 °C, receiving injections from two different titrant solutions. To ensure consistent oxygen isotope water values, both titrants were prepared with deionized water collected at the same time as that used for their associated starting solution. The titrant conditions varied with intended solution pH: one included ACS grade $NaHCO_3$, Na_2CO_3, and NaCl, while the other was comprised of ACS grade $CaCl_2•2H_2O$, $B(OH)_3$, and NaCl. In response to the decrease in dissolved boron during experiments with no constant boron addition, as observed by Klochko et al. (2006), boron was constantly supplied to the reaction vessel via titrant solution throughout the experiments. Specific solution chemistries and experimental conditions are outlined in Table 4.1.

The experimental solution was sampled before and after each synthesis experiment with a 60 mL plastic syringe then deposited in a 50 mL vial. A final rinse of the vials with experimental solution occurred immediately prior to a second aliquot injection of the water sample. The water samples were stored in the refrigerator for oxygen and boron isotopic analysis at a later date. The latter required the sample to be filtered through a Millipore 0.45 μm Durapore® syringe filter then stored in 1.5 mL vials, which had been precleaned in 3M HCl at 80 °C overnight, rinsed five times with 18 MΩ Milli-Q water, oven-dried and stored in a closed high-density polyethylene bottle. Upon collection of water samples, the remaining solution was run through a vacuum filtration system using 0.45 μm Durapore® membrane filters to isolate the suspended calcium carbonate crystals. Borosilicate glassware was avoided to ensure isotopic exchange with the boron in the experimental solution did not occur. Salts were thoroughly rinsed with 2 liters of 18 MΩ Milli-Q water followed by ultra-pure methanol. The filtered calcium carbonate sample was oven-dried at ~ 70 °C overnight then collected and weighed. An average carbonate yield from a 3-week precipitation experiment was ~ 50 mg (aragonite) and ~ 200 mg (calcite).

4.2.3 Seawater pH buffer

The pH scale used to determine the pK_B value must be identical to that used for the dissociation constants for CO_2 equilibria to ensure an accurate estimation of pCO_2 from pH. The pH can be identified using the total scale (pH_T), free scale (pH_F), seawater scale (pH_{SWS}), or NBS scale (pH_{NBS}). The latter is defined by low ionic-strength (I = ~ 0.1 mol/kg), standard buffer solutions, each having an assigned pH. Such pH quantification methodology is incompatible with high ionic-strength solutions such as seawater (I = ~ 0.7 mol/kg), which alters the liquid junction potential by several millivolts (Dickson, 1993; Hansson, 1973). Application of the boron isotope-pH proxy in paleoseawater pH reconstructions is founded on the origin of marine foraminifera in natural seawater, thus ionic strength is an important inorganic experiment consideration to mimic the incorporation of boron into carbonates in the natural environment. To convert experimental pH measurements, a Tris buffer is used to accurately compare the pH_T values to the dissociation of boric acid in seawater (Dickson, 1993; Hansson, 1973).

Experimental solutions were designed to simulate the ionic strength of natural seawater. The Tris buffer was prepared according to Millero et al. (1993), in which ACS grade KCl, Na_2SO_4, and NaCl salts are dried at 90°C for twenty-four hours, and then the buffer is prepared gravimetrically using the salts, deionized water, Tris and Tris-HCl. To account for any degradation over time, a second Tris buffer solution was made one year after the first. A Tris correction factor (determined to be ~ 0.28 and ~ 0.15 pH units for the two different buffers prepared) must be quantified to accurately scale the pH values, and is calculated by differentiating the RmV for a pH of 8.10 using the calibrated NIST buffer solutions from the RmV measured with the pH electrode for the Tris buffer. This correction factor is then applied to all pH values recorded by the electrode, calibrated by the NIST buffers. The total scale communication of pH measurements ensures consistent reporting of results to accurately depict their relationship with the dissociation of boric acid in seawater.

4.2.4 Oxygen ($\delta^{18}O$) isotope analysis

All synthesized calcium carbonate minerals were identified as pure aragonite or calcite using the x-ray diffraction (XRD) analytical facility at McMaster University. The oxygen isotope compositions of the samples were quantified by the MRSI VG OPTIMA isotope ratio mass spectrometer equipped with an ISOCARB automated common acid bath at 90 °C (precision ± 0.08 ‰). Oxygen isotope compositions were normalized to the recommended values for standards NBS 18 (7.16 ‰) and NBS 19 (28.65 ‰) relative to SMOW. To calculate the $\delta^{18}O$ specific to aragonite and calcite, corresponding acid fractionation factors of 1.01063 and 1.01030 were applied (Kim et al., 2007).

The classic CO_2-H_2O equilibration technique (Epstein and Mayeda, 1953) was modified slightly for oxygen isotope analysis of experimental solution samples. Using the

Gas Bench II headspace autosampler with a Thermo Finnigan Delta plus XP isotope ratio mass spectrometer at McMaster University (precision ± 0.05 ‰), Exetainer® vials were flushed and filled with a 0.2% CO_2 and 99.8% He mixture with a double needle at a flow rate of 100 mL/min. A 1 mL syringe dispensed 0.2 mL quantity of sample into each vial. Twenty-seven hours was allotted for equilibration at 25 ± 0.1 °C, after which time the CO_2 in the headspace was analyzed. Analyses were run as duplicates, with previously calibrated laboratory water standards MRSI-STD-W1 (0.58 ‰) and MRSI-STD-W2 (28.08 ‰), measured at the onset and conclusion of each session.

4.2.5 Boron ($\delta^{11}B$) isotope analysis

Boron samples were sent to the United Kingdom for isotopic analysis. Using multicollector inductively coupled plasma mass spectrometry (MC-ICPMS), the boron isotope compositions of aragonite and calcite samples were analyzed at The National Oceanography Centre, Southampton (NOCS). Synthetic aragonite and calcite samples of 1-3 mg were rinsed with ~ 500 µL of boron-free MilliQ (18.2 MΩ cm) water, ultrasonicated for 30 seconds and then centrifuged for 4 minutes, in an effort to remove any boron that may have adhered to the carbonates from the experimental solution. This procedure was repeated five times; each supernatant extract was subjected to B/Ca analysis on the Thermo XSeries II Quadropole ICPMS to assess rinsing efficiency. The cleaned samples were transferred to Teflon centrifuge tubes, leached in weak acid (0.0005M HNO_3) to rid any remaining adsorbed boron, rinsed three times in MilliQ water to remove the weak acid, and finally dissolved in 0.5M HNO_3. The boron was separated from the calcium carbonate matrix to obtain accurate boron isotope compositions (Foster and Rohling, 2013). Samples were buffered with boron-free 2M sodium acetate-0.5M acetic acid then directed through 20 μL columns of boron-specific anion exchange resin, Amberlite IRA 743 (Lemarchand et al., 2002). The matrix and buffer were rinsed ten times with 160 μl of boron-free MilliQ water while the sample boron was eluted five times with 160 μl of 0.5M HNO_3. One more rinse with 160 μl of 0.5M HNO_3 was passed through the columns before measuring boron concentrations in this elution tail to ensure > 99.9% elution efficiency. Boron isotopes were then analyzed with a Thermo Neptune MC-ICPMS, a highly sensitive instrument (600-800 mV for a 50 ppb boron solution) equipped with an adaptable and customizable introduction system, ideal for boron isotope measurements due to its fine-tuning ability. Complete procedural replicates of seawater and an in-house coral standard indicate the reproducibility of MC-ICPMS measurements to be ± 0.25 ‰ at a 95% confidence level (Foster et al., 2008).

Preventative measures were taken to ensure that boron contamination (external to the system) did not bias experimental δ^{11}B data. Caution was exercised to (1) reduce airborne particulate boron; (2) purify all reagents involved in sample preparation; (3) ensure effective cleaning protocols for sample vessels; and (4) implement correct analyst practices. "Blank pots", consisting of 1.5 mL autosampler vials filled with HNO_3 equal to sample volumes, were measured every three samples to allow accurate characterization of fall-in blank, reagent-borne blank, and any possible contamination from the autosampler vials. At NOCS, samples are assessed in duplicates, with independent replicate measurements that do not share bracketing standards or blanks, and the mean δ^{11}B is calculated. Intralaboratory precision was quantified using standards and corals containing a range of boron concentrations, providing a δ^{11}B external reproducibility at 2σ of 0.23 ‰ (50 ppb) and 0.33 ‰ (10 ppb).

4.3 Results and discussion

4.3.1 Oxygen isotope fractionation between $CaCO_3$ and H_2O

Calcium carbonate samples ranging from 43-389 mg (aragonite) and 91-330 mg (calcite) were successfully precipitated using the modified constant addition method. Table 4.1 shows that these masses were a function of both the chemical composition and duration of the experiment.

Oxygen isotope analyses were used to corroborate the existence of isotopic equilibrium conditions during carbonate precipitation. The relationship between the each sample's oxygen isotope compositions of the synthesized carbonate and precipitating solution was compared with the published equilibrium carbonate-water oxygen isotope fractionation equation. Specifically, as determined by Kim et al. (2007) and Kim and O'Neil (1997) respectively,

$$1000\ln\alpha_{\text{aragonite-water}} = 17.88\ (10^3/T) - 31.14$$

$$1000\ln\alpha_{\text{calcite-water}} = 18.03\ (10^3/T) - 32.42$$

The oxygen isotope fractionation ($1000\ln\alpha_{\text{aragonite-water}}$) for the aragonite samples synthesized in this study at 25 °C ranged from 28.80 to 29.15 ‰ and averaged 28.97 ± 0.11 ‰ (Table 4.2) while the oxygen isotope fractionation ($1000\ln\alpha_{\text{calcite-water}}$) for the calcite samples spanned 28.40 to 28.71 ‰ with an average of 28.56 ± 0.08 ‰ (Table 4.2). The overlap of our aragonite oxygen isotope fractionation data with the published relationship (28.83 ‰, as per Kim et al., 2007) indicates that our experimental system was in isotopic equilibrium throughout aragonite synthesis. However, our calcite samples consistently lie at the upper bound or outside the analytical error range of the published relationship for calcite oxygen isotope fractionation (28.05 ‰, as per Kim and O'Neil, 1997) and thus appear to be non-equilibrium products. Several factors may be responsible for this apparent contrast in data, including: (1) kinetic effects were at play during abiotic calcite synthesis; (2) the accuracy of using well-established oxygen isotope equilibrium values to ascertain the overall equilibrium nature of the experimental system; (3) the influence of ionic strength on precipitation mechanism; and (4) mineral-specific effects of boron uptake into the crystal lattice. These possibilities are each explored below.

The calcite growth samples may indeed have been subjected to systematic kinetic effects. Calcite yield far outweighed that of aragonite over similar timespans, indicating faster precipitation and thereby samples in disequilibrium, which is highly sensitive to crystal growth and/or precipitation rate (Dietzel et al., 2009; Gabitov et al., 2012). Possible oxygen isotope effects observed during calcite precipitation can be attributed to the preferential deprotonation of isotopically heavy HCO_3^- ions and the incorporation of isotopically light CO_3^{2-} during mineral growth (Figure 4.1). The observed departure from oxygen equilibrium among these samples provides further evidence of its rapid growth, disallowing re-equilibration of the calcite surface with its ambient water. It appears that a "fast" injection rate of 0.50 mL/hr does not allow sufficient time to elapse for the DIC to isotopically equilibrate; in this scenario, preferentially-incorporated CO_3^{2-} ions thus possess the isotopic signature of the heavier HCO_3^- ion, yielding products heavier than predicted equilibrium. A slower injection rate would ensure isotopic equilibrium is achieved. Our observations indicate that growth rate is an important consideration, in addition to the pH of the precipitating fluid, when evaluating the boron isotope composition of carbonates due to their possible influences on amount of boron incorporated and, by extension, the associated isotopic signature.

Notably, our study is the first to employ the constant addition method for abiotic calcite growth; under laboratory conditions at 25 °C, the current published oxygen isotope equilibrium for calcite was generated using the CO_2 degassing technique (Kim and O’Neil, 1997) whereas that of aragonite has been tested using the degassing as well as constant addition techniques. In theory, the state of equilibrium exists as a standalone entity, independent of synthesis methodology. The synthesis of aragonite employing two experimental methodologies yielded no statistical difference in the determination of the equilibrium oxygen isotope fractionation factor between aragonite and water (Kim et al, 2007; Kim et al., 2014). It is therefore assumed that oxygen isotope fractionation behaviour for calcite samples synthesized via CO_2 degassing will be within the analytical error range of those grown using the constant addition method. However, it is worthwhile to try an alternative precipitation technique to corroborate the accuracy of the degassing equilibrium value for calcite, as it is possible that true equilibrium lies elsewhere. This consideration cannot be discounted until the calcite sample set from our study is indeed determined to be in disequilibrium, and/or further investigations (employing different methodology) support the initial equilibrium quantified by Kim and O’Neil (1997).

Moreover, previous reports of calcite-water oxygen isotope equilibrium were conducted in low ionic strength solutions. To simulate oceanic salinity, this study used solutions of high ionic strength akin to natural seawater (~ 0.7 mol/kg). Such a difference may alter the carbonate precipitation mechanism, inducing kinetic effects in the calcite samples otherwise not observed in aragonite possibly due to heightened reaction rates generating disequilibrium carbonate products. Kim et al. (2014) determined the equilibrium aragonite-water oxygen isotope fractionation factor to be independent of the ionic strength of the parent solution up to 0.7 mol/kg, although this relationship for calcite has yet to be investigated.

It is also possible that the oxygen isotope data is affected by boron incorporation into the calcite crystal lattice. To ascertain the influence of boron uptake on oxygen isotope equilibrium, two artificial seawater solutions should be prepared identically, with one as the “control group” and the other excepting only the inclusion of boric acid. Subsequent comparisons of the data will reveal whether or not the presence of boron disturbs oxygen isotope equilibrium. Quantification of various percentages of DIC-precipitated in two separate solutions (each containing only one of the two aqueous boron species, i.e., boric acid and borate) will also provide insight into the validity of the proxy. For example, if the overall boron isotope composition of the precipitated carbonate shifts with the percentage of DIC precipitated (e.g., 20% versus 40% versus 80%) then the speciation basis of the proxy is called into question. Of course, each of these variables must be examined independently. An additional consideration, specific to boron isotope composition as suggested by Ruiz-Agudro et al. (2012), attributes the deviation from equilibrium to isotopic fractionation associated with the potential change in coordination from tetrahedrally-coordinated to trigonally-coordinated boron upon incorporation into the crystal lattice. This possibility begs further investigation beyond the scope of this study.

Spontaneously precipitated calcite has never been unequivocally proven to be in true isotopic equilibrium at low temperatures (< 100 °C). Kim and O'Neil (1997) serve as the "gold standard" (i.e., baseline reference) for measured oxygen isotope fractionation factors derived for slow-growth calcite precipitates at 25 °C, reporting values consistent with statistical mechanical calculations of enrichment factors (27.67 ‰) (Chacko and Deines, 2008). However, Coplen's (2007) study sequence from Devils Hole, Nevada, revealed natural samples known to be near equilibrium but exhibiting a significantly larger oxygen isotopic fractionation factor (29.80 ‰). Dietzel et al. (2009) provided supportive evidence for these findings, suggesting that kinetic effects were at play in studies preceding Coplen's. Such a discrepancy indicates that equilibrium values may be underestimated for low temperatures (5-40 °C). Notably, Dietzel et al. (2009) did not allow for establishment of initial isotopic equilibrium prior to carbonate synthesis, which was conducted using the CO_2 diffusion technique, possibly introducing further methodological error into the investigation. Furthermore, Kluge et al. (2014) recently reported that the Devils Hole site temperature was, in fact, stable while $\delta^{18}O_{carbonate}$ varied – this is in direct contrast to the data interpretation provided by Coplen (2007). To resolve the current controversy of oxygen isotope fractionation factors for calcite, it is necessary to re-evaluate the currently adopted "equilibrium" values.

4.3.2 Boron isotope compositions in synthetic carbonate samples

The boron isotope compositions of inorganic aragonite and calcite ($\delta^{11}B_{aragonite}$ and $\delta^{11}B_{calcite}$) precipitated from pH values spanning 7.10 to 9.15 (aragonite) and 7.46 to 8.53 (calcite) are reported in Table 4.3. The pH trends and stability throughout carbonate syntheses are illustrated in Appendix A.2. While the $\delta^{11}B$ value of the experimental solution remained constant at ~ 39.85 ‰ over the course of carbonate growth, as pH increased from 7.10 to 9.15, $\delta^{11}B_{aragonite}$ also increased from 14.54 ‰ to 34.96 ‰, while $\delta^{11}B_{calcite}$ increased from 18.32 ‰ to 23.31 ‰ as pH increased from 7.25 to 8.15 (Figure 4.2). This direct correlation, in addition to the observed decrease in boron isotope fractionation between carbonate and solution with increasing pH, strongly supports the hypothesis that $B(OH)_4^-$ is incorporated into the crystal lattice (e.g., Spivack et al., 1993; Sanyal et al., 1995). Its exclusive incorporation cannot be confirmed in this study, however, particularly due to the unresolved boron isotope fractionation behavior in calcite, currently masked by kinetic effects.

Interestingly, both low-pH (7.4-7.6) and mid-pH (8.4-8.6) calcite samples share a common offset (~ 0.5 ‰) from oxygen isotope equilibrium, however this same difference is not reflected along the estimated aqueous borate curve which accounts for a variety of pK_B characterizations. Rather, the mid-pH calcites are in relatively good agreement with the mid-pH aragonites as well as the aqueous borate curve, compared to the low-pH calcites which are situated ~ 3 ‰ above the low-pH aragonites corresponding closely with the borate curve.

Incorporation of ^{11}B-enriched boric acid along with borate ion in the carbonate lattice during mineralization may account for the non-equilibrium enrichment of ^{11}B in the experimental calcites, resulting in a heavier overall boron isotopic composition of the carbonate compared to the expected value assuming exclusive incorporation of borate. Previous literature (e.g., Sanyal et al., 2000) indicates that boron incorporated into synthetic carbonate minerals precipitated under pH-controlled conditions possesses an isotopic signature very similar to that of aqueous borate, offering quantitative evidence for preferential incorporation of borate into the carbonate. However, a progressive enrichment in ^{11}B relative to aqueous borate is registered at lower pH values, as observed by the positive offset between δ^{11}B of inorganic calcite (Sanyal et al., 2000) and aqueous borate (Klochko et al., 2006) observed to be ~ 4, 2 and 1 ‰ at pH values of 7.6, 8.2 and 8.5, respectively. Equal proportions of aqueous boron species are found at pH = 8.597 (Dickson, 1990) with the relative concentration of boric acid increasing as pH decreases (Klochko et al., 2006); thus, its contribution to the incorporation of boron into the carbonate also increases, progressively amplifying deviations in $\delta^{11}B_{carbonate}$ from the borate curve.

These inorganic carbonate precipitation experiments proved time-consuming, with earlier synthesis attempts marked by non-ideal pH variability given the primary objective of this project is to constrain boron isotopic composition and speciation by isolating these parameters (i.e., precipitating carbonates at a stable pH). Evaluation of the pH trend associated with synthesized $\delta^{11}B_{carbonate}$ versus calculated $\delta^{11}B_{B(OH)4-}$ is further complicated by pK_B and $^{11\text{-}10}K_B$ constants unique to experimental conditions employed in this study (see Table 4.4 for details). Rather, to accurately interpret the boron isotope compositions of synthesized carbonate samples, the most appropriate constants must be selected based on similarities in experimental solution compositions.

The makeup of our system yields a pK_B value between 8.597 (Dickson, 1990) and 8.830 (Hershey et al., 1986), as well as $^{11-10}K_B$ values ranging from 1.0250 to 1.0272 (Klochko et al., 2006). The acid dissociation constants (pK_B) are differentiated based on the chemical constituents of the parent solution: Na^+, Mg^{2+}, Ca^{2+}, K^+, SO_4^{2-} and Cl^- were all included in Dickson's (1990) experimental media while only Na^+ and Cl^- were added to Hershey et al. (1986) aqueous solution. Similarly, the two varying boron isotope fractionation factors ($^{11-10}K_B$) reported by Klochko et al. (2006) were empirically observed as chemical equilibrium in a 0.6 mol/kg KCl-H_2O mixture (1.0250) and a 0.7 mol/kg synthetic seawater solution ($S = 35$, $B_T = 0.01$ mol/kg H_2O) were 1.0250 and 1.0272, respectively. If only borate is being incorporated into the crystal lattice, then pK_B and $^{11-10}K_B$ lie nearer 8.597 and 1.0250, respectively. A line of 'best fit' for our assumed equilibrium aragonite data generates a pK_B value of 8.64 and a $^{11-10}K_B$ value ~ 1.0254; however, possible incorporation of any $B(OH)_3$ renders these constants invalid in calculating $\delta^{11}B_{B(OH)4-}$ with pH. Since exclusive incorporation of borate ion into the crystal lattice has not been confirmed, previously established values for pK_B and $^{11-10}K_B$ were applied to compare $\delta^{11}B_{carbonate}$ and $\delta^{11}B_{B(OH)4-}$.

Notably, the chemical composition of the synthetic seawater solutions in this study does not contain sulfate ion or potassium, which are both components of true seawater, rendering the Tris correction factor imperfect. Application of a different correction factor will inevitably affect the positioning of the pK_B curve. Therefore, usage of a Tris buffer will be more appropriate with the inclusion of additional seawater constituents in follow-up studies. Daily calibration of the buffer will allow any drift to be monitored and rectified by regularly renewing buffer solution.

This study comprises two intermediate steps in the establishment of the boron isotope paleo-pH proxy, namely the examination of inorganic aragonite and calcite oxygen and boron isotope behaviour at 25 °C under a variety of stable pH conditions. Subsequent experimental work will include other ion constituents to closer mimic natural seawater conditions, improving the pK_B and ${}^{11\text{-}10}K_B$ selection processes, and providing a more realistic depiction of oxygen and boron stable isotope systematics in the oceans. Carbonate samples from this study will next be subjected to ^{11}B magic angle spinning nuclear magnetic resonance (MAS NMR) spectroscopy analysis to further classify boron coordination within the crystal lattice. This insight will be invaluable to identify the presence of trigonal or tetrahedral boron however cannot identify any changes in coordination that may have occurred upon uptake.

4.4 Conclusions

Calcium carbonate in the form of aragonite and calcite was synthesized from high ionic strength solutions at 25 °C with stable pH values ranging from 7.10 to 9.18 using a modified constant addition method. The boron isotope composition of each sample was compared to the predicted equilibrium boron isotope composition of $B(OH)_4^-$ in seawater at the same pH value. Boron isotope compositions analyzed by MC-ICPMS were interpreted by considering pK_B constants 8.597 and 8.830, as well as $^{11\text{-}10}K_B$ values of 1.0250 and 1.0272. These double-bounded constants were necessary due to the unique chemical compositions of this study's experimental solutions, which were neither as simple nor complex as those from which the constants were derived. The direct correlation of increasing $\delta^{11}B_{carbonate}$ with pH indicates the preferential incorporation of $B(OH)_4^-$ into the crystal lattice, an observation consistent with a fundamental supposition underlying the boron isotope paleo-pH proxy.

Carbon isotope behavior plays a potentially important role for the boron-pH proxy due to certain elemental similarities with boron, perhaps offering further insight into the power of a multi-element approach in the refinement of paleoclimate proxies. However, the experimental system must first be developed to control its isotopic variance spanning the carbonate growth period. To ascertain the point at which isotopic drift is minimized, different injection rates can be implemented as a trial-and-error attempt to yield zero fluctuation. Alternatively, the initial solution can be left in a closed system for calcium carbonate crystal growth to proceed without the addition of titrant solution; upon quantification of precipitation rate, the rate of ion replenishment can be calculated appropriately and implemented as a function of titrant injection rate. Investigation of these various permutations and interrelationships is essential to the development of a multi-element approach targeted to refine the boron isotope paleo-pH proxy.

Controversy remains as to as to the exact mechanism of boron incorporation into carbonate, specifically whether only borate ion or both boric acid and borate ion can be incorporated. The debate aside, the isotopic composition of boron in carbonate precipitated from seawater is strongly pH-dependent (Sanyal et al., 2000), allowing reconstruction of paleo-seawater pH from marine carbonates. Growth rate is an additional consideration when using boron as a pH proxy due to its possible influence on the amount of boron incorporated and its associated isotopic signature. A fundamental understanding of laboratory-synthesized samples, in which chemical composition and temperature are carefully calibrated, will allow for quantification and correction of vital effects in natural samples. Eventually, the boron isotopic composition of marine biogenic carbonates preserved in sediment will reveal important information about the environment from which they were precipitated.

This study serves as a stepping-stone chronicling the development of the boron isotope paleo-pH proxy. While the pH-dependence of boron isotope compositions in marine carbonates requires further investigation under conditions more likened to true seawater, our results demonstrate the feasibility of the proxy in reconstructing seawater pH. This parameter can then be used in conjunction with seawater alkalinity or the dissolved inorganic carbon concentrations to outline variations in $p\mathrm{CO}_2$ spanning Earth's history (Zeebe and Wolf-Gladrow, 2001). Subsequent application of ancient seawater pH values to general circulation models documenting historical trends will provide a more intricate understanding of the cause-and-effect relationships underlying climate change.

Table 4.1: Experimental conditions for modified constant addition experiments.

Sample Name	Start[a] (mmolal)	Titrant 1[b] (mmolal)	Titrant 2[c] (mmolal)	Duration (hrs)	Sample Size (mg)	Average Temp. (°C)	Average pH (total scale)
CKG-Oct511	5/5/0.5/2/7.9/685	60/20/620	3/20/695	375.23	70	25.04	8.52
CKG-Mar2112-C	5/5/0.5/2/7.9/685	60/20/620	3/20/695	411.05	45	25.01	8.51
CKG-Apr2712-D	5/5/0.5/2/7.9/685	60/20/620	3/20/695	405.87	43	24.99	8.56
CKG-Aug312-D2	0/10/0.25/1/7.9/685	0/80/510	5/20/695	406.88	264	25.05	8.99
CKG-Aug3012-E	5/5/0.5/2/7.9/685	60/20/620	3/20/695	626.88	79	24.94	8.49
CKG-Sept2512-D2	0/10/0.25/1/7.9/685	0/80/510	5/20/695	595.17	92	25.06	9.18
CKG-Oct2912-E	5/5/0.5/2/7.9/685	60/20/620	3/20/695	595.17	71	25.03	8.52
CKG-Oct2912-E2	5/5/0.5/2/7.9/685	60/20/620	3/20/695	599.73	88	25.06	8.49
CKG-Dec512-D	0/10/0.25/1/7.9/685	0/80/510	5/20/695	599.73	80	25.08	9.14
CKG-Dec512-D2	0/10/0.25/1/7.9/685	0/80/510	5/20/695	479.40	67	25.05	9.14
CKG-Dec1412-C	7.5/2.5/10/40/7.9/592	16/4/685	5/20/695	599.73	270	25.03	7.27
CKG-Feb2513-C	0/10/0.25/1/7.9/685	0/80/510	5/20/695	450.82	75	25.05	9.15
CKG-Feb2513-D	0/10/0.25/1/7.9/685	0/80/510	5/20/695	450.82	59	25.07	9.15
CKG-Feb2513-E	10/0/10/40/7.9/570	60/20/620	10/20/695	283.03	389	25.08	7.10
CKG-Apr313-C	10/0/10/40/7.9/570	60/20/620	10/20/695	307.25	340	25.03	7.31
CKG-Apr313-D	10/0/10/40/7.9/570	60/20/620	10/20/695	211.58	335	25.06	7.28
CKG-Apr313-E	10/0/10/40/7.9/570	60/20/620	10/20/695	67.22	67	25.06	7.32
JW-June2813-C	7.5/2.5/1/0.13/7.9/692	16/4/685	10/20/685	358.50	100	25.01	8.40
JW-June2813-D	7.5/2.5/1/0.13/7.9/692	16/4/685	10/20/685	358.50	92	25.04	8.58
JW-June2813-E	7.5/2.5/1/0.13/7.9/692	16/4/685	10/20/685	358.50	110	25.04	8.70
JW-July3013-D	7.5/2.5/1/0.13/7.9/692	16/4/685	10/20/685	594.75	91	25.09	8.46
JW-July3013-E	7.5/2.5/1/0.13/7.9/692	16/4/685	10/20/685	594.75	113	25.09	8.42
JW-Nov1313-A	10/0/10/1.3/7.9/673	20/0/690	10/20/685	452.17	330	25.03	7.40
JW-Nov1313-C	10/0/10/1.3/7.9/673	20/0/690	10/20/685	452.17	325	25.03	7.43
JW-Dec0413-A	10/0/10/1.3/7.9/673	20/0/690	10/20/685	385.33	212	25.01	7.46
JW-Dec0413-C	10/0/10/1.3/7.9/673	20/0/690	10/20/685	385.33	188	25.02	7.46

[a] $NaHCO_3/Na_2CO_3/Ca/Mg/B/NaCl$

[b] $NaHCO_3/Na_2CO_3/NaCl$

[c] Ca/B/NaCl

Table 4.2: Oxygen isotope compositions confirming isotopic equilibrium.

Sample Name	$\delta^{18}O_{aragonite}$ (‰)	$\delta^{18}O_{water}$ (‰)	$\alpha_{(aragonite\text{-}H2O)}$	$1000\ln\alpha_{(aragonite\text{-}H2O)}$
CKG-Oct511	22.45	-6.76	1.0294	28.99
CKG-Mar2112-C	22.52	-6.63	1.0293	28.92
CKG-Apr2712-D	22.45	-6.70	1.0293	28.92
CKG-Aug312-D2	22.59	-6.73	1.0295	29.09
CKG-Aug3012-E	22.51	-6.62	1.0293	28.90
CKG-Sept2512-D2	22.59	-6.52	1.0293	28.88
CKG-Oct2912-E	22.56	-6.51	1.0293	28.84
CKG-Oct2912-E2	22.53	-6.49	1.0292	28.80
CKG-Dec512-D	22.67	-6.41	1.0293	28.84
CKG-Dec512-D2	22.69	-6.43	1.0293	28.89
CKG-Dec1412-C	22.96	-6.43	1.0296	29.15
CKG-Feb2513-C	22.65	-6.60	1.0294	29.02
CKG-Feb2513-D	22.63	-6.57	1.0294	28.97
CKG-Feb2513-E	22.67	-6.64	1.0295	29.08
CKG-Apr313-C	22.64	-6.69	1.0295	29.10
CKG-Apr313-D	22.60	-6.68	1.0295	29.05
CKG-Apr313-E	22.49	-6.74	1.0294	29.01
		*Average:	1.0294	28.97

*Stdev = 0.10

Sample Name	$\delta^{18}O_{calcite}$ (‰)	$\delta^{18}O_{water}$ (‰)	$\alpha_{(calcite\text{-}H2O)}$	$1000\ln\alpha_{(calcite\text{-}H2O)}$
JW-June2813-C	22.03	-6.63	1.0288	28.44
JW-June2813-D	22.09	-6.66	1.0289	28.53
JW-June2813-E	22.20	-6.52	1.0289	28.49
JW-July3013-D	22.06	-6.58	1.0288	28.42
JW-July3013-E	22.19	-6.62	1.0290	28.59
JW-Nov1313-A	22.53	-6.36	1.0290	28.66
JW-Nov1313-C	22.51	-6.44	1.0290	28.73
JW-Dec0413-A	22.50	-6.31	1.0290	28.59
JW-Dec0413-C	22.57	-6.32	1.0290	28.66
		**Average:	1.0289	28.57

**Stdev = 0.08

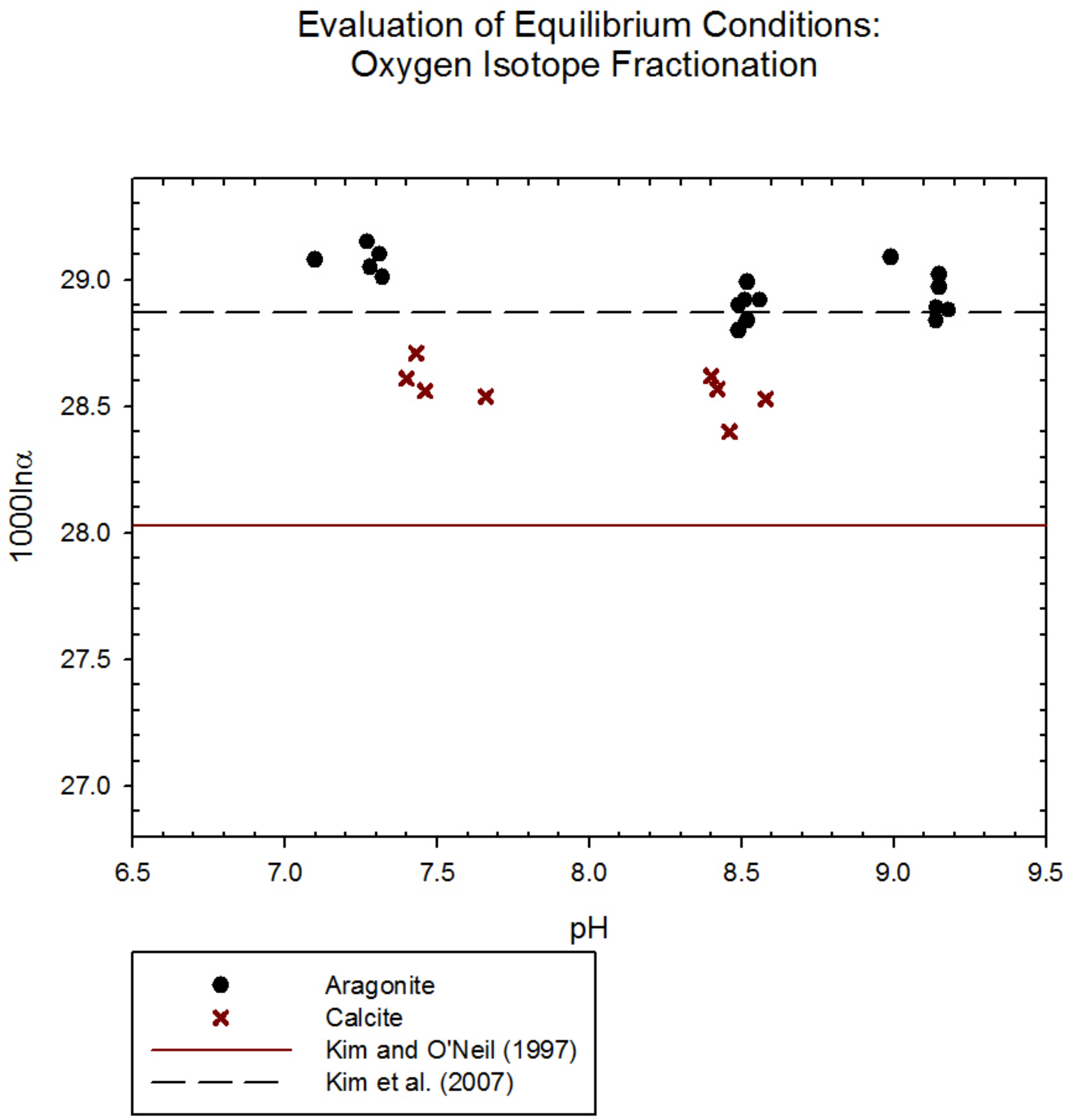

Figure 4.1: Comparison of this study with published oxygen isotope equilibrium values.

Using the modified constant addition method, the oxygen isotope fractionation of synthesized aragonite samples fall within the analytical error range reported by Kim et al. (2007) whereas that of the calcite samples are systematically offset ~ 0.5-0.7 ‰ from the equilibrium value proposed by Kim and O’Neil (1997) using the degassing technique. A combined analytical error is approximately 0.2 ‰.

Table 4.3: Boron isotope compositions in synthetic calcium carbonate.

Sample	Average pH	σ	$\delta^{11}B_{carb}$ (‰)
CKG-Oct511	8.52	0.03	24.81
CKG-Mar2112-C	8.51	0.02	24.62
CKG-Apr2712-D	8.56	0.04	24.50
CKG-Aug312-D2	8.99	0.05	31.26
CKG-Aug3012-E	8.49	0.03	24.45
CKG-Sept2512-D2	9.18	0.03	34.19
CKG-Oct2912-E	8.52	0.02	24.65
CKG-Oct2912-E2	8.49	0.03	24.65
CKG-Dec512-D	9.14	0.06	34.81
CKG-Dec512-D2	9.14	0.05	34.85
CKG-Dec1412-C	7.27	0.08	15.62
CKG-Feb2513-C	9.15	0.05	34.96
CKG-Feb2513-D	9.15	0.05	24.85
CKG-Feb2513-E	7.10	0.03	14.54
CKG-Apr313-C	7.31	0.13	14.94
CKG-Apr313-D	7.28	0.11	14.84
CKG-Apr313-E	7.32	0.12	14.86
JW-June2813-C	8.40	0.12	21.07
JW-June2813-D	8.58	0.07	21.23
JW-June2813-E	8.70	0.12	22.85
JW-July3013-D	8.46	0.03	21.86
JW-July3013-E	8.42	0.02	23.31
JW-Sept0413-D	7.66	0.10	19.37
JW-Nov1313-A	7.40	0.12	18.62
JW-Nov1313-C	7.43	0.11	18.32
JW-Dec0413-A	7.46	0.12	18.62
JW-Dec0413-C	7.46	0.12	18.55

σ = Standard deviation based on population (stdevp).

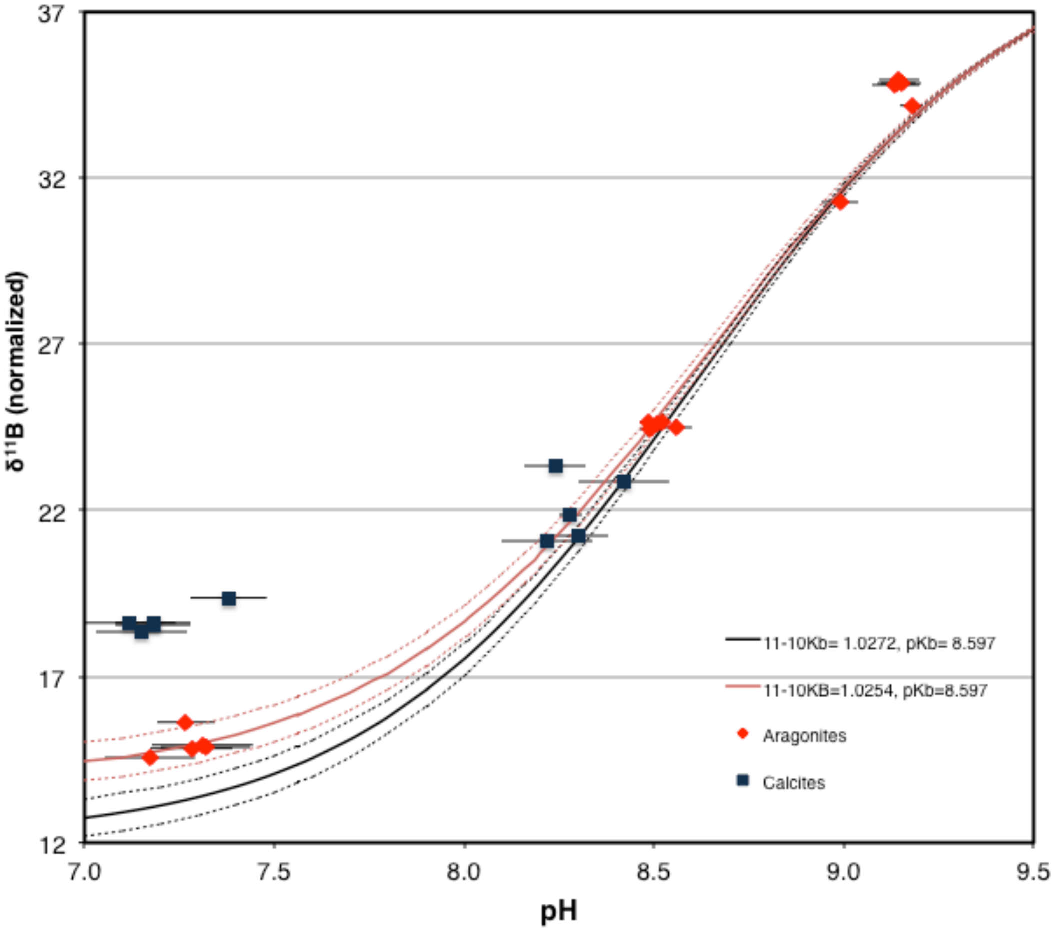

Figure 4.2: Estimated *in situ* fit (red line) of inorganic carbonate data with theoretical approximation (black line).

To best simulate experimental conditions in this study, an acid dissociation constant (pK_B) of 8.597 was used (as per Dickson, 1990) and a Tris correction factor of 0.28 was applied to the total scale pH readings compiled for all boron-measured aragonite and calcite samples. Our data yields an *in situ* boron equilibrium constant ($^{11-10}K_B$) of ~ 1.0254 relative to that empirically derived from Klochko et al. (2006), a discrepancy attributable to the unique chemical constituents in this study's synthetic seawater solution.

Table 4.4: Acid dissociation constants (pK_B) for $B(OH)_3$ at 25 °C (from Klein-Gebbinck, 2013).

Author(s)	pH scale	Ionic Strength (mol kg^{-1})	Media	pK_B^*
Buch (1933)	uncertain	(34.4)[a]	Na^+, Ca^{2+}, Cl^-	8.74
Owen and King (1945)	pH_{NBS}	0.725	Na^+, Cl^-	8.831
Lyman (1957)	pH_{NBS}	(33)[a]	Seawater	8.54[b]
Dyrssen and Hansson, (1973)	uncertain	0	pure water	9.237
		0.7	Na^+, Cl^-	8.85
		0.7	synthetic seawater (Na^+, Cl^-, Ca^{2+}, Mg^{2+}, SO_4^{2-})	8.61
Hansson (1973)	pH_T	0.7	Na^+, Mg^{2+}, Ca^{2+}, Cl^-, SO_4^{2-}	8.61
Bryne and Kester (1974)	pH_{NBS}	0.7	Na^+, Ca^{2+}, Cl^-	8.774[c]
			Na^+, Mg^{2+}, Cl^-	8.715[c]
Hershey et al. (1986)	pH_T	0.68	Na^+, Cl^-	8.83
			Na^+, Mg^{2+}, Cl^-	8.725
			Na^+, Ca^{2+}, Cl^-	8.675
Dickson (1990)	pH_T	0.7	Na^+, Mg^{2+}, Ca^{2+}, Cl^-, K^+,SO_4^{2-}	8.597
Tossell (2005)	n/a	n/a	computational	9.2
Bryne et al. (2006)	pH_T	0.6	K^+, Cl^-	8.64

[a] In salinity (psu).

[b] calculated from Pitzer interaction parameters in Hershey et al., (1986).

[c] corrected by Millero (1982).

References

Atekwana, E. A., & Krishnamurthy, R. V. (1998). Seasonal Variations of Dissolved Inorganic Carbon and d13C of Surface Waters: Application of a Modified Gas Evolution Technique. *Journal of Hydrology*, *205*, 265–278.

Barnola, J. M., Raynaud, D., Korotkevich, Y. S., & Lorius, C. (1987). Vostok ice core provides 160,000-year record of atmospheric CO2. *Nature*, *329*, 408–414.

Beck, W. C., Grossman, E. L., & Morse, J. W. (2005). Experimental studies of oxygen isotope fractionation in the carbonic acid system at 15°, 25°, and 40°C. *Geochimica et Cosmochimica Acta*, *69*(14), 3493–3503. doi:10.1016/j.gca.2005.02.003

Chacko, T., & Deines, P. (2008). Theoretical calculation of oxygen isotope fractionation factors in carbonate systems. *Geochimica et Cosmochimica Acta*, *72*(15), 3642–3660. doi:10.1016/j.gca.2008.06.001

Coplen, T. B. (2007). Calibration of the calcite–water oxygen-isotope geothermometer at Devils Hole, Nevada, a natural laboratory. *Geochimica et Cosmochimica Acta*, *71*(16), 3948–3957. doi:10.1016/j.gca.2007.05.028

Dickson, A. (1990). Thermodynamics of the dissociation of boric acid in synthetic seawater from 273.15 to 318.15 K. *Deep Sea Research Part A. Oceanographic Research Papers, 37(5),* 755-766.

Dickson, A. G. (1993). The measurement of sea water pH. *Marine Chemistry*, *44*(2-4), 131–142. doi:10.1016/0304-4203(93)90198-W

Dietzel, M., Tang, J., Leis, A., & Köhler, S. (2009). Oxygen isotopic fractionation during inorganic calcite precipitation — Effects of temperature, precipitation rate and pH. *Chemical Geology*, *268*(1-2), 107–115. doi:10.1016/j.chemgeo.2009.07.015

Epstein, S., & Mayeda, T. (1953). Variation of O18 content of waters from natural sources. *Geochimica et Cosmochimica Acta*, *4*, 213–224.

Foster, G. L., & Rohling, E. J. (2013). Relationship between sea level and climate forcing by CO2 on geological timescales. *Proceedings of the National Academy of Sciences of the United States of America*, *110*(4), 1209–14. doi:10.1073/pnas.1216073110

Hansson, I. (1973). A new set of pH-scales and standard buffers for sea water. *Deep-Sea Research*, *20*, 479–491.

Hemming, N G, & Hanson, G. N. (1992). Boron isotopic composition and concentration in modern marine carbonates. *Geochimica et Cosmochimica Acta*, *56*, 537–543.

Hemming, N Gary, Reeder, R. J., & Hanson, G. N. (1995). Mineral-fluid partitioning and isotopic fractionation of boron in synthetic calcium carbonate. *Geochimica et Cosmochimica Acta*, *59*(2), 371–379.

Hershey, J. P., Fernandez, M., Milne, P. J., Millero, J., & Hal, F. (1986). The ionization of boric acid in NaCI , Na-Ca-Cl and Na-Mg-Cl solutions at 25 ° C. *Geochimica et Cosmochimica Acta*, *50*(4), 143–148.

Hoefs, J. (2009). Stable Isotope Geochemistry. Sixth Edition. Springer. 285p.

Hönisch, B., Hemming, N. G., Archer, D., Siddall, M., & McManus, J. F. (2009). Atmospheric carbon dioxide concentration across the mid-Pleistocene transition. *Science*, *324*(5934), 1551–4. doi:10.1126/science.1171477

Jouzel, J., Lorius, C., Petit, J. R., Genthon, C., Barkov, N., Kotlyakov, V. M., & Petrov, V. M. (1987). Vostok ice core: a continuous isotope temperature record over the last climatic cycle (160,000 years). *Nature*, *329*, 403–407.

Kakihana, H., Kotaka, M., Satoh, S., Nomura, M., & Okamoto, M. (1977). Fundamental Studies on the Ion-Exchange Separation of Boron Isotopes. *Bulletin of the Chemical Society of Japan*, *50*(1), 158–163.

Kim, S., O'Neil, J., Hillaire-Marcel, C., & Mucci, A. (2007). Oxygen isotope fractionation between synthetic aragonite and water: Influence of temperature and Mg2+ concentration. *Geochimica et Cosmochimica Acta*, *71*(19), 4704–4715. doi:10.1016/j.gca.2007.04.019

Kim, S.-T., & O'Neil, J. (1997). Equilibrium and nonequilibrium oxygen isotope effects in synthetic carbonates. *Geochimica et Cosmochimica Acta*, *61*(16), 3461–3475.

Klochko, K., Kaufman, A. J., Yao, W., Byrne, R. H., & Tossell, J. A. (2006). Experimental measurement of boron isotope fractionation in seawater. *Earth and Planetary Science Letters*, *248*(1-2), 276–285. doi:10.1016/j.epsl.2006.05.034

Kluge, T., Affek, H. P., Dublyanski, Y., & Spotl, C. (2014). Devils Hole Paleotemperatures and Implications for Oxygen Isotope Equilibrium Fractionation. *Earth & Planetary Science Letters, 400,* 251-260.

Lemarchand, D., Gaillardet, J., Lewin, E., & Allegre, C. J. (2002). Boron isotope systematics in large rivers: implications for the marine boron budget and paleo-pH reconstruction over the Cenozoic. *Chemical Geology*, *190*, 123–140.

Lowenstein, T. K., Timofeeff, M. N., Brennan, S. T., Hardie, L. A., & Demicco, R. V. (2001). Oscillations in Phanerozoic Seawater Chemistry: Evidence From Fluid Inclusions. *Science*, *294*, 1086–1089.

Millero, F. J., Zhang, J., Fiol, S., Sotolongo, S., Roy, R. N., & Lee, K. (1993). The use of buffers to measure the pH of seawater m (SO24-)/ K (HSO ;). *Marine Chemistry*, *44*, 143–152.

Milliman, J. D. (1974). Marine Carbonates. Springer-Verlag (1974), 375p.

Morse, J. W., Arvidson, R. S., & Lüttge, A. (2007). Calcium carbonate formation and dissolution. *Chemical reviews*, *107*(2), 342–81. doi:10.1021/cr050358j

Pagani, M., Lemarchand, D., Spivack, A., & Gaillardet, J. (2005). A critical evaluation of the boron isotope-pH proxy: The accuracy of ancient ocean pH estimates. *Geochimica et Cosmochimica Acta*, *69*(4), 953–961. doi:10.1016/j.gca.2004.07.029

Palmer, T., & Wilson, M. (2004). Calcite precipitation and dissolution of biogenic aragonite in shallow Ordovician calcite seas. *Lethaia*, *37*(4), 417–427. doi:10.1080/00241160410002135

Petit, J. R., Raynaud, D., Basile, I., Chappellaz, J., Ritz, C., Delmotte, M., … Pe, L. (1999). Climate and atmospheric history of the past 420,000 years from the Vostok ice core, Antarctica. *Nature*, *399*, 429–436.

Rollion-Bard, C., Chaussidon, M., & France-Lanord, C. (2011). Biological control of internal pH in scleractinian corals: Implications on paleo-pH and paleo-temperature reconstructions. *Comptes Rendus Geoscience*, *343*(6), 397–405. doi:10.1016/j.crte.2011.05.003

Romanek, C., Grossman, E., & Morse, J. (1992). Carbon isotopic fractionation in synthetic aragonite and calcite : Effects of temperature and precipitation rate. *Geochimica et Cosmochimica Acta*, *56*, 419–430.

Sanyal, A., Hemming, N. G., Hanson, G. N., & Broecker, W. (1995). Evidence for a higher pH in the glacial ocean from boron isotopes in foraminifera. *Nature*, *373*, 234–236.

Sanyal, A., Nugent, M., Reeder, R. J., & Bijma, J. (2000). Seawater pH control on the boron isotopic composition of calcite : Evidence from inorganic calcite precipitation experiments. *Geochimica et Cosmochimica Acta*, *64*(9), 1551–1555.

Spivack, A. J., Palmer, M. R., & Edmond, J. M. (1987). The sedimentary cycle of the boron isotopes. *Geochimica et Cosmochimica Acta*, *51*, 1939–1949.

Usdowski, E., & Hoefs, J. (1990). Kinetic 13C/12C and 18O/16O effects upon dissolution and outgassing of CO2 in the system CO2-H2O. *Chemical Geology (Isotope Geosciences Edition)*, *80*, 109–118.

Vengosh, A., Kolodny, Y., Starinsky, A., Chivas, A. R., & McCulloch, M. T. (1991). Coprecipitation and isotopic fractionation of boron in modern biogenic carbonates. *Geochimica et Cosmochimica Acta*, *55*(10), 2901–2910. doi:10.1016/0016-7037(91)90455-E

Zeebe, R. (2007). An explanation of the effect of seawater carbonate concentration on foraminiferal oxygen isotopes. *Geochimica et Cosmochimica Acta*, *63*(13), 2001–2007.

Zeebe, R. E., Sanyal, A., Ortiz, J. D., & Wolf-Gladrow, D. A. (2001). A theoretical study of the kinetics of the boric acid–borate equilibrium in seawater. *Marine Chemistry*, *73*(2), 113–124. doi:10.1016/S0304-4203(00)00100-6

Zeebe, R. E., & Wolf-Gladrow, D. (2001). *CO2 in Seawater: Equilibrium, Kinetics, Isotopes: Equilibrium, Kinetics, Isotopes*. Elsevier. 325p.

CHAPTER 5:

TEMPERATURE DEPENDENCE AND OXYGEN ISOTOPE EFFECTS IN THE CALCITE-CO_2-H_2O-NaCl SYSTEM

Temperature Dependence and Oxygen Isotope Effects in the Calcite-CO_2-H_2O-NaCl System

Jillian Wyman[a] and Sang-Tae Kim[a]

[a]School of Geography and Earth Sciences, McMaster University, 1280 Main Street West, Hamilton, ON L8S 4K1, Canada

Abstract

This study is the first to examine kinetic effects in synthetic calcite over a spectrum of pH and temperature ranges using the modified constant addition method. Oxygen isotope systematics were quantified in abiotic calcite samples grown in a high ionic strength solution (~ 0.7 mol/kg) at three different temperatures (10, 25 and 40 °C) and over three different pH ranges (low pH ~ 7.15, mid pH ~ 8.35 and high pH ~ 9.15). Oxygen isotope fractionation between calcite and H_2O was found to be dependent on both temperature and pH. Injection rate was adjusted with temperature to conform to known reaction rate constants in an attempt to contrast equilibrium products with those experiencing kinetic effects. Preliminary results support Kim et al. (2006), who postulated the link between injection rate, precipitation rate and state of isotopic equilibrium. Solution chemistry was also determined to be an important factor when differentiating the temperature- and pH-dependence spanning the various permutations in experimental conditions; the presence of bicarbonate and/or carbonate ions (HCO_3^- and CO_3^{2-}, respectively) was found to be instrumental to the derivation and – predictably – deviation from oxygen isotope equilibrium. Several causalities for oxygen isotope effects were identified, ultimately providing strong support for the calcite-water oxygen isotope equilibrium fractionation factor reported by Kim and O'Neil (1997) relative to other published values.

5.1 Introduction

The discovery and development of stable isotope geothermometry is fundamental to the field of paleoclimatology. Geologists have long contemplated how Earth's climate has varied in the past but were unable to quantify historical temperature changes until Urey's 1947 groundbreaking contribution, in which he calculated the temperature dependence of oxygen isotope fractionation between calcium carbonate and water, highlighting the potential of marine carbonates to act as a paleothermometer. Urey (1947) determined that an empirically-derived calcite-water oxygen isotope fractionation ($1000\ln\alpha_{\text{calcite-water}}$) change from 30 to 31 ‰ yielded a temperature change from 8 °C to 12 °C. While isotopic fractionation behaviour has proven to be more complex than initially believed, this remarkable relationship provided an important and inspiring foundation for paleoclimatology researchers to build upon. The temperature dependence of calcium carbonate mineral growth is an important parameter to be examined when chronicling the variation in relative abundances of abiotic marine carbonate polymorphs over time. The critical Mg:Ca ratio at which calcite versus aragonite precipitates decreases sharply with increasing temperature (Morse et al., 1997).

The validity of oxygen isotope fractionation as a temperature proxy is affected by non-equilibrium fractionation effects due to calcium carbonate growth solution chemistry and/or precipitation rate (McCrea, 1950; Tarutani et al., 1969; De Villiers et al., 1995; Kim and O'Neil, 1997; Spero et al., 1997; Zeebe, 1999; Jiménez-López et al., 2001; Kim et al., 2006). Using the CO_2 diffusion technique, Dietzel et al. (2009) previously observed kinetic effects affecting oxygen isotope fractionation for disequilibrium calcite growth. Their results call into question the accuracy of the currently adopted calcite-water oxygen equilibrium fractionation factor (Kim and O'Neil, 1997) however it must be noted that Dietzel et al. (2009) did not account for establishment of isotopic equilibration prior to experimentation, rendering it difficult to disentangle the contributing factors. The temperature-sensitive nature of achieving isotopic equilibrium within the parent solution, prior to experimentation, proved to be an integral consideration for the outcome of this study. Both thermal and chemical equilibrium must be individually established prior to attaining a state of isotopic equilibrium (Beck et al., 2005). A change in temperature or pH will directly impact isotope exchange kinetics and thus the time required to achieve isotopic equilibrium. Decreasing temperature and/or increasing pH will retard reaction rates, whereas increasing temperature and/or decreasing pH are associated with faster reactions; exact relationships detailed in Beck et al. (2005) are valuable to ensure apparent oxygen isotopic equilibrium has been reached among DIC species before initiating a precipitation experiment.

Apparent oxygen isotopic fractionation between carbonates and water is further influenced by a combination of kinetic effects in the aqueous carbonate species (Mills and Urey, 1940; McConnaughey, 1989, Kim et al., 2006) as well as surface entrapment of isotopically light CO_3^{2-} ions (Watson, 2004). At higher precipitation rates, kinetic effects in solution largely control the state of (dis)equilibrium, which itself is a function of changing solution chemistry, pH, and/or precipitation rate. At slower precipitation rates, aqueous carbonate species are in oxygen isotopic equilibrium, thus fractionation is governed by the entrapment of CO_3^{2-} in the surface layer, minimizing the role of solution pH and amplifying the influence of precipitation rate (Dietzel et al., 2009). Predictably, discrepancy exists among theoretical, empirical and experimental reports of the oxygen isotope fractionation equation between calcite and water, however a range of uncertainty must be considered to accurately identify overlap between approaches. As noted by Coplen (2007), Horita and Clayton (2007) did not include the error associated with their statistical-mechanical calculations, rendering the possibility that, under a larger umbrella of uncertainty, these calculations may agree with Coplen's measured values.

Given the ongoing debate in the literature over appropriate selection of equilibrium carbonate-water fractionation factors and varied interpretations of observed kinetic effects, it is necessary to further investigate oxygen isotopic fractionation during slow carbonate precipitation; a thorough evaluation of the potential acting mechanisms will reveal important insights to distinguish equilibrium from disequilibrium oxygen isotope fractionation effects. Our study is the first to oxygen isotope effects in synthetic calcite over a variety of pH and temperature ranges using the modified constant addition method, abiding by Beck et al. (2005)'s recommended guidelines to ensure parent solutions had established isotopic equilibrium preceding the onset of experimentation. Oxygen isotope systematics were quantified in abiotic calcite samples grown in a seawater-like solution (~ 0.7 mol/kg) at three different temperatures (10, 25 and 40 °C) and over three different pH ranges (low pH ~ 7.15, mid pH ~ 8.35 and high pH ~ 9.15). Numerous permutations of these experimental conditions were trialed to provide insight into the relationship linking temperature, pH, and non-equilibrium isotope effects.

5.2 Experimental methods

5.2.1 Overview

This study employed the unseeded pH-stat method, a modified version of the constant addition technique. In this approach, reactant solution is simply added to the reactor at a constant rate, thereby attaining and maintaining steady state conditions throughout the experimental duration. A dual syringe pump dispenses two titrants in equal amounts, which are injected simultaneously at a continuous, predetermined rate of 0.25 mL/hr or 0.50 ml/hr into an airtight Teflon® reaction vessel. The starting solution reaches a state of supersaturation (with respect to calcite) just prior to the addition of the two titrant solutions, with subsequent spontaneous nucleation and carbonate precipitation. Calcium carbonate is thus precipitated without the use of seed material under a closed system. The constant addition method allows ongoing replenishment of aqueous ions as they are consumed during carbonate precipitation in a given period of time.

The temperature of experimental solutions is held constant by circulating water from a temperature-controlled water bath and a water-jacketed glass reaction vessel. In this study, experimental chambers were connected to three different water baths, each set at a different temperature (i.e., 10 ± 0.01 °C, 25 ± 0.01 °C and 40 ± 0.01 °C). Solution homogeneity is maintained with a floating magnetic stirrer throughout precipitation. Aliquots of experimental solution are collected at the onset and conclusion of each experiment. Solution temperature and pH are monitored daily using a Thermo Scientific Traceable® digital thermometer and ROSS® Sure-Flow combination pH electrode, respectively; the electrode is calibrated with NIST-traceable pH buffers (4.00, 7.00, and

10.00) which are also stored in their respective temperature-controlled water baths to ensure consistency between all experimental solutions. Upon termination of each experiment, solutions are filtered, with the carbonate crystals dried overnight in a 70 °C oven then subsequently collected for isotopic analysis.

Once pH was deemed "stable" (e.g., $\sigma = 0.10$) after conducting multiple trials under the closed system, identical conditions across both mid- and low-pH ranges (8.4-8.6 and 7.6-7.8 total scale, respectively) were employed to isolate temperature effects, examining trends across three different synthesis temperatures (10, 25 and 40 °C). The chemical compositions of all involved solutions were carefully controlled over the experimental duration and precipitation of the desired polymorph, as illustrated in Appendix A.3. Calcite was precipitated for all reported experimental runs (n=32) in this study.

5.2.2 Solution preparation

Calcite was precipitated from Na-Cl-Ca-Mg-(B)-CO_2 solutions of seawater-like ionic strength (0.7 mol/kg). Experimental starting solutions were gravimetrically prepared using deionized water (~18 MΩ cm) and ACS grade $NaHCO_3$ and Na_2CO_3, the ratio of which was dependent on the targeted initial pH as well as the concentrations of boric acid and sodium chloride. The solution was stored in a high-density polytheylene (HDPE) bottle immersed in a temperature-monitored water bath specific to the desired temperature for experimentation (i.e., 10, 25 or 40 °C) to ensure that the DIC species and water reached oxygen isotopic equilibrium at a given temperature. This study adhered to the kinetic parameters describing rates of oxygen isotope exchange among dissolved species reported by Beck et al. (2005) who estimated isotopic equilibrium to occur at 24, 9 and 2 h for 15, 25 and 40 °C, respectively. These values are consistent with Halas and Wolacewicz (1982), who reported equilibration times of 8.8, 2 and <1 h at 25, 35 and 40 °C. As an added precaution, all prepared parent solutions were left to equilibrate in a temperature-controlled water bath at least one week prior to commencing the precipitation experiment.

Once the minimum guideline equilibration time had elapsed, ACS grade $MgCl_2•6H_2O$ and $CaCl_2•2H_2O$ were added to the equilibrated starting solutions immediately preceding experimental synthesis. Using the Geochemist's Workbench® package (Bethke, 1996, 1998), these chemicals were added gravimetrically in a known Mg:Ca ratio of 0.13 to generate precipitation of calcite versus other polymorphs, promoting reaction with the bicarbonate to produce calcium carbonate. The completed starting solution was then enclosed in a temperature-controlled reaction chamber, receiving injections from two different titrant solutions. To ensure consistent oxygen isotope water values, both titrants were prepared with deionized water collected at the same time as that used for their associated starting solution. The titrant conditions varied with intended solution pH: one included ACS grade $NaHCO_3$ and/or Na_2CO_3 and NaCl, while the other was comprised of ACS grade $CaCl_2•2H_2O$, $B(OH)_3$ and NaCl. Mid-pH bulk solutions were prepared employing a 3:1 ratio of $NaHCO_3$:Na_2CO_3 (i.e., 7.5:2.5 mmolal) with one titrant solution replenishing these ions at a 4:1 ratio. In contrast, all low-pH solutions were comprised solely of $NaHCO_3$. Specific solution chemistries and experimental conditions are outlined in Table 5.1.

Since the solubility of CO_2 decreases with increasing temperature, it is impossible to hold constant both saturation of calcite and calcium concentration over the range of temperatures investigated (10-40 °C). Therefore, to maintain the saturation index of the system, calcium ion concentration should be reduced with increasing experiment temperature. The temperature spectrum observed in this experiment yielded negligible influence of calcium ion concentration on the system's state of saturation, all of which were calculated using Geochemist's Workbench® (Bethke, 1996, 1998).

5.2.3 Collection and filtration of samples

The experimental solution was sampled before and after each synthesis experiment with a 60 mL plastic syringe then deposited in a 10 mL vial. A final rinse of the vials with experimental solution occurred immediately prior to a second injection of the water sample. The water samples were stored in the refrigerator for oxygen isotopic analysis at a later date. Upon collection of water samples, a glass rod with a rubber policeman was used to destabilize crystals adhering to the sides of the chamber and join the suspended precipitates. The solution was run through a vacuum filtration system using a 0.45 μm Durapore® membrane filter overlying a plastic funnel support with a silicone stopper inserted into a 1 L Büchner flask. A 300 mL Büchner funnel was secured to the setup with a clamp, fitted atop with a rubber hose to withdraw air from the flask, creating a vacuum. The remaining precipitate was thoroughly rinsed with 2 liters of 18 MΩ Milli-Q water followed by ultra-pure methanol. The filtered calcium carbonate sample was oven-dried at ~ 70 °C overnight then collected and weighed for subsequent x-ray diffraction and stable isotopic analyses. Carbonate yield was found to be a function of both the temperature and pH at which it was synthesized (see Discussion). All of the calcium carbonate samples were identified as calcite at McMaster University's X-Ray Diffraction Facility (see Appendix).

5.2.4 Isotopic analysis of calcite

Small samples (~ 100 μg) of precipitates were weighed on the MRSI Mettler Toledo scale, placed into small stainless steel sample cups then inserted into an Isocarb carbonate preparation device attached to a Fisions Optima dual-inlet mass spectrometer for determination of isotopic composition (precision ± 0.08 ‰). The samples were run against two standards, NBS 19 and NBS 18, with oxygen isotope compositions normalized to the recommended values for NBS 18 (7.16 ‰) and NBS 19 (28.65 ‰) relative to SMOW. To calculate the δ^{18}O specific to calcite, a corresponding acid fractionation factor of 1.01030 was applied (Kim et al., 2007).

5.2.5 Isotopic analysis of solutions

The classic CO_2-H_2O equilibration technique (Epstein and Mayeda, 1953) was modified slightly for oxygen isotope analysis of experimental samples. Using the Gas Bench II headspace autosampler with a Thermo Finnigan Delta plus XP isotope-ratio mass spectrometer at McMaster University (precision ± 0.05 ‰), Exetainer® vials were flushed and filled with a 0.2% CO_2 and 99.8% He mixture with a double needle at a flow rate of 100 mL/min. A 1 mL syringe dispensed 0.2 mL quantity of sample into each vial.

Twenty-seven hours was allotted for equilibration at 25 ± 0.1 °C, after which time the CO_2 in the headspace was analyzed. Analyses were run as duplicates, with laboratory water standards MRSI-STD-W1 (0.58 ‰) and MRSI-STD-W2 (28.08 ‰) previously calibrated against SMOW and SLAP, analyzed to begin and end each session.

5.3 Results

5.3.1 Oxygen isotope fractionation trends at 10 °C

At this low-temperature regime, in which a titrant injection rate of 0.50 mL/hr was employed for all experiments, the oxygen isotope fractionation between calcite and water ($1000\ln\alpha_{CaCO3\text{-}H2O}$) displayed a predictable trend at both low- and high-pH experiments, with an apparent anomaly occurring under mid-pH conditions (Figure 5.1). A higher $1000\ln\alpha_{CaCO3\text{-}H2O}$ was observed at low-pH, attributable to the greater proportion of HCO_3^- ions present in the parent solution; likewise, the sole high-pH product was associated with a lower $1000\ln\alpha_{CaCO3\text{-}H2O}$ due to the dominant influence of CO_3^{2-} ions in the parent solution. However, the mid-pH experiments were statistically distinguishable from one another and noticeably offset from both predicted equilibrium (Kim and O'Neil, 1997) and oxygen isotope fractionation trend, a result explored in the Discussion.

5.3.2 Oxygen isotope fractionation trends at 25 °C

The oxygen isotope fractionation trend was examined at 25 °C under two different injection rates (0.50 mL/hr for low-pH experiments, 0.25 mL/hr for high-pH experiments, with both trialled for mid-pH experiments) while Ca:Mg concentration was also halved in two mid-pH experiments. The low- and high-pH data are similarly offset from the published calcite-water oxygen isotope equilibrium value (Kim and O'Neil, 1997), however they approach equilibrium from opposite directions (i.e., low-pH nearer HCO_3^- and high-pH nearer CO_3^{2-}) (Figure 5.2). Interestingly, the mid-pH samples straddle the calcite-water equilibrium line as a function of titrant injection rate and/or Ca:Mg concentration in the parent solution (see Table 5.1). Both these variables were altered to quantify the shift in their respective $1000\ln\alpha_{CaCO3\text{-}H2O}$ values. Calcites (n=5) synthesized using 0.50 mL/hr lie slightly above published equilibrium, whereas those grown with a slower injection rate (n=1), halved Ca:Mg (n=1) and a hybrid of these alterations (n=1) lie slightly below published equilibrium.

5.3.3 Oxygen isotope fractionation trends at 40 °C

Data compiled at this upper temperature regime, in which calcites were grown using a "slow" titrant injection rate of 0.25 mL/hr, display the most consistent trend of the three temperature ranges. However, no high-pH experiments are reported in this study due to tubing contamination issues (see Discussion), which generated carbonate products < 100% pure calcite. The low- and mid-pH calcites were determined to be within the analytical error of oxygen isotope equilibrium, as provided by Kim and O'Neil (1997) (Figure 5.3). A slight but noticeable, negative linear data trend can be observed in $1000\ln\alpha_{CaCO3\text{-}H2O}$ with pH. High-pH experiments must be repeated to yield pure calcite to improve the statistical significance of this apparent trend.

5.3.4 Oxygen isotope fractionation trends with temperature

To ascertain the hypothesized influences of HCO_3^- and CO_3^{2-} on oxygen isotope fractionation behaviour, a compiled plot of the calculated $1000\ln\alpha_{CaCO3\text{-}H2O}$ spanning the three temperature permutations can be assessed with the oxygen isotope fractionation between bicarbonate-water and carbonate-water components of the carbonic acid system, as determined by Beck et al. (2005). Deviation from calcite-water oxygen isotope equilibrium (Kim and O'Neil, 1997) can also be compared for all tested temperature and pH conditions.

Our data strongly trend along the reported oxygen isotope equilibrium values reported by both Beck et al. (2005) and Kim and O'Neil (1997) (Figure 5.4). A negative, linear relationship exists between $1000\ln\alpha_{\mathrm{CaCO3\text{-}H2O}}$ with temperature. Noticeably, the spread of data (i.e., sample variance under the same temperature conditions) lessens with increasing temperature, which is consistent with the temperature-dependent solution isotopic equilibration times recommended by Beck et al. (2005).

5.4 Discussion

5.4.1 Influences on carbonate yield

Carbonate minerals exhibit retrograde solubility, marked by a decrease in solubility with increasing temperature, attributable to the temperature influence on the solubility of carbon dioxide and dissolved carbonate species. The resulting difficulty in collecting samples can be further amplified by the positive relationship between precipitation rate and temperature. That is, colder growing conditions yield less calcite precipitation, which also dissolve more easily. This combined effect is clearly observed when contrasting mid-pH calcite samples synthesized at 10 °C compared to amounts collected at 25 and 40 °C (Table 5.2). Since our experimental design is characterized by spontaneous nucleation, it is not practical or appropriate to calculate surface area- or weight-normalized precipitation rates. Instead, to approximate calcite precipitation rate, bulk precipitation rate (subsequent to spontaneous nucleation) is communicated. This approach is proportional to the titrant injection rate at fixed titrant concentrations (Zuddas and Mucci, 1994).

As per Watkins et al. (2013), in which oxygen isotope behaviour was examined at the calcite-water interface, injection rate was varied according to temperature. Variations in oxygen isotope makeup within aqueous marine carbonate samples can create disequilibrium conditions if the precipitate forms quickly and is not given sufficient time to achieve equilibrium (Kim and O'Neil, 1997). At the lower and mid-temperature ranges of this study (10 and 25 °C), an injection rate of both 0.25 mL/hr ("slow") and 0.50 mL/hr ("fast") was employed, while only 0.25 mL/hr was used for experiments conducted at 40 °C. Since precipitation rate increases with temperature, a slower injection rate was employed in an attempt to slow crystal growth, minimize kinetic effects to the system and thus synthesize carbonates nearer equilibrium conditions. No distinct trend between calcite yield, temperature and pH was observed as a function of bulk precipitation rate (Figure 5.5), which accounts for experimental duration and total solution input (mg $CaCO_3$ precipitated/kg solution/day).

5.4.2 Effect of DIC species on oxygen isotope fractionation

The oxygen isotope compositions of precipitated calcite are controlled by both the kinetics of surface nucleation and the reactants, primarily CO_3^{2-} ions, present at areas of precipitate growth (Given and Wilkinson, 1985). At 25 °C, Beck et al. (2005) reported oxygen isotope fractionation of $1000\ln\alpha_{CO3\text{-}H2O} = 31.00 \pm 0.15$ ‰ and $1000\ln\alpha_{HCO3\text{-}H2O} =$

24.19 ± 0.26 ‰, within the analytical error of Kim et al. (2006) who determined $1000\ln\alpha_{CO3\text{-}H2O}$ = 30.53 ± 0.08 ‰ and $1000\ln\alpha_{HCO3\text{-}H2O}$ = 23.71 ± 0.08 ‰ at the same temperature.

Typically, temperature is the controlling factor affecting the direction and magnitude of equilibrium isotope fractionations, with only one equilibrium isotope fractionation factor expected at a given temperature. However, Zeebe (1999) suggested that the oxygen isotope composition of carbonates is dependent on both temperature and the relative abundance of the individual carbonic acid species (e.g., H_2CO_3, HCO_3^-, and CO_3^{2-}) in the parent solution (i.e., pH) at the time of precipitation. A follow-up investigation conducted by Kim et al. (2006) (also predicted by Deines, 2005) indicates that oxygen isotope fractionation factors between orthorhombic carbonate and water are independent of the relative contribution of the carbonic acid species to the DIC.

The duality of solution chemistry carbon speciation and oxygen isotope fractionation behaviour is an important consideration in our laboratory-controlled study. Mid-pH parent solutions were prepared employing a hybrid of $NaHCO_3$:Na_2CO_3 (in a 3:1 ratio of 7.5:2.5 mmolal) whereas low-pH parent solutions were prepared using solely $NaHCO_3$ (10 mmolal) and high-pH parent solutions contained Na_2CO_3 as the only DIC source. Each of these DIC species is associated with its own oxygen isotope equilibrium fractionation factor with water, as reported by Beck et al. (2005), producing a fractionation factor bias intrinsic to parent solution pH due to the sheer availability of HCO_3^- versus CO_3^{2-} ions available in solution. Furthermore, while CO_3^{2-} ions are preferentially incorporated into the calcite solid during precipitation (Given and Wilkinson, 1985), during rapid calcite precipitation, kinetic effects observed at the low-pH range can be attributed to the preferential deprotonation of isotopically light HCO_3^- ions into CO_3^{2-} and its subsequent incorporation into the calcite crystal; insufficient time elapses for the isotopic equilibrium between HCO_3^- and CO_3^{2-} species, therefore the recently-transformed CO_3^{2-} (from HCO_3^-) ions still carry the isotopic signature of HCO_3^-. Calcite samples then adopt an isotopic signature closer to that of the HCO_3^- equilibrium line. Similarly, the CO_3^{2-} species is dominant for samples synthesized at high-pH. Rapidly precipitated calcites under these conditions would yield oxygen isotope fractionation values nearer the CO_3^{2-}–H_2O equilibration line reported by Beck et al. (2005). Notably, the HCO_3^--CO_3^{2-} speciation occurs in near-equal proportions at the mid-pH realm, balancing the contributing factors. Even under rapid precipitation, more CO_3^{2-} is available for incorporation into the crystal lattice (versus that at lower-pH) such that deviation from the calcite-water oxygen isotope equilibrium fractionation is lessened, minimizing the influence of HCO_3^- ions altering the isotopic signature upon deprotonation. The magnitude of this differential appears further reduced at 40 °C but it must be noted that injection rate was halved in an attempt to slow precipitation rate.

Several permutations of the available parameters have yet to undergo experimentation, however our apparent data trend is consistent with the predicted role of each dominant carbonic acid species oxygen isotope equilibrium fractionation with water, as a function of pH. For the low-pH growth conditions, slower-growth calcites would approach the calcite-water equilibrium value (Kim and O'Neil, 1997) from "top-down", due to a greater timespan allotted for isotopic equilibration to be achieved during precipitation. Similarly, the dominance of CO_3^{2-} at high pH indicates that oxygen isotope fractionation values would approach equilibrium from the "bottom-up". Completion of these final combinations is targeted in the near future to quantitatively confirm this trend in its entirety.

5.4.3 Effect of temperature on oxygen isotope fractionation

This study used the calcite-water oxygen isotope fractionation equation proposed by Kim and O'Neil (1997), which has been widely employed and proven consistent with experimental and theoretical results (e.g., O'Neil et al., 1969; Tarutani et al., 1969; Horita and Clayton, 2007). A significantly smaller $1000\ln\alpha_{CaCO3-H2O}$ was observed in this study with increasing temperature, aligning with previous work conducted by Kim and O'Neil (1997).

Of additional significance is the similarity in bulk precipitation rate across samples nearest predicted equilibrium for all three experimental temperature ranges. Notably, the "outlier" set amongst the nine permutations (i.e., low-mid-high pH at 10-25-40 °C) occurred for mid-pH at 10 °C. Calcites grown under these conditions possessed a distinctly low bulk precipitation rate, and generated samples far below expected equilibrium. These experiments were conducted using new tubing of different chemical composition than past shipments, unbeknownst to our lab until amorphous precipitate collected in the tubes and leaked into the experimental chamber. Presumably formed as a result of tubing leaching, this foreign substance generated carbonate products of lighter oxygen isotope composition than its pure calcite counterparts, indicating its preference for the uptake of heavy oxygen isotopes. A weak, unidentifiable peak (as determined by XRD analysis) provides further evidence that these samples were likely anomalous; a repeat investigation into the mid-pH, 10 °C calcite synthesis experiment will prove illuminating.

A stark contrast in the variation of oxygen isotope fractionation with temperature can also be observed in Figure 5.4. Most notably, the spread among samples (within a given temperature range) drastically decreases with increasing temperature. Since equilibration time is reduced with temperature, it can be deduced that experiments conducted at the lower temperature regime were not given sufficient time to attain isotopic equilibrium. Therefore, it appears that another mechanism is involved in the $CaCO_3$-H_2O isotopic exchange process following exchange with DIC, H_2O and carbonate.

5.5 Conclusions and future work

Stable isotope geothermometry has been used extensively to reconstruct Earth's past and present climate variability, specifically the oxygen isotope carbonate-water paleothermometer pertaining to biogenic marine carbonates. Most of these calibration studies, however, were conducted in solutions of ionic strengths differing from seawater. Given that a majority of calcium carbonates used for paleoclimate research are marine in origin, the similarity of our seawater-like study with current paleothermometry calibrations, which are founded on the stable isotope systematics studies of carbonates precipitated from low ionic strength solutions (e.g., Kim and O'Neil, 1997; Kim et al., 2007), indicate that these calibrations may be suitable for paleoclimatic reconstructions based on the analysis of marine carbonates.

In this experimental investigation, the synthesis of abiotic calcite samples displaying oxygen isotope effects provides further insight into distinguishing equilibrium versus non-equilibrium fractionation and growth behaviour in calcium carbonates. Furthermore, the culmination of select contributing factors (i.e., injection rate, precipitation rate and incorporation of DIC species) indicates that equilibrium $1000\ln\alpha_{CaCO3\text{-}H2O}$ values for oxygen isotopic fractionation between calcite and water at 25 °C are in close approximation with the empirical value proposed by Kim and O'Neil (1997) (28.05 ‰) as well as the theoretical value (27.67 ‰) calculated by Chacko and Deines (2008).

Our study is the first to examine oxygen isotope effects in synthetic calcite over a spectrum of pH and temperature ranges using the modified constant addition method. Several distinct trends emerged over each of the tested parameters (i.e., pH and temperature). Less calcite was collected for experiments conducted at 10 °C than at 25 °C and 40 °C, due to decreased reaction rates (i.e., precipitation) and retrograde solubility behaviour displayed by carbonates at lower temperatures. Deviations from predicted oxygen isotope equilibrium at each of the three pH and temperature regimes are attributable to the chemical composition of starting parents solutions, given the presence of $NaHCO_3$ and/or Na_2CO_3, as well as varying control over injection/precipitation rate. This parameter was adjusted with temperature to conform to known reaction rate constants, in an attempt to contrast equilibrium products with those experiencing kinetic effects. Calcites synthesized at the upper temperature regime of 40 °C achieved nearest-equilibrium conditions (within the published analytical error range), providing evidence to support Kim et al. (2006) and Zuddas and Mucci (1994), who proposed that isotope equilibrium is controlled by precipitation rate, which itself is controlled by titrant injection rate. This apparent trend can be confirmed by testing the two remaining experimental permutations (i.e., 10 °C with slow injection and 40 °C with a fast injection) (Figure 5.6), as well as a repeated trial for mid-pH calcites at 10 °C to confirm the presumably anomalous contribution of the amorphous precipitate, providing empirical evidence for the influence of injection rate on equilibrium oxygen isotope fractionation.

The role of temperature on stable oxygen isotope systematics may also be calibrated by clumped isotope paleothermometry (Ghosh et al., 2006). An inherent weakness of the carbonate-water thermometer is that temperature determination requires knowledge of oxygen isotope compositions of both carbonates and the water from which they grew. Other marine paleothermometers (e.g., speciation of planktonic organisms, relative abundances of alkenones, or the Mg/Ca or Sr/Ca ratios of corals, foraminifera, and other carbonate-producing organisms) are useful for Pleistocene temperature reconstruction but are not viable options to extrapolate beyond this timeframe. The clumped isotope approach involves a homogeneous equilibrium and allows rigorous constraints of carbonate growth temperatures based on the isotopic composition of carbonate alone. This is a promising avenue for circumstances under which it is difficult to obtain original oxygen isotope compositions (i.e., for ancient waters).

Table 5.1: Experimental conditions for modified constant addition experiments.

Sample Name	Start[a] (mmolal)	Titrant 1[b] (mmolal)	Titrant 2[c] (mmolal)	Duration (hrs)	Sample Size (mg)	Average Temp. (°C)	Initial pH (total scale)	Final pH (total scale)
10 C								
#11-JWApril0314-A	7.5/2.5/1/0.13/7.9/692	16/4/685	10/20/685	431.5	28	9.91	8.40	8.45
#11-JWApril0314-C	7.5/2.5/1/0.13/7.9/692	16/4/685	10/20/685	431.5	25	9.95	8.40	8.47
#11-JWApril0314-D	7.5/2.5/1/0.13/7.9/692	16/4/685	10/20/685	624.0	12	10.21	8.52	8.39
#5-JWNov1313-D	10/0/10/1.3/7.9/673	20/0/690	10/20/685	432.5	332	9.99	7.67	7.68
#5-JWNov1313-E	10/0/10/1.3/7.9/673	20/0/690	10/20/685	432.5	327	10.03	7.67	7.58
#6-JWDec0413-D	10/0/10/1.3/7.9/673	20/0/690	10/20/685	387.8	160	9.98	7.47	7.65
#6-JWDec0413-E	10/0/10/1.3/7.9/673	20/0/690	10/20/685	387.8	156	10.00	7.48	7.63
#7-JWFeb1114-E	0/10/0.15/0.019/7.9/685	0/80/510	5/20/695	339.5	23	9.99	9.43	9.62
25 C								
#3-JWJune2813-C	7.5/2.5/1/0.13/7.9/692	16/4/685	10/20/685	358.5	100	25.01	8.59	8.29
#3-JWJune2813-D	7.5/2.5/1/0.13/7.9/692	16/4/685	10/20/685	358.5	92	25.04	8.59	8.51
#3-JWJune2813-E	7.5/2.5/1/0.13/7.9/692	16/4/685	10/20/685	358.5	110	25.04	8.58	8.73
#4-JWJuly3013-D	7.5/2.5/1/0.13/7.9/692	16/4/685	10/20/685	594.8	91	25.09	8.48	8.46
#4-JWJuly3013-E	7.5/2.5/1/0.13/7.9/692	16/4/685	10/20/685	594.8	113	25.09	8.46	8.24
#10-JWMarch1014-A	7.5/2.5/0.5/0.065/7.9/692	16/4/685	10/20/685	331.0	82	24.99	8.44	8.41
#10-JWMarch1014-C	7.5/2.5/0.5/0.065/7.9/692	16/4/685	10/20/685	331.0	234	24.99	8.43	8.41
#10-JWMarch1014-E	7.5/2.5/1/0.13/7.9/692	16/4/685	10/20/685	498.0	48	24.99	8.44	8.52
#5-JWSept0413-A	10/0/10/1.3/7.9/673	20/0/690	10/20/685	341.0	240	25.03	7.49	7.79
#5-JWSept0413-C	10/0/10/1.3/7.9/673	20/0/690	10/20/685	341.0	235	25.03	7.49	7.79
#5-JWSept0613-D	10/0/10/1.3/7.9/673	20/0/690	10/20/685	382.5	235	25.04	7.47	7.76
#5-JWSept0613-E	10/0/10/1.3/7.9/673	20/0/690	10/20/685	382.5	360	25.04	7.47	7.77
#5-JWNov1313-A	10/0/10/1.3/7.9/673	20/0/690	10/20/685	452.2	330	25.03	7.58	7.55
#5-JWNov1313-C	10/0/10/1.3/7.9/673	20/0/690	10/20/685	452.2	325	25.03	7.58	7.57
#6-JWDec0413-A	10/0/10/1.3/7.9/673	20/0/690	10/20/685	385.3	212	25.01	7.46	7.62
#6-JWDec0413-C	10/0/10/1.3/7.9/673	20/0/690	10/20/685	385.3	188	25.02	7.46	7.62
#7-JWFeb1114-A	0/10/0.15/0.019/7.9/685	0/80/510	5/20/695	335.5	35	25.09	9.43	9.81
#7-JWFeb1114-C	0/10/0.15/0.019/7.9/685	0/80/510	5/20/695	335.5	35	25.09	9.43	9.79
#12-JWMay2614-A	0/10/0.15/0.019/7.9/685	0/80/510	5/20/695	503.0	29	22.55	9.41	9.59
#12-JWApril3014-A	7.5/2.5/1/0.13/7.9/692	16/4/685	10/20/685	288.5	121	39.87	8.39	8.20
#12-JWApril3014-C	7.5/2.5/1/0.13/7.9/692	16/4/685	10/20/685	288.5	110	39.79	8.39	8.20
#12-JWMay2714-D	10/0/10/1.3/7.9/673	20/0/690	10/20/685	483.2	187	39.95	7.52	7.33
#12-JWMay2714-E	10/0/10/1.3/7.9/673	20/0/690	10/20/685	483.2	198	39.95	7.52	7.88
#13-JWJune1814-D	10/0/10/1.3/7.9/673	20/0/690	10/20/685	312.0	170	39.96	7.54	7.30
#13-JWJune1814-E	10/0/10/1.3/7.9/673	20/0/690	10/20/685	312.0	221	39.95	7.56	7.86
40 C								
#12-JWApril3014-A	7.5/2.5/1/0.13/7.9/692	16/4/685	10/20/685	288.5	121	39.87	8.39	8.20
#12-JWApril3014-C	7.5/2.5/1/0.13/7.9/692	16/4/685	10/20/685	288.5	110	39.79	8.39	8.20
#12-JWMay2714-D	10/0/10/1.3/7.9/673	20/0/690	10/20/685	483.2	187	39.95	7.52	7.33
#12-JWMay2714-E	10/0/10/1.3/7.9/673	20/0/690	10/20/685	483.2	198	39.95	7.52	7.88
#13-JWJune1814-D	10/0/10/1.3/7.9/673	20/0/690	10/20/685	312.0	170	39.96	7.54	7.30
#13-JWJune1814-E	10/0/10/1.3/7.9/673	20/0/690	10/20/685	312.0	221	39.95	7.56	7.86

[a] $NaHCO_3/Na_2CO_3/Ca/Mg/B/NaCl$

[b] $NaHCO_3/Na_2CO_3/NaCl$

[c] Ca/B/NaCl

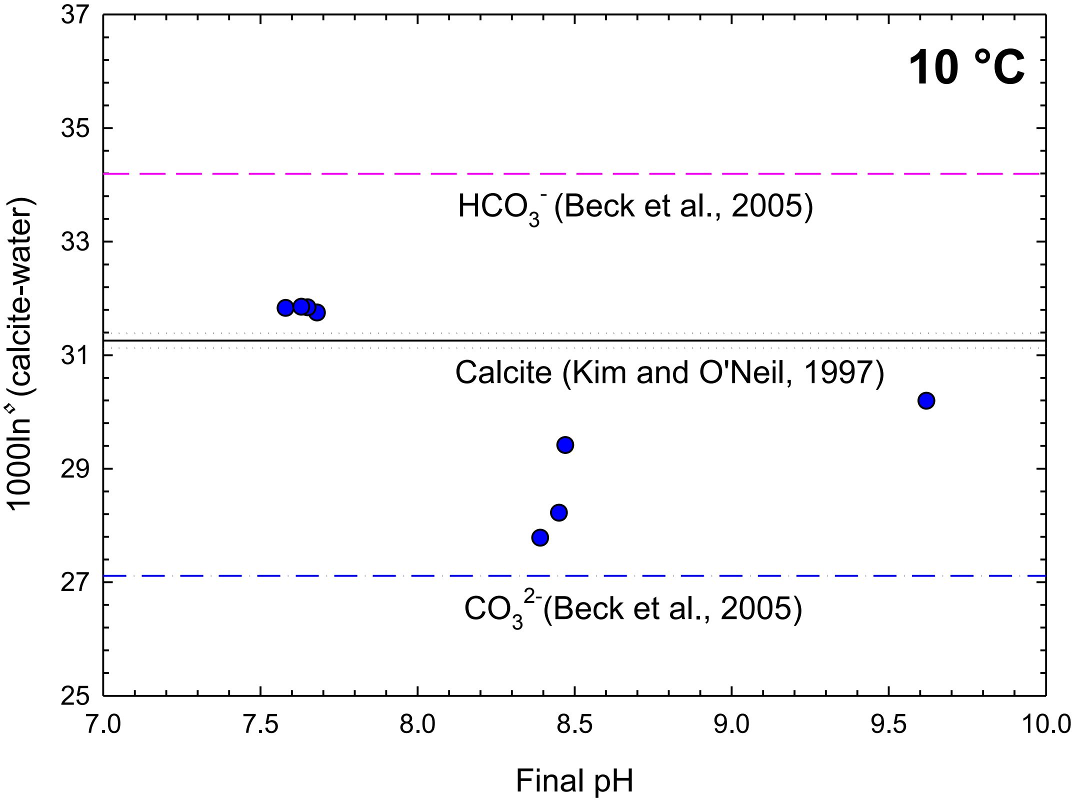

Figure 5.1: Oxygen isotope fractionation at 10 °C.

Note that mid-pH samples were synthesized during a period of tubing contamination in the experimental setup, necessitating a rerun to ascertain the true oxygen isotope fractionation for pure calcite at this pH range. A combined analytical error is estimated to be 0.2 ‰.

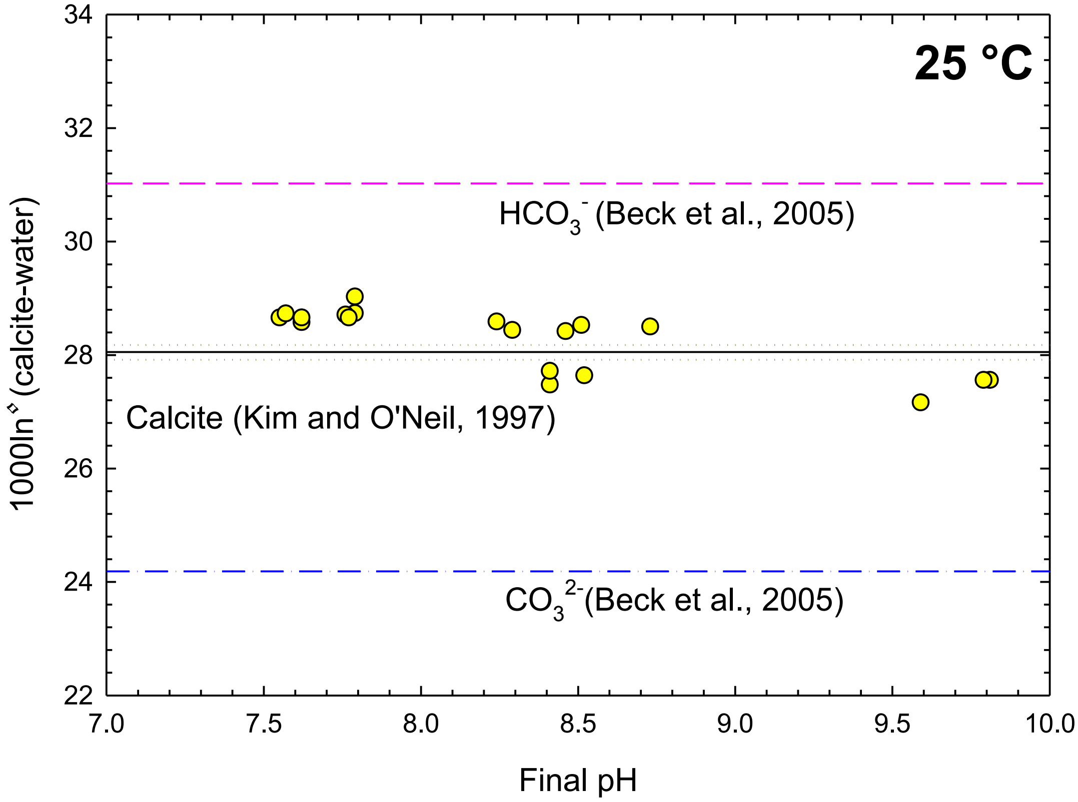

Figure 5.2: Oxygen isotope fractionation at 25 °C.

Note that mid-pH samples were synthesized using several combinations of injection rates and Ca/Mg concentrations. To add statistical significance to the observed trend, further calcite samples will be grown and examined under each of these trialled conditions. A combined analytical error is estimated to be 0.2 ‰.

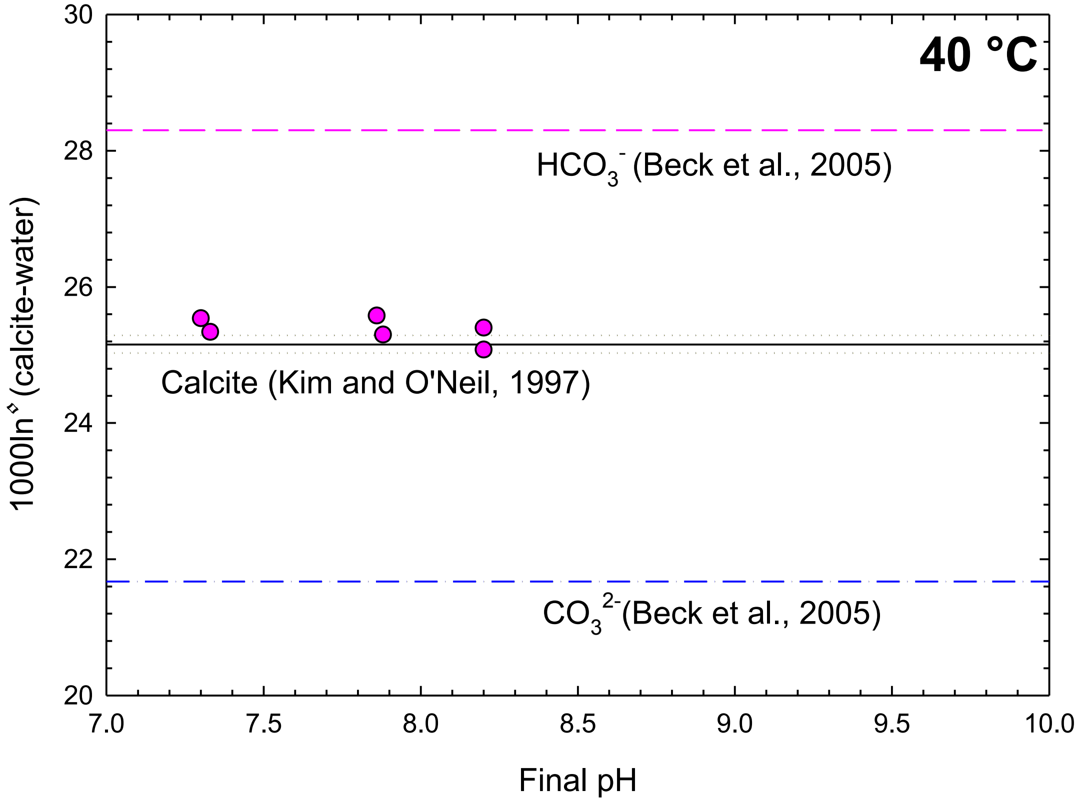

Figure 5.3: Oxygen isotope fractionation at 40 °C.

A combined analytical error is estimated to be 0.2 ‰.

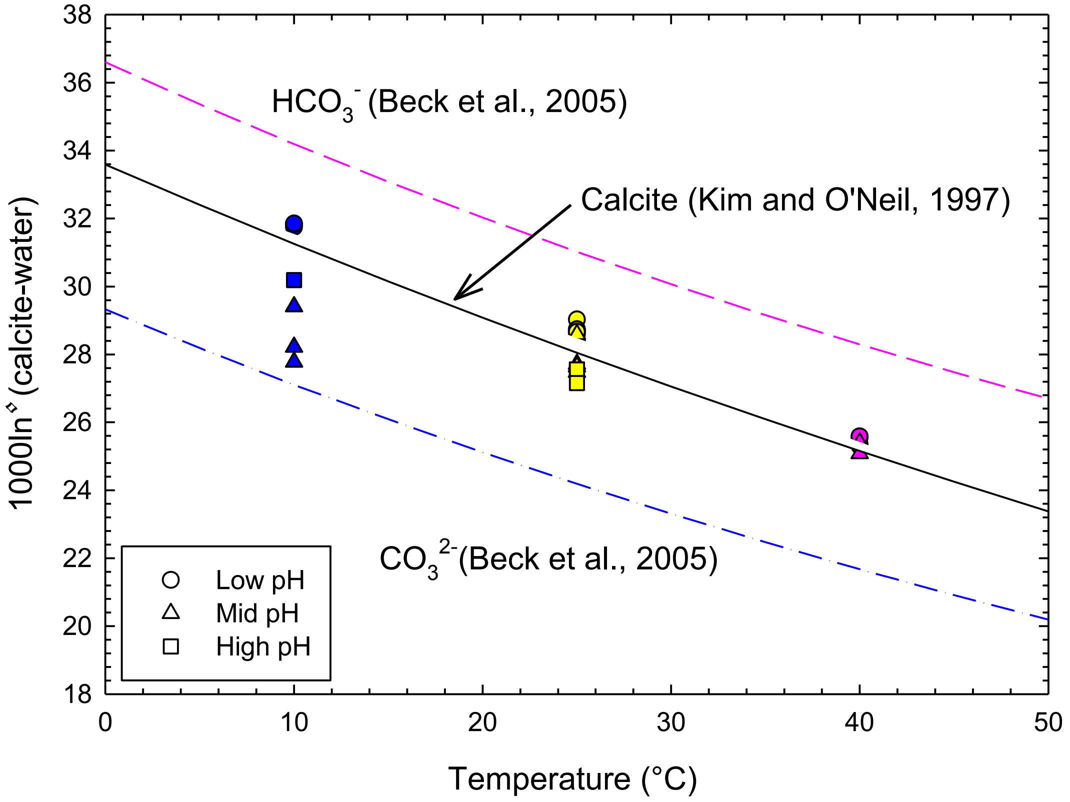

Figure 5.4: Oxygen isotope fractionation trends with temperature.

A combined analytical error is estimated to be 0.2 ‰.

Table 5.2: Oxygen isotope data experimental results from synthetic calcite growth trials, as a function of pH and temperature.

Sample Name	Start Sol'n	Sample Size (mg)	Duration (hrs)	Bulk ppt rate (mg/kg/d)	Ave Temp (C)	Stdev Temp	Inj. Rate (mL/h)	Initial pH	Final pH	Change pH	$\delta^{18}O_{calcite}$ (‰)	$\delta^{18}O_{water(initial)}$ (‰)	$\delta^{18}O_{water(final)}$ (‰)	*Difference* (‰)	$1000\ln\alpha_{(calcite\text{-}H2O)}$	Kim & O'Neil	*Difference*
10 C																	
#11-JWApril0314-A	mid	28	431.5	1.28	9.91	0.00	0.5	8.40	8.45	-0.05	22.22	-6.27	-6.22	0.05	28.22	31.28	-3.06
#11-JWApril0314-C	mid	25	431.5	1.14	9.95	0.01	0.5	8.40	8.47	-0.07	23.37	-6.22	-6.29	-0.07	29.41	31.27	-1.86
#11-JWApril0314-D	mid-0.25	12	624.0	0.40	10.21	0.04	0.25	8.52	8.39	0.13	22.29	-6.45	-5.72	0.73	27.78	31.21	-3.43
#5-JWNov1313-D	low	332	432.5	15.15	9.99	0.01	0.5	7.67	7.68	-0.01	25.77	-6.54	-6.29	0.25	31.75	31.26	0.49
#5-JWNov1313-E	low	327	432.5	14.92	10.03	0.02	0.5	7.67	7.58	0.09	25.76	-6.41	-6.38	0.04	31.83	31.25	0.58
#6-JWDec0413-D	low	160	387.8	8.29	9.98	0.01	0.5	7.47	7.65	-0.18	25.86	-6.42	-6.29	0.13	31.84	31.26	0.58
#6-JWDec0413-E	low	156	387.8	8.09	10.00	0.01	0.5	7.48	7.63	-0.15	25.86	-6.38	-6.30	0.08	31.85	31.26	0.59
#7-JWFeb1114-E	high	23	339.5	14.15	9.99	0.01	0.5	9.43	9.62	-0.19	24.37	-6.34	-6.09	0.25	30.19	31.26	-1.07
25 C																	
#3-JWJune2813-C	mid	100	358.5	5.68	25.01	0.02	0.5	8.59	8.29	0.3	22.03	-6.88	-6.63	0.25	28.44	28.05	0.39
#3-JWJune2813-D	mid	92	358.5	5.22	25.04	0.02	0.5	8.59	8.51	0.08	22.09	-6.82	-6.66	0.16	28.53	28.04	0.49
#3-JWJune2813-E	mid	110	358.5	6.24	25.04	0.04	0.5	8.58	8.73	-0.15	22.20	-6.79	-6.52	0.27	28.50	28.04	0.46
#4-JWJuly3013-D	mid	91	594.8	2.83	25.09	0.04	0.5	8.48	8.46	0.02	22.06	-6.71	-6.58	0.13	28.42	28.03	0.39
#4-JWJuly3013-E	mid	113	594.8	3.51	25.09	0.03	0.5	8.46	8.24	0.22	22.19	-6.66	-6.62	0.04	28.59	28.03	0.56
#10-JWMarch1014-A	mid-halved	82	331.0	5.10	24.99	0.00	0.5	8.44	8.41	0.03	21.97	-5.85	-5.73	0.12	27.48	28.05	-0.57
#10-JWMarch1014-C	mid-halved	234	331.0	14.56	24.99	0.00	0.5	8.43	8.41	0.02	22.15	-5.81	-5.79	0.02	27.72	28.05	-0.33
#10-JWMarch1014-E	mid-0.25	48	498.0	2.06	24.99	0.00	0.25	8.44	8.52	-0.08	22.20	-5.85	-5.67	0.18	27.64	28.05	-0.41
#5-JWSept0413-A	low	240	341.0	14.43	25.03	0.01	0.5	7.49	7.79	-0.3	22.66	-6.65	-6.60	0.04	29.03	28.05	0.98
#5-JWSept0413-C	low	235	341.0	14.13	25.03	0.03	0.5	7.49	7.79	-0.3	22.43	-6.55	-6.54	0.02	28.74	28.05	0.69
#5-JWSept0613-D	low	235	382.5	12.38	25.04	0.04	0.5	7.47	7.76	-0.29	22.43	-6.66	-6.51	0.15	28.71	28.04	0.67
#5-JWSept0613-E	low	360	382.5	18.96	25.04	0.04	0.5	7.47	7.77	-0.3	22.34	-6.65	-6.54	0.11	28.66	28.04	0.62
#5-JWNov1313-A	low	330	452.2	14.29	25.03	0.01	0.5	7.58	7.55	0.03	22.53	-6.52	-6.36	0.16	28.66	28.05	0.61
#5-JWNov1313-C	low	325	452.2	14.07	25.03	0.02	0.5	7.58	7.57	0.01	22.52	-6.53	-6.44	0.09	28.73	28.05	0.68
#6-JWDec0413-A	low	212	385.3	16.29	25.01	0.00	0.5	7.46	7.62	-0.16	22.50	-6.37	-6.31	0.06	28.58	28.05	0.53
#6-JWDec0413-C	low	188	385.3	15.04	25.02	0.01	0.5	7.46	7.62	-0.16	22.57	-6.16	-6.32	-0.15	28.66	28.05	0.61
#7-JWFeb1114-A	high	35	335.5	2.14	25.09	0.00	0.5	9.43	9.81	-0.38	21.70	-6.41	-6.07	0.34	27.56	28.03	-0.47
#7-JWFeb1114-C	high	35	335.5	2.14	25.09	0.00	0.5	9.43	9.79	-0.36	21.79	-6.33	-5.99	0.34	27.56	28.03	-0.47
#12-JWMay2614-A	high-0.25	29	503.0	1.23	22.55	0.04	0.25	9.41	9.59	-0.18	20.85	-6.50	-6.50	0.00	27.16	28.55	-1.39
40 C																	
#12-JWApril3014-A	mid	121	288.5	9.39	39.87	0.01	0.25	8.39	8.20	0.19	19.52	-6.53	-6.05	0.48	25.40	25.18	0.22
#12-JWApril3014-C	mid	110	288.5	8.54	39.79	0.01	0.25	8.39	8.20	0.19	19.36	-6.53	-5.89	0.64	25.08	25.19	-0.11
#12-JWMay2714-D	low	187	483.2	8.29	39.95	0.03	0.25	7.52	7.33	0.19	19.46	-6.53	-6.05	0.48	25.34	25.17	0.17
#12-JWMay2714-E	low	198	483.2	8.77	39.95	0.03	0.25	7.52	7.88	-0.36	19.58	-6.53	-5.89	0.64	25.30	25.17	0.13
#13-JWJune1814-D	low	170	312.0	12.13	39.96	0.01	0.25	7.54	7.30	0.24	19.62	-6.52	-6.09	0.43	25.54	25.16	0.38
#13-JWJune1814-E	low	221	312.0	15.77	39.95	0.01	0.25	7.56	7.86	-0.30	19.60	-6.48	-6.15	0.33	25.58	25.17	0.41

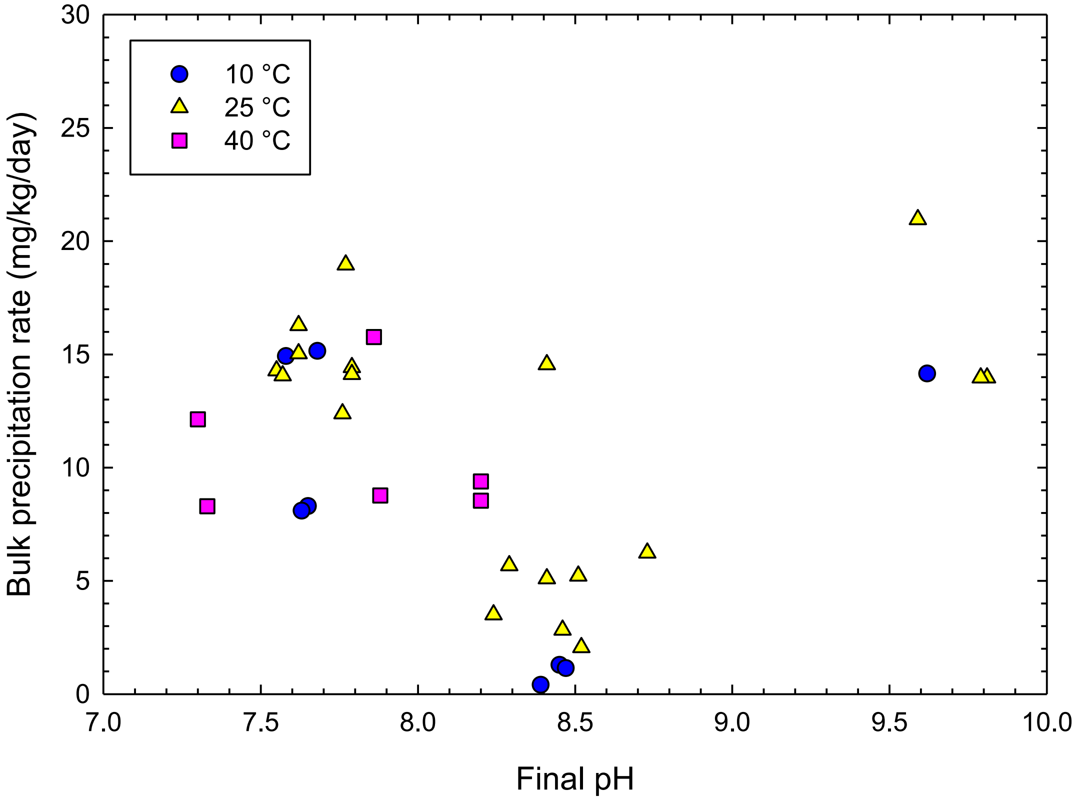

Figure 5.5: Interplay of carbonate yield, temperature and pH, calculated as a function of bulk precipitation rate (mg $CaCO_3$/kg solution/day).

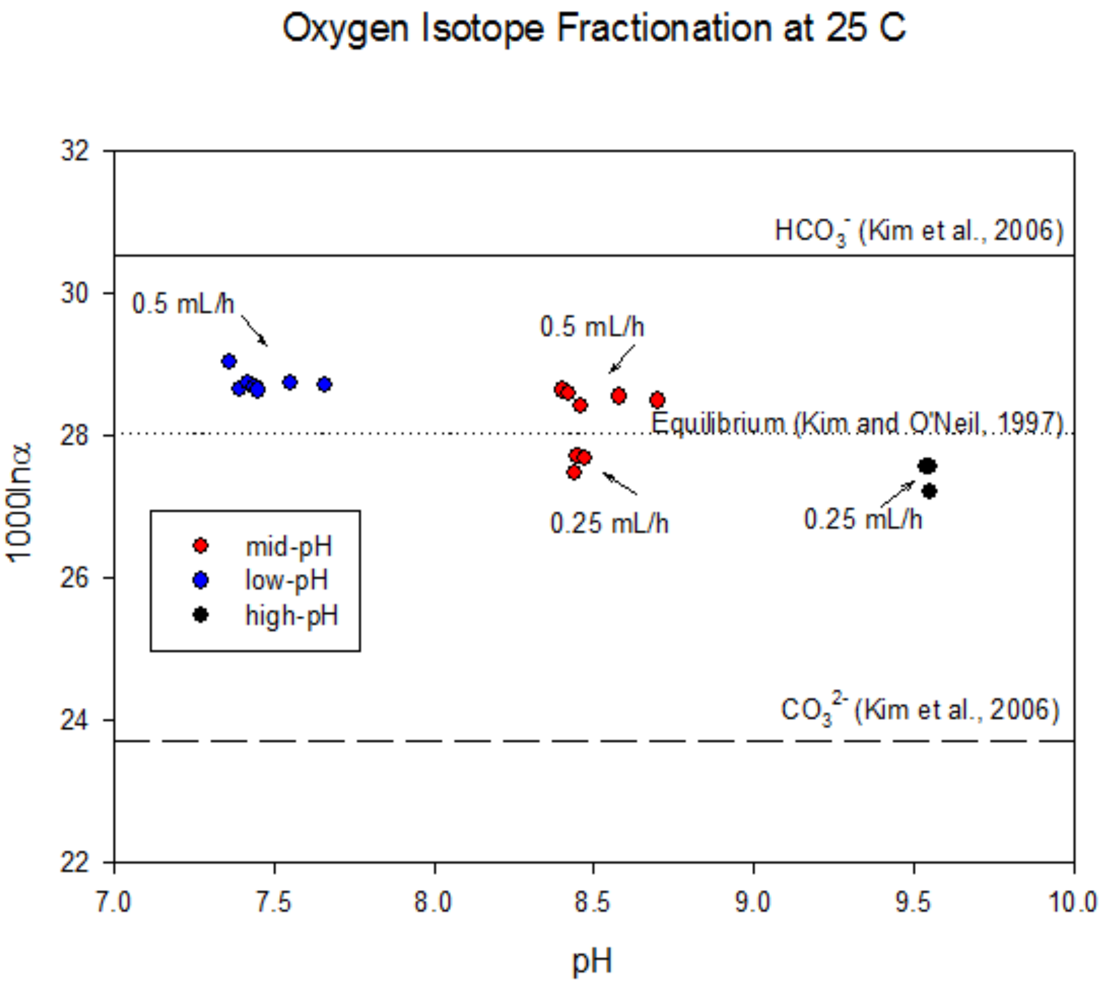

Figure 5.6: The interplay of temperature, pH and injection rate with predicted isotopic equilibrium at 25 °C.

A combined analytical error is estimated to be 0.2 ‰.

References

Arrhenius, S. On the Influence of Carbonic Acid in the Air upon the Temperature of the Ground. *Philosophical Magazine and Journal of Science, 5(41),* 237-276.

Allen, K. A., & Hönisch, B. (2012). The planktic foraminiferal B/Ca proxy for seawater carbonate chemistry: A critical evaluation. *Earth and Planetary Science Letters*, *345-348*, 203–211. doi:10.1016/j.epsl.2012.06.012

Atekwana, E. A., & Krishnamurthy, R. V. (1998). Seasonal Variations of Dissolved Inorganic Carbon and $\delta^{13}C$ of Surface Waters: Application of a Modified Gas Evolution Technique. *Journal of Hydrology*, *205*, 265–278.

Bar-Matthews, M., Ayalon, A., Gilmour, M., Matthews, A., & Hawkesworth, C. J. (2003). Sea-land oxygen isotopic relationships from planktonic foraminifera and speleothems in the Eastern Mediterranean region and their implication for paleorainfall during interglacial intervals. *Geochimica et Cosmochimica Acta*, *67*(17), 3181–3199.

Barnola, J. M., Raynaud, D., Korotkevich, Y. S., & Lorius, C. (1987). Vostok ice core provides 160,000-year record of atmospheric CO2. *Nature*, *329*, 408–414.

Barras, C., Duplessy, J.-C., Geslin, E., Michel, E., & Jorissen, F. J. (2010). Calibration of $\delta^{18}O$ of cultured benthic foraminiferal calcite as a function of temperature. *Biogeosciences*, *7*(4), 1349–1356. doi:10.5194/bg-7-1349-2010

Beck, W. C., Grossman, E. L., & Morse, J. W. (2005). Experimental studies of oxygen isotope fractionation in the carbonic acid system at 15°, 25°, and 40°C. *Geochimica et Cosmochimica Acta*, *69*(14), 3493–3503. doi:10.1016/j.gca.2005.02.003

Berner, R. A. (1975). The Role of Magnesium in the Crystal Growth of Calcite and Aragonite From Sea Water. *Geochimica et Cosmochimica Acta*, *39*, 489–504.

Billups, K. (2002). Late Miocene through early Pliocene deep water circulation and climate change viewed from the sub-Antarctic South Atlantic. *Palaeogeography, Palaeoclimatology, Palaeoecology*, *185*, 287–307.

Bottinga, Y. (1966). Calculation of Fractionation Factors for Carbon and Oxygen Isotopic Exchange in the System Calcite-Carbon Dioxide-Water. *The Journal of Physical Chemistry*, *287*(1), 800–808.

Broecker, W. S. (1982). Glacial to Interglacial Changes in Ocean Chemistry. *Prog. Oceanog.*, *11*, 151–197.

Broecker, W. S. (1986). Oxygen isotope constraints on surface ocean temperatures. *Quaternary Research*, *26*(1), 121–134. doi:10.1016/0033-5894(86)90087-6

Busenberg, E., & Plummer, L. N. (1986). The solubility of BaCO3 (witherite) in CO3-H2O solutions between 0 and 90 C , evaluation of the association constants of BaHCO3(aq) and BaCO3(aq) between 5 and 80 C , and a preliminary evaluation of the thermodynamic properties of Ba. *Geochimica et Cosmochimica Acta*, *50*, 2225–2233.

Chacko, T., & Deines, P. (2008). Theoretical calculation of oxygen isotope fractionation factors in carbonate systems. *Geochimica et Cosmochimica Acta*, *72*(15), 3642–3660. doi:10.1016/j.gca.2008.06.001

Chacko, T., Mayeda, T. K., Clayton, R. N., & Goldsmith, J. R. (1991). Oxygen and carbon isotope fractionations between CO2 and calcite. *Geochimica et Cosmochimica Acta*, *55*(10), 2867–2882. doi:10.1016/0016-7037(91)90452-B

Chamberlin, T.C. (1898). An attempt to frame a working hypothesis of the cause of glacial periods on an atmospheric basis. *Journal of Geology,* 6, 609-621.

Coplen, T. B. (2007). Calibration of the calcite–water oxygen-isotope geothermometer at Devils Hole, Nevada, a natural laboratory. *Geochimica et Cosmochimica Acta*, *71*(16), 3948–3957. doi:10.1016/j.gca.2007.05.028

Day, C. C., & Henderson, G. M. (2011). Oxygen isotopes in calcite grown under cave-analogue conditions. *Geochimica et Cosmochimica Acta*, *75*(14), 3956–3972. doi:10.1016/j.gca.2011.04.026

Dickson, A. G. (1992). pH buffers for sea water media based on the total hydrogen ion concentration scale ANDREW G. *Deep-Sea Research*, *40*(1), 107–118.

Dickson, A. G. (1993). The measurement of sea water pH. *Marine Chemistry*, *44*(2-4), 131–142. doi:10.1016/0304-4203(93)90198-W

Dietzel, M., Tang, J., Leis, A., & Köhler, S. (2009). Oxygen isotopic fractionation during inorganic calcite precipitation — Effects of temperature, precipitation rate and pH. *Chemical Geology*, *268*(1-2), 107–115. doi:10.1016/j.chemgeo.2009.07.015

Dietzel, M., Tang, J., Leis, A., & Köhler, S. J. (2009). Oxygen isotopic fractionation during inorganic calcite precipitation — Effects of temperature, precipitation rate and pH. *Chemical Geology*, *268*(1-2), 107–115. doi:10.1016/j.chemgeo.2009.07.015

Dietzel, M., & Usdowski, E. (1996). Coprecipitation of Ni2+, Co2+, and Mn2+ with galena and covellite, and of Sr2+ with calcite during crystallization via diffusion of

H2S and CO2 through polyethylene at 20C: Power law and Nernst law control of trace element partitioning. *Chemical Geology*, *131*, 55–65.

Dreybrodt, W., & Scholz, D. (2011). Climatic dependence of stable carbon and oxygen isotope signals recorded in speleothems: From soil water to speleothem calcite. *Geochimica et Cosmochimica Acta*, *75*(3), 734–752. doi:10.1016/j.gca.2010.11.002

Dromgoole, E. L., & Walter, L. M. (1990). Inhibition of calcite growth rates by Mn2+ in CaC12 solutions at 10, 25, and 50°C. *Geochimica et Cosmochimica Acta*, *54*(1984), 2991–3000.

Duplessy, J., Shackleton, N. J., Matthewsa, R. K., Prell, W., Ruddiman, W. F., Hendy, C. H., … Yvette, G. (1984). 13C Record of Benthic Foraminifera in the Last Interglacial Ocean : Implications for the Carbon Cycle and the Global Deep Water Circulation. *Quaternary Research*, *21*, 225–243.

Emrich, K., Ehhalt, D., & Vogel, J. (1970). Carbon Isotope Fractionation During the Precipitation of Calcium Carbonate. *Earth and Planetary Science Letters*, *8*(September 1969), 363–371.

Epstein, S., Buchsbaum, R., Lowenstam, H., & Urey, H. (1953). Revised Carbonate-Water Isotopic Temperature Scale. *Geological Society of America Bulletin*, *11*, 1315–1326. doi:10.1130/0016-7606(1953)64

Epstein, S., & Mayeda, T. (1953). Variation of O18 content of waters from natural sources. *Geochimica et Cosmochimica Acta*, *4*, 213–224.

Feely, R. A., Sabine, C. L., Lee, K., Berelson, W., Kleypas, J., Fabry, V. J., and Millero, F. J. (2004). Impact of anthropogenic CO_2 on the $CaCO_3$ system in the oceans. *Science,* 305, 362-366.

Foster, G.L. (2008). Seawater pH, pCO2 and [CO2−3] variations in the Caribbean Sea over the last 130 kyr: A boron isotope and B/Ca study of planktic foraminifera. *Earth and Planetary Science Letters*, *271*(1-4), 254–266. doi:10.1016/j.epsl.2008.04.015

Foster, G.L., & Rohling, E. J. (2013). Relationship between sea level and climate forcing by CO2 on geological timescales. *Proceedings of the National Academy of Sciences of the United States of America*, *110*(4), 1209–14. doi:10.1073/pnas.1216073110

Foster, G.L., Ni, Y., Haley, B., & Elliott, T. (2006). Accurate and precise isotopic measurement of sub-nanogram sized samples of foraminiferal hosted boron by total evaporation NTIMS. *Chemical Geology*, *230*(1-2), 161–174. doi:10.1016/j.chemgeo.2005.12.006

Foster, G. L., von Strandmann, P. A. P., & Rae, J. W. (2010). Boron and magnesium isotopic composition of seawater. *Geochem. Geophys. Geosyst., 11,* Q08015, doi:10.1029/2010GC003201.

Friedman, I., & O'Neil, J. R. (1977). Data of Geochemistry. Chapter KK. Compilation of Stable Isotope Fractionation Factors of Geochemical Interest. US Government Printing Office.

Furst, M., Lowestam, H.A., & Burnett, D. S. (1976). Radiographic study of the distribution of boron in recent mollusc shells. *Geochim. Cosmochim. Acta, 40*, 1381–1386

Fung, B. M. (2002). 13C NMR studies of liquid crystals. *Progress in Nuclear Magnetic Resonance Spectroscopy*, *41*(3-4), 171–186. doi:10.1016/S0079-6565(02)00048-1

Gabitov, R. I., Watson, E. B., & Sadekov, A. (2012). Oxygen isotope fractionation between calcite and fluid as a function of growth rate and temperature: An in situ study. *Chemical Geology*, *306-307*, 92–102. doi:10.1016/j.chemgeo.2012.02.021

Gabitov, R., Watson, B., & Sadekov, A. (2012). Oxygen isotope fractionation between calcite and fluid as a function of growth rate and temperature: An in situ study. *Chemical Geology*, *306-307*, 92–102. doi:10.1016/j.chemgeo.2012.02.021

Garside, J. (1982). Nucleation. In G H Nancollas (Ed.), *Biological Mineralization and Demineralization SE - 3* (Vol. 23, pp. 23–35). Springer Berlin Heidelberg. doi:10.1007/978-3-642-68574-3_3

Ghosh, P., Adkins, J., Affek, H., Balta, B., Guo, W., Schauble, E. A., … Eiler, J. M. (2006). 13C–18O bonds in carbonate minerals: A new kind of paleothermometer. *Geochimica et Cosmochimica Acta*, *70*(6), 1439–1456. doi:10.1016/j.gca.2005.11.014

Grossman, E., & Ku, T. (1986). Oxygen and carbon isotope fractionation in biogenic aragonite: Temperature effects. *Chemical Geology*, *59*, 59–74.

Gruzensky, P. M. (1967). Growth of Calcite Crystals. In H. S. Peiser (Ed.), *Crystal Growth* (pp. 365–367). Oxford University Press.

Hansson, I. (1973). A new set of pH-scales and standard buffers for sea water. *Deep-Sea Research*, *20*, 479–491.

Hemming, N.G., & Hanson, G. N. (1992). Boron isotopic composition and concentration in modern marine carbonates. *Geochimica et Cosmochimica Acta*, *56*, 537–543.

Hemming, N.G., Reeder, R. J., & Hanson, G. N. (1995). Mineral-fluid partitioning and isotopic fractionation of boron in synthetic calcium carbonate. *Geochimica et Cosmochimica Acta*, *59*(2), 371–379.

Hershey, J. P., Fernandez, M., Milne, P. J., Millero, J., & Hal, F. (1986). The ionization of boric acid in NaCI , Na-Ca-Cl and Na-Mg-Cl solutions at 25 ° C. *Geochimica et Cosmochimica Acta*, *50*(4), 143–148.

Hoefs, J. (2009). Stable Isotope Geochemistry. Sixth Edition. Springer. 285p.

Hönisch, B., Hemming, N. G., Grottoli, A. G., Amat, A., Hanson, G. N., & Bijma, J. (2004). Assessing scleractinian corals as recorders for paleo-pH: Empirical calibration and vital effects. *Geochimica et Cosmochimica Acta*, *68*(18), 3675–3685. doi:10.1016/j.gca.2004.03.002

Hönisch, B., Hemming, N. G., Archer, D., Siddall, M., & McManus, J. F. (2009). Atmospheric carbon dioxide concentration across the mid-Pleistocene transition. *Science*, *324*(5934), 1551–4. doi:10.1126/science.1171477

Hönisch, B., Hemming, N. G., & Loose, B. (2007). Comment on "A critical evaluation of the boron isotope-pH proxy: The accuracy of ancient ocean pH estimates" by M. Pagani, D. Lemarchand, A. Spivack and J. Gaillardet. *Geochimica et Cosmochimica Acta*, *71*(6), 1636–1641. doi:10.1016/j.gca.2006.07.045

Horita, J., & Clayton, R. N. (2007). Comment on the studies of oxygen isotope fractionation between calcium carbonates and water at low temperatures by Zhou and Zheng (2003; 2005). *Geochimica et Cosmochimica Acta*, *71*(12), 3131–3135. doi:10.1016/j.gca.2005.11.033

Jimenez-Lopez, C., Caballero, E., Huertas, F. J., & Romanek, C. S. (2001). Chemical, mineralogical and isotope behavior, and phase transformation during the precipitation of calcium carbonate minerals from intermediate ionic solution at 25 ° C. *Geochimica et Cosmochimica Acta*, *65*(19), 3219–3231.

Jiménez-López, C., Romanek, C. S., Huertas, F. J., Ohmoto, H., & Caballero, E. (2004). Oxygen isotope fractionation in synthetic magnesian calcite. *Geochimica et Cosmochimica Acta*, *68*(16), 3367–3377. doi:10.1016/j.gca.2003.11.033

Jouzel, J., Lorius, C., Petit, J. R., Genthon, C., Barkov, N., Kotlyakov, V. M., & Petrov, V. M. (1987). Vostok ice core: a continuous isotope temperature record over the last climatic cycle (160,000 years). *Nature*, *329*, 403–407.

Kakihana, H., Kotaka, M., Satoh, S., Nomura, M., & Okamoto, M. (1977). Fundamental Studies on the Ion-Exchange Separation of Boron Isotopes. *Bulletin of the Chemical Society of Japan*, *50*(1), 158–163.

Kim, S-T., & O'Neil, J. (1997). Equilibrium and nonequilibrium oxygen isotope effects in synthetic carbonates. *Geochimica et Cosmochimica Acta*, *61*(16), 3461–3475.

Kim, S-T., Hillaire-Marcel, C., & Mucci, A. (2006). Mechanisms of equilibrium and kinetic oxygen isotope effects in synthetic aragonite at 25°C. *Geochimica et Cosmochimica Acta*, *70*(23), 5790–5801. doi:10.1016/j.gca.2006.08.003

Kim, S-T., O'Neil, J., Hillaire-Marcel, C., & Mucci, A. (2007). Oxygen isotope fractionation between synthetic aragonite and water: Influence of temperature and Mg2+ concentration. *Geochimica et Cosmochimica Acta*, *71*(19), 4704–4715. doi:10.1016/j.gca.2007.04.019.

Kim, S-T., Klein-Gebbinck, C.D., Mucci, A., & Coplen, T. (2014). Oxygen isotope systematics in the aragonite–CO_2–H_2O–NaCl system up to 0.7mol/kg ionic strength at 25°C. *Geochimica et Cosmochimica Acta*, *137*, 147-158.

Kitano, Y., Okumura, M., & Idogaki, M. (1978). Coprecipitation of borate-boron with calcium carbonate. *Geochemical Journal*, *12*, 183–189.

Kitano, Y., Okumura, M., & Idogaki, M. (1979). Influence of borate-boron on crystal form of calcium carbonate. *Geochemical Journal*, *13*, 223–224.

Klochko, K., Cody, G. D., Tossell, J. A., Dera, P., & Kaufman, A. J. (2009). Re-evaluating boron speciation in biogenic calcite and aragonite using 11B MAS NMR. *Geochimica et Cosmochimica Acta*, *73*(7), 1890–1900. doi:10.1016/j.gca.2009.01.002

Klochko, K., Kaufman, A. J., Yao, W., Byrne, R. H., & Tossell, J. A. (2006). Experimental measurement of boron isotope fractionation in seawater. *Earth and Planetary Science Letters*, *248*(1-2), 276–285. doi:10.1016/j.epsl.2006.05.034

Lea, D., Pak, D., & Spero, H. (2000). Climate impact of late quaternary equatorial pacific sea surface temperature variations. *Science (New York, N.Y.)*, *289*(5485), 1719–24. Retrieved from http://www.ncbi.nlm.nih.gov/pubmed/10976060

Lemarchand, D., Gaillardet, J., Lewin, E., & Allegre, C. J. (2002). Boron isotope systematics in large rivers: implications for the marine boron budget and paleo-pH reconstruction over the Cenozoic. *Chemical Geology*, *190*, 123–140.

Lemarchand, D., Wasserburg, G., & Papanastassiou, D. (2004). Rate-controlled calcium isotope fractionation in synthetic calcite. *Geochimica et Cosmochimica Acta*, *68*(22), 4665–4678. doi:10.1016/j.gca.2004.05.029

Liu, Y., & Tossell, J. (2005). Ab initio molecular orbital calculations for boron isotope fractionations on boric acids and borates. *Geochimica et Cosmochimica Acta*, *69*(16), 3995–4006. doi:10.1016/j.gca.2005.04.009

Lowenstein, T. K., Timofeeff, M. N., Brennan, S. T., Hardie, L. A., & Demicco, R. V. (2001). Oscillations in Phanerozoic Seawater Chemistry: Evidence From Fluid Inclusions. *Science*, *294*, 1086–1089.

Lynch-Stieglitz, J., Stocker, T. F., Broecker, W. S., & Fairbanks, R. G. (1995). The Influence of Air-Sea Exchange on the Isotopic Composition of Oceanic Carbon: Observations and Mo. *Global Biogeochemical Cycles*, *9*(4), 653–665.

McConnaughey, T. (1989). 13C and 18O isotopic disequilibrium in biological carbonates : II . In vitro simulation of kinetic isotope effects. *Geochimica et Cosmochimica Acta*, *53*, 163–171.

McCrea, J. M. (1950). On the isotopic chemistry of carbonates and a paleotemperature scale. *Journal of Chemical Physics*, *18*(6), 849–857.

Mickler, P. J., Banner, J. L., Stern, L., Asmerom, Y., Edwards, R. L., & Ito, E. (2004). Stable isotope variations in modern tropical speleothems: Evaluating equilibrium vs. kinetic isotope effects. *Geochimica et Cosmochimica Acta*, *68*(21), 4381–4393. doi:10.1016/j.gca.2004.02.012

Millero, F. J., Zhang, J., Fiol, S., Sotolongo, S., Roy, R. N., & Lee, K. (1993). The use of buffers to measure the pH of seawater m (SO24-)/ K (HSO ;). *Marine Chemistry*, *44*, 143–152.

Milliman, J. D. (1974). Marine Carbonates. Springer-Verlag (1974), 375p.

Mix, A. C., & Fairbanks, R. G. (1985). North Atlantic surface-ocean control of Pleistocene deep-ocean circulation. *Earth and Planetary Science Letters*, *73*, 231–243.

Mook, W., Bommerson, J., & Staverman, W. (1974). Carbon isotope fractionation between dissolved bicarbonate and gaseous carbon dioxide. *Earth and Planetary Science Letters*, *22*, 169–176.

Morse, J. W., Arvidson, R. S., & Lüttge, A. (2007). Calcium carbonate formation and dissolution. *Chemical reviews*, *107*(2), 342–81. doi:10.1021/cr050358j

Morse, J. W., Wang, Q., & Tsio, M. Y. (1997). Influences of temperature and Mg : Ca ratio on CaCO 3 precipitates from seawater. *Geology*, *25*(1), 85–87. doi:10.1130/0091-7613(1997)025<0085

Mucci, A. (1986). Influence of temperature on the composition of magnesian calcite overgrowths precipitated from seawater. *Geochimica et Cosmochimica Acta*, *51*, 1977–1984.

Mucci, A., & Morse, J. W. (1982). The incorporation of Mg and Sr into calcite overgrowths : influences of growth rate and solution composition. *Geochimica et Cosmochimica Acta*, *47*, 217–233.

Mucci, A., & Morse, J. W. (1984). The solubility of calcite in seawater solutions of various magnesium concentration , Zi = 0.697 m at 25 °C and one atmosphere total pressure. *Geochimica et Cosmochimica Acta*, *48*(1982), 815–822.

Muth-Bohm, J., Becker, A., & Faisal, F. (2000). Suppressed molecular ionization for a class of diatomics in intense femtosecond laser fields. *Physical review letters*, *85*(11), 2280–3. Retrieved from http://www.ncbi.nlm.nih.gov/pubmed/10977991

Nancollas, G. H., & Purdie, N. (1945). The Kinetics of Crystal Growth. *Quarterly Reviews*, 1–20.

Nancollas, G. H., & Gardner, G. L. (1974). Kinetics of crystal growth of calcium oxalate monohydrate. *Journal of Crystal Growth*, *21*(2), 267–276. doi:10.1016/0022-0248(74)90014-1

O'Neil, J. R., Adami, L. H. and Epstein, S. (1975). Revised value for the ^{18}O fractionation between CO_2 and H_2O at 25^0C. *Journal of Research of the U.S. Geological Survey*, *3(5)*, 623-624.

Oppo, D. W., & Fairbanks, R. G. (1987). Variability in the deep and intermediate water circulation of the Atlantic Ocean during the past 25,000 years : Northern Hemisphere modulation of the Southern Ocean. *Earth and Planetary Science Letters*, *86*, 1–15.

Pagani, M., Lemarchand, D., Spivack, A., & Gaillardet, J. (2005). A critical evaluation of the boron isotope-pH proxy: The accuracy of ancient ocean pH estimates. *Geochimica et Cosmochimica Acta*, *69*(4), 953–961. doi:10.1016/j.gca.2004.07.029

Palmer, T., & Wilson, M. (2004). Calcite precipitation and dissolution of biogenic aragonite in shallow Ordovician calcite seas. *Lethaia*, *37*(4), 417–427. doi:10.1080/00241160410002135

Paquette, J., & Reeder, R. J. (1990). New Type of Compositional Zoning in Calcite: Insights Into Crystal Growth Mechanisms. *Geology*, *18*, 1244–1247.

Paquette, J., & Reeder, R. J. (1995). Relationship between surface structure , growth mechanism , and trace element incorporation in calcite. *Science*, *59*(4), 735–749.

Pearson, P. N., & Palmer, M. R. (2000). Atmospheric carbon dioxide concentrations over the past 60 million years. *Nature*, *406*(6797), 695–9. doi:10.1038/35021000

Petit, J. R., Raynaud, D., Basile, I., Chappellaz, J., Ritz, C., Delmotte, M., … Pe, L. (1999). Climate and atmospheric history of the past 420,000 years from the Vostok ice core, Antarctica. *Nature*, *399*, 429–436.

Raymo, M. E., Ruddiman, W. F., Shackleton, N. J., & Oppo, D. W. (1990). Evolution of Atlantic-Pacific d13C gradients over the last 2.5 m.y. *Earth and Planetary Science Letters*, *97*, 353–368.

Reddy, M. M. (1977). Crystallization of calcium carbonate in the presence of trace concentrations of phosphorus-containing anions. *Journal of Crystal Growth*, *41*, 287–295.

Reddy, M. M., & Wang, K. K. (1980). Crystallization of calcium carbonate in the presence of metal ions. *Journal of Crystal Growth*, *50*(2), 470–480. doi:10.1016/0022-0248(80)90095-0

Rollion-Bard, C., Erez, J., & Zilberman, T. (2008). Intra-shell oxygen isotope ratios in the benthic foraminifera genus Amphistegina and the influence of seawater carbonate chemistry and temperature on this ratio. *Geochimica et Cosmochimica Acta*, *72*(24), 6006–6014. doi:10.1016/j.gca.2008.09.013

Rollion-Bard, C., Chaussidon, M., & France-Lanord, C. (2011). Biological control of internal pH in scleractinian corals: Implications on paleo-pH and paleo-temperature reconstructions. *Comptes Rendus Geoscience*, *343*(6), 397–405. doi:10.1016/j.crte.2011.05.003

Romanek, C.S., Grossman, E., & Morse, J. (1992). Carbon isotopic fractionation in synthetic aragonite and calcite : Effects of temperature and precipitation rate. *Geochimica et Cosmochimica Acta*, *56*, 419–430.

Romanek, C. S., Jiménez-López, C., Navarro, A. R., Sánchez-Román, M., Sahai, N., & Coleman, M. (2009). Inorganic synthesis of Fe–Ca–Mg carbonates at low temperature. *Geochimica et Cosmochimica Acta*, *73*(18), 5361–5376. doi:10.1016/j.gca.2009.05.065

Romanek, C.S., Grossman, E., & Morse, J. (1992). Carbon isotopic fractionation in synthetic aragonite and calcite: Effects of temperature and precipitation rate. *Geochimica et Cosmochimica Acta*, *56*(1), 419–430. doi:10.1016/0016-7037(92)90142-6

Romanov, D., Kaufmann, G., & Dreybrodt, W. (2008). δ^{13}C profiles along growth layers of stalagmites: Comparing theoretical and experimental results. *Geochimica et Cosmochimica Acta*, *72*(2), 438–448. doi:10.1016/j.gca.2007.09.039

Rosenbaum, J., & Sheppard, S. (1986). An isotopic study of siderites, dolomites and ankerites at high temperatures*. *Geochimica et Cosmochimica Acta*, *50*(645), 4–7.

Royer, D. L., Wing, S. L., Beerling, D. J., Jolley, D. W., Koch, P. L., Hickey, L. J., & Berner, R. a. (2001). Paleobotanical evidence for near present-day levels of atmospheric CO2 during part of the tertiary. *Science (New York, N.Y.)*, *292*(5525), 2310–3. doi:10.1126/science.292.5525.2310

Rubinson, M., & Clayton, R. N. (1969). Carbon-13 fractionation between aragonite and calcite. *Geochimica et Cosmochimica Acta*, *33*, 997–1002.

Ruiz-Agudo, E., Putnis, C. V., Kowacz, M., Ortega-Huertas, M., & Putnis, a. (2012). Boron incorporation into calcite during growth: Implications for the use of boron in carbonates as a pH proxy. *Earth and Planetary Science Letters*, *345-348*, 9–17. doi:10.1016/j.epsl.2012.06.032

Sanyal, A., Hemming, N. G., Hanson, G. N., & Broecker, W. (1995). Evidence for a higher pH in the glacial ocean from boron isotopes in foraminifera. *Nature*, *373*, 234–236.

Sanyal, A., Nugent, M., Reeder, R. J., & Bijma, J. (2000). Seawater pH control on the boron isotopic composition of calcite : Evidence from inorganic calcite precipitation experiments. *Geochimica et Cosmochimica Acta*, *64*(9), 1551–1555.

Sanyal, A., Bijma, J., Spero, H. J., & Lea, D. W. (2001). Empirical relationship between pH and the boron isotopic composition of Globigerinoides sacculifer: Implications for the boron isotope paleo-pH proxy. *Paleoceanography*, *16*(5), 515–519.

Schauble, E. A., Ghosh, P., & Eiler, J. M. (2006). Preferential formation of 13C–18O bonds in carbonate minerals, estimated using first-principles lattice dynamics. *Geochimica et Cosmochimica Acta*, *70*(10), 2510–2529. doi:10.1016/j.gca.2006.02.011

Schwarcz, H. P., Agyei, E., & Mcmullen, C. (1969). Boron Isotopic Fractionation During Clay Adsorption From Seawater. *Earth and Planetary Science Letters*, *6*, 1–5.

Sen, S., Stebbins, J. F., Hemming, N. G., & Ghosh, B. (1994). Coordination environments of B impurities in calcite and aragonite polymorphs; A ^{11}B MAS NMR study. *American Mineralogist, 79*, p. 819-825

Sharma, T., & Clayton, R. N. (1985). Measurement of O18/O16 ratios of total oxygen of carbonates. *Geochimica et Cosmochimica Acta*, *29*, 1347–1353.

Sigman, D. M., & Boyle, E. A. (2000). Glacial/Interglacial Variations in Atmospheric Carbon Dioxide. *Nature*, *407*(October), 859–869.

Spero, H. J., Bijma, J., Lea, D. W., & Bemis, B. E. (1997). Effect of seawater carbonate concentration on foraminiferal carbon and oxygen isotopes. *Nature*, *390*, 497–500.

Spivack, A. J., Palmer, M. R., & Edmond, J. M. (1987). The sedimentary cycle of the boron isotopes. *Geochimica et Cosmochimica Acta*, *51*, 1939–1949.

Stanley, S. M., & Hardie, L. A. (1998). Secular oscillations in the carbonate mineralogy of reef-building and sediment-producing organisms driven by tectonically forced shifts in seawater chemistry. *Palaeogeography, Palaeoclimatology, Palaeoecology*, *144*, 3–19.

Tang, J., Köhler, S. J., & Dietzel, M. (2008). Sr2+/Ca2+ and 44Ca/40Ca fractionation during inorganic calcite formation: I. Sr incorporation. *Geochimica et Cosmochimica Acta*, *72*(15), 3718–3732. doi:10.1016/j.gca.2008.05.031

Tarutani, T., Clayton, R. N., & Mayeda, T. K. (1969). The effect of polymorphism and magnesium substitution on oxygen isotope fractionation between calcium carbonate and water. *Geochimica et Cosmochimica Acta*, *33*, 987–996.

Tossell, J. A. (2006). Boric acid adsorption on humic acids: Ab initio calculation of structures, stabilities, 11B NMR and 11B,10B isotopic fractionations of surface complexes. *Geochimica et Cosmochimica Acta*, *70*(20), 5089–5103. doi:10.1016/j.gca.2006.08.014

Tremaine, D. M., Froelich, P. N., & Wang, Y. (2011). Speleothem calcite farmed in situ: Modern calibration of δ18O and δ13C paleoclimate proxies in a continuously-monitored natural cave system. *Geochimica et Cosmochimica Acta*, *75*(17), 4929–4950. doi:10.1016/j.gca.2011.06.005

Turner, J. V. (1982). Kinetic fractionation of carbon-13 during calcium carbonate precipitation. *Geochimica et Cosmochimica Acta*, *46*(7), 1183–1191. doi:10.1016/0016-7037(82)90004-7

Urey, H. C. (1947). The Thermodynamic Properties of Isotopic Substances. *Journal of the Chemical Society,* 562-581.

Usdowski, E., & Hoefs, J. (1990). Kinetic 13C/12C and 18O/16O effects upon dissolution and outgassing of CO2 in the system CO2-H2O. *Chemical Geology (Isotope Geosciences Edition)*, *80*, 109–118.

Vengosh, A., Kolodny, Y., Starinsky, A., Chivas, A. R., & McCulloch, M. T. (1991). Coprecipitation and isotopic fractionation of boron in modern biogenic carbonates. *Geochimica et Cosmochimica Acta*, *55*(10), 2901–2910. doi:10.1016/0016-7037(91)90455-E

Venz, K. A., & Hodell, D. A. (2002). New evidence for changes in Plio ^ Pleistocene deep water circulation from Southern Ocean ODP Leg 177 Site 1090. *Palaeogeography, Palaeoclimatology, Palaeoecology*, *182*, 197–220.

Vincent, E., & Berger, W. H. (n.d.). Carbon Dioxide and Polar Cooling in the Miocene: The Monterey Hypothesis. *Geophysical Monograph Series*, *32*, 455–468.

Watkins, J. M., Nielsen, L. C., Ryerson, F. J., & DePaolo, D. J. (2013a). The influence of kinetics on the oxygen isotope composition of calcium carbonate. *Earth and Planetary Science Letters*, *375*, 349–360. doi:10.1016/j.epsl.2013.05.054

Watkins, J. M., Nielsen, L. C., Ryerson, F. J., & DePaolo, D. J. (2013b). The influence of kinetics on the oxygen isotope composition of calcium carbonate. *Earth and Planetary Science Letters*, *375*, 349–360. doi:10.1016/j.epsl.2013.05.054

Watkins, J., & Nielsen, L. C. (2013). The influence of kinetics on the oxygen isotope composition of calcium carbonate. *Earth and Planetary Science Letters*, *375*, 349–360. doi:10.1016/j.epsl.2013.05.054

Watson, E. B. (2004). A conceptual model for near-surface kinetic controls on the trace-element and stable isotope composition of abiogenic calcite crystals. *Geochimica et Cosmochimica Acta*, *68*(7), 1473–1488. doi:10.1016/j.gca.2003.10.003

Wilkinson, B. H., & Algeo, T. J. (1989). Sedimentary Carbonate Record of Calcium-Magnesium Cycling. *American Journal of Science*, *289*, 1158–1194.

Wilson, J. D., Barker, S., & Ridgwell, A. (2012). Assessment of the spatial variability in particulate organic matter and mineral sinking fluxes in the ocean interior: Implications for the ballast hypothesis. *Global Biogeochemical Cycles*, *26*(4), 15p. doi:10.1029/2012GB004398

Winland, H. D. (1969). Stability of Calcium Carbonate Polymorphs in Warm, Shallow Seawater. *SEPM Journal of Sedimentary Research*, *Vol. 39*(4). doi:10.1306/74D71E92-2B21-11D7-8648000102C1865D

Wolf-Gladrow, D. A., Zeebe, R. E., Klaas, C., Körtzinger, A., & Dickson, A. G. (2007). Total alkalinity: The explicit conservative expression and its application to biogeochemical processes. *Marine Chemistry*, *106*(1-2), 287–300. doi:10.1016/j.marchem.2007.01.006

Zachos, J. C., Dickens, G. R., & Zeebe, R. E. (2008). An early Cenozoic perspective on greenhouse warming and carbon-cycle dynamics. *Nature*, *451*(7176), 279–83. doi:10.1038/nature06588

Zachos, J., Pagani, M., Sloan, L., Thomas, E., & Billups, K. (2014). Trends, Global Rhythms, and Aberrations in Global Climate 65 Ma to Present. *Science*, *292*(5517), 686–693.

Zeebe, R. (2007). An explanation of the effect of seawater carbonate concentration on foraminiferal oxygen isotopes. *Geochimica et Cosmochimica Acta*, *63*(13), 2001–2007.

Zeebe, R. E., Sanyal, A., Ortiz, J. D., & Wolf-Gladrow, D. A. (2001). A theoretical study of the kinetics of the boric acid–borate equilibrium in seawater. *Marine Chemistry*, *73*(2), 113–124. doi:10.1016/S0304-4203(00)00100-6

Zeebe, R. E., & Wolf-Gladrow, D. A. (2001). *CO2 in Seawater: Equilibrium, Kinetics, Isotopes: Equilibrium, Kinetics, Isotopes*. Elsevier.

Zeebe, R. E., Wolf-Gladrow, D. A., & Jansen, H. (1999). On the time required to establish chemical and isotopic equilibrium in the carbon dioxide system in seawater. *Marine Chemistry*, *65*(3-4), 135–153.

Zhong, S., & Mucci, A. (1993). Calcite precipitation in seawater using a constant addition technique: A new overall reaction kinetic expression. *Geochimica et Cosmochimica Acta*, *57*(7), 1409–1417. doi:10.1016/0016-7037(93)90002-E

Zhou, G-T., & Zheng, Y.-F. (2003). An experimental study of oxygen isotope fractionation between inorganically precipitated aragonite and water at low temperatures. *Geochimica et Cosmochimica Acta*, *67*(3), 387–399.

Zuddas, P., & Mucci, A. (1994). Kinetics of calcite precipitation from seawater : I . A classical chemical kinetics description for strong electrolyte solutions. *Science*, *58*(20), 4353–4362.

CHAPTER 6:

CONCLUSIONS AND RESEARCH CONTRIBUTIONS

6.1 Introduction

The refined calibration of the boron isotope-pH proxy will greatly enhance our understanding of historical atmospheric CO_2 fluctuations and the effect of this greenhouse gas on Earth's climate. Any change in atmospheric CO_2 concentrations will be reflected in seawater pH due to equilibrium exchange of atmospheric CO_2 with CO_2 dissolved in the ocean. Elevated atmospheric CO_2 concentrations (presumably from anthropogenic emissions) will cause ocean acidification, marked by a reduction in seawater pH. Research conducted in this study involved the synthesis of calcium carbonate by spontaneous nucleation at stable pH values, with subsequent boron and oxygen isotope analysis of both precipitated carbonate crystals and the precipitating solutions. Specifically, this thesis examined the dependence of the boron isotope composition ($\delta^{11}B$) of synthetic calcite on the pH of the precipitating solution. A systematic increase in $\delta^{11}B_{calcite}$ was observed, with decreasing boron isotope fractionation between calcite and solution as pH increased, supporting the hypothesis that $B(OH)_4^-$ ion is incorporated into the crystal lattice. However, the exclusive incorporation of borate cannot be confirmed, as it appears that boric acid may also be integrated into the crystal structure, as evidenced by heavier boron isotope compositions in the low-pH samples. While this is to be expected given the dominance of boric acid at pH < 8.597 (Dickson, 1990), the magnitude of the deviation from the aqueous borate curve suggests that either the samples were not precipitated in isotopic equilibrium and/or more than a single aqueous boron species is incorporated into the carbonate lattice.

This thesis also employed the modified constant addition method to examine oxygen isotope behavior across three temperature and pH ranges in high (0.7 mol/kg) ionic strength solutions. The oxygen isotope composition of water ($\delta^{18}O_{H2O}$) was analyzed to confirm equilibrium conditions within the experimental system. Numerous variables impacting oxygen isotope effects and fractionation behavior in solution were identified and proven consistent with theoretically predicted acting influences, and subsequent suggestions were made to correct for them.

Chapter 1 discussed the importance of aqueous stable isotope geochemistry to the field of climatology, with Chapter 2 detailing the mechanisms of oxygen isotope fractionation between calcium carbonate and its growth solution ($\delta^{18}O_{CaCO3\text{-}H2O}$). The second chapter also introduced the boron isotope paleo-pH proxy and isotopic analysis procedures in the laboratory. Chapter 3 served as an overview of the methodological options to synthesize abiotic calcium carbonate minerals, providing context for the following two chapters. The sequential nature of the boron isotope paleo-pH proxy development was advanced in Chapter 4, which investigated the boron isotope compositions of synthetic aragonite and calcite samples from a range of stable pH values. Finally, Chapter 5 evaluated the temperature dependence of oxygen isotopes in synthesized calcite crystals across three different growth temperature and three distinct stable pH conditions. This sixth chapter summarizes each research chapter's major findings and/or purpose, outlines the candidate's contributions to Chapters 3, 4 and 5, identifies each study's relevance to the field, and explores future avenues of research specific to the two experimental projects presented in this thesis.

6.2 Candidate's Contributions to Collaborative Research

6.2.1 Evaluation of abiotic carbonate synthesis techniques in stable isotope geochemistry

In this review paper, the candidate conducted the literature review, compiled the information and provided a comprehensive summary (of which only a portion appears in this thesis) of the current methodological options available to synthesize abiotic calcium carbonates and the considerations involved in their selection. The candidate then integrated editorial suggestions made by the candidate's supervisor (the collaborative author).

6.2.2 Investigation of oxygen and boron stable isotope systematics in the calcium carbonate-CO_2-H_2O-NaCl system

This collaborative study was a continuation of Christa Klein-Gebbinck et al. (2013) investigation into the boron isotope paleo-pH proxy. Experimental work was split according to each thesis focus (i.e., aragonite and calcite synthesis experiments). The candidate conducted all modified constant addition experiments yielding calcite mineralogy, analyzing the resultant carbonate samples via IRMS and solution samples for oxygen and carbon via CF-IRMS, as well as normalizing and interpreting the mass spectrometry output data. The candidate then wrote up the paper targeted for publication, designed figures/tables, and incorporated feedback suggested by the collaborating authors.

6.2.3 Temperature dependence and kinetic effects in the calcite-CO_2-H_2O-NaCl system

This partnership again involved the candidate and the candidate's supervisor. The candidate was responsible for all modified constant addition experiments, the preparation of standard solutions, subsequent isotopic analyses of carbonate crystals and their precipitating solutions, as well as data interpretation. Upon discussion with the supervisor, the candidate completed the research paper, with recommended changes made by the supervisor.

6.3 Research relevance and applicability to field of geochemistry

The reconstruction of variations in Earth's concentration of atmospheric carbon dioxide is fundamental to the field of climatology. Understanding and characterizing past climatic shifts is essential to accurately predict future climate change, particularly with modern environmental concerns surrounding the effect of anthropogenic CO_2 emissions on global climate. A variety of geochemical proxies have been developed to chronicle past climate aberrations, in lieu of direct measurements for timeframes exceeding the limits of practical measurement. These proxies supplement and/or complement current global circulation climate models in an overarching effort to minimize prediction uncertainties. Specific to this thesis, the boron isotope paleo-pH proxy is used to estimate the pH of ancient seawater, which reflects changes in the atmospheric-dissolved CO_2 equilibrium. Once quantified, pH can be used in conjunction with either alkalinity or total inorganic carbon concentration to reconstruct atmospheric $p\mathrm{CO}_2$.

The robustness of the boron-pH proxy is challenged in this thesis by experimentally evaluating the contribution of the aqueous borate ($B(OH)_4^-$) species to the total boron isotope composition of calcite. The inorganic synthesis of abiotic minerals permits a targeted variable to be assessed in isolation, eliminating auxiliary environmental components and thus minimizing unknown influences on the system. This thesis is one step in a series investigating the boron isotope systematics in marine carbonates, to assess the proxy's validity and its legitimacy for paleoclimate research applications.

Identification of temperature-dependent oxygen isotope fractionation trends is important to consistently synthesize calcium carbonate samples in oxygen isotope equilibrium, under a wide range of temperature and pH conditions. Such ability requires a fundamentally sound understanding of all the underlying mechanisms. Lesser known variables can then be more easily isolated and studied, allowing ongoing augmentation of our current state of knowledge.

6.4 Future research

While the research findings presented in this thesis advance our understanding of the boron-pH proxy, several amendments can be made to improve the overall precision and thus further refine the proxy. For example, inclusion of other seawater constituents to the synthetic seawater-like solution will better reflect the isotopic fractionation behavior of true seawater. Artificial seawater solutions in this thesis were comprised solely of $NaHCO_3$, Na_2CO_3, $MgCl_2$, $CaCl_2$, NaCl and $B(OH)_3$. Similarly, the addition of SO_4^{2-} and K^+ will better approximate the use of Tris buffer to correct for seawater pH data from a standard electrode measurement in RmV, and allow for more appropriate applications of pK_B and $^{11\text{-}10}K_B$. The complexity of the system must be increased sequentially to ensure reliable control over important parameters such as pH and ionic strength. A comprehensive understanding of controls on the system requires evaluation of boron incorporation into calcium carbonates over a range of ionic strengths and temperatures, expanding upon this study which precipitated aragonite and calcite at 25 °C in high ionic strength (0.7 mol/kg) solutions. An additional consideration involves the abiotic synthesis of carbonate minerals in the laboratory, which allow experiments to be conducted under controlled conditions, thus isolating the variable of interest. In the future, this knowledge base can be transferred to natural samples to evaluate the existence of species-specific vital effects. Certain foraminiferal species will be identified as suitable candidates for pH reconstructions, which can then be compared with historical models to confirm past pCO_2 conditions.

A potential revolution to the proxy involves control over carbon isotope equilibrium, which may reveal important insights linking fractionation trends between carbon and boron isotopes. Notably, these two elements are one atomic number apart and share similar atomic properties. Ultimately, developing a multi-element approach to the boron isotope paleo-pH proxy will better identify its true applicability and limitations over a range of ionic strengths, temperatures and growth environments.

The onset of precipitation and nature of crystal growth also offer future avenues for research. Theoretically, the constant addition technique is ideally designed to control carbon and oxygen isotope drift, achieved with the titrant addition of ions to replenish those consumed by precipitation. This objective, however, is not consistently met. To ascertain the point at which isotopic drift is minimized, different injection rates can be implemented as a trial-and-error attempt to yield zero fluctuation. Alternatively, the initial solution can be left in a closed system for calcium carbonate crystal growth to proceed without the addition of titrant solution; upon quantification of precipitation rate, the rate of ion replenishment can be calculated appropriately and implemented as a function of titrant injection rate. The use of seeded material within the constant addition system will also provide insight into the linearity of growth. For this study, a bulk precipitation rate (mg $CaCO_3$ precipitated/kg solution/day) was quantified. This is a coarse representation of growth rate, assuming it is constant and ongoing. Unlike spontaneous precipitation experiments, the overgrowth approach allows reliable measurement of the crystal growth rate in the presence, as the nucleation process is eliminated such that mineral growth upon nuclei allows isolation of the growth kinetics parameter.

While this study quantified the boron isotope composition of laboratory-synthesized calcium carbonates, sufficient carbonate samples and precipitating solutions remain to undergo MAS NMR spectroscopy analysis. These results will identify the presence of trigonal and/or tetrahedral forms of boron in the carbonate lattice. While NMR studies will not confirm whether boric acid is contributing to the overall boron isotope composition of the carbonate, boron coordination will be established and coordination changes during uptake will be revealed for both aragonite and calcite polymorphs. Examining the mechanisms of boron incorporation and potential influences of boric acid on the carbonate's boron isotope compositions will deepen our fundamental understanding of the proxy. Tossell (2006) hypothesized a mineral-specific coordination change in carbonate crystal structure may occur upon $B(OH)_4^-$ uptake, necessitating independent investigations for aragonite and calcite since systematic processes occurring at the carbonate surface may depend on crystal habit.

Assessing the temperature- and pH-dependence of oxygen isotope effects in synthetic calcite has yielded promising results, consistent with previous literature from both a theoretical and empirical standpoint. Several permutations of the available parameters (i.e., injection rate and temperature) have yet to undergo experimentation, however this knowledge will quantitatively fill in the remaining gaps. Such information adds to the ever-growing database linking carbonic acid speciation, calcium carbonate precipitation rates, oxygen isotope effects, pH and temperature variables. MRSI colleague Chris Spencer is currently tweaking the constant addition method for carbonate synthesis in an attempt to improve control over carbon isotope drift. Application of other abiotic calcium carbonate synthesis techniques, as described in Chapter 3, under identical experimental conditions (i.e., solution chemistry, injection rates and temperatures), will supplement our oxygen isotope equilibrium fractionation knowledge across a spectrum of growth conditions.

Information generated by oxygen stable isotope analyses in marine carbonates has already been widely used to piece together Earth's past environmental conditions, including fluctuations in temperature, ocean circulation patterns and biotic productivity; inclusion of historical pH changes allows quantitative determination of atmospheric $p\mathrm{CO}_2$. The boron isotope paleo-pH proxy is currently undergoing sequential development, which is essential to substantiate its validity. Once refined, this proxy can be cross-verified with other established proxies to reconstruct past environmental conditions, informing discussions of global warming and enabling scientists to predict future climate with more certainty. Furthermore, the development of a multi-element approach to stable isotope geochemistry analyses, as explored in this thesis, may prove to be a tremendously powerful tool in the evaluation, refinement and augmentation of the current paleoclimate archive.

APPENDIX

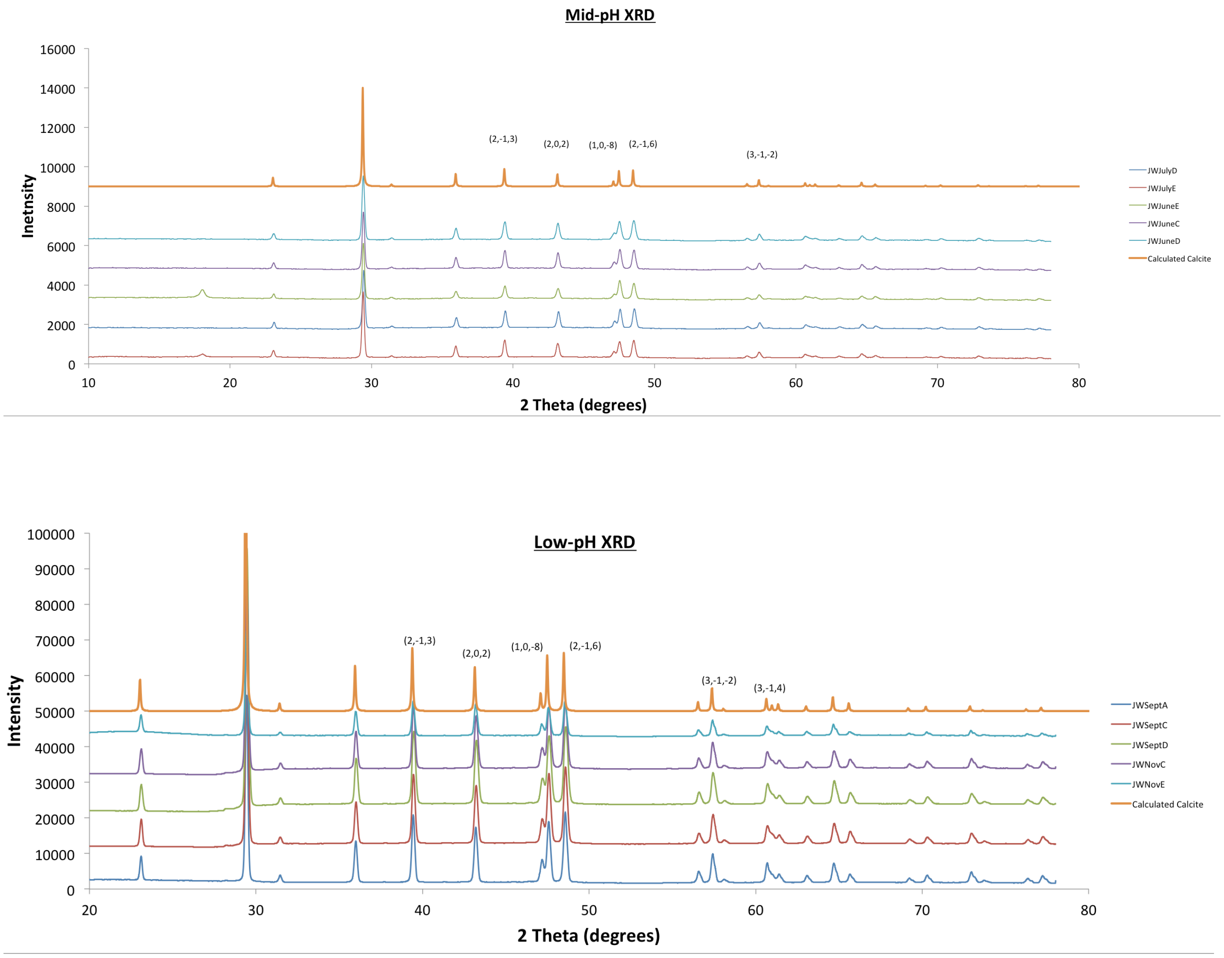

Figure A.1: X-ray diffraction (XRD) data alignment of selected calcite samples.

Mineralogy is determined by measuring the angles and intensities of diffracted x-ray beams, specific to the crystalline atoms within the mineral. An arbitrary vertical stacking of selected carbonate samples from this study illustrates the alignment of peaks along identical diffracted angles, which also position exactly with the calculated, theoretical calcite peaks (uppermost plot). Thus, these samples are identified as "pure" (100%) calcite via XRD crystallographic analysis.

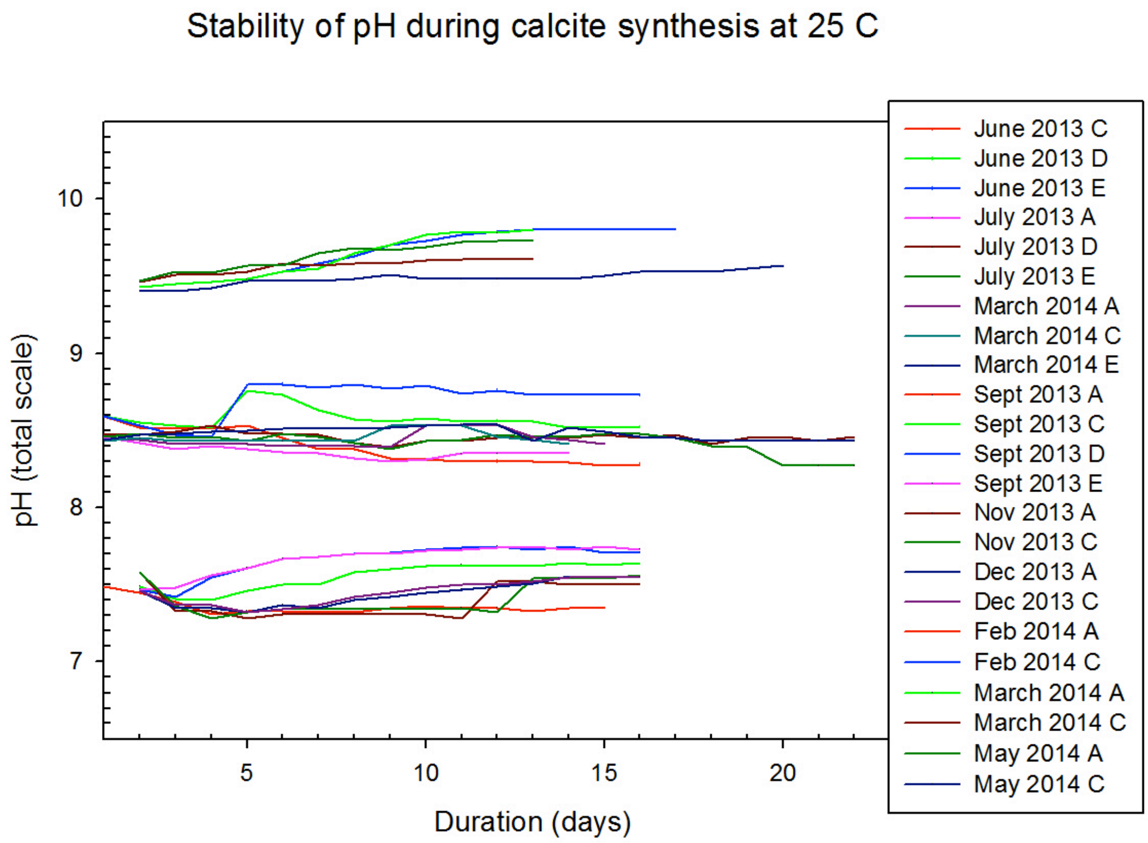

Figure A.2: Stability of pH during calcite synthesis experiments for boron analysis at 25 °C.

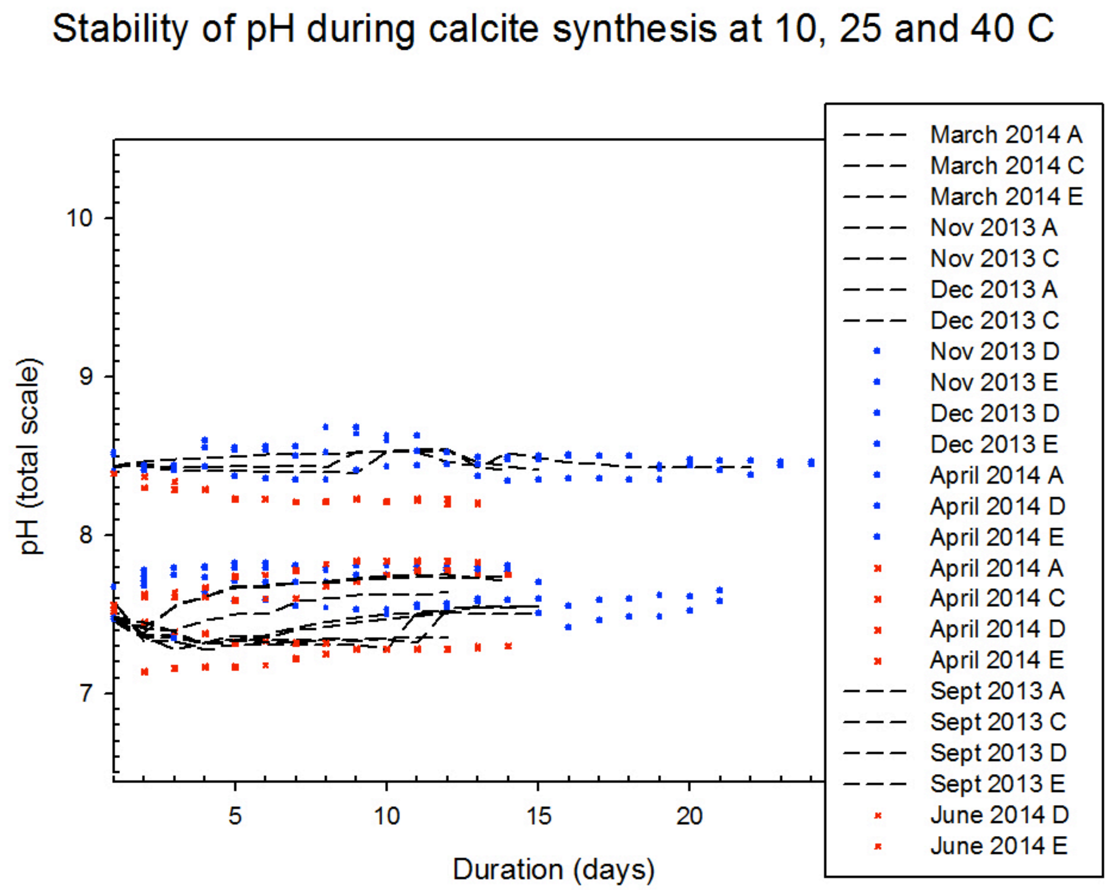

Figure A.3: Stability of pH during calcite temperature-dependence experiments (black dashed lines for 25 °C, blue dots represent 10 °C and red x's indicate 40 °C carbonate growth conditions).

Table A.1a: Compilation of oxygen isotope data for synthesized calcites at 10 °C.

Sample Name	Sample size (mg)	Bulk ppt rate (mg/kg/d)	Average pH	$\delta^{18}O_{calcite}$ (‰)	Average	Stdev
#11-JWApril0314-A	28	1.28	8.38	22.23		
				22.20	22.22	0.02
#11-JWApril0314-C	25	1.14	8.48	23.06		
				23.45		
				23.76		
				23.20	23.37	0.31
#11-JWApril0314-D	12	0.40	8.50	22.33		
				22.24	22.29	0.06
#5-JWNov1313-D	332	15.15	7.70	25.74		
				25.80	25.77	0.04
#5-JWNov1313-E	327	14.92	7.65	25.70		
				25.82	25.76	0.08
#6-JWDec0413-D	160	8.29	7.55	25.83		
				25.89	25.86	0.04
#6-JWDec0413-E	156	8.09	7.61	25.87		
				25.84	25.86	0.02
#7-JWFeb1114-E	23	1.39	9.54	24.32		
				24.42	24.37	0.07

Table A.1b: Compilation of oxygen isotope data for synthesized calcites at 25 °C.

Sample Name	Sample size (mg)	Bulk ppt rate (mg/kg/d)	Average pH	$\delta^{18}O_{calcite}$ (‰)	Average	Stdev
#3-JWJune2813-C	100	5.68	8.40	22.01		
				22.04	22.03	0.02
#3-JWJune2813-D	92	5.22	8.58	21.99		
				22.14		
				22.12		
				22.10	22.09	0.01
#3-JWJune2813-E	110	6.24	8.70	22.30		
				22.09	22.20	0.15
#4-JWJuly3013-D	91	2.83	8.46	22.06		
				22.05	22.06	0.01
#4-JWJuly3013-E	113	3.51	8.42	22.18		
				22.19	22.19	0.01
#10-JWMarch1014-A	82	5.10	8.44	21.81		
				22.12	21.97	0.22
#10-JWMarch1014-C	234	14.56	8.45	22.15	22.15	n/a
#10-JWMarch1014-E	48	2.06	8.47	22.20		
				22.20	22.20	0.00
#5-JWSept0413-A	240	14.43	7.36	22.69		
				22.63	22.66	0.04
#5-JWSept0413-C	235	14.13	7.55	22.43	22.43	n/a
#5-JWSept0613-D	235	12.38	7.66	22.43		
				22.42	22.43	0.01
#5-JWSept0613-E	360	18.96	7.66	22.34	22.34	n/a
#5-JWNov1313-A	330	14.29	7.39	22.49		
				22.57	22.53	0.06
#5-JWNov1313-C	325	14.07	7.42	22.53		
				22.50	22.52	0.03
#6-JWDec0413-A	212	16.29	7.44	22.51		
				22.49	22.50	0.01
#6-JWDec0413-C	188	15.04	7.45	22.58		
				22.56	22.57	0.01
#7-JWFeb1114-A	35	2.14	9.75	21.64		
				21.67		
				21.66		
				21.72		
				21.79		
				21.74	21.70	0.06
#7-JWFeb1114-C	35	2.14	9.74	21.78		
				21.74		
				21.84		
				21.79	21.79	0.04
#12-JWMay2614-A	29	1.23	9.53	20.72		
				20.98	20.85	0.18

Table A.1c: Compilation of oxygen isotope data for synthesized calcites at 40 °C.

Sample Name	Sample size (mg)	Bulk ppt rate (mg/kg/d)	Average pH	$\delta^{18}O_{calcite}$ (‰)	Average	Stdev
#12-JWApril3014-A	121	9.39	8.25	19.53		
				19.51	19.52	0.01
#12-JWApril3014-C	110	8.54	8.26	19.34		
				19.37	19.36	0.02
#12-JWMay2714-D	87	3.86	7.68	19.47		
				19.44	19.46	0.02
#12-JWMay2714-E	98	4.34	7.34	19.60		
				19.55	19.58	0.04
#13-JWJune1814-D	170	12.13	7.25	19.62		
				19.61	19.62	0.01
#13-JWJune1814-E	221	15.77	7.74	19.62		
				19.58	19.60	0.03

Table A.2a: Compilation of carbon isotope data for synthesized calcites at 10 °C.

Sample Name	Sample size (mg)	Bulk ppt rate (mg/kg/d)	Average pH	$\delta^{18}O_{calcite}$ (‰)	Average	σ
#11-JWApril0314-A	28	1.28	8.38	-0.26		
				-0.30	-0.28	0.03
#11-JWApril0314-C	25	1.14	8.48	-4.11		
				-4.05		
				-4.17		
				-4.07	-4.10	0.05
#11-JWApril0314-D	12	0.40	8.50	-3.21		
				-3.77	-3.49	0.39
#5-JWNov1313-D	332	15.15	7.70	-2.60		
				-2.55	-2.58	0.04
#5-JWNov1313-E	327	14.92	7.65	-3.41		
				-3.30	-3.36	0.08
#6-JWDec0413-D	160	8.29	7.55	-2.00		
				-2.01	-2.01	0.01
#6-JWDec0413-E	156	8.09	7.61	-2.32		
				-2.30	-2.31	0.01
#7-JWFeb1114-E	23	1.39	9.54	1.70		
				1.76	1.73	0.05

Table A.2b: Compilation of carbon isotope data for synthesized calcites at 25 °C.

Sample Name	Sample Size (mg)	Bulk ppt rate (mg/kg/d)	Average pH	$\delta^{13}C_{calcite}$ (‰)	Average	σ
#3-JWJune2813-C	100	5.68	8.40	-18.40		
				-17.66	-18.03	0.52
#3-JWJune2813-D	92	5.22	8.58	-18.74		
				-18.91	-18.82	0.12
#3-JWJune2813-E	110	6.24	8.70	-16.09		
				-16.56	-16.33	0.33
#4-JWJuly3013-D	91	2.83	8.46	-17.76		
				-17.82	-17.79	0.04
#4-JWJuly3013-E	113	3.51	8.42	-14.68		
				-14.49	-14.58	0.13
#10-JWMarch1014-A	82	5.10	8.44	-4.06		
				-4.09	-4.08	0.02
#10-JWMarch1014-C	234	14.56	8.45	-4.40		
				-0.60	-4.48	2.68
#10-JWMarch1014-E	48	2.06	8.47	-3.81		
				-3.70	-3.76	0.07
#5-JWSept0413-A	240	14.43	7.36	-3.47		
				-3.62	-3.55	0.11
#5-JWSept0413-C	235	14.13	7.55	-2.28		
				-2.58	-2.43	0.21
#5-JWSept0613-D	235	12.38	7.66	-1.40		
				-1.30	-1.35	0.07
#5-JWSept0613-E	360	18.96	7.66	-1.26		
				-1.41	-1.34	0.11
#5-JWNov1313-A	330	14.29	7.39	-3.00		
				-2.96	-2.98	0.03
#5-JWNov1313-C	325	14.07	7.42	-2.49		
				-3.62	-3.05	0.80
#6-JWDec0413-A	212	16.29	7.44	-2.42		
				-2.59		
				-2.37		
				-2.53	-2.51	0.10
#6-JWDec0413-C	188	15.04	7.45	-2.34		
				-2.32	-2.33	0.01
#7-JWFeb1114-A	35	2.14	9.75	-0.28		
				-0.15		
				-0.16		
				-0.29		
				-0.31		
				-0.29	-0.25	0.07
#7-JWFeb1114-C	35	2.14	9.74	-0.22		
				-0.50		
				-0.24		
				-0.22	-0.23	0.14
#12-JWMay2614-A	29	1.23	9.53	-2.55		
				-2.60	-2.57	0.04

Table A.2c: Compilation of carbon isotope data for synthesized calcites at 40 °C.

Sample Name	Sample size (mg)	Bulk ppt rate (mg/kg/d)	Average pH	$\delta^{18}O_{calcite}$ (‰)	Average	σ
#12-JWApril3014-A	121	9.39	8.25	-4.22		
				-4.15	-4.19	0.05
#12-JWApril3014-C	110	8.54	8.26	-4.42		
				-4.39	-4.41	0.02
#12-JWMay2714-D	87	3.86	7.68	-1.43		
				-1.38	-1.40	0.04
#12-JWMay2714-E	98	4.34	7.34	-3.53		
				-3.58	-3.55	0.04
#13-JWJune1814-D	170	12.13	7.25	-3.79		
				-3.74	-3.77	0.03
#13-JWJune1814-E	221	15.77	7.74	-1.75		
				-1.70	-1.73	0.03

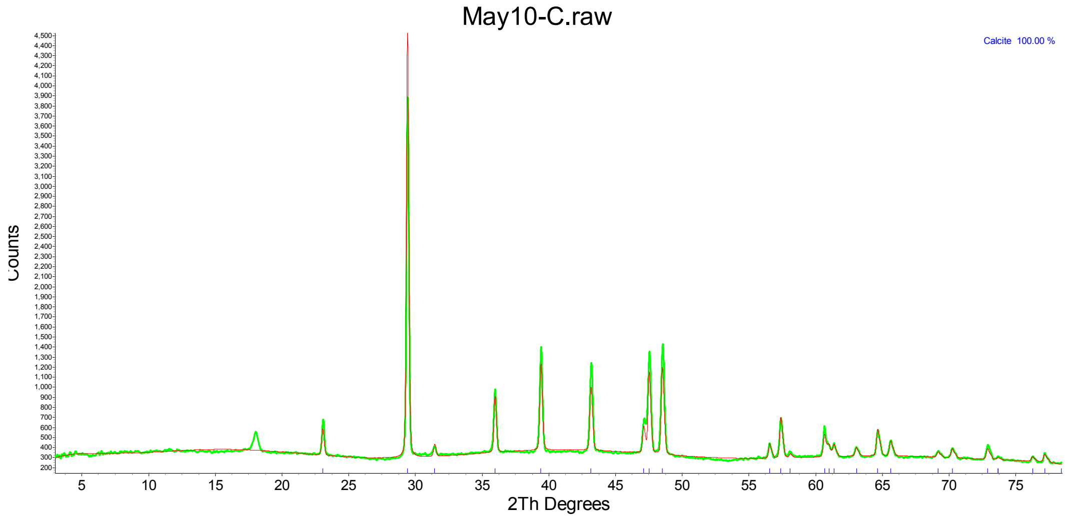
May10-C.raw
Calcite 100.00 %
Counts
200
300
400
500
600
700
800
900
1,000
1,100
1,200
1,300
1,400
1,500
1,600
1,700
1,800
1,900
2,000
2,100
2,200
2,300
2,400
2,500
2,600
2,700
2,800
2,900
3,000
3,100
3,200
3,300
3,400
3,500
3,600
3,700
3,800
3,900
4,000
4,100
4,200
4,300
4,400
4,500
5
10
15
20
25
30
35
40
45
50
55
60
65
70
75
2Th Degrees

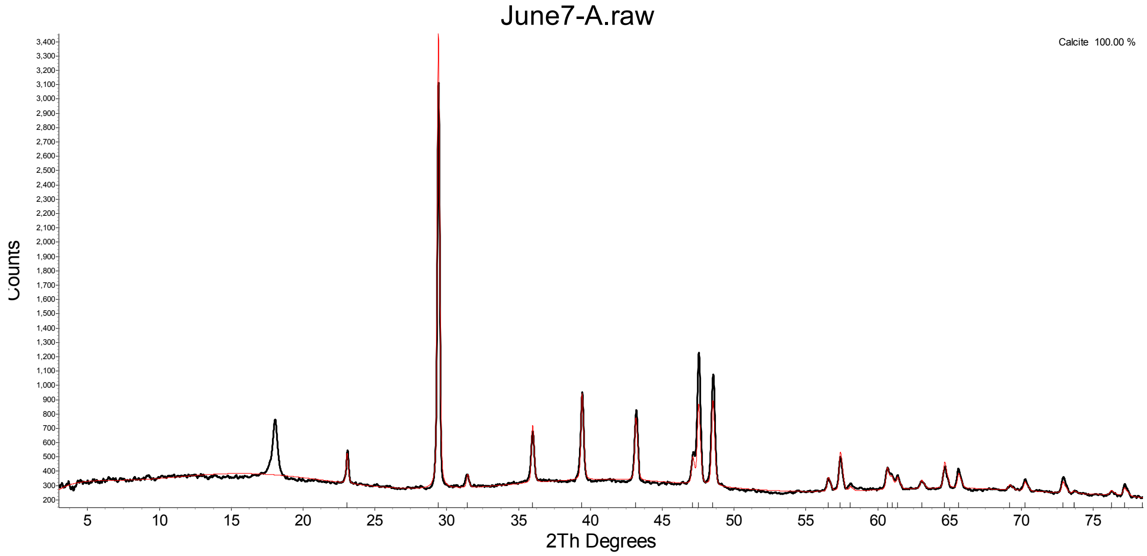
June7-A.raw
Calcite 100.00 %
Counts
200
300
400
500
600
700
800
900
1,000
1,100
1,200
1,300
1,400
1,500
1,600
1,700
1,800
1,900
2,000
2,100
2,200
2,300
2,400
2,500
2,600
2,700
2,800
2,900
3,000
3,100
3,200
3,300
3,400
5
10
15
20
25
30
35
40
45
50
55
60
65
70
75
2Th Degrees

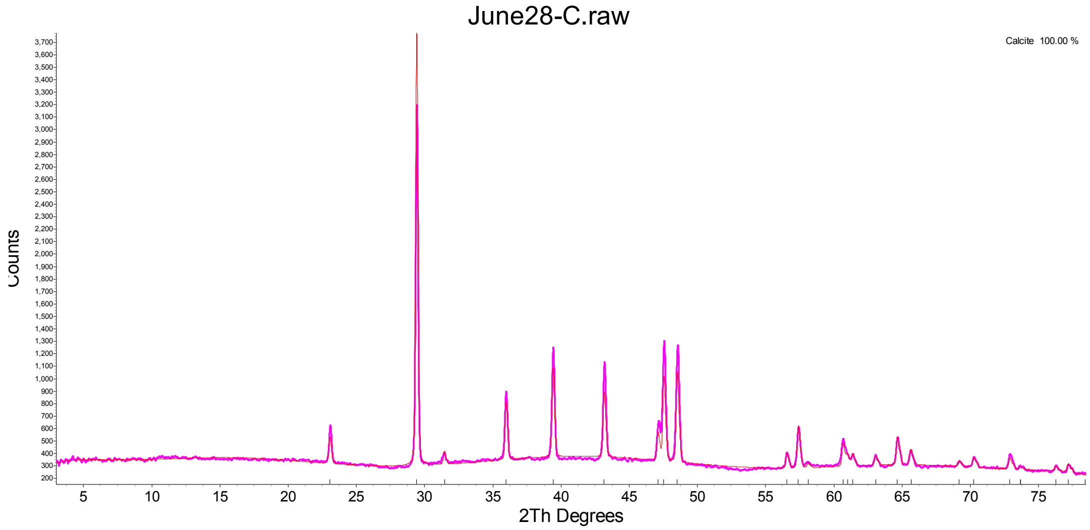
June28-C.raw
Calcite 100.00 %
Counts
200
300
400
500
600
700
800
900
1,000
1,100
1,200
1,300
1,400
1,500
1,600
1,700
1,800
1,900
2,000
2,100
2,200
2,300
2,400
2,500
2,600
2,700
2,800
2,900
3,000
3,100
3,200
3,300
3,400
3,500
3,600
3,700
5
10
15
20
25
30
35
40
45
50
55
60
65
70
75
2Th Degrees

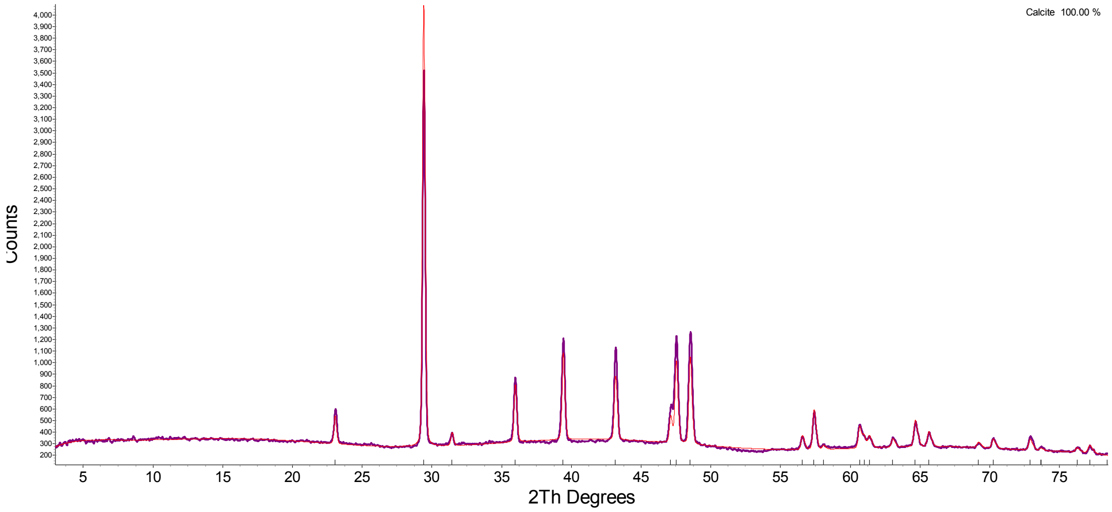
June28-D.raw

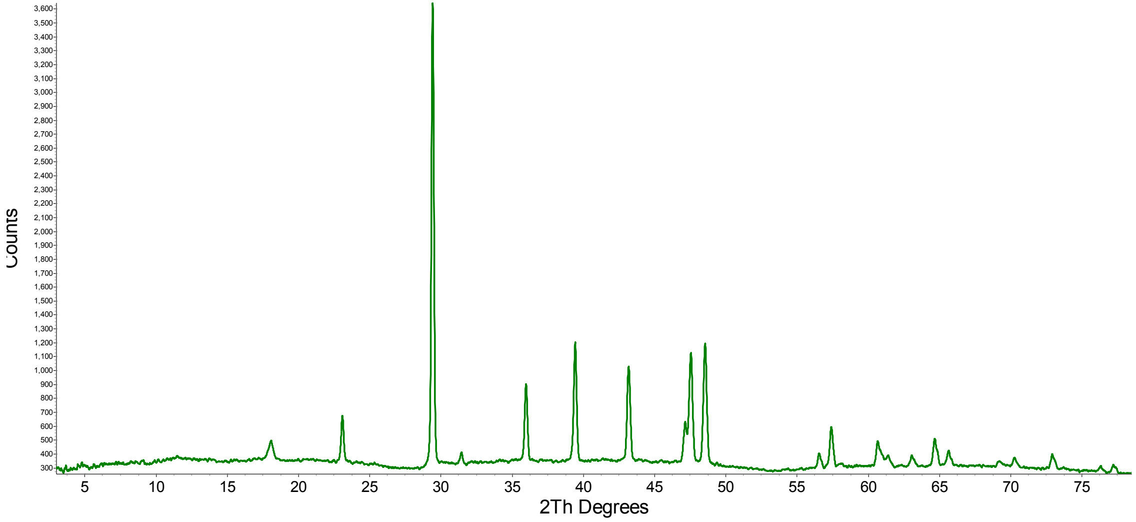
July18-C.raw

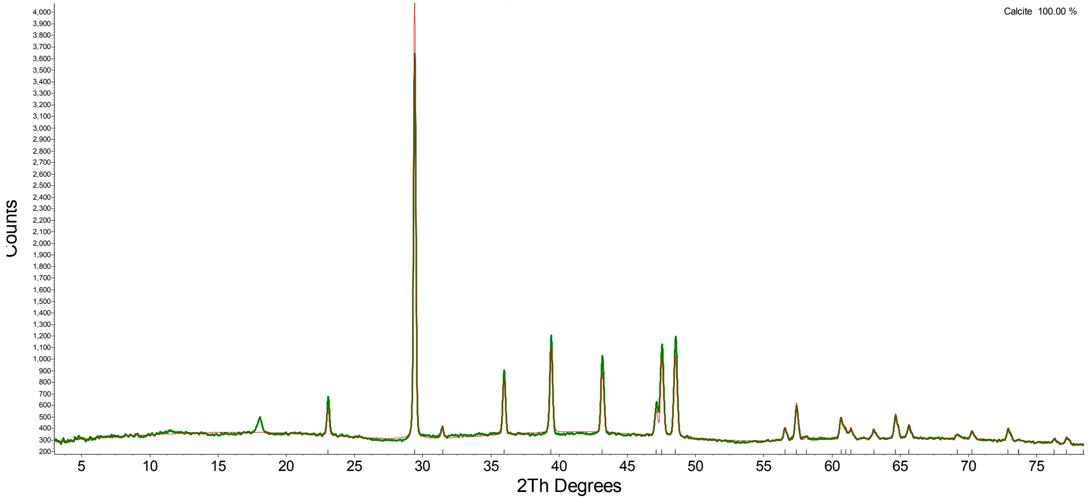
July18-C.raw

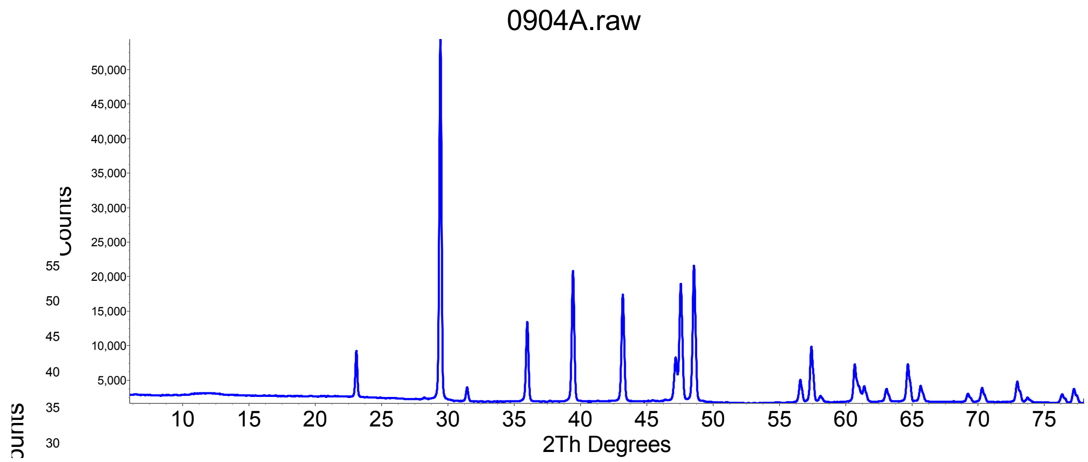
0904A.raw
Counts
50,000
45,000
40,000
35,000
30,000
25,000
20,000
15,000
10,000
5,000
55
50
45
40
35
30
ounts
10
15
20
25
30
35
40
45
50
55
60
65
70
75
2Th Degrees

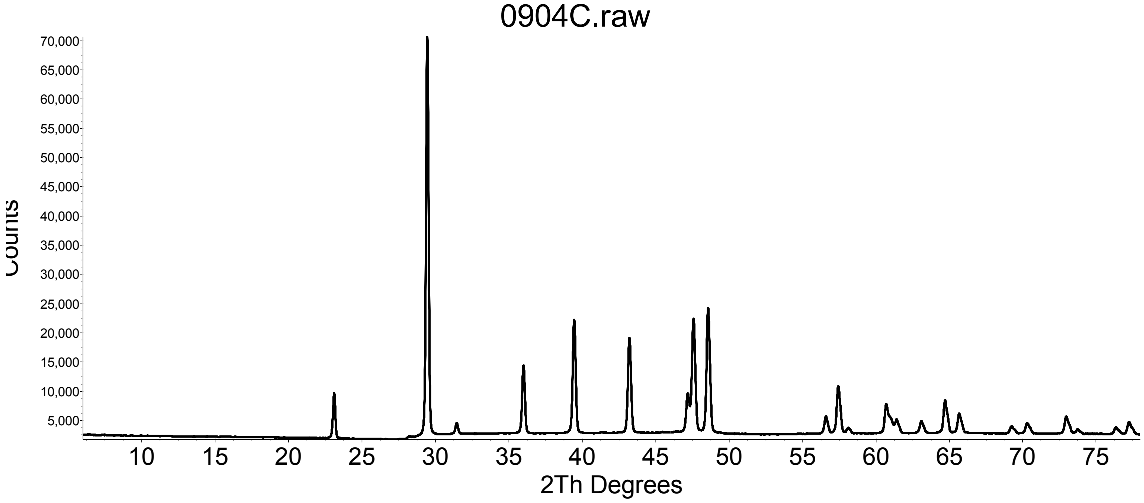
0904C.raw
Counts
70,000
65,000
60,000
55,000
50,000
45,000
40,000
35,000
30,000
25,000
20,000
15,000
10,000
5,000
10
15
20
25
30
35
40
45
50
55
60
65
70
75
2Th Degrees

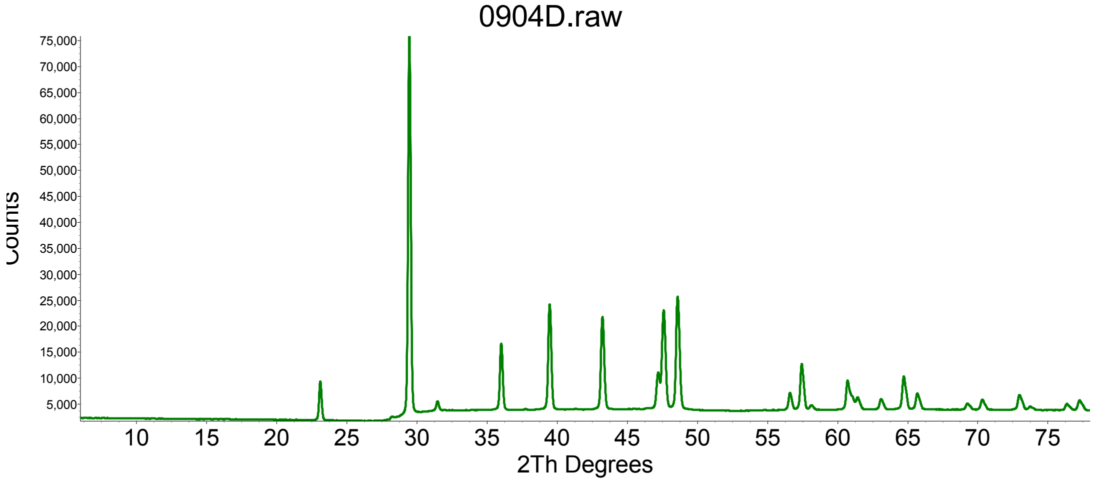
0904D.raw
Counts
75,000
70,000
65,000
60,000
55,000
50,000
45,000
40,000
35,000
30,000
25,000
20,000
15,000
10,000
5,000
10
15
20
25
30
35
40
45
50
55
60
65
70
75
2Th Degrees

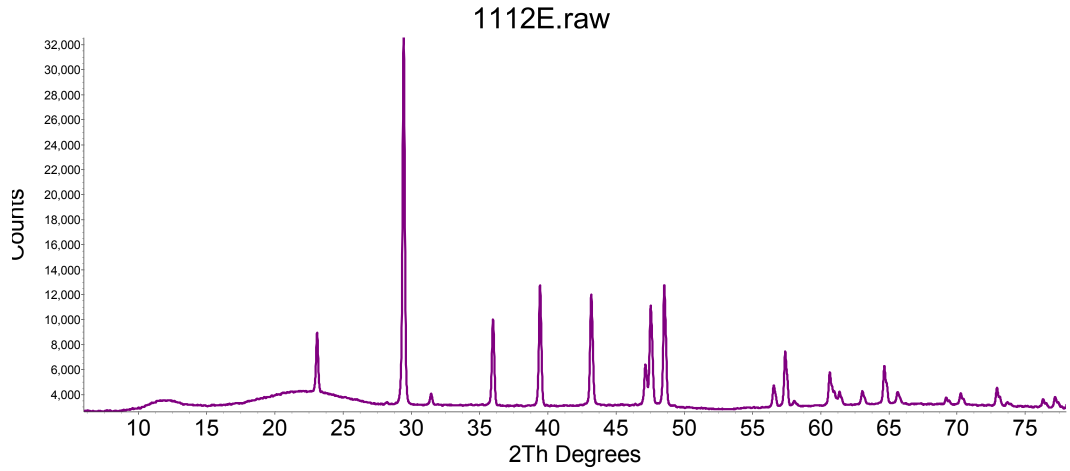
1112E.raw
Counts
32,000
30,000
28,000
26,000
24,000
22,000
20,000
18,000
16,000
14,000
12,000
10,000
8,000
6,000
4,000
10
15
20
25
30
35
40
45
50
55
60
65
70
75
2Th Degrees

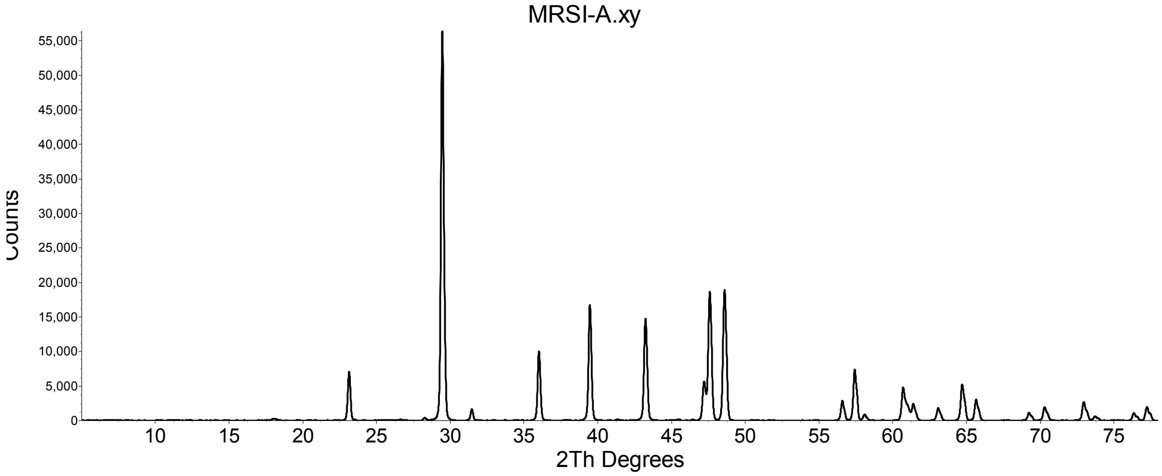
MRSI-A.xy
Counts
55,000
50,000
45,000
40,000
35,000
30,000
25,000
20,000
15,000
10,000
5,000
0
10
15
20
25
30
35
40
45
50
55
60
65
70
75
2Th Degrees

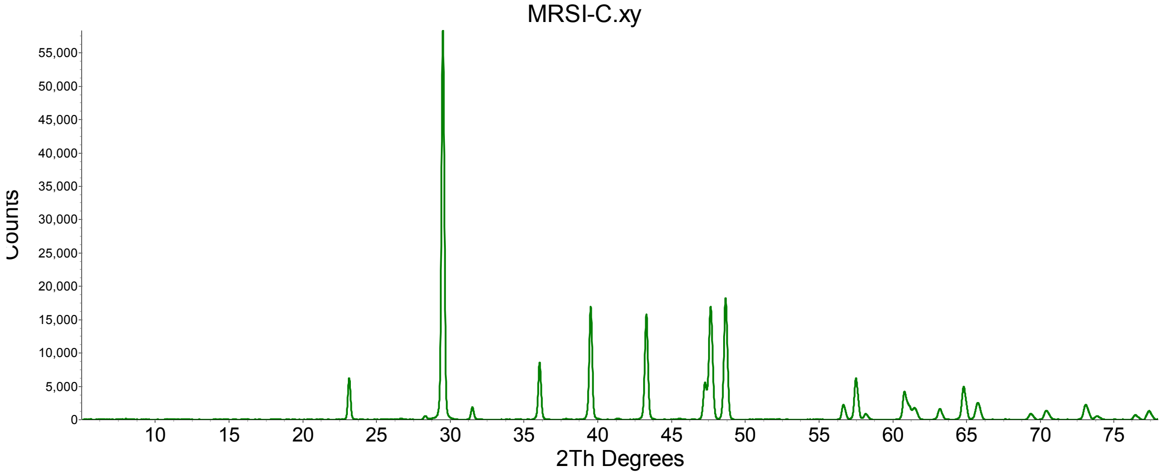
MRSI-C.xy
Counts
55,000
50,000
45,000
40,000
35,000
30,000
25,000
20,000
15,000
10,000
5,000
0
10
15
20
25
30
35
40
45
50
55
60
65
70
75
2Th Degrees

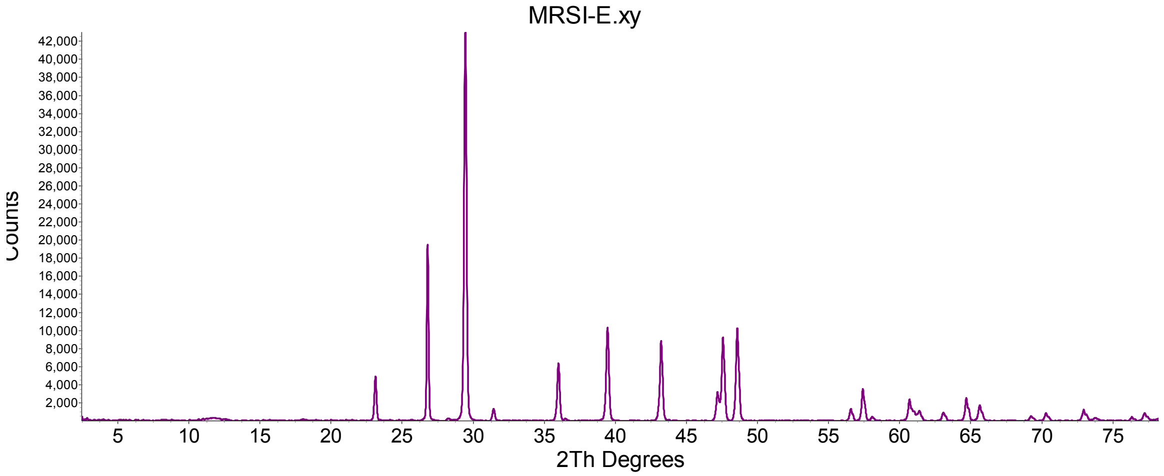
MRSI-E.xy
Counts
42,000
40,000
38,000
36,000
34,000
32,000
30,000
28,000
26,000
24,000
22,000
20,000
18,000
16,000
14,000
12,000
10,000
8,000
6,000
4,000
2,000
5
10
15
20
25
30
35
40
45
50
55
60
65
70
75
2Th Degrees

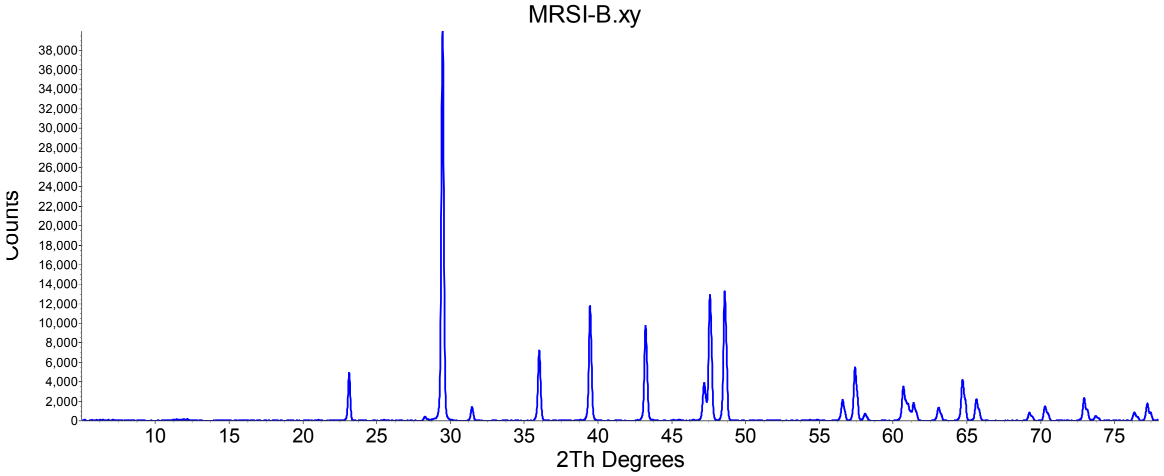
MRSI-B.xy
Counts
38,000
36,000
34,000
32,000
30,000
28,000
26,000
24,000
22,000
20,000
18,000
16,000
14,000
12,000
10,000
8,000
6,000
4,000
2,000
0
10
15
20
25
30
35
40
45
50
55
60
65
70
75
2Th Degrees

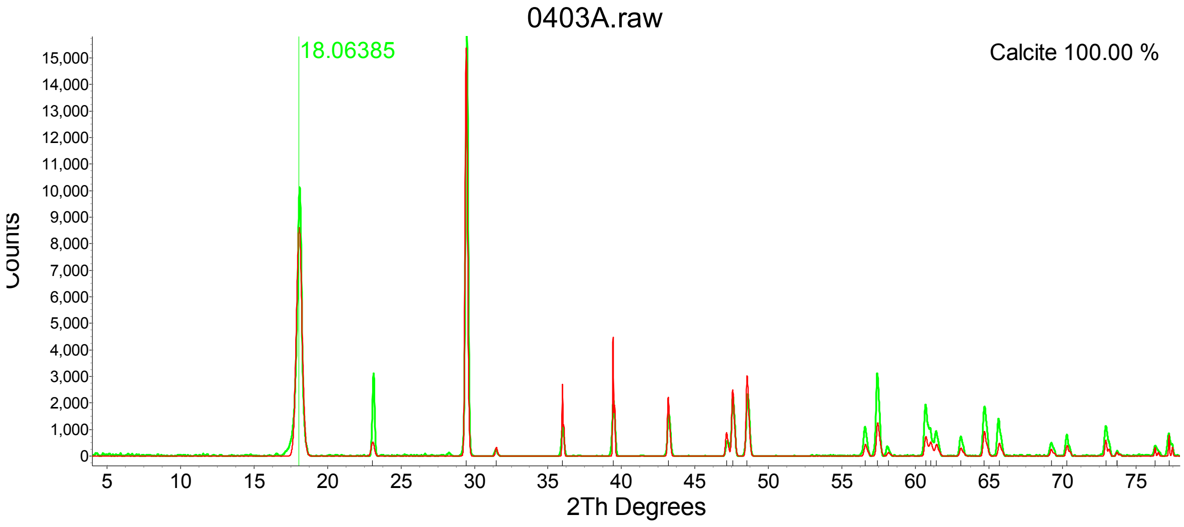
0403A.raw
18.06385
Calcite 100.00 %
Counts
15,000
14,000
13,000
12,000
11,000
10,000
9,000
8,000
7,000
6,000
5,000
4,000
3,000
2,000
1,000
0
5
10
15
20
25
30
35
40
45
50
55
60
65
70
75
2Th Degrees

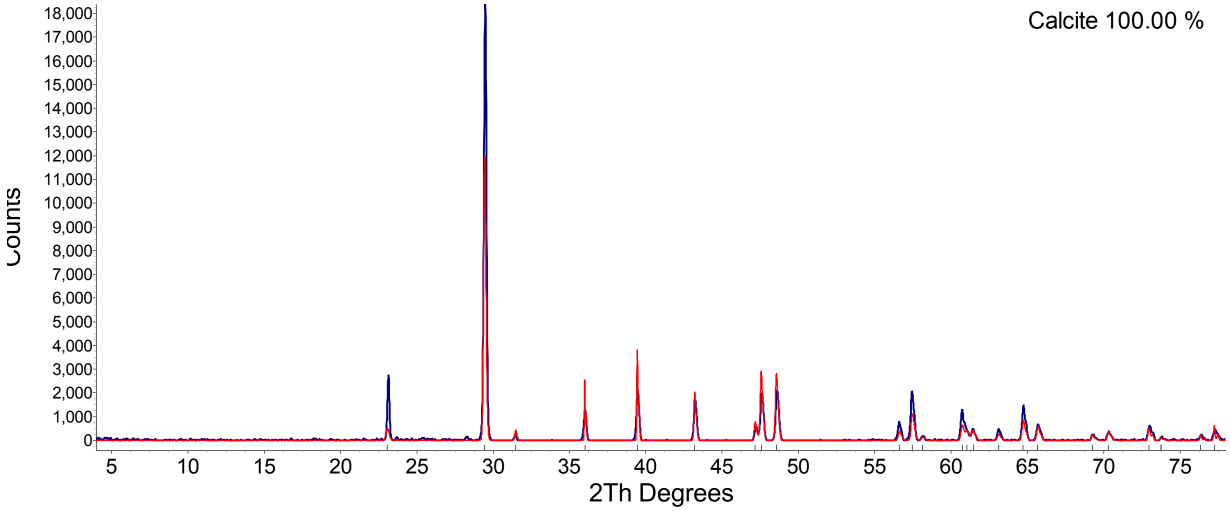
0616A.raw

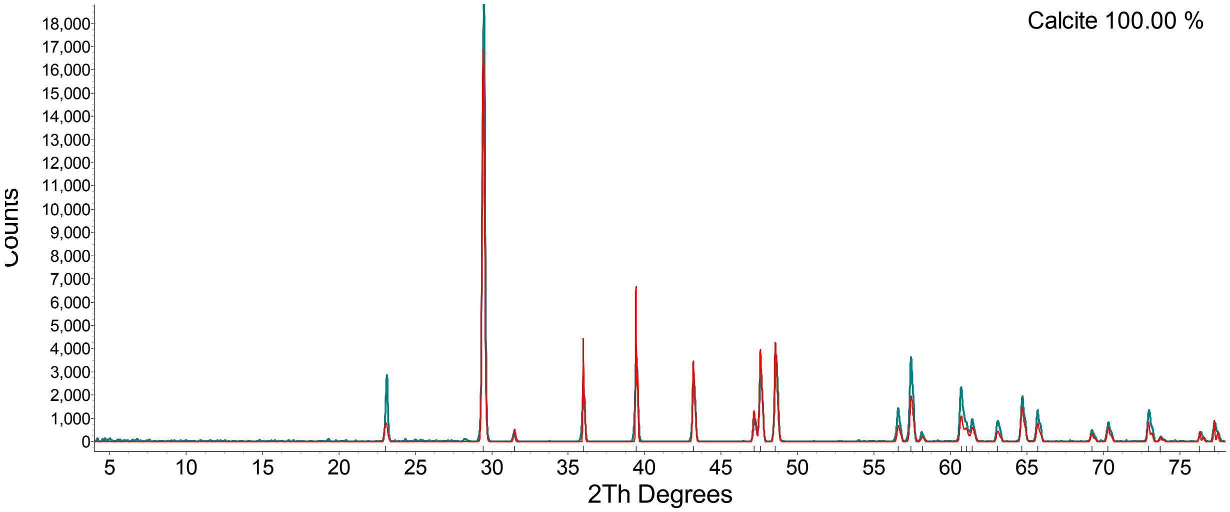
0616E.raw

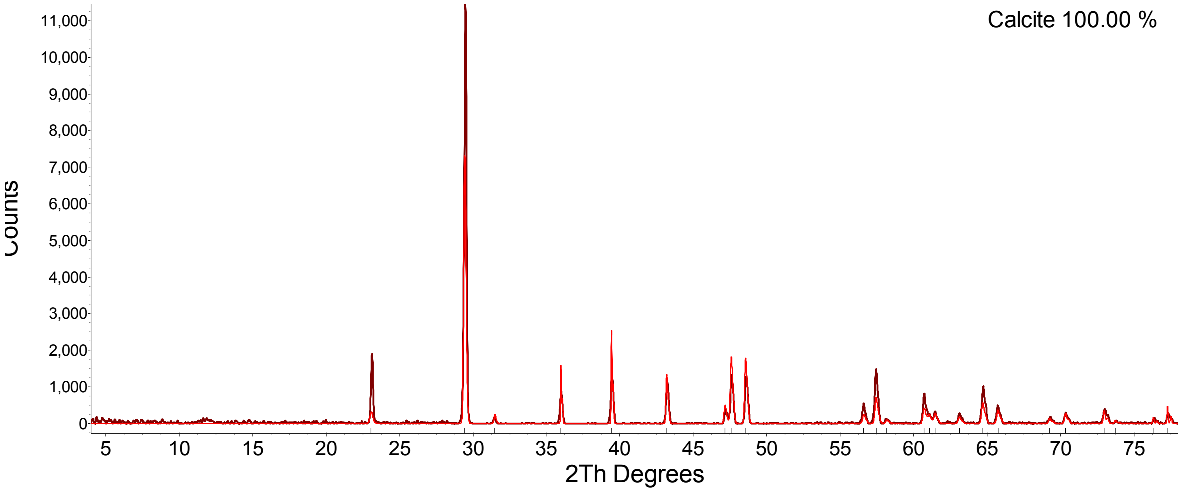
0512A.raw